5-29-2009

Diagnosis and Inhibition Tools in Medicinal Chemistry

Senol Akay
Georgia State University

DIAGNOSIS AND INHIBITION TOOLS IN MEDICINAL CHEMISTRY

by

SENOL AKAY

PART I: SYNTHESIS AND EVALUATION OF DUAL WAVELENGTH FLUORESCENT BENZO[B]THIOPHENE BORONIC ACID DERIVATIVES FOR SUGAR SENSING

Under the Direction of Dr. Binghe Wang

PART II: SYNTHESIS OF DIAMIDINES AND ARYLIMIDAMIDES FOR DNA MINOR GROOVE BINDERS AS ANTIPARASITIC AGENTS

Under the Direction of Dr. Dave Boykin

ABSTRACT

Cell surface saccharides are involved in a variety of essential biological events. Fluorescent sensors for saccharides can be used for detection, diagnosis, analysis and monitoring of pathological processes. The boronic acid functional group is known to bind strongly and reversibly to compounds with diol groups, which are commonly found on saccharides. Sensors that have been developed for the purpose of saccharide recognition have shown great potential.

However, they are very hydrophobic and this lack of essential water-solubility makes them useful in biological applications. The first section of this dissertation details the process of developing water-soluble saccharide sensors that change fluorescent properties upon binding to saccharides.

The second section of the dissertation focuses on the development of DNA-minor groove binders as antiparasitical agents. Parasitical diseases comprise some of the world's largest health problems and yet current medication and treatments for these parasitical diseases are often difficult to administer, costly to the patients, and have disruptive side effects. Worse yet, these parasites are developing drug resistance, thus creating an urgent need for new treatments. Dicationic molecules constitute a class of antimicrobial drug candidates that possess high activity against various parasites. The second section details the development of a series of di-cationic agents that were then screened in *in vitro* activities against parasitical species.

INDEX WORDS: Boronolectins**,** Carbohydrate sensing, Benzo[b]thiophene boronic acid, Physiological pH, DNA-minor groove, DNA-binders, HAT, Leishmaniasis, Malaria

DIAGNOSIS AND INHIBITION TOOLS IN MEDICINAL CHEMISTRY

PART I: SYNTHESIS AND EVALUATION OF DUAL WAVELENGTH FLUORESCENT BENZO[B]THIOPHENE BORONIC ACID DERIVATIVES FOR SUGAR SENSING

PART II: SYNTHESIS OF DIAMIDINES AND ARYLIMIDAMIDES FOR DNA MINOR GROOVE BINDERS AS ANTIPARASITIC AGENTS

by

SENOL AKAY

A Dissertation Submitted in Partial Fulfillment of the Requirements for the Degree of

Doctor of Philosophy

in the College of Arts and Sciences

Georgia State University

2009

DIAGNOSIS AND INHIBITION TOOLS IN MEDICINAL CHEMISTRY

PART I: SYNTHESIS AND EVALUATION OF DUAL WAVELENGTH FLUORESCENT BENZO[B]THIOPHENE BORONIC ACID DERIVATIVES FOR SUGAR SENSING

PART II: SYNTHESIS OF DIAMIDINES AND ARYLIMIDAMIDES FOR DNA MINOR GROOVE BINDERS AS ANTIPARASITIC AGENTS

by

SENOL AKAY

Committee Chair: Dr. David Boykin

Committee: Dr. Al Baumstrak
Dr. Binghe Wang
Dr. Gabor Patonay

Electronic Version Approved:

Office of Graduate Studies
College of Arts and Sciences
Georgia State University
August 2009

DEDICATION

For my wife, Christina. Your love, patience, and endless support truly made this possible.

To my family, whose love and encouragement is always with me.

To the Jordan and Paret families in gratitude for all your unwavering support.

ACKNOWLEDGMENTS

No great feat is accomplished alone. I would like to thank my wife and family who supported me through long hours in the lab and who were always there to celebrate my successes and offer encouragement along the way.

I would like to thank my research advisors Dr. David Boykin and Dr. Binghe Wang for the incredible opportunities that I was able to participate in during my graduate studies, as well as for their invaluable guidance and exceptional mentoring throughout my research experience.
I would also like to thank the group members of both Dr. Boykin's and Dr. Wang's labs. In particular, Dr. Junfeng Wang, Dr. Arvind Kumar and Abdelbasset Farahat for their all support, advice and encouragement. Our discussions over coffee will be a memory that I take with me as I move forward.

Finally, I would like to thank Georgia State University, the Chemistry Department and the Molecular Disease Fellowship program for their institutional and financial support.

TABLE OF CONTENTS

LIST OF TABLES

LIST OF FIGURES

LIST OF SCHEMES

LIST OF ABBREVIATIONS

Abs. Absorbance

ARS Alizarin Red S.

DCM Dichloromethane

DMF *N,N*-dimetnylformamide

DMSO Dimethylsulfoxide

ICT Internal Charge Transfer

If Fluorescence Intensity

i.v. Intravenous

J Coupling constant

Ka-acid Acid dissociation constant of the boronic acid

Ka-ester Acid dissociation constant of the boronic ester

Keq-trig Equilibrium constant of the trigonal boronic acid with the diol

Keq-tet Equilibrium constant of the tetrahedral boronic acid with the diol

M Molar

m Multiplet

m/z Mass/charge

mp Melting point

MS Mass spectrometry

NMR Nuclear magnetic resonance

PBA Phenylboronic acid

PET Photoinduced electron transfer

rt Room temperature

psi Pounds per square inch

q quartet

s singlet

t triplet

T.b.g. Trypanosoma brucei gambiense

T.b.r. Trypanosoma brucei rhodesiense

TEA Triethylamine

THF Tetrahydrofuran

TLC Thin layer chromatography

T_m Thermal melting

UV Ultralviolet

SECTION I

BORONIC ACID BASED SENSOR FOR CELL SURFACE GLYCOLIPIDS

1. Introduction

1.1. The Importance of Cell Surface Glycolipids Sensors

Mammalian cell surfaces are coated with saccharides. These saccharides, in the forms of glycosylated proteins, peptides, and lipids, are characteristic fingerprints of different cell types.[1-5] These glycosylated biomolecules are involved in a variety of essential biological events such as adhesion, blood generation, cancer metastasis, cell-cell communications, and viral infection.[4, 6 , 7, 8] For example, cell-cell adhesion in the inflammatory processes involves lectin-carbohydrate interactions, and neutrophils inflammation was found to be mediated in part by the endothelial leukocyte adhesion molecule-1 (ELAM-1). ELAM-1 is part of a selectin family of adhesion molecules that contain a lectin motif thought to recognize carbohydrate ligands.[9] Embryonic development at early stages is known to rely on Lewis X for cell-cell adhesion.[10]

Virus glycoproteins specifically attach to the sialic acid region on the host cell surface. The human influenza virus prefers to bind to sialic acid attached to galactose in α 2, 6 linkage. However, the Avian influenza virus, in contrast to the human influenza virus, binds in α 2, 3 linkages.[11-13] HIV infection is mediated by glycoprotein binding with cell surface receptors.[14, 15]

The altered cell-surface protein glycosylation or the expressions of certain glycoproteins have been associated with many cancer types.[3, 16, 17] Certain cell surface saccharides involved in cancer and that are over expressed on cancer cells include sialyl Lewis X (sLex), sialyl Lewis A (sLea), Lewis Y (Ley), Lewis X. [18-21] Therefore, artificially designed small molecules, which

are mimics of proteins that bind to cell surface carbohydrates, could potentially be used for diagnosis and therapeutics.

1.2. Interaction Between Boronic Acid and Carbohydrate Containing Diols

The first observation reported the ability of boronic and boric acid to bind with diols, resulting in the acidity increase of the boric acid solution after the addition of sugars. The comprehensive study of phenyl boronic acid and different diols demonstrated that different diols show different affinity for the boronic acid group, lowering the acidity of the boron species to different levels.[22] Boronic acids have found to covalently react with 1,2 or 1,3 diols to form reversible five- or six-membered complexes.[22] It is important to understand the interaction mechanism between diols and boronic acid. The acidity of boronic acid is unlike that of carboxylic acids. The acidity relays on the proton release from the boronate species, which forms by reaction with water molecules. This is shown in Figure 1.1.

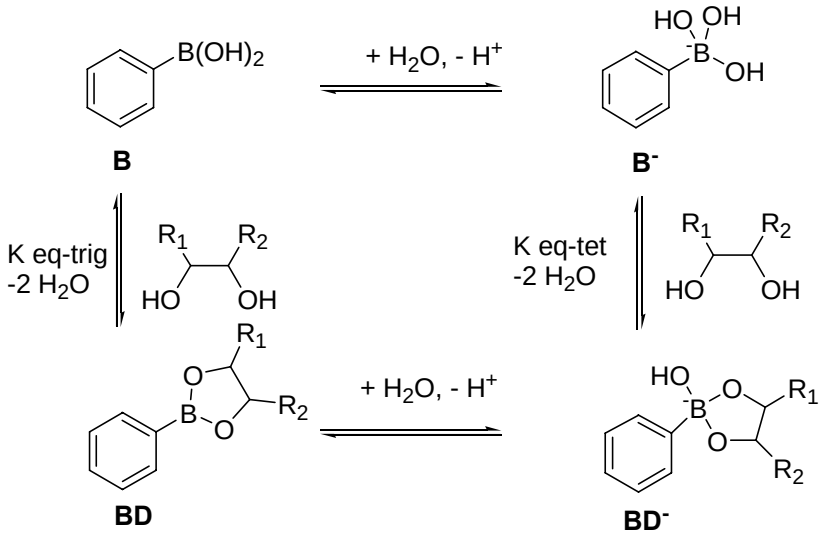

Figure 1.1. Binding process between phenylboronic acid and a diol.

Boronic acids are Lewis acids and they react with the long pair electrons of an oxygen atom of water to form the neutral trigonal form **(B)** to the anionic tetrahedral form (**B**$^-$). The same

mechanism is true for the diol – boronic complex; (**BD**) is also an acid and can react with water to release a proton.

1.3. Binding Constants Determination

In order to evaluate the binding interactions between boronic acids and diols, it is essential to have sensitive and accurate methods for the determination of their binding constants. The pH depression method and the ^{11}B-NMR method were the first two methods commonly used for determining binding constants. However, these techniques have drawbacks because of insensitivity, the requirement of large samples, and long experiment times. Recent efforts have focused on spectroscopic methods, which are highly sensitive, rapid, and require a smaller sample.

1.3.1. pH-Depression Method

This method is based on the detection of pH changes according to diol boronic acid interaction. The diol addition to a boronic acid solution lowers the pH of the solution. The extent of the pH lowering effect of a particular diol can be correlated with the "binding constant" between these two species.

1.3.2. ^{11}B-NMR Method

The other method that has been used is based on the detection of ^{11}B-NMR chemical shift differences. The addition of sugar to the boronic acid solution forms the ester complex. The pKa of the boronic acid is lower than the free form. This change results in physical changes on the boron atom. The boron atom converts from the neutral trigonal form to the anionic tetrahedral form. The ^{11}B-NMR can detect the significant chemical shift differences. Using a similar mathematical derivation, as used in pH-depression method, the binding constants of

boric acid with diols are determined. However, the ^{11}B-NMR method requires high concentration of the sensor compound and longer NMR detection for boron atom.[23-25]

1.3.3. Spectroscopic Methods

Because of the low sensitivity and the requirement of large samples, the preferred binding determination method has now changed to spectroscopic methods, which are generally more sensitive than classical methods. However, for using spectroscopic applications, the complex formation between diols and boronic acids needs to trigger a change in the spectroscopic properties of the boronic acid component. These changes can be evaluated depending on the esters complex spectroscopic properties such as CD, absorption, and fluorescence. The association constant is determined from the plot of spectroscopic intensity change verses several of the diol concentrations.

1.4. Spectroscopic Boronic Acid Compounds

1.4.1. Photoelectron Transfer (PET)

The requirement for spectroscopic detection for boronic acid reporter compounds is the boronic acid unit has to change the spectroscopic properties upon diol binding. Czarnick *et. al.* determined the binding constant of anthrylboronic acid with D-fructose at physiological pH using fluorescence spectroscopy.[26] Their fluorescent sensor, 2- anthrylboronic acid, was design based on the modulation of an excited state photoelectron transfer (PET) process that is responsible for the quenching of fluorescence. The free 2-anthrylboronic acid apparent pKa is about 8.8. The addition of fructose lowers the complex apparent pKa to about 5.9. The complex is exits in the anionic tetrahedral form at physiological pH. The formation of boronate anion quenched the anthracene fluorescence.

The other mostly used anthracene system was developed by Shinkai *et. al.* The amino group was positioned in a 1,5- relationship with the boron atom. The long pair electrons of nitrogen promote B-N bound formation. This system also showed a significant fluorescence intensity change by addition of sugars.[27, 28] The initial explanation of the fluorescence change mechanism was suggested by the modulation of the excited state PET through the formation of the B-N bond. It is known that long pair electron on the benzylic amine quenched the anthracene fluorescence.

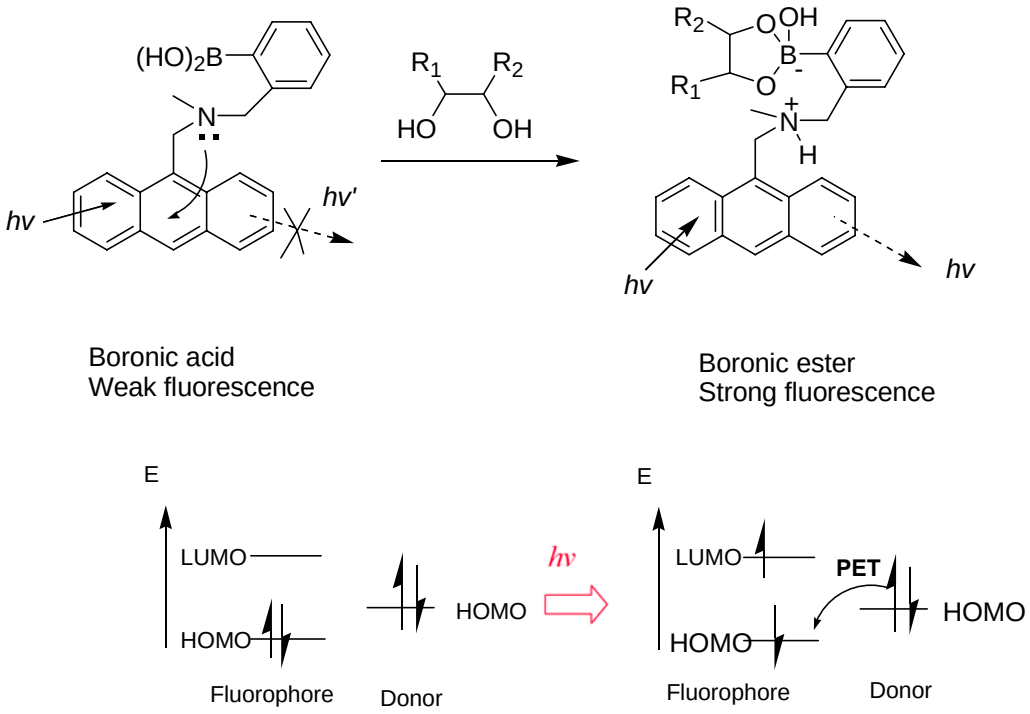

Figure 1.2. Suggested mechanism of an anthracene-based photoinduced electron transfer system.

The anthracene boronic acid is weakly fluorescence at free boronic acid formation. Upon addition of sugar, the acidity of boron increase. As a result, long pair electrons forms a B-N bound. Therefore, the fluorescence quenching long pair electrons is not available to quench the anthracene system and fluorescence increase. Wang *et.al.* suggested a different mechanism for

the fluorescent intensity change by hydrolysis mechanism. In this theory, the protonation of nitrogen also could responsible for fluorescence change by tie up the long pair electrons.

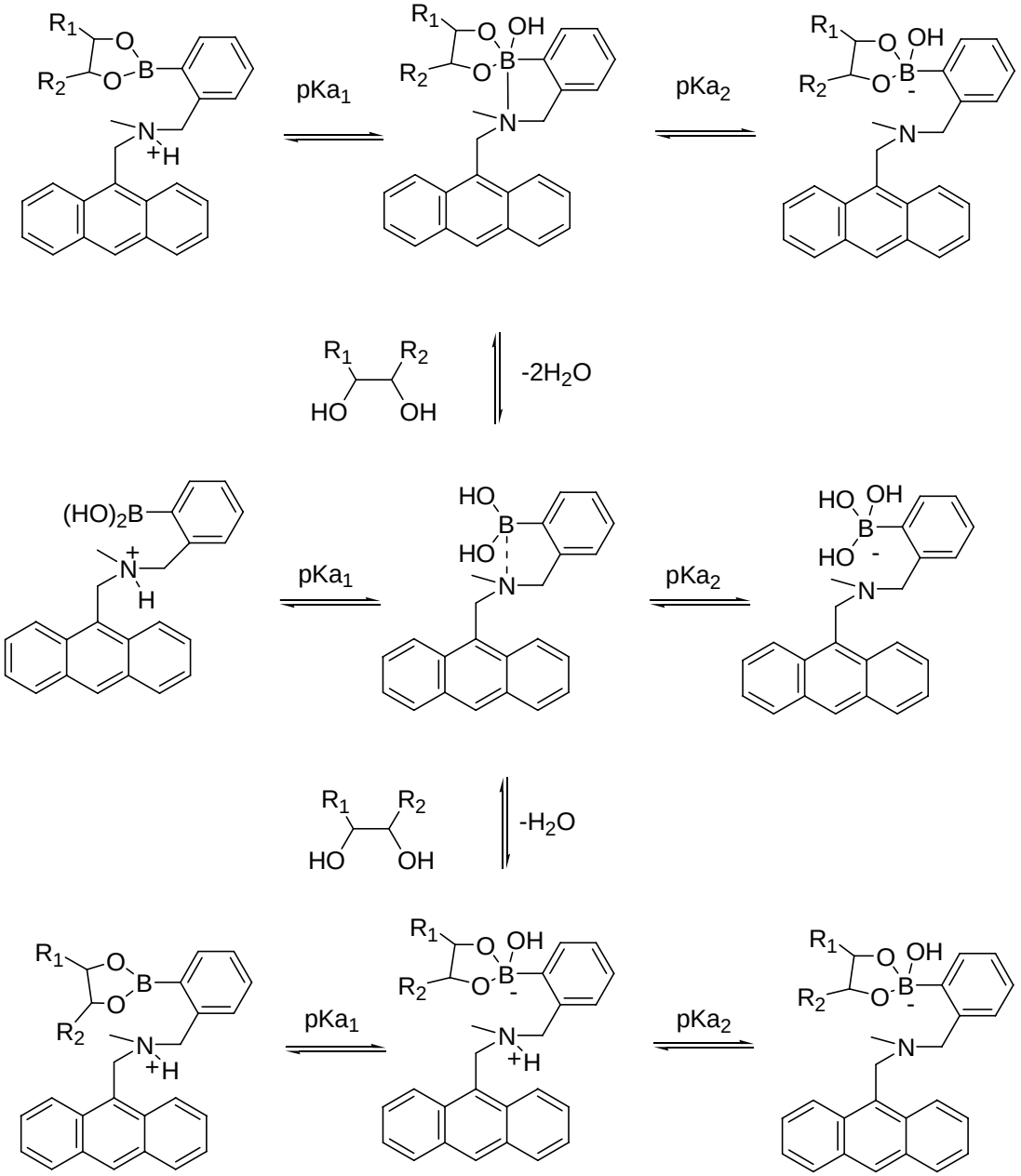

Figure 1.3. The possible mechanisms for the anthracene boronic acid fluorescence intensity change.

The detail examination of pH profile of the free boronic acid and the ester complex supported the hydrolysis mechanism, Figure 1.3.[29, 30]

1.4.2. Internal Charge Transfer

The first internal charge transfer based fluorescent boronic acid compounds as a carbohydrate sensor introduced by s Shinkai group in 1994.[31] The ICT system contains an electron donor group and electron acceptor in the same fluorophore. The empty valance orbital on boronic acid acts as an electron acceptor in the natural form. Upon addition of sugar, boronic acid group turns into its tetrahedral anionic form at certain pH and it is no longer an electron acceptor. This physical change of the molecule leads to the spectral changes because of the perturbation of charge transfer nature of the excited state and triggers the change of the fluorescence spectrum.[32]

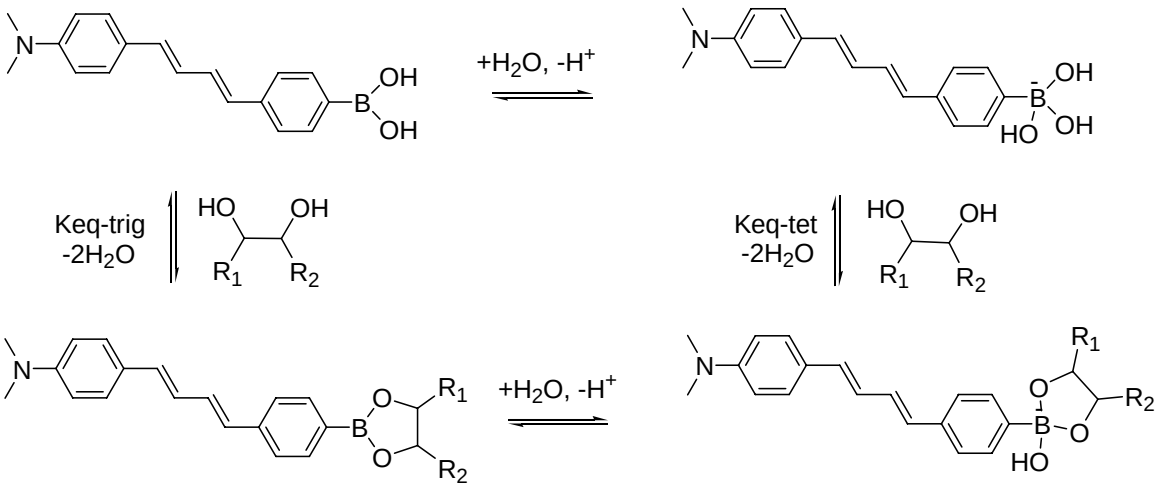

Figure 1.4. The possible binding mechanism of ICT based fluorescent boronic acid compounds.

1.4.3. Alizarin Red S. (ARS)

Boronic acids compound has been found to be a great tools for carbohydrate recognition. The spectroscopic/fluorescent boronic acid showed a great interest for carbohydrate sensing. However, because of the limitations of the fluorescence properties of the boronic acid compounds, there was a need for the development of a general and sensitive method for the

determination of the binding constants between boronic acids and diols regardless of the boronic acids are fluorescent or not. Wang *et. al.* developed a generally applicable, highly sensitive method for the determination of the binding constants between boronic acids and diols by a three-component competition assay, Figure 1.5.[33] ARS has been used for detection of boric acid.[34] ARS is not a fluorescent molecule, because of the possible excited state proton transfer from one of the catechol dihydroxyl groups to the carbonyl oxygen.[7] The binding of the catechol hydroxyl groups to the boronic acid should remove the phenol hydroxyl protons and abolish the excited state proton transfer process, which is responsible for the fluorescence.[7]

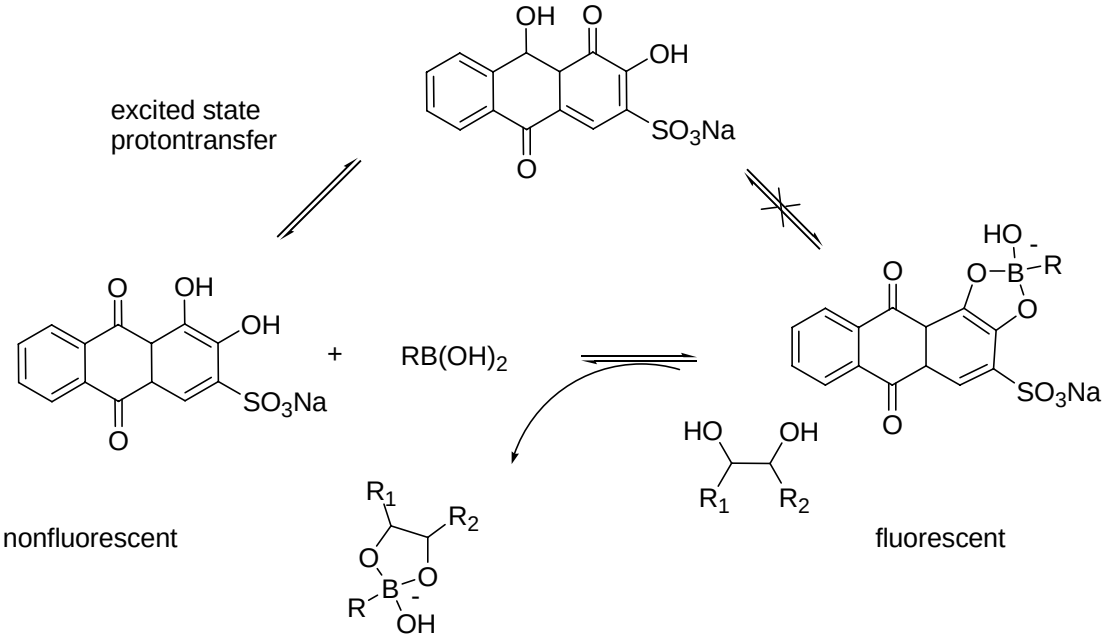

Figure 1.5. Proposed Alizarin Red S. (ARS) binding mechanism with boronic acid.

1.5. Design of Fluorescent Boronic Acid Sensor

Boronic acid compounds have been found to be a great tool for carbohydrate diol binding because of their tight and reversible interactions with 1,2- or 1,3- diols. [22] Arylboronic acids are often used for this purpose. In selecting arylboronic acids for carbohydrate recognition, those

that change fluorescent properties upon binding [26, 35-40] and are functional under physiological conditions [41-48] are especially useful. [7, 49]

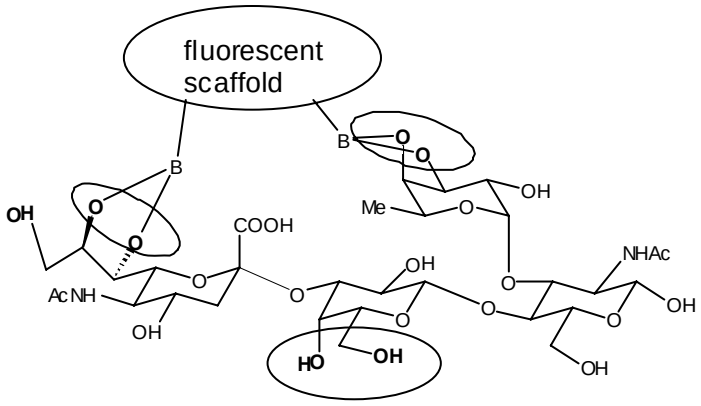

Figure 1.6. Proposed binding di-boronic acid for Sialyl Lewis X tetrasaccharide.

Such boronic acids have been used for a wide variety of applications including solution carbohydrate sensing, [50-61] cell labeling based on cell surface carbohydrate biomarkers, [62, 63] erythrocyte agglutination [64] and carbohydrate transport and separations. [65-71] From this hypothesis, our strategically designed di-boronic acid compounds for specific recognition for certain cell lines.

The first time Wang laboratory was demonstrated that synthetic fluorescent chemosensors can be used for a fluorescent labeling agent for over expressed saccharides in cancer cells. [28, 72] This study showed that boronic acid compounds are able to specifically bind to over express targeted cells. SLex are over expressed in HEPG2 and HEP3B cancer cell lines. The picture on the right shows that non-expressing control cells (COS7) are not labeled. In Figure 1.7. SLex is over express in HEPG2 and HEP3B cancer cell lines. As a control, COS7 does not contain SLex saccharide. Presence of di-boronic acid HEPG2 and HEP3B cancer lines glove under UV.

However, COS7 cancer cell line does not glove under UV In this vendor, for many of the possible applications, the availability of a large number of structurally diverse fluorescent boronic acid moieties that change fluorescent properties will be very useful, especially for combinatorial synthesis of lectin mimics. Moreover, fluorescent boronic acid base chemosensors shows strong ability to binds to the carbohydrates. Chemical modifications of boronic acid sensors shown increase the specific gylycolipid binding. However, currently developed boronic acid sensors have highly conjugated hydrophobic properties. They required dissolving in organic co-solvent system for binding determination. However, these sensors were required large amount of organic co-solvents for increase the solubility. The solubility of fluorescent compounds is still one of the biggest challenges to apply these chemosensors in *in vivo* studies for medical applications.

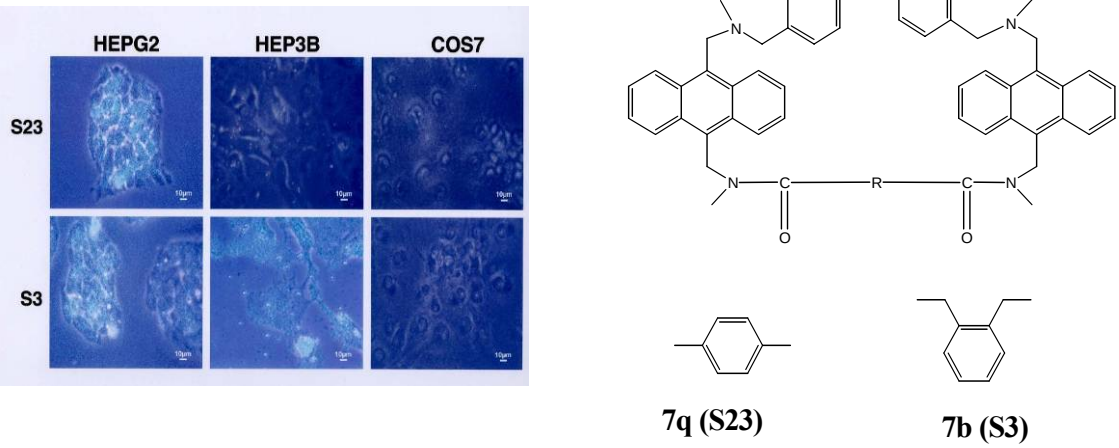

Figure 1.7. Fluorescent labeling of HEPG2, HEP3B, and COS7 with S23 and S3 at 5 mM.

The purpose of this project is development of fluorescence carbohydrate sensors can be used in carbohydrate detection, diagnosis, analysis, and monitoring pathological processes in biomedical purposes.

Our first plan is develop small boronic acid compounds which are functional at physiological pH, change fluorescent upon binding with sugars and water soluble.

References

1. Karlsson, K. A. On the Character and Functions of Sphingolipids. *Acta. Biochem.Polo.* **1998,** 45,429-438.

2. Fukuda, M.; Hindsgaul, O. *Molecular Glycobiology*. Oxford University Press: New York, 1994; p 1-52.

3. Fukuda, M. Possible Roles of Tumor-associated Carbohydrate Antigens. *Cancer Res.* **1996,** 56, 2237-2244.

4. Fukuda, M. *Cell Surface Carbohydrates and Cell Development*. CRC Press: Boca Raton, 1992.

5. Fukuda, M. Cell Surface Carbohydrates: Cell-type Specific Expression. In *Molecular Glycobiology*, Fukuda, M.; Hindsgaul, O., Eds. Oxford University Press: New York, 1994; pp 1-52.

6. Xiong, L.; Andrews, D.; Regnier, F. Comparative Proteomics of Glycoproteins Based on Lectin Selection and Isotope Coding. *J. Proteome. Res.* **2003,** 2, 618-625.

7. Yan, J.; Fang, H.; Wang, B. Boronolectins and Fluorescent Boronolectins-An Examination of the Detailed Chemistry Issues Important for their Design. *Med. Res. Rev.* **2005,** 25, 490-520.

8. Kannagi, R.; Izawa, M.; Koike, T.; Miyazaki, K.; Kimura, N. Carbohydrate-Mediated Cell Adhesion in Cancer Metastasis and Angiogenesis. *Cancer Science* **2004,** 95, 377-384.

9. Phillips, M.; Nudelman, E.; Gaeta, F.; Perez, M.; Singhal, A.; Hakomori, S.; Paulson, J. ELAM-1 mediates cell adhesion by recognition of a carbohydrate ligand, sialyl-Lex. *Science* **1990,** 250, 1130-1132.

10. Clark, G. F.; Oehninger, S.; Patankar, M. S.; Koistinen, R.; Dell, A.; Morris, H. R.; Koistinen, H.; Seppala, M. A Role for Glycoconjugates in Human Development: The Human Feto-Embryonic Defence System Hypothesis. *Human Reprod.* **1996,** 11, 467-473.

11. Brunngraber, E.; Witting, L.; Haberland, C.; Brown, B. Glycoproteins in Tay-sachs disease: isolation and carbohydrate composition of glycopeptides. *Brain Res* **1972,** 38, 151-162.

12. Li, M.; Wang, B. Computational studies of H5N1 hemagglutinin binding with SA-[alpha]-2, 3-Gal and SA-[alpha]-2, 6-Gal. *Biochemical and Biophysical Research Communications* **2006,** 347, 662-668.

13. Wang, B.; Brand-Miller, J. The role and potential of sialic acid in human nutrition. *Eur J Clin Nutr* 57, 1351-1369.

14. Grundner, C.; Pancera, M.; Kang, J.; Koch, M.; Sodroski, J.; Wyatt, R. Factors limiting the immunogenicity of

HIV-1 gp120 envelope glycoproteins. *Virology* **2004,** 330, 233-248.

15. Azevedo-Pereira, J. M.; Santos-Costa, Q.; Mansinho, K.; J., M.-P. Identification and characterization of

HIV-2 strains obtained from asymptomatic patients that do not use CCR5 or CXCR4coreceptors. *Virology* **2003,** 313.

16. Dennis, J. W. Changes in Glycosylation Associated with Malignant Transformation and Tumor Progression. In *Cell Surface Carbohydrates and Cell Development*, Fukuda, M., Ed. CRC Press: Boca Raton, 1992; pp 161-194.

17. Meyer, T.; Hart, I. R. Mechanisms of Tumour Metastasis. *Eur. J. Cancer* **1998,** 34, 214-221.

18. Sun, J.; Thurin, J.; Cooper, H. S.; Wang, P.; Mackiewicz, M.; Steplewiski, Z.; Blaszczykthurin, M. Elevated Expression of H-Type GDP-L-Fucose-Beta-D-Galactoside Alpha-2-L-Fucosyl-Transferase Is Associated with Human Colon Adenocarcinoma Progression. *Proc. Natl. Acad. Sci. USA* **1995,** 92, 5723-5728.

19. Windmuller, R.; Schmidt, R. R. Efficient Synthesis of *lactoneo* Series Antigens H, Lewis X (Le^x), and Lewis Y (Le^y). *Tetrahedron Lett.* **1994,** 35, 7927-7930.

20. Myers, R. B.; Grizzle, W. E. Biomarker Expression in Prostatic Intraepithelial Neoplasia. *Eur. Urol.* **1996,** 30, 153-166.

21. Hallouin, F.; Goupille, C.; Bureau, V.; Meflah, K.; Le Pendu, J. Increased Tumorigenicity of Rat Colon Carcinoma Cells after Alpha 1,2-Fucosyltransferase FTA Anti-Sense cDNA Transfection. *Int. J. Cancer* **1999,** 80, 606-611.

22. Lorand, J. P.; Edwards, J. O. Polyol Complexes and Structure of the Benzeneboronate Ion. *J. Org. Chem.* **1959,** 24, 769-774.

23. Vanduin, M.; Peters, J.; Kieboom, A.; Vanbekkum, H. The pH-dependence of the stability of esters

of boric-acid and borate in aqueous-medium as studied by B-11 NMR. *Tetrahedron* **1984,** 40, 2901-2911.

24. Vandenberg, R.; Peters, J. A.; Vanbekkum, H. The Structure and (Local) Stability-Constants of Borate Esters of Monosacchharides and Disaccharides as Studied by B-11 and C-13 Nmr-Spectroscopy. *Carbohydr. Res.* **1994,** 253, 1-12.

25. Vanduin, M.; Peters, J. A.; Kieboom, A. P. G.; Vanbekkum, H. Studies on Borate Esters .2. Structure and Stability of Borate Esters of Polyhydroxycarboxylates and Related Polyols in Aqueous Alkaline Media as Studied by B-11 Nmr. *Tetrahedron* **1985,** 41, 3411-3421.

26. Yoon, J.; Czarnik, A. W. Fluorescent Chemosensors of Carbohydrates. A Means of Chemically Communicating the Binding of Polyols in Water Based on Chelation-Enhanced Quenching. *J. Am. Chem. Soc.* **1992,** 114, 5874-5875.

27. Springsteen, G.; Wang, B. A Detailed Examination of Boronic Acid-Diol Complexation. *Tetrahedron* **2002,** 58, 5291-5300.

28. Wang, W.; Gao, X.; Wang, B. Boronic Acid-based Sensors for Carbohydrates. *Curr. Org. Chem.* **2002,** 6, 1285-1317.

29. Ni, W.; Kaur, G.; Springsteen, G.; Wang, B.; Franzen, S. Regulating the Fluorescence Intensity of an Anthracene Boronic Acid System: A B-N Bond or a Hydrolysis Mechanism? *Bioorgan. Chem.* **2004,** 32, manuscript accepted.

30. Franzen, S.; Ni, W.; Wang, B. A Study of the Mechanism of Electron Transfer Quenching by Boron-Nitrogen Adducts in Fluorescent Sensors. *J. Phys. Chem. B* **2003,** 107, 12942-12948.

31. Shinmori, H.; Takeuchi, M.; Shinkai, S. Spectroscopic Sugar Sensing by a Stilbene Derivative with Push (Me_2N-)-Pull((HO)2B-)-Type Substituents. *Tetrahedron* **1994,** 51, 1893-1902.

32. DiCesare, N.; Lakowicz, J. R. Chalcone-analogue Fluorescent Probes for Saccharides Signaling Using the Boronic Acid Group. *Tetrahedron Lett.* **2002,** 43, 2615-2618.

33. Szebellady, L.; Tomay, S. Beitrage zum nachweis der borsaure mit alizarin. *Z. Anal. Chem.* **1936,** 107, 26-30.

34. Palit, D.; Pal, H.; Mukherjee, T.; Mittal, J. Photodynamics of the S1 state of some hydroxy and amino substituted napthoquinones and anthraquinones. *J. Chem. Soc. Faraday Trans.* **1990,** 86, 3861-3869.

35. Davis, C. J.; Lewis, P. T.; McCarroll, M. E.; Read, M. W.; Cueto, R.; Strongin, R. M. Simple and Rapid Visual Sensing of Saccharides. *Org. Lett.* **1999,** 1, 331-334.

36. James, T. D.; Sandanayake, K. R. A. S.; Iguchi, R.; Shinkai, S. Novel Saccharide-Photoinduced Electron Transfer Sensors Based on the Interaction of Boronic Acid and Amine. *J. Am. Chem. Soc.* **1995,** 117, 8982-8987.

37. Cao, H.; Diaz, D. I.; DiCesare, D.; Lakowicz, J. R.; Heagy, M. D. Monoboronic Acid Sensor That Displays Anomalous Fluorescence Sensitivity to Glucose. *Org. Lett.* **2002,** 4, 1503 -1505.

38. Cao, H. S.; Heagy, M. D. Fluorescent Chemosensors for Carbohydrates: A Decade's worth of Bright Spies for Saccharides in Review. *J. Fluor.* **2004,** 14, 569-584.

39. Cao, H.; McGill, T.; Heagy, M. D. Substituent Effects on Monoboronic Acid Sensors for Saccharides Based on N-Phenyl-1,8-Naphthalenedicarboximides. *J. Org. Chem.* **2004,** 69, 2959-2966.

40. DiCesare, N.; Lakowicz, J. R. Wavelength-ratiometric Probes for Saccharides Based on Donor-acceptor Diphenylpolyenes. *J. Photochem. Photobiol. A-Chem.* **2001,** 143, 39-47.

41. Yang, W.; Springsteen, G.; Yan, J.; Deeter, S.; Wang, B. A Novel Type of Fluorescent Boronic Acid that Shows Large Fluorescence Intensity Changes upon Binding with a Diol in Aqueous Solution at Physiological pH. *Bioorg. Med. Chem. Lett.* **2003,** 13, 1019 - 1022.

42. Gao, X.; Zhang, Y.; Wang, B. New Boronic Acid Fluorescent Reporter Compounds II. A Naphthalene-based Sensor Functional at Physiological pH. *Org. Lett.* **2003,** 5, 4615-4618.

43. Yang, W.; Lin, L.; Wang, B. A New Type of Water-Soluble Fluorescent Boronic Acid Suitable for Construction of Polyboronic Acids for Carbohydrate Recognition. *Heterocycl. Commun.* **2004,** 10, 383-388.

44. Gao, X.; Zhang, Y.; Wang, B. A Highly Fluorescent Water-soluble Naphthalene-based Boronic Acid Reporter for Saccharide Sensing that also Shows Ratiometric UV Changes. *Tetrahedron* **2005,** 61, 9111-9117.

45. Wang, J.; Jin, S.; Wang, B. A New Boronic Acid Fluorescent Reporter that Changes Emission Intensity at Three Wavelengths upon Sugar Binding. *Tetrahedron Lett.* **2005,** 46, 7003-7006.

46. Yang, W.; Lin, L.; Wang, B. A Novel Type of Fluorescent Boronic Acid for Carbohydrate Recognition. *Tetrahedron Lett.* **2005,** 46, 7981-7984.

47. Zhang, Y.; Gao, X.; Hardcastle, K.; Wang, B. Water-soluble Fluorescent Boronic Acid Compounds for Saccharide Sensing: Structural Effect on Their Fluorescence Properties. *Chem.-Eur. J.* **2006,** 12, 1377-1384.

48. Wang, J.; Lin, N.; Jin, S.; Wang, B. Indolylboronic acids Fluorescent Reporters for Sugar Sensing and Recognition. *Chem. Biol. Drug Design* **2006,** 67, 137-144.

49. Yang, W.; Gao, X.; Wang, B. Boronic Acid Compounds as Potential Pharmaceutical Agents. *Med. Res. Rev.* **2003,** 23, 346-368.

50. Zhong, Z.; Anslyn, E. V. A Colorimetric Sensing Ensemble for Heparin. *J. Am. Chem. Soc.* **2002,** 124, 9014 -9015.

51. James, T. D.; Sandanayake, K. R. A. S.; Shinkai, S. A Glucose-selective Molecular Fluorescent Sensor. *Angew. Chem. Int. Ed. Engl.* **1994,** 33, 2207-2209.

52. James, T. D.; Linnane, P.; Shinkai, S. Fluorescent Saccharide Receptors: A Sweet Solution to the Design, Assembly and Evaluation of Boronic Acid Derived PET Sensors. *Chem. Commun.* **1996**, 281-288.

53. Kabilan, S.; Marshall, A. J.; Sartain, F. K.; Lee, M. C.; Hussain, A.; Yang, X.; Blyth, J.; Karangu, N.; James, K.; Zeng, J.; Smith, D.; Domschke, A.; Lowea, C. R. Holographic Glucose Sensors. *Biosen. Bioelectron.* **2005,** 20, 1602–1610.

54. Zhao, J.; James, T. D. Enhanced Fluorescence and Chiral Discrimination for Tartaric Acid in a Dual Fluorophore Boronic Acid Receptor. *Chem. Commun.* **2005,** 14, 1889 - 1891.

55. Alexeev, V. L.; Sharma, A. C.; Goponenko, A. V.; Das, S.; Lednev, I. K.; Wilcox, C. S.; Finegold, D. N.; Asher, S. A. High Ionic Strength Glucose-Sensing Photonic Crystal. *Anal. Chem.* **2003,** 75, 2316 -2323.

56. Asher, S. A.; Alexeev, V. L.; Goponenko, A. V.; Sharma, A. C.; Lednev, I. K.; Wilcox, C. S.; Finegold, D. N. Photonic Crystal Carbohydrate Sensors: Low Ionic Strength Sugar Sensing. *J. Am. Chem. Soc.* **2003,** 125, 3322 -3329.

57. Jiang, S.; Rusin, O.; Escobedo, J. O.; Kim, K. K.; Yang, Y.; Fakode, S.; Warner, I. M.; Strongin, R. M. Stereochemical and Regiochemical Trends in the Selective Spectrophotometric Detection of Saccharides *J. Am. Chem. Soc.* **2006,** 12221-12228.

58. Samoie, G.; Wang, W.; Xu, X.; Escobedo, J. O.; Schneider, H.-J.; Strongin, R. M. A Chemomechanical Polymer that Functions in Blood Plasma with High Glucose Selectivity *Angew. Chem., Int. Ed. Engl.* **2006,** In press

59. Karnati, V.; Gao, X.; Gao, S.; Yang, W.; Sabapathy, S.; Ni, W.; Wang, B. A Selective Fluorescent Sensor for Glucose. *Bioorg. Med. Chem. Lett.* **2002,** 12, 3373-3377.

60. Kaur, G.; Fang, H.; Gao, X.; Li, H.; Wang, B. Diboronic Glucose Sensors. *Tetrahedron* **2006,** 62, 2583-2589.

61. Kaur, G.; Lin, N.; Fang, H.; Wang, B. Boronic Acid-based Glucose Sensors. In *Glucose Sensing*, Geddes, C. D.; Lakowicz, J. R., Eds. Springer Press: 2006; Vol. 11, pp 377-397.

62. Yang, W.; Gao, S.; Gao, X.; Karnati, V. R.; Ni, W.; Wang, B.; Hooks, W. B.; Carson, J.; Weston, B. Diboronic Acids as Fluorescent Probes for Cells Expressing Sialyl Lewis X. *Bioorg. Med. Chem. Lett* **2002,** 12, 2175-2177.

63. Yang, W.; Fan, H.; Gao, S.; Gao, X.; Ni, W.; Karnati, V.; Hooks, W. B.; Carson, J.; Weston, B.; Wang, B. The First Fluorescent Diboronic Acid Sensor Specific for Hepatocellular Carcinoma Cells Expressing Sialyl Lewis X. *Chem. Biol.* **2004,** 11, 439-448.

64. Burnett, T. J.; Peebles, H. C.; Hageman, J. H. Synthesis of a Fluorescent Boronic Acid which Reversibly Binds to Cell Walls and a Diboronic Acid which Agglutinates Erythrocytes. *Biochem. Biophy. Res. Comm.* **1980,** 96, 157-162.

65. Hageman, J. H.; Kuehn, G. D. Boronic Acid Matrices for the Affinity Chromatography of Glycoproteins and Enzymes. *Met. Mol. Biol.* **1992,** 11, 45-71.

66. Soundaramani, S.; Badawi, M.; Montaño-Kohlrust, C.; Hageman, J. H. Boronic Acids for Affinity Chromatography: Spectral Methods for Determination of Ionization and Diol-binding Constants. *Anal. Biochem.* **1989,** 178, 125-134.

67. Paugam, M.-F.; Bien, J. T.; Smith, B. D.; Chrisstoffels, L. A. J.; de Jong, F.; Reinhoudt, D. N. Facilitated Catecholamine Transport through Bulk and Polymer-Supported Liquid Membrane. *J. Am. Chem. Soc.* **1996,** 118, 9820-9825.

68. Westmark, P. R.; Gardiner, S. J.; Smith, B. Selective Monosaccharide Transport through Lipid Bilayers Using Boronic Acid Carriers. *J. Am. Chem. Soc.* **1996,** 118, 11093-11100.

69. Westmark, P. R.; Gardiner, S. J.; Smith, B. D. Selective Monosaccharide Transport through Lipid bilayers using Boronic Acid Carriers. *J. Am. Chem. Soc.* **1996,** 118, 11093-11100.

70. Draffin, S. P.; Duggan, P. J.; Duggan, S. A. M. Highly Fructose Selective Transport Promoted by Boronic Acids Based on a Pentaerythritol Core. *Org. Lett.* **2001,** 3, 917-920.

71. Gardiner, S. J.; Smith, B. D.; Duggan, P. J.; Karpa, M. J.; Griffin, G. J. Selective Fructose Transport Through Supported Liquid Membranes Containing Diboronic Acid or Conjugated Monoboronic Acid- Quaternary Ammonium Carriers. *Tetrahedron* **1999,** 55, 2857-2864.

72. Yang, W.; Yan, J.; Fang, H.; Wang, B. The First Fluorescent Sensor for D-Glucarate Based on the Cooperative Action of Boronic Acid and Guanidinium Groups. *Chem. Commun.* **2003**, 792 - 793.

2. Synthesis and Evaluation of Dual Wavelength Fluorescent Benzo[b]thiophene Boronic Acid Derivatives for Sugar Sensing

This part of the study has been published in *Chemical Biology & Drug Design* **2007,** 70, 279-289.

Abstract

Cell surface glycoproteins have been known to play very important roles in various physiological and pathological processes. Small molecule compounds capable of carbohydrate recognition can be very useful for the development of sensing, diagnostic, and therapeutic agents. Along this line, we are interested in developing water soluble fluorescent boronic acid compounds for carbohydrate recognition. As such, a series of benzo[b]thiophene boronic acid derivatives have been synthesized and their fluorescent properties analyzed at physiological pH. Benzo[b]thiophene derivatives were found to be a new type of fluorescent reporter compounds capable of dual fluorescent emission under physiological pH conditions. Compounds **1, 3, 4, 5** and **6** showed unusual emission wavelength shifts upon binding of sugars. These boronic acids will be useful tools for ts a unique example of a dual fluorescence carbohydrate sensor with an emission band shift. In order to exam whether this unusual dual emission fluorescent intensity phenomenon is general with different sugars, the binding of **1** with sorbitol, galactose, mannose, and glucose was also tested. All tested sugars demonstrated the same dual emission spectral changes as fructose at physiological pH, Figure 2.3.

2.1.Introduction

Carbohydrates on cell surfaces are involved in many biological and pathological processes.[1, 2] Oligosaccharide binding proteins, lectins, specifically recognize certain oligosaccharides on the cell surface and trigger various biological events [3] such as HIV infection, [4] cancer metastasis, [5]

embryo development, [4] neural development, [6-8] and inflammation.[9-11] Therefore, small molecules that mimic the function of lectins in recognizing carbohydrates can be used for various sensing, diagnosis, and therapeutic applications. [12] Development of such small molecule lectin mimics requires special recognition moieties capable of strong binding under physiological conditions. Along this line, boronic acid compounds hold a special place due to their strong interactions with sugars. Boronic acid compounds bind tightly and reversibly to cis 1,2 or 1,3 diol moieties to form five- or six- membered rings, respectively.[7, 13, 14] Arylboronic acids are often used for this purpose. In selecting arylboronic acids for carbohydrate recognition, those that change fluorescent properties upon binding [15-21] and are functional under physiological conditions [22-29] are especially useful. [12, 30] Such boronic acids have been used for a wide variety of applications including solution carbohydrate sensing, [31-42] cell labeling based on cell surface carbohydrate biomarkers, [43, 44] erythrocyte agglutination [45] and carbohydrate transport and separations. [46-52] For many of the possible applications, the availability of a large number of structurally diverse fluorescent boronic acid moieties that change fluorescent properties will be very useful, especially for combinatorial synthesis of lectin mimics. Herein, we describe the synthesis and evaluation of five different benzo[b]thiophene boronic acid derivatives that change fluorescent properties upon binding to sugars at physiological pH, and can potentially be utilized for the synthesis of small molecule lectin mimics for carbohydrate biomarkers recognition. These compounds are 2-benzo[b]thiophene boronic acid (2-BTBA, **1**), 3-benzo[b]thiophene boronic acid (3-BTBA, **2**), 5-benzo[b]thiophene boronic acid (5-BTBA, **3**), 7-benzo[b]thiophene boronic acid (7-BTBA, **4**), 4-benzo[b]thiophene boronic acid (4-BTBA, **5**), and 6-benzo[b]thiophene boronic acid (6-BTBA, **6**), Figure 2.1.

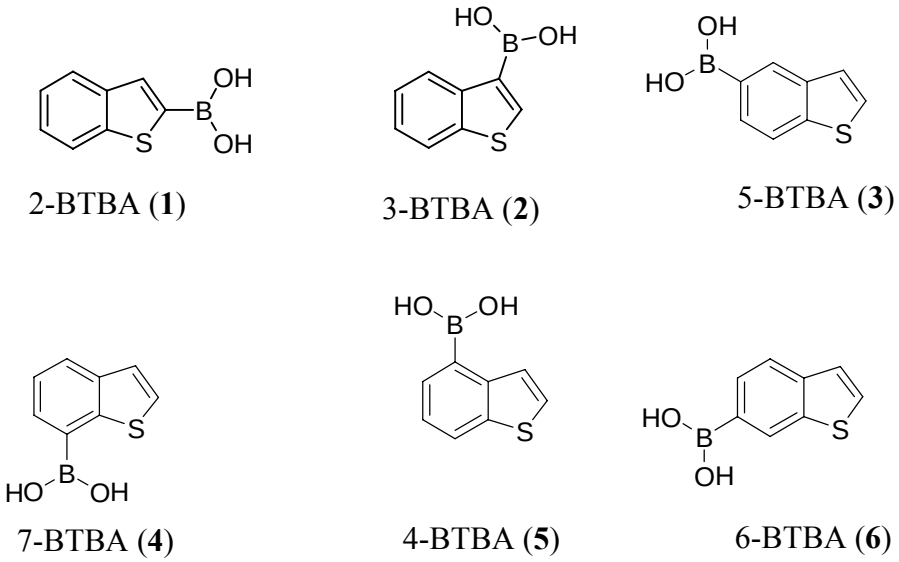

Figure 2.1. The structures of benzo[b]thiophene boronic acid compounds.

2.2. Synthesis

The synthesis of 3-BTBA (**2**) is shown in Scheme 2.1. Bromination of **7** with molecular bromine at room temperature resulted in the dibrominated compound (**8**).[53] The bromo group at the 2-position was removed with butyl lithium at -78 ^{o}C resulting in compound **9.** The protected boronic acid ester **10** was synthesized through a palladium catalyzed coupling reaction. [54-56] Deprotection of boronic acid ester[57] was carried out via treatment with aqueous potassium hydrogen fluoride in methanol resulting in potassium benzo[b]thiophene trifluoroboronate salt **11.** Hydrolysis of trifluoroborate with alkali metal hydroxide in acetonitrile resulted in free boronic acid compound **2**.

Benzo[b]thiophene boronic acid derivatives **3, 4, 5** and **6** were synthesized from their respective bromothiopenol derivatives in a similar fashion.[7] Deprotonation of bromothiophenol with a strong base, NaH, followed by substitution with bromoacetaldehyde dimethyl acetal

resulted in compounds **13**. Polyphosphoric acid-catalyzed aromatization at high temperatures resulted in

bromobenzo[b]thiophenes **14**.[58] Catalytic borylation with bis(pinacolato)diboron was followed by hydrolysis to give the free boronic acid derivatives **3-6.** [54-56]

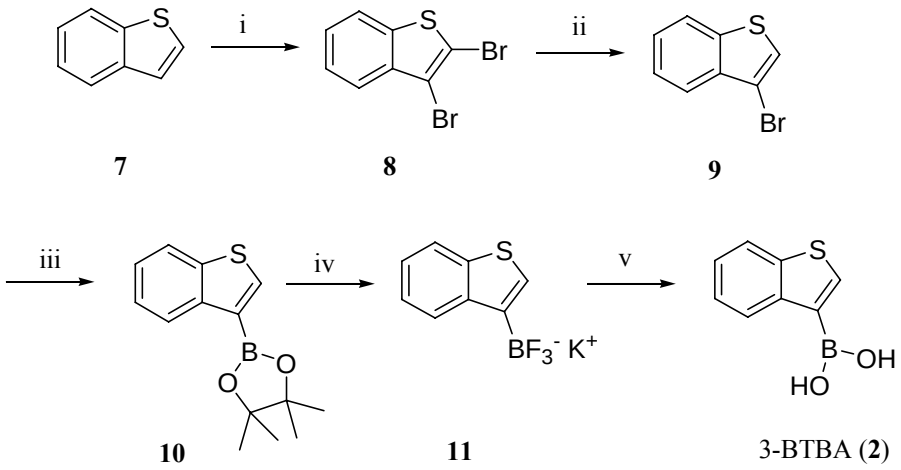

Scheme 2.1. Synthesis of 3-BTBA (**2**).
Reagents and conditions: i) Br_2, DCM, rt, 82%; ii) BuLi, THF, -78 ^oC, 81%; iii) bis(pinacolato)diboron, KOAc, [$PdCl_2$(dppf)], DMSO, 80 ^oC, 61%; iv) KHF_2, MeOH, rt, 85%; v) LiOH, CH_3CN, rt, 90%.

2.3. Fluorescent Studies

The aim of the study was to search for boronic acid compounds that change fluorescent properties upon sugar binding. Therefore, the fluorescent properties of the compounds synthesized **2-6** and a commercially available analog **1** were examined in 0.1 M phosphate buffer at pH 7.4. We first examined compound **1**, 2-BTBA. The fluorescent spectral changes of **1** with addition of fructose at different concentrations are shown in Figure 2.2. In the absence of sugar, 2-BTBA shows two emission bands at 305 and 334 nm, respectively.

Following the addition of fructose, the fluorescent spectrum of **1** showed an increase in emission intensity at 305 nm and a wavelength shift of the 334 nm peak to 317 nm with a

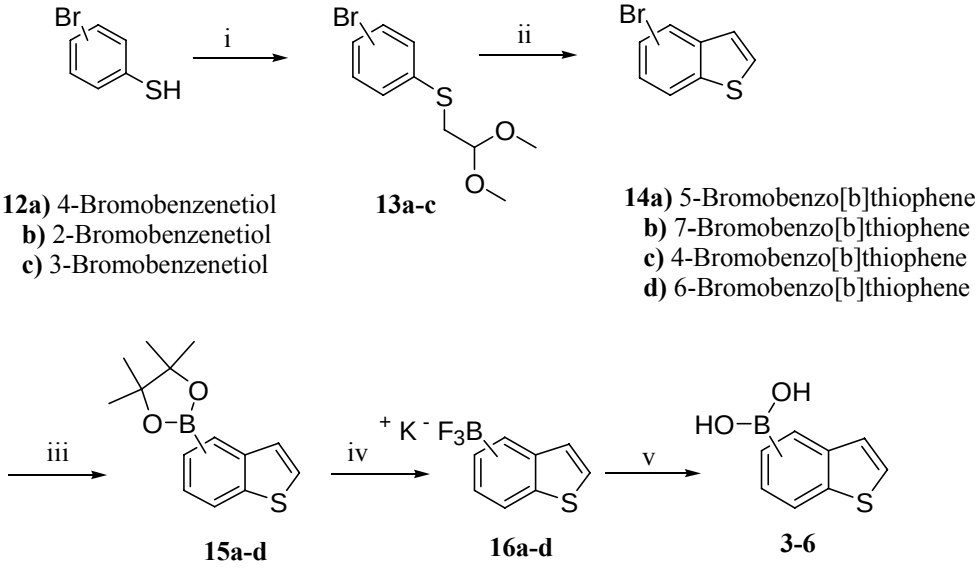

12a) 4-Bromobenzenetiol
b) 2-Bromobenzenetiol
c) 3-Bromobenzenetiol

13a-c

14a) 5-Bromobenzo[b]thiophene
b) 7-Bromobenzo[b]thiophene
c) 4-Bromobenzo[b]thiophene
d) 6-Bromobenzo[b]thiophene

15a-d **16a-d** **3-6**

Scheme 2.2. Synthesis of benzo[b]thiophene boronic acid derivatives **3**, **4**, **5** and **6.**
Reagents and conditions: i) NaH, bromoacetaldehyde dimethyl acetal, THF, reflux, 95-97%; ii) polyphosphoric acid, chlorobenzene, 160 ^{o}C, 82-96%; iii) bis(pinacolato)diboron, KOAc, [$PdCl_2$(dppf)], DMSO, 80 ^{o}C, 47-65%; iv) KHF_2, MeOH, rt, 60-70%; v) LiOH, CH_3CN, rt, 61-66%.

somewhat decreased intensity. An isosbestic point was observed at 322 nm. This represents a unique example of a dual fluorescence carbohydrate sensor with an emission band shift. In order to exam whether this unusual dual emission fluorescent intensity phenomenon is general with different sugars, the binding of **1** with sorbitol, galactose, mannose, and glucose was also tested. All tested sugars demonstrated the same dual emission spectral changes as fructose at physiological pH, Figure 2.3.

The apparent association constants (Ka) of compound **1** and five different sugars were also determined assuming 1:1 binding, Table 2.1. It is interesting to note that 2-BTBA showed somewhat higher binding constants than simple phenylboronic acid (**PBA**).

For example, under similar conditions, PBA showed the following binding constants: 370 M^{-1} for sorbitol, 160 M^{-1} for fructose, 15 M^{-1} for galactose, 13 M^{-1} for mannose, and 4.6 M^{-1} for glucose. [59]

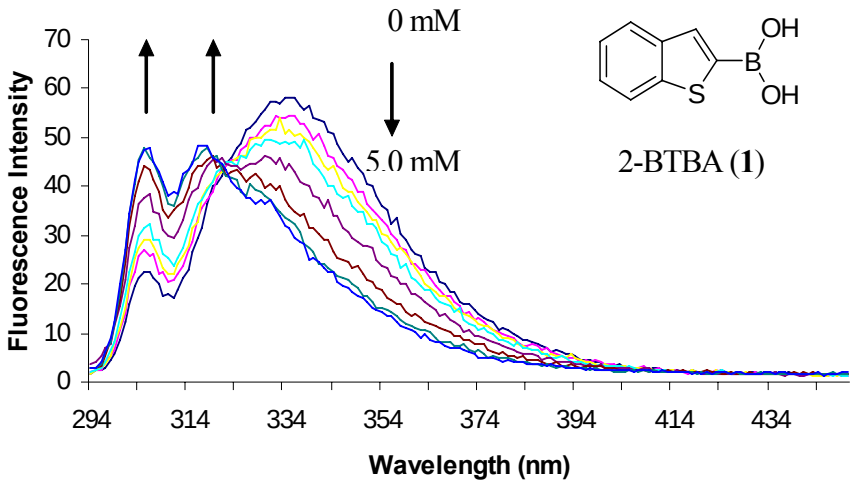

Figure 2.2. Fluorescence spectra change of **1** (1×10^{-5} M) upon addition of D-fructose (0-5.0 mM) in 0.1 M phosphate buffer at pH 7.4: λ_{ex} = 274 nm.

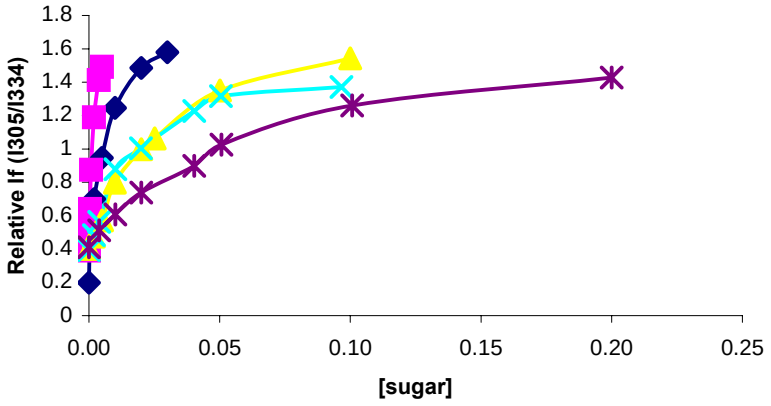

Figure 2.3. Relative fluorescence intensity of **1** (1×10^{-5} M) in 0.10 M phosphate buffer at pH 7.4 in the presence of D-Sorbitol (■), D-fructose (♦), D-galactose (▲), D-mannose (x), and D-glucose (*): λ_{ex} = 274 nm, λ_{em} = 305 and 334 nm.

In contrast, the binding constants of 2-BTBA with the same sugars are as follows: 1008, 656, 19, 27, and 30 M^{-1} respectively. The binding affinity trend for 2-BTBA also showed some difference from that of PBA with the binding constant for glucose higher than that of galactose and mannose.

As has been shown before, boronic acid binding constants are affected by many factors such as the boronic acid pKa, boronic ester pKa, sugar pKa, pH, steric effect, buffer and its concentration, and the optimal binding pH of the boronic acid. [59, 60] The convoluted results of all these factors combined are not entirely predictable. In the absence of any sugar, the fluorescent intensity of 2-BTBA at 334 nm decreased upon changing pH from 3 to 12. An apparent pKa of 7 was observed, which is assigned to the boronic acid moiety, Figure 2.4. In the presence of fructose, fluorescent intensity was tested in the region of pH 2 to 11. Similar to the situation in the absence of a sugar, the fluorescent intensity decreased at 334 nm with increasing pH. An apparent pKa of 4 was observed.

Table 2.1. Apparent association constants (*K*a) of boronic acid sensors with different sugars and their apparent p*K*a values in the absence and presence of fructose.

	2-BTBA (1)	**3-BTBA (2)**	**5-BTBA (3)**	**7-BTBA (4)**	**4-& 6-BTBA (5 & 6)**	**Phenylboronic acid (PBA)[13]**
Sorbitol	1008 ± 54	1883 ± 32	324 ± 33	4561 ± 90	349 ± 5	370
Fructose	656 ± 28	1015 ± 30	256 ± 35	1342 ± 64	338 ± 37	160
Galactose	19 ± 1	95 ± 29	6 ± 2	153 ± 2	12 ± 3	15
Glucose	30 ± 1	22 ± 8	23 ± 3	38 ± 11	24 ± 11	13
Mannose	27 ± 5	25 ± 2	2 ± 1	51 ±18	18 ±12	4.5
pKa	7.0	8.5	8.6	8.0	8.2	8.8
pKa +fructose	4.0	5.0	5.4	4.5	4.8	4.6

As has been demonstrated by past studies, boronic acids with lower pKa values than PBA tend to have higher binding constants. The apparent pKa of 7 for 2-BTBA is much lower than that of PBA (8.8) determined under similar conditions. [59, 60] This might be a major contributing factor for the higher binding constant for 2-BTBA. The observed lowering of the boron pKa with fructose binding is also in line with what have been observed in the past with similar monoboronic acids. [59, 60] These results indicate that the boronic acid moiety of 2-BTBA exists partially in the tetrahedral ionized state, (**1b**, Scheme 2.3) at physiological pH even in the absence of a sugar, while in the presence of fructose the complex exists predominantly in the anionic state (**1d**, Scheme 2.3). The results further indicate that the free boronate (**1b**) fluorescent intensity is much higher than that of the free boronic acid (**1a**), while the fluorescent intensity of the sugar complex in the anionic state (**1d**) is much higher than that of the free boronate (**1b)**.

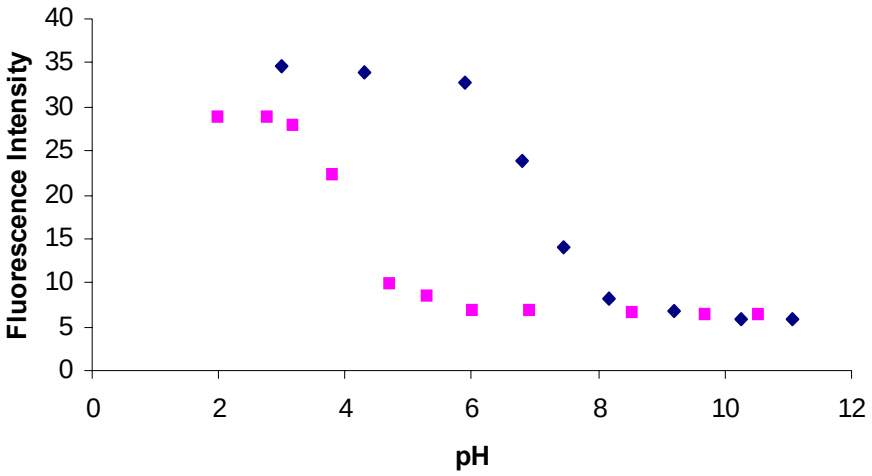

Figure 2.4. Fluorescence intensity pH profile of **1** (1×10^{-5} M) in 0.10 M phosphate buffer: [saccharide] = 0.5 M, λ_{ex} = 274 nm, λ_{em} = 334 nm. ♦ **1**, ■**1** + 0.5 M D-fructose.

Next, we were interested in studying whether positional analogs of **1** would show similar fluorescent property changes upon sugar binding. Saccharide induced fluorescent changes of 3-BTBA (**2**) were studied in a fashion similar to that of 2-BTBA (**1b**). However, 3-BTBA exhibited significantly different fluorescent properties than 2-BTBA. Without sugar and at physiological pH, 3-BTBA displays two emission bands at 302 nm and 317 nm, respectively. Upon addition of fructose, the emission band at 302 nm exhibited little change, while the intensity of the emission band at 317 nm decreased. Furthermore, there was no wavelength shift observed either, Figure 2.5A. The lack of significant intensity changes at two wavelengths and emission shift are in direct contrast to 2-BTBA (**1**). The effect of other carbohydrates was also tested with 3-BTBA (**2**). All sugars behaved similarly in changing the fluorescent properties of 3-BTBA, Figures 2.6A, 7A.

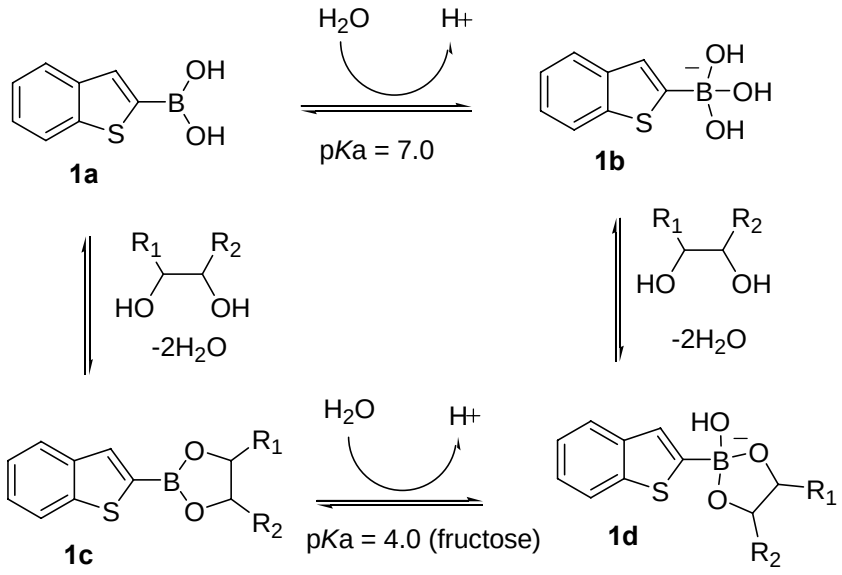

Scheme 2.3. Proposed binding mechanism for compound **1** at different pH.

The apparent association constants (Ka, Table 2.1) between 3-BTBA (**2**) and five different carbohydrates were determined. These binding constants were also found to be higher than that

of PBA. pH induced fluorescent changes were also studied; fluorescence emission at 317 nm in the absence and presence of 0.5 M of sugar decreased upon changing pH from 2 to 12, Figure 2.8A. An apparent pKa was observed at 8.5 in the absence of sugar and 5.2 in the presence of fructose, Figure 2.8A. In this case, the improved binding constant cannot be readily associated with the p*K*a change as in the case of 2-BTBA.

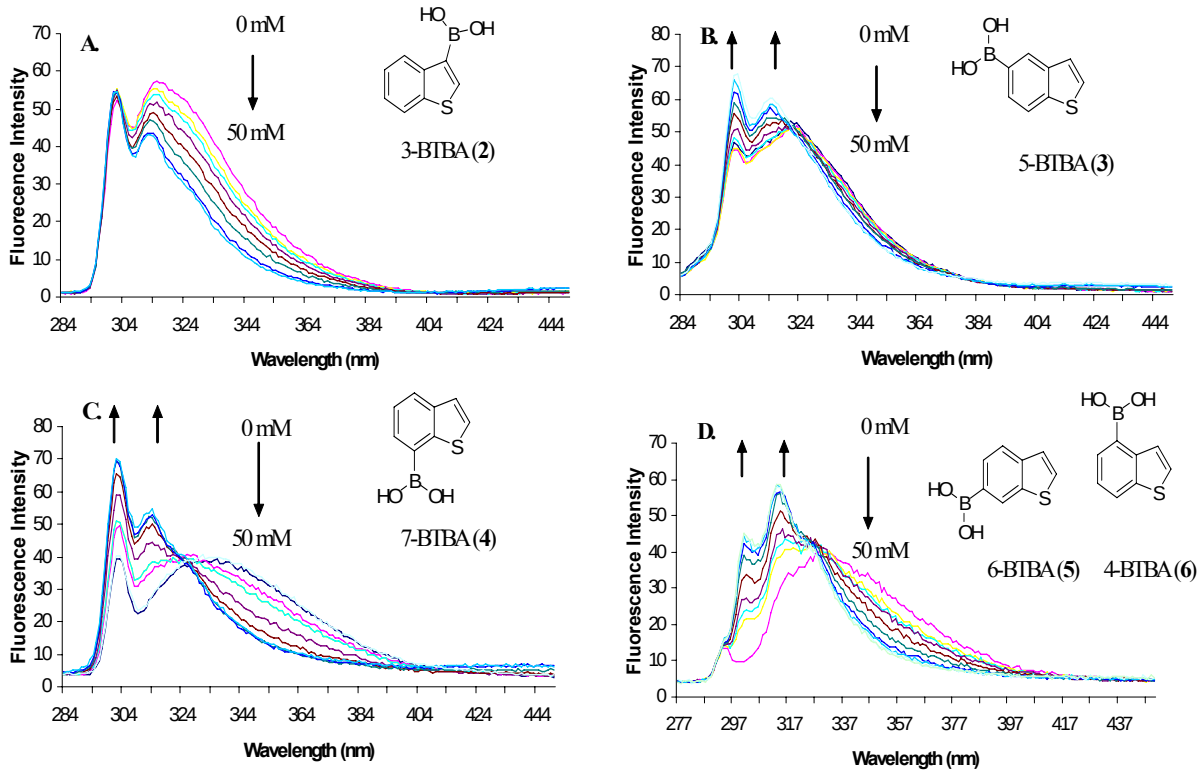

Figure 2.5. Fluorescence spectral changes of boronic acid compounds **2-6** with different concentrations of D-fructose (0-50 mM) in 0.1 M aqueous phosphate buffer at pH 7.4. **A)** 3-BTBA (**2**, 1.0×10^{-5} M), λ_{ex} = 274 nm; **B)** 5-BTBA (**3**, 1.0×10^{-5} M), λ_{ex} = 274 nm; **C)** 7-BTBA (**4**, 1.0×10^{-5} M), λ_{ex} = 274 nm; **D)** 4 & 6-BTBA (**5 & 6**, 1.0×10^{-5} M), λ_{ex} = 264 nm.

However, this is not strange as the binding constants are affected by many factors and there are numerous cases that the boronic acid binding constants do not correlate with its pKa. [59, 60] In other words, there is no good way to predict precise boronic acid-sugar binding constants yet with the state of the art knowledge. The results with these two compounds (**1** and **2**) also

indicate that positional isomers within this series of compounds may show very different fluorescent property changes upon sugar binding. For 5-BTBA (**3**), two emission bands at 303 and 322 nm were observed in the absence of a sugar. Upon the addition of fructose, the fluorescent spectrum of **3** showed an increase in emission intensity at 303 nm. The emission band at 322 nm shifted to 315 nm and showed an isosbestic point at 322 nm (Figure 2.5B). This is very similar to the situation of 2-BTBA (**1**).

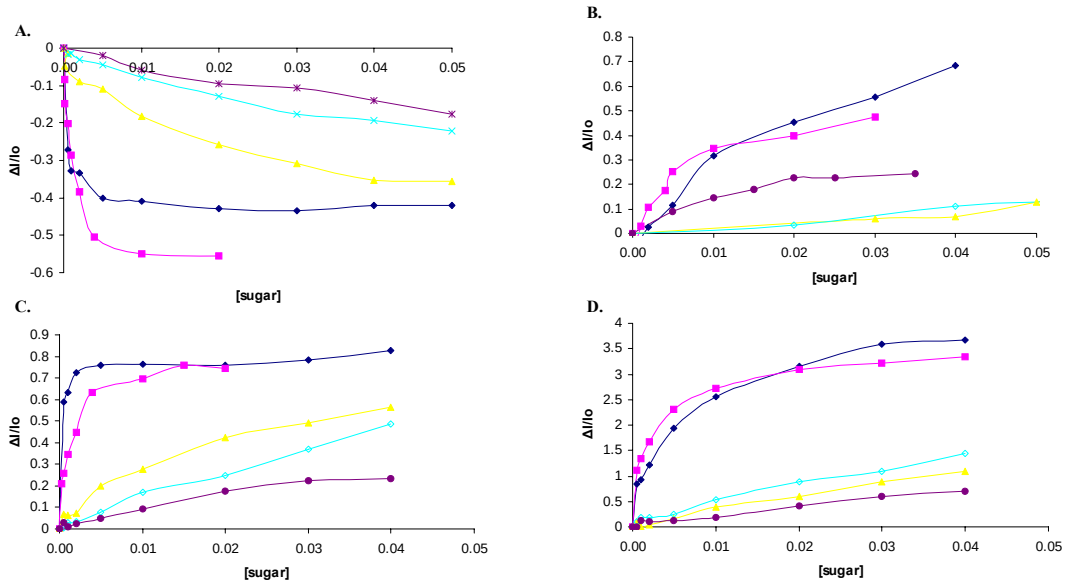

Figure 2.6. Fluorescence intensity changes (ΔI/Io) of boronic acid **2-6** (1×10^{-5} M) in aqueous phosphate buffer at pH 7.4 in the presence of D-Sorbitol (♦), D-fructose (■), D-galactose (▲), D-mannose (◊), and D-glucose (●) with different sugar concentration: **A.** 3-BTBA (**2**), λ_{ex} = 274 nm, λ_{em} = 317 nm. **B.** 5-BTBA (**3**), λ_{ex} = 274 nm, λ_{em} = 302 nm. **C**. 7-BTBA (**4**), λ_{ex} = 274 nm, λ_{em} = 303 nm. **D.** 4-BTBA (**5**) and 6-BTBA (**6**), λ_{ex} = 267 nm, λ_{em} = 303 nm.

To study the generality of this fluorescent behavior, we also tested sorbitol, galactose, mannose, and glucose. Similar to the situation of boronic acids **1** and **2**, all sugars induced similar trends in fluorescent property changes, Figures 2.6B, 7B. The apparent binding constants (*K*a) between compound **3** and five sugars were further investigated. 5-BTBA (**3**) showed moderate binding affinity to sorbitol (324 M^{-1}) and fructose (256 M^{-1}) and low affinity

for galactose, mannose, and glucose, Table 2.1. However, it still exhibited higher association constants than PBA for glucose. The apparent pKa was found to be 8.6 in the absence of fructose and 5.2 in the presence of fructose, Figure 2.8B.

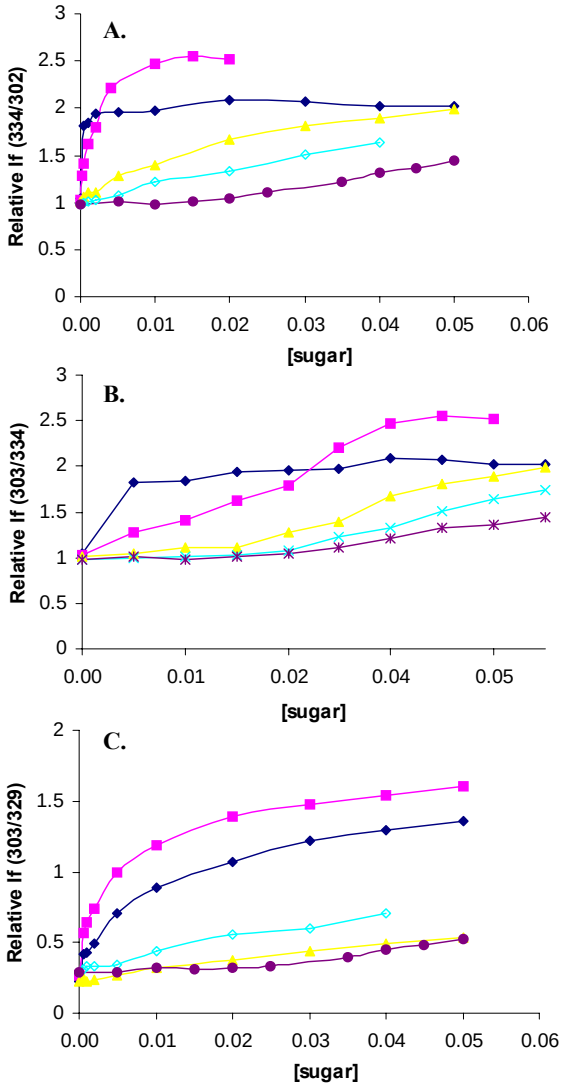

Figure 2.7. Relative fluorescence intensity of boronic acid compounds **3-6** (1×10^{-5} M) in 0.10 M phosphate buffer at pH 7.4 in the presence of D-Sorbitol (♦), D-fructose (■), D-galactose (▲), D-mannose (◊), and D-glucose (●): **A.** 5-BTBA (**3**), λ_{ex} = 274 nm, λ_{em} = 302 nm and 334nm. **B**. 7-BTBA (**4**), λ_{ex} = 274 nm, λ_{em} = 303 nm and 334 nm. **C.** 4-BTBA (**5**) and 6-BTBA (**6**), λ_{ex} = 267 nm, λ_{em} = 303 nm and 329 nm.

7-BTBA (**4**) exhibited similar fluorescent property changes upon sugar addition as 2-BTBA (**1**) and 5-BTBA (**3**), Figure 2.5C. Without sugar, **4** exhibited two emission bands at 303 nm and 334 nm when excited at 274 nm in phosphate buffer at pH 7.4.

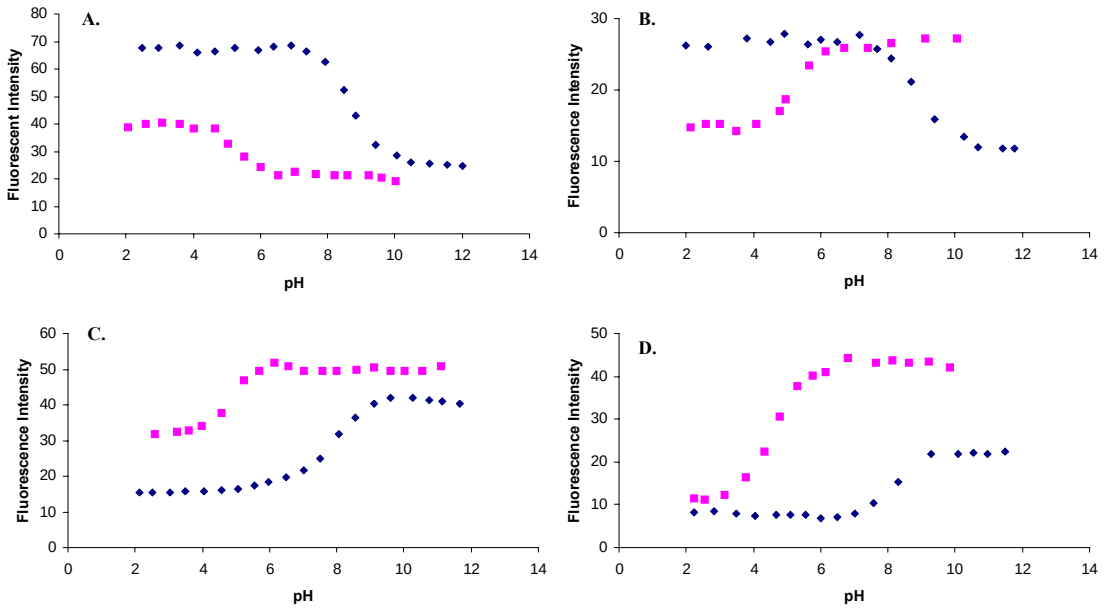

Figure 2.8. pH profiles of fluorescence intensity changes of boronic acids **2-6** (1×10^{-5} M) in the absence and presence of D-fructose (0.5 M) in 0.1 M aqueous phosphate buffer. **A.** 3-BTBA (**2**), λ_{ex} = 274 nm, λ_{em} = 318 nm; **B.** 5-BTBA (**3**), λ_{ex} = 270 nm , λ_{em} = 324 for free boronic acid, λ_{em} = 313 nm for boronic acid + 0.5 M D-fructose; **C.** 7-BTBA (**4**), λ_{ex} = 274 nm, λ_{em} = 315 nm; **D.** 4-BTBA (**5**) and 6-BTBA (**6**), λ_{ex} = 267 nm, λ_{em} = 332 nm; ♦boronic acid, ■ boronic acid + 0.5 M D-fructose.

With the addition of fructose, compound **4** showed fluorescence intensity increases at 303 nm, while the emission band at 334 nm shifted to 314 nm with a somewhat increased intensity. An isosbestic point was observed at 326 nm. Other tested sugars showed dual band emission phenomena similar to fructose, Figure 2.6c and 7c. The apparent pKa was observed at 8.0 in the absence of sugar and 5.0 in the presence of fructose, which is consistent with the general phenomena that binding to sugars lowers the p*K*a of a boronic acid. [13] One very unique feature

that stands out with 7-BTBA is its large apparent binding constants with various sugars. For example, the binding constants of 7-BTBA with sorbitol, fructose, galactose, mannose, and glucose were 4561, 1342, 153, 51, and 38 M^{-1}, respectively. In contrast, the apparent binding constants with the same sugars under identical conditions for PBA were much smaller, Table 2.1. [59, 60] Again, it does not seem that there is a direct correlation between the pKa of either the free boronic acid or the boronic ester with the drastically improved binding constants for 7-BTBA. Further theoretical studies are underway to examine this issue.

The fluorescent properties of 4-BTBA (**5**) and 6-BTBA (**6**) were examined as a mixture due to the difficulty in separating these two compounds. Without sugar, the mixture of **5** and **6** showed two emission bands at 293 nm and 329 nm when excited at 267 nm, Figure 2.5D. Upon addition of fructose, the emission band at 293 nm shifted to 303 nm and increased in fluorescent intensity. Additionally, the emission band at 329 nm shifted to 314 nm with a slight increase in fluorescent intensity. An isosbestic point was observed at 327 nm. Among the tested benzo[b]thiophene boronic acid derivatives, only the mixture of **5** and **6** showed both a red shift and a blue shift at the same time. The results were similar when tested with other sugars such as sorbitol, galactose, glucose, and mannose. The apparent association constants (*K*a) for this mixture were also determined, Table 2.1. These binding constants are comparable to that of 5-BTBA, but much smaller than that of 7-BTBA. The apparent p*K*a of this mixture was determined to be 8.2 in the absence of any sugar and 4.8 in the presence of 0.5 M fructose, consistent with all previous findings that sugar addition lowers the pKa of the boronic acid moiety. It is interesting to note that the fluorescence studies indicate that the 4-BTBA and 6-BTBA mixture shows dual fluorescent properties. Since these isomers were not isolated, it is hard to make an assumption of characteristic fluorescent properties of each isomer. Since the

mixture of 4- and 6-BTBA showed similar fluorescent properties with other isomers and their separation was very hard, we did not pursue the study with individual isomers.

2.4. Conclusion

In conclusion, six benzo[b]thiophene boronic acid derivatives have been examined for their fluorescent property changes upon sugar binding. All six compounds showed significant fluorescent property changes upon sugar addition. Among them, 2-, 5, and 7-BTBA showed a pattern of fluorescent property changes with intensity increase at one wavelength and a blue shift coupled with an intensity change in another. Such changes allow for ratiometric sensing. 3-BTBA only showed fluorescent intensity changes at one wavelength. The mixture of 4- and 6-BTBA showed a very unique red shift at one wavelength and blue shift in another upon sugar addition. Work is currently underway to use these new fluorescent reporter compounds for the synthesis of di- and polyboronic acid sensors for high selectivity identification and detection of carbohydrates of biological interest.

2.5. Experimental

2.5.1. General Information

2-Benzothiophene boronic acid was purchased from Frontier Scientific (Logan, UT, USA) and other reagents and sugars from Acros (Morris Plains, NJ, USA) and Aldrich (St Louis, MO, USA). Moisture sensitive reactions were carried out under dried N_2 with oven dried glassware. Purification of crude materials was completed with flash chromatography with silica gel 60 (230-400 mesh) from Sorbient Technology (Atlanta, GA, USA). THF was distilled from Na and benzophenone. ^{1}H NMR and ^{13}C NMR spectra were recorded at 400 MHz and 100 MHz, respectively. Mass spectrum analyses were performed by the Georgia State University

Analytical Facilities. Chemical shifts (δ) are given in ppm relative to TMS for ^{1}H spectra and residual solvents for ^{13}C spectra.

2.5.2. Fluorescence binding studies

Fluorescent spectra were recorded on a Shimadzu RF-5301 PC spectrofluorometer. Absorption spectra were recorded on a Shimadzu UV-1700 UV/Vis spectrometer. pH values were determined by a UB-10 Ultra Basic Benchtop pH meter (Denver Instrument, Denver, CO, USA). Distinct solutions of the sensors (1.0×10^{-5} M) were prepared in 0.1 M phosphate buffer at pH 7.40. Stock sugar solution was prepared by using sensor solution and the required amount of sugar dissolved in a volumetric flask. To prepare various concentrations of sugars, the stock sugar-sensor solution was diluted with sensor solution. Binding constants and apparent pKa values were measured as described earlier. [23, 25, 28]

2.5.3. Synthetic Procedures

2,3-Dibromobenzo[b] thiophene (8).[53]

2.3-Dibromobenzo[b]thiophene **8** was synthesized by following literature procedures.

3-Bromobenzo[b]thiophene (9).[61]

3-Bromobenzo[b]thiophene **9** was prepared by following literature procedures.

2-Benzo[b]thiophen-3-yl-4,4,5,5-tetramethyl-[1,3,2]dioxaborolane (10).

KOAc (1.1 g 11.4 mmol) was added to a solution of compound **9** (485 mg, 2.28 mmol), bis(pinacolato)diboron (867 mg, 3.41 mmol), and $PdCl_2$(dppf) (93 mg, 0.01 mmol) in anhydrous DMSO (7 mL). The reaction mixture was stirred at 80 ^{o}C overnight. Solution was dissolved in ethyl acetate 100 mL and washed with 5% $NaHCO_3$ (5 × 20 mL) and dried over Na_2SO_4. After filtration and evaporation of the solvent, the crude product was purified by column chromatography with 30 g of silica gel eluting with hexanes/ethyl acetate (5:1) to give

compound **10** as a colorless solid (360 mg, 61%). ^{1}H NMR ($CDCl_3$): δ 8.37 (d, J = 7.2 Hz, 1H), 8.06 (s, 1H), 7.87 (d, J = 7.6 Hz, 1H), 7.41-7.02 (m, 2H), 1.37 (s, 12H); ^{13}C NMR ($CDCl_3$): δ 142.8, 140.7, 139.0, 125.4, 124.3, 124.1, 122.1, 83.5, 24.9; GC-MS: m/z calculated for $C_{14}H_{17}BO_2S$: 260, found: 260 (M).

Potassium 3-benzo[b]thiophene trifluoroborate (11).

To the solution of compound **10** (213 mg, 0.8 mmol) in 10 mL of methanol was added aqueous potassium hydrogen fluoride (351 mg, 4.5 mmol, 4.5 M). The mixture was stirred at room temperature for 4 hr. Then solvent was removed under vacuum and the residue was dissolved in hot acetone. The mixture was filtered. The filtrate was collected and solvent was removed *in vacuo*. An oily yellow residue was obtained, which was crystallized in a minimum amount of acetone and 10 mL of ethyl ether to give compound **11** as a white solid (163 mg, 85%). ^{1}H NMR (d_6-acetone): δ 8.18 (m, 1H), 7.80 (m, 1H), 7.24 (s, 1H), 7.22-7.14 (m, 2H). ^{13}C NMR (d_6-acetone): δ 142.8, 140.7, 139.0, 125.4, 124.3, 124.1, 122.1; ESI-MS: m/z calculated for $C_8H_5BF_3SK$: 240; found: 201 (M-K).

3-Benzo[b]thiophene boronic acid (3-BTBA, 2).[62]

Compound **11** (163 mg, 0.68 mmol) and lithium hydroxide were dissolved in acetonitrile (5 mL) and water (1 mL). The solution was stirred at room temperature for 36 hr and then acidified with conc. hydrochloric acid. Then solvent was removed *in vacuo* to give a residue, which was dissolved in ethyl acetate (30 mL) and washed with 5% $NaHCO_3$ (2 × 20 mL). The organic layer was dried over Na_2SO_4. Removal of solvent through filtration and rota-evaporation afforded a white solid compound **2** (107 mg, 90%). ^{1}H NMR (d_6-DMSO, D_2O): δ 8.37 (d, J = 7.6 Hz, 1 H), 8.24 (s, 2H), 8.21 (s, 1H), 7.98 (d, J = 7.2 Hz, 1H), 7.38-7.30, (m,

2H). ^{13}C NMR (d_6-DMSO, D_2O): δ 143.3, 140.7, 137.7, 126.0, 124.3, 124.2, 122.6. ESI-MS: m/z calculated for $C_8H_7BO_2S$:178, found: 177 (M - H).

1-Bromo-4-(2,2-dimethoxy-ethylsulfanyl)-benzene (13a).

3-Bromobenzothiol **12a** (500 mg, 2.6 mmol) was dissolved in 20 mL fresh distilled THF; sodium hydride (140 mg, 3.4 mmol, in 60% mineral oil) was added in the flask. The mixture was stirred for 10 min. at rt and then bromoacetaldehyde dimethylacetal (41 mL, 3.4 mmol) was injected into the flask. Next, the reaction mixture was refluxed for 24 hr. After solvent evaporation, the residue was dissolved in ethyl acetate (50 mL), washed with a saturated solution of $NaHCO_3$ (3 × 30 mL), and dried over Na_2SO_4. After filtration and evaporation of the solvent, the crude product was purified by column chromatography with 10 g of silica gel eluting with hexanes/DCM (5:1) to give a pale green oil, compound **13a** (680 mg, 95%). ^{1}H NMR ($CDCl_3$): δ 7.41-7.38 (m, 2H), 7.26-7.23 (m, 2H), 4.50 (t, J = 5.6 Hz, 1H), 3.36 (s, 6H), 3.09 (d, J = 5.6 Hz, 2H). ^{13}C NMR ($CDCl_3$): δ 135.4, 131.9, 131.0, 120.1, 103.1, 53.6, 36.5. GC-MS: m/z calculated for $C_{10}H_{13}BrO_2S$: 276, found: 276 (M).

5-Bromobenzo[b]thiophene (14a).

Polyphosphoric acid (500 mg) and cholorobenzene (15 mL) mixture was refluxed for 3 hours and then compound **13a** in 3 mL of cholorobenzene (240 mg, 0. 8 mmol) was injected into the flask. The reaction mixture was refluxed for an additional 24 hr while silicon oil temperature at was maintained at 180 ^{o}C . Cholorobenzene was then evaporated *in vacuo* and the resulting residue dissolved in DCM (50 mL). The solution was washed with $NaHCO_3$ solution (3 × 30 mL) and dried over Na_2SO_4. After filtration and evaporation of the solvent, the crude product was purified by column chromatography with 10 g of silica gel eluting with hexanes to give a pale yellow oil (180 mg, 82%). ^{1}H NMR ($CDCl_3$): δ 7.91 (d, J = 2.0 Hz, 1H), 7.68 (d, J = 9.0

Hz, 1 H), 7.42 (d, J = 5.6 Hz, 1H), 7.39 (dd, J_1 = 2.0 Hz, J_2 = 9.0 Hz, 1H), 7.21 (dd, J_1 = 0.4 Hz, J_2 = 5.6 Hz, 1H); ^{13}C NMR ($CDCl_3$): δ 141.1, 138.2, 128.0, 127.1, 126.1, 123.6, 123.0, 118.1; GC-MS: m/z calculated for C_8H_4BrS: 212, found: 212 (M).

2-Benzo[b]thiophen-5-yl-4,4,5,5-tetramethyl-[1,3,2]dioxaborolane (15a).

Compound **15a** was synthesized from compound **14a** by following similar procedures used for the synthesis of **10**. The crude product was purified by silica gel column chromatography eluting with hexanes/ethyl acetate (2:1) to give compound **15a** as a colorless solid (60%). ^{1}H NMR ($CDCl_3$): δ 8.31 (s, 1 H), 7.89 (d, J = 8.0 Hz, 1H), 7.74 (d, J = 8.0 Hz, 1H), 7.41 (d, J = 5.6 Hz, 1H), 7.35 (d, J = 5.6 Hz, 1H), 1.37 (s, 12H); ^{13}C NMR ($CDCl_3$): δ 142.7, 139.1, 130.7, 129.7, 126.0, 124.1, 121.8, 83.8, 24.9; GC-MS: m/z calculated for $C_{14}H_{17}BO_2S$: 260, found: 260 (M).

Potassium 5-benzo[b]thiophene trifluoroborate (16a).

Compound **16a** was synthesized from compound **15a** by following the same procedure as for the synthesis of **11**. The crude product was purified by crystallization with minimum amount of acetone and 10 mL of ether to give compound **16a** as a white solid (70%). ^{1}H NMR (d_6-acetone): δ 7.98 (s, 1H), 7.69 (d, J = 7.6 Hz, 1H), 7.56 (d, J = 8.0 Hz, 1H), 7.40 (d, J = 5.6 Hz, 1H), 7.28 (d, J = 5.6 Hz, 1H); ^{13}C NMR (d_6-acetone): δ 139.0, 137.0, 129.0, 126.4, 124.1, 123.6, 119.8; ESI-MS: m/z calculated for $C_8H_5BF_3SK$: 240; found: 201 (M - K).

5-Benzo[b]thiophene boronic acid (5-BTBA, 3).

Compound **3** was synthesized from hydrolysis of **16a** by following the same procedures used for the synthesis of **2**, to give **3** as a white solid (66%). ^{1}H NMR (d_6-DMSO): δ 8.31 (s, 1H), 8.09 (s, 2H), 7.95 (d, J = 8.4 Hz, 1H), 7.76 (d, J = 8.2 Hz, 1H), 7.72 (d, J = 5.6 Hz, 1H), 7.46

(d, J = 5.4 Hz, 1H); ^{13}C NMR (d_6-DMSO): δ 141.3, 139.0, 130.3, 130.0, 127.1, 124.6, 121.9; ESI-MS: m/z calculated for $C_8H_7BO_2S$: 178; found: 177 (M - H).

1-Bromo-2-(2,2-dimethoxy-ethylsulfanyl)-benzene (13b).

Compound **13b** was synthesized from 2-bromobenzothiol by following the procedure used for the synthesis of **13a**, and the crude product was purified by column chromatography with silica gel eluting with hexanes to give **13b** as pale yellow oil (95%). ^{1}H NMR ($CDCl_3$): δ 7.53 (dd, J_1 = 1.2 Hz, J_2 = 8.0 Hz, 1H), 7.33 (dd, J_1 = 1.6 Hz, J_2 = 7.6 Hz, 1H), 7.32 (dt, J_1 = 1.2 Hz, J_2 = 7.2 Hz, 1H), 7.03 (dt, J_1 = 1.6 Hz, J_2 = 7.6 Hz, 1H), 4.58 (t, J = 5.6 Hz, 1H), 3.37 (s, 6H), 3.13 (d, J = 5.6 Hz, 2H);),^{13}C NMR ($CDCl_3$): δ 137.5, 133.0, 129.1, 127.7, 127.0, 124.2, 103.1, 53.6, 36.0; GC-MS: m/z calculated for $C_{10}H_{13}BrO_2S$: 276, found: 276 (M).

7-Bromobenzo[b]thiophene (14b).

Compound **14b** was synthesized from **13b** by following the same procedure used for the synthesis of **14a**, and the crude product purified by column chromatography with silica gel eluting with hexanes to give **14b** as a colorless oil (85%). ^{1}H NMR ($CDCl_3$): δ 7.73 (dd, J_1 = 0.8 Hz, J_2 = 8.0 Hz, 1H), 7.47-7.45 (m, 2H), 7.39 (d, J = 5.6 Hz, 1H), 7.21 (t, J = 8.0 Hz, 1H); ^{13}C NMR ($CDCl_3$): δ 141.5, 140.5, 127.2, 127.0, 125.4, 124.7, 122.5, 115.8; GC-MS: m/z calculated for C_8H_4BrS: 212; found: 212 (M).

2-Benzo[b]thiophen-7-yl-4,4,5,5-tetramethyl-[1,3,2]dioxaborolane (15b).

Compound **15b** was synthesized via palladium catalyzed coupling with **14b** by following the same procedure used for the synthesis of **15a**. The crude product was purified by column chromatography eluting with hexanes/ethyl acetate (2:1) to give compound **15b** as a white solid (65%). ^{1}H NMR (400 MHz, $CDCl_3$): δ 7.91 (dd, J_1 = 1.2 Hz, J_2 = 8.0 Hz, 1H), 7.82 (dd, J_1 = 0.8 Hz, J_2 = 6.8 Hz, 1H), 7.46 (d, J = 5.6 Hz, 1H), 7.36 (t, J = 7.6 Hz, 1H), 7.33 (d, J = 5.6 Hz,

1H), 1.42 (s, 12H) ; ^{13}C NMR ($CDCl_3$): δ 145.7, 139.2, 131.8, 127.4, 126.5, 123.5, 123.2, 84.2, 24.9; GC-MS: m/z calculated for $C_{14}H_{17}BO_2S$: 260, found: 260 (M).

Potassium 5-benzo[b]thiophene trifluoroborate (16b).

Compound **16b** was synthesized from compound **15b** by following equivalent reaction procedures to those used for synthesis of **11**. The crude product was purified by crystallization with a minimum amount of acetone and 10 mL of ether, to give compound **16b** as a white solid crystals (60%). ^{1}H NMR (MHz, d_6-acetone): δ 7.59 (dd, J_1 = 0.8 Hz, J_2 = 7.6 Hz, 1H), 7.46 (d, J = 6.8 Hz, 1H), 7.42 (d, J = 5.6 Hz, 1H), 7.25 (d, J = 5.6 Hz, 1H), 7.17 (dt, J_1=0.4 Hz, J_2 = 7.4 Hz, 1H); ^{13}C NMR (d_6- acetone): δ 143.5, 138.2, 127.0, 126.9, 122.8, 122.6, 120.6; ESI-MS: m/z calculated for $C_8H_5BF_3SK$: 240, found: 201 (M - K).

7-Benzo[b]thiophene boronic acid (7-BTBA, 4).

Compound **4** was synthesized by hydrolysis of **16b** following the procedure used for the synthesis of **2** to give **4** as a white solid (61%). ^{1}H NMR (d_6-DMSO, D_2O): δ 8.38 (s, 2H), 7.93 (d, J = 8.0 Hz, 1H), 7.83 (d, J = 6.8 Hz, 1H), 7.71 (d, J = 5.6 Hz, 1H), 7.42-7.35 (m, 2H); ^{13}C NMR (d_6-DMSO, D_2O): δ 145.1, 139.5, 131.2, 128.7, 126.0, 123.8, 123.6; ESI-MS: m/z calculated for $C_8H_7BO_2S$: 178, found: 177 (M-H).

1-Bromo-3-(2,2-dimethoxy-ethylsulfanyl)-benzene (13c).

Compound **13c** was synthesized from 3-bromobenzothiol by following the same procedure used for the synthesis of **13a**, and the crude product was purified by column chromatography with silica gel eluting with hexanes/DCM (5:1) to give **13c** as pale yellow oil (97%). ^{1}H NMR ($CDCl_3$): δ 7.52 (m, 1H), 7.33-7.29 (m, 2H), 7.17-7.13 (m, 1H), 4.55 (t, J = 5.6 Hz, 1H), 3.39 (s, 6H), 3.13 (d, J = 5.6 Hz, 2H); ^{13}C NMR ($CDCl_3$): δ138.7, 131.4, 130.1, 129.1, 127.5, 122.7, 103.0, 53.6, 36.2; GC-MS: m/z calculated for $C_{10}H_{13}BrO_2S$: 276, found: 276 (M).

4-Bromo benzo[b]thiophene and 6-bromo benzo[b]thiophene (14c,d).[63]

Aromatic cyclization of **13c** was accomplished by following the same procedure used for the synthesis of **14a**. After purification by column chromatography with silica gel eluting with hexanes/DCM (5:1) a mixture of 4-bromo benzo[b]thiophene and 6-bromo benzo[b]thiophene was obtained as yellow oil (96%). ^{1}H NMR ($CDCl_3$): δ 7.96 (m, 1H), 7.74 (d, J = 8.4 Hz, 1H), 7.59 (d, J =8.4 Hz, 1H), 7.49 (dd, J_1 = 0.8 Hz, J_2 = 7.8 Hz, 1H), 7.44-7.40 (m, 3H), 7.34 (d, J = 5.6 Hz, 1H), 7.22 (dd, J_1= 0.4, J_2 = 5.6 Hz, 1H), 7.12 (t, J = 5.6 Hz, 1H); ^{13}C NMR ($CDCl_3$): δ 141.3, 140.5, 139.5, 138.3, 127.6, 127.5, 127.3, 127.0, 125.2, 125.0, 124.7, 124.3, 123.6, 121.6, 118.2, 117.5; GC-MS: m/z calculated for C_8H_4BrS: 212, found: 212 (M).

2-Benzo[b]thiophen-4-yl-4,4,5,5-tetramethyl-[1,3,2]dioxaborolane (15c) and 2-benzo [b]thiophen-6-yl-4,4,5,5-tetramethyl-[1,3,2]dioxaborolane (15d).

Boronic acid ester mixture (**15c,d)** was synthesized via palladium catalyzed coupling with the 4-bromo benzo[b]thiophene and 6-bromo benzo[b]thiophene mixture by following the same procedure used for the synthesis of **15a**. The crude product was purified by column chromatography eluting with hexanes/ethyl acetate (2:1) to give a mixture of the ester compounds (**15c,d**) as a white solid (47%). ^{1}H NMR ($CDCl_3$): δ 8.40 (s, 1H), 8.05-7.787 (m, 5H), 7.50 (t, J = 5.6 Hz, 2H), 7.35 (t, J = 8.8 Hz, 2H), 1.45 (s, 12H), 1.40 (s, 12H); ^{13C} NMR ($CDCl_3$): δ 144.1, 141.8, 139.6, 139.3, 132.4, 129.8, 129.6, 128.2, 126.5, 125.9, 125.4, 123.9, 123.4, 123.0, 83.9, 83.8, 25.0, 24.9; GC-MS: m/z calculated for $C_{14}H_{17}BO_2S$: 260; found: 260 (M).

4- and 6-Benzo[b]thiophene boronic acid mixture (4-BTBA, 5; 6-BTBA, 6).

Boronic acid mixture (**5**, **6**) was synthesized from the mixture of **15c,d** following the same procedures used for the synthesis of **11**. The crude product was purified with crystallization

with a minimum amount of acetone and 10 mL of ether to give the potassium trifluoroborate mixture as a white solid. Hydrolysis of the salt following the same procedure used for the synthesis of **2** gave **5** and **6** as a white solid (61%). Proton NMR and carbon NMR is given for the mixture. 4-BTBA: ^{1}H NMR (d_6-DMSO, D_2O): δ 8.50 (s, 2H), 7.92 (d, *J*= 8.0 Hz, 1H), 7.78 (d, *J* = 6.8 Hz, 1H), 7.73 (d, *J* = 5.2 Hz, 1H), 7.39 (d, *J* = 5.6 Hz, 1H), 7.35 (t, *J* = 7.6 Hz, 1H); 6-BTBA: ^{1}H NMR (d_6-DMSO, D_2O): δ 8.28 (s, 1H), 8.24 (s, 2H), 7.92 (d, *J* = 8.4 Hz, 1H), 7.73 (d, *J* = 8.0 Hz, 1H), 7.65 (d, *J* = 5.2 Hz, 1H), 7.44 (d, *J* = 5.2 Hz, 1H).^{13}C NMR (DMSO, d_6, D_2O): δ 145.0, 141.5, 139.5, 139.4, 131.2, 130.2, 129.9, 128.5, 127.2, 126.1, 124.7, 123.9, 123.6, 122.0; ESI-MS: m/z calculated for $C_8H_7BO_2S$: 178, found: 177 (M-H).

References

1. Feizi, T. Demonstration by Monoclonal Antibodies that Carbohydrate Structures of Glycoproteins and Glycolipids Are Oncodevelopmental Antigens. *Nature* **1985,** 314, 53-57.

2. Brodesser, S.; Sawatzki, P.; Kolter, T. Bioorganic Chemistry of Ceramide. *Euro. J. Org. Chem.* **2003,** 11, 2021-2034.

3. Gabius, H.-J.; Gabius, S. *Lectins and Cancer*. Springer-Verlag: New York, 1991.

4. Clark, G. F.; Oehninger, S.; Patankar, M. S.; Koistinen, R.; Dell, A.; Morris, H. R.; Koistinen, H.; Seppala, M. A Role for Glycoconjugates in Human Development: The Human Feto-Embryonic Defence System Hypothesis. *Human Reprod.* **1996,** 11, 467-473.

5. Danguy, A.; Camby, I.; Kiss, R. Galectins and Cancer. *Biochem. Biophys. Acta-Gen. Subj.* **2002,** 1572, 285-293.

6. Liedtke, S.; Geyer, H.; Wuhrer, M.; Geyer, R.; Frank, G.; Gerardy-Schahn, R.; Zahringer, U.; Schachner, M. Characterization of N-Glycans from Mouse Brain Neural Cell Adhesion Molecule. *Glycobiol.* **2001,** 11, 373-384.

7. Takeuchi, K.; Kohn, T. J.; Sall, D. J.; Denney, M. L.; McCowan, J. R.; Smith, G. F.; Gifford-Moore, D. S. Dibasic benzo[b]thiophene derivatives as a novel class of active site directed thrombin inhibitors: 4. SAR studies on the conformationally restricted C3-side chain of hydroxybenzo[b]thiophenes. *Bioorganic & Medicinal Chemistry Letters* **1999,** 9, 759-764.

8. Nagase, T.; Sanai, Y.; Nakamura, S.; Asato, H.; Harii, K.; Osumi, N. Roles of HNK-1 Carbohydrate Epitope and its Synthetic Glucuronyltransferase Genes on Migration of Rat Neural Crest Cells. *J. Anat.* **2003,** 203, 77-88.

9. Ley, K. The Role of Selectins in Inflammation and Disease. *Trends Mol. Med.* **2003,** 9, 263-268.

10. Takeuchi, M.; Kijima, H.; Hamachi, I.; Shinkai, S. A Novel Sugar Sensing System Designed with a Cooperative Action of a Boronic-Acid-Appended Zinc Porphyrin and a 3-Pyridylboronic Acid Axial Ligand. *Bull. Chem. Soc. Jpn.* **1997,** 70, 699-705.

11. Almkvist, J.; Karlsson, A. Galectins as Inflammatory Mediators. *Glycoconjug. J.* **2004,** 19, 575–581.

12. Yan, J.; Fang, H.; Wang, B. Boronolectins and Fluorescent Boronolectins-An Examination of the Detailed Chemistry Issues Important for their Design. *Med. Res. Rev.* **2005,** 25, 490-520.

13. Lorand, J. P.; Edwards, J. O. Polyol Complexes and Structure of the Benzeneboronate Ion. *J. Org. Chem.* **1959,** 24, 769-774.

14. Springsteen, G.; Deeter, S.; Gao, X.; Wang, B. The Optiml pH for Boronic Acid-Diol Binding. *Tetrahedron* **2002,** manuscript in preparation.

15. Davis, C. J.; Lewis, P. T.; McCarroll, M. E.; Read, M. W.; Cueto, R.; Strongin, R. M. Simple and Rapid Visual Sensing of Saccharides. *Org. Lett.* **1999,** 1, 331-334.

16. Yoon, J.; Czarnik, A. W. Fluorescent Chemosensors of Carbohydrates. A Means of Chemically Communicating the Binding of Polyols in Water Based on Chelation-Enhanced Quenching. *J. Am. Chem. Soc.* **1992,** 114, 5874-5875.

17. James, T. D.; Sandanayake, K. R. A. S.; Iguchi, R.; Shinkai, S. Novel Saccharide-Photoinduced Electron Transfer Sensors Based on the Interaction of Boronic Acid and Amine. *J. Am. Chem. Soc.* **1995,** 117, 8982-8987.

18. Cao, H.; Diaz, D. I.; DiCesare, D.; Lakowicz, J. R.; Heagy, M. D. Monoboronic Acid Sensor That Displays Anomalous Fluorescence Sensitivity to Glucose. *Org. Lett.* **2002,** 4, 1503 -1505.

19. Cao, H. S.; Heagy, M. D. Fluorescent Chemosensors for Carbohydrates: A Decade's worth of Bright Spies for Saccharides in Review. *J. Fluor.* **2004,** 14, 569-584.

20. Cao, H.; McGill, T.; Heagy, M. D. Substituent Effects on Monoboronic Acid Sensors for Saccharides Based on N-Phenyl-1,8-Naphthalenedicarboximides. *J. Org. Chem.* **2004,** 69, 2959-2966.

21. DiCesare, N.; Lakowicz, J. R. Wavelength-ratiometric Probes for Saccharides Based on Donor-acceptor Diphenylpolyenes. *J. Photochem. Photobiol. A-Chem.* **2001,** 143, 39-47.

22. Yang, W.; Springsteen, G.; Yan, J.; Deeter, S.; Wang, B. A Novel Type of Fluorescent Boronic Acid that Shows Large Fluorescence Intensity Changes upon Binding with a Diol in Aqueous Solution at Physiological pH. *Bioorg. Med. Chem. Lett.* **2003,** 13, 1019 - 1022.

23. Gao, X.; Zhang, Y.; Wang, B. New Boronic Acid Fluorescent Reporter Compounds II. A Naphthalene-based Sensor Functional at Physiological pH. *Org. Lett.* **2003,** 5, 4615-4618.

24. Yang, W.; Lin, L.; Wang, B. A New Type of Water-Soluble Fluorescent Boronic Acid Suitable for Construction of Polyboronic Acids for Carbohydrate Recognition. *Heterocycl. Commun.* **2004,** 10, 383-388.

25. Gao, X.; Zhang, Y.; Wang, B. A Highly Fluorescent Water-soluble Naphthalene-based Boronic Acid Reporter for Saccharide Sensing that also Shows Ratiometric UV Changes. *Tetrahedron* **2005,** 61, 9111-9117.

26. Wang, J.; Jin, S.; Wang, B. A New Boronic Acid Fluorescent Reporter that Changes Emission Intensity at Three Wavelengths upon Sugar Binding. *Tetrahedron Lett.* **2005,** 46, 7003-7006.

27. Yang, W.; Lin, L.; Wang, B. A Novel Type of Fluorescent Boronic Acid for Carbohydrate Recognition. *Tetrahedron Lett.* **2005,** 46, 7981-7984.

28. Zhang, Y.; Gao, X.; Hardcastle, K.; Wang, B. Water-soluble Fluorescent Boronic Acid Compounds for Saccharide Sensing: Structural Effect on Their Fluorescence Properties. *Chem.-Eur. J.* **2006,** 12, 1377-1384.

29. Wang, J.; Lin, N.; Jin, S.; Wang, B. Indolylboronic acids Fluorescent Reporters for Sugar Sensing and Recognition. *Chem. Biol. Drug Design* **2006,** 67, 137-144.

30. Yang, W.; Gao, X.; Wang, B. Boronic Acid Compounds as Potential Pharmaceutical Agents. *Med. Res. Rev.* **2003,** 23, 346-368.

31. Zhong, Z.; Anslyn, E. V. A Colorimetric Sensing Ensemble for Heparin. *J. Am. Chem. Soc.* **2002,** 124, 9014 -9015.

32. James, T. D.; Sandanayake, K. R. A. S.; Shinkai, S. A Glucose-selective Molecular Fluorescent Sensor. *Angew. Chem. Int. Ed. Engl.* **1994,** 33, 2207-2209.

33. James, T. D.; Linnane, P.; Shinkai, S. Fluorescent Saccharide Receptors: A Sweet Solution to the Design, Assembly and Evaluation of Boronic Acid Derived PET Sensors. *Chem. Commun.* **1996**, 281-288.

34. Kabilan, S.; Marshall, A. J.; Sartain, F. K.; Lee, M. C.; Hussain, A.; Yang, X.; Blyth, J.; Karangu, N.; James, K.; Zeng, J.; Smith, D.; Domschke, A.; Lowea, C. R. Holographic Glucose Sensors. *Biosen. Bioelectron.* **2005,** 20, 1602–1610.

35. Zhao, J.; James, T. D. Enhanced Fluorescence and Chiral Discrimination for Tartaric Acid in a Dual Fluorophore Boronic Acid Receptor. *Chem. Commun.* **2005,** 14, 1889 - 1891.

36. Alexeev, V. L.; Sharma, A. C.; Goponenko, A. V.; Das, S.; Lednev, I. K.; Wilcox, C. S.; Finegold, D. N.; Asher, S. A. High Ionic Strength Glucose-Sensing Photonic Crystal. *Anal. Chem.* **2003,** 75, 2316 -2323.

37. Asher, S. A.; Alexeev, V. L.; Goponenko, A. V.; Sharma, A. C.; Lednev, I. K.; Wilcox, C. S.; Finegold, D. N. Photonic Crystal Carbohydrate Sensors: Low Ionic Strength Sugar Sensing. *J. Am. Chem. Soc.* **2003,** 125, 3322 -3329.

38. Jiang, S.; Rusin, O.; Escobedo, J. O.; Kim, K. K.; Yang, Y.; Fakode, S.; Warner, I. M.; Strongin, R. M. Stereochemical and Regiochemical Trends in the Selective Spectrophotometric Detection of Saccharides *J. Am. Chem. Soc.* **2006,** 12221-12228.

39. Samoie, G.; Wang, W.; Xu, X.; Escobedo, J. O.; Schneider, H.-J.; Strongin, R. M. A Chemomechanical Polymer that Functions in Blood Plasma with High Glucose Selectivity *Angew. Chem., Int. Ed. Engl.* **2006,** In press

40. Karnati, V.; Gao, X.; Gao, S.; Yang, W.; Sabapathy, S.; Ni, W.; Wang, B. A Selective Fluorescent Sensor for Glucose. *Bioorg. Med. Chem. Lett.* **2002,** 12, 3373-3377.

41. Kaur, G.; Fang, H.; Gao, X.; Li, H.; Wang, B. Diboronic Glucose Sensors. *Tetrahedron* **2006,** 62, 2583-2589.

42. Kaur, G.; Lin, N.; Fang, H.; Wang, B. Boronic Acid-based Glucose Sensors. In *Glucose Sensing*, Geddes, C. D.; Lakowicz, J. R., Eds. Springer Press: 2006; Vol. 11, pp 377-397.

43. Yang, W.; Gao, S.; Gao, X.; Karnati, V. R.; Ni, W.; Wang, B.; Hooks, W. B.; Carson, J.; Weston, B. Diboronic Acids as Fluorescent Probes for Cells Expressing Sialyl Lewis X. *Bioorg. Med. Chem. Lett* **2002,** 12, 2175-2177.

44. Yang, W.; Fan, H.; Gao, S.; Gao, X.; Ni, W.; Karnati, V.; Hooks, W. B.; Carson, J.; Weston, B.; Wang, B. The First Fluorescent Diboronic Acid Sensor Specific for Hepatocellular Carcinoma Cells Expressing Sialyl Lewis X. *Chem. Biol.* **2004,** 11, 439-448.

45. Burnett, T. J.; Peebles, H. C.; Hageman, J. H. Synthesis of a Fluorescent Boronic Acid which Reversibly Binds to Cell Walls and a Diboronic Acid which Agglutinates Erythrocytes. *Biochem. Biophy. Res. Comm.* **1980,** 96, 157-162.

46. Hageman, J. H.; Kuehn, G. D. Boronic Acid Matrices for the Affinity Chromatography of Glycoproteins and Enzymes. *Met. Mol. Biol.* **1992,** 11, 45-71.

47. Soundaramani, S.; Badawi, M.; Montaño-Kohlrust, C.; Hageman, J. H. Boronic Acids for Affinity Chromatography: Spectral Methods for Determination of Ionization and Diol-binding Constants. *Anal. Biochem.* **1989,** 178, 125-134.

48. Paugam, M.-F.; Bien, J. T.; Smith, B. D.; Chrisstoffels, L. A. J.; de Jong, F.; Reinhoudt, D. N. Facilitated Catecholamine Transport through Bulk and Polymer-Supported Liquid Membrane. *J. Am. Chem. Soc.* **1996,** 118, 9820-9825.

49. Westmark, P. R.; Gardiner, S. J.; Smith, B. Selective Monosaccharide Transport through Lipid Bilayers Using Boronic Acid Carriers. *J. Am. Chem. Soc.* **1996,** 118, 11093-11100.

50. Westmark, P. R.; Gardiner, S. J.; Smith, B. D. Selective Monosaccharide Transport through Lipid bilayers using Boronic Acid Carriers. *J. Am. Chem. Soc.* **1996,** 118, 11093-11100.

51. Draffin, S. P.; Duggan, P. J.; Duggan, S. A. M. Highly Fructose Selective Transport Promoted by Boronic Acids Based on a Pentaerythritol Core. *Org. Lett.* **2001,** 3, 917-920.

52. Gardiner, S. J.; Smith, B. D.; Duggan, P. J.; Karpa, M. J.; Griffin, G. J. Selective Fructose Transport Through Supported Liquid Membranes Containing Diboronic Acid or Conjugated Monoboronic Acid- Quaternary Ammonium Carriers. *Tetrahedron* **1999,** 55, 2857-2864.

53. Ogawa, S.; Kikuta, K.; Muraoka, H.; Saito, F.; Sato, R. Synthesis, Structure, and Both Cathodic and Anodic Reversible Redox Reactions of Benzochalcogenophenes Containing Ferrocene Units. *Tetrahedron Letters* **2006,** 47, 2887-2891.

54. Ishiyama, T.; Miyaura, N. Synthesis of Arylboronates via Palladium-Catalyzed Cross-Coupling Reactions of Alkoxydiboron with Aryl Halides or Triflates. In *Advances in Boron Chemistry*, Siebert, W., Ed. The Royal Society of Chemistry: Cambridge, 1997; pp 92-95.

55. Ishiyama, T.; Miyaura, N. Chemistry of Group 13 Element-transition Metal Linkage-the Platinum and Palladium-catalyzed Reactions of (Alkoxo)diborons. *J. Organomet. Chem.* **2000,** 611, 392-402.

56. Ishiyama, T.; Itoh, Y.; Kitano, T.; Miyaura, N. Synthesis of Arylboronates via the Palladium(0)-catalyzed Cross-coupling Reaction of Tetra(alkoxo)Diborons with Aryltriflates. *Tetrahedron. Lett.* **1997,** 38, 3447-3450.

57. Yuena, A. K. L.; Huttona, C. A. Deprotection of Pinacolyl Boronate Esters via Hydrolysis of Intermediate Potassium Trifluoroborates. *Tetrahedron Letters* **2005,** 46, 7899-7903.

58. Ple, P. A.; Marnett, L. J. Synthesis of Substituted Benzo[b]thiophenes by Acid-Catalyzed Cyclization of Thiophenylacetals and Ketones. *J. Heterocyclic Chem.* **1988,** 25.

59. Springsteen, G.; Wang, B. A Detailed Examination of Boronic Acid-Diol Complexation. *Tetrahedron* **2002,** 58, 5291-5300.

60. Yan, J.; Springsteen, G.; Deeter, S.; Wang, B. The Relationship among pKa, pH, and Binding Constants in the Interactions between Boronic Acids and Diols-It is not as Simple as It Appears. *Tetrahedron* **2004,** 60, 11205-11209.

61. Heynderickx, A.; Samat, A.; Guglielmetti, R. A One-Pot Synthesis of Hindered 2,3-diarylbenzo[b]thiophenes via Suzuki Reaction. *Synthesis* **2002,** 2, 213-216.

62. Thompson, W. J.; Jones, J. H.; Lyle, P. A.; Thies, J. E. An Efficient Synthesis of Arylpyrazines and Bipyridines. *J. Org. Chem.* **1988,** 53, 2052-2055.

63. Titus, R. L.; Choi, M.; Hutt, M. P. Benzo[b]thiophene Derivatives. II 4- and 6-Substituted Benzo[b]thiophenes. *J. Heterocyclic Chem.* **1967,** 4, 651-652.

SECTION II

DNA-MINOR GROOVE BINDERS AS ANTIPARASITIC AGENTS

3. Parasitical Diseases

The classical Greek word “parasite” was described as “a guest who comes to dinner and doesn't leave.” However, today’s biology uses the term to describe eukaryotic organisms, which range from a single cell protozoa to complex multicellular worms, which grow and multiply in host organelles. The diseases caused by these organisms represent some of the world's greatest health problems.

3.1. Human African Trypanosomiasis (HAT, Sleeping Sickness)

Human African Trypanosomiasis (HAT), or sleeping sickness, is one of the most deadly diseases in sub-Saharan Africa. The most common form of human African trypanosomiasis is caused by the vector borne parasite, *Trypanosoma brucei.* The parasite is transmitted by tsetse fly (*Glossina* Genus) bites. Devastating epidemics of *Trypanosoma brucei* have occurred in large areas of Central Africa, especially the Southern Sudan, Congo-Zaire, Angola, Uganda and the Central African Republic.[1] According to the World Health Organization, the annual incidence of the disease is approximately 300,000 cases, with 500,000 people already carrying trypanosomes and the majority of these cases will die if left untreated. In addition, the large habitat area of the tsetse fly threatens 60 million people over approximately ten million square kilometers in sub Saharan Africa.[2, 3]

Trypanosomiasis sickness in humans is caused by two different subspecies of *Trypanosoma brucei*: *Trypanosoma brucei rhodensiense* (***T.b.r.***) *in* Eastern Africa and *Trypanosoma brucei gambiense* (***T.b.g.***) *in* Western Africa. Both forms of the parasite affect the central nervous system.

Trypanosoma brucei rhodesiense causes an acute infection within a few weeks after infection with the parasite. The disease develops rapidly and invades the central nervous system.

Trypanosoma brucei gambiense also causes an acute infection. However, the first symptoms may become apparent only months or even years after the initial infection. Because of the slow developing symptoms, the disease is often not diagnosed until the disease is in an advanced state.

Infections occur during a blood meal by the tsetse fly when the parasite is transmitted to the mammalian host. However, the parasite does not keep the same kinetoplastic form after leaving the insect. Different morphological forms are associated with different life cycle stages in the various species. The different life forms of the parasite are distinguished by the position of the kinetoplastid in relation to the nucleus and the presence or absence of an undulating membrane. Four major morphological forms are found in kinetoplastids that cause sleeping sickness. First, the tsetse fly injects metacyclic trypomastigotes into mammalian skin tissue. The parasites enter the lymphatic system through the skin and travel to different organs via the blood stream. In the bloodstream of the host, the parasite transforms into trypomastigotes and continues the replication by binary fission. The tsetse fly becomes infected with trypomastigotes when taking blood from an infected mammalian host. The parasites transform into procyclic trypomastigotes in the fly's midgut and multiply by binary fission. The new form then leaves the midgut and transforms into epimastigotes in the fly's salivary glands and again multiply by binary fission. The next cycle starts again with an infected fly bite. [4]

The symptoms of trypanosomiasis vary between subspecies of the invading parasite. During the trypomastigotes' incubation period, the infection is characterized by irregular episodes of fever and headache. In the case of ***T.b.g.***, the number of parasites in the blood tends to be very low

and often the infected person shows no symptoms. However, the patients infected with ***T.b.r.*** show much higher parasitemias and a more pronounced fever.

Trypanosomes that cross the blood-brain barrier result in a generalized meningoencephalitis which causes central nervous system (CNS) damage and shows worsening symptoms including apathy, fatigue, confusion, somnolence, and motor changes (such as tics, slurred speech, and lack of coordination). Neurological manifestations can occur within weeks after ***T.b.r.*** infections. If patients are not treated at the CNS stage of the disease, it will usually progress to convulsions or coma followed by death in both ***T. b.g.*** and ***T.b.r.*** infections.

Advanced identification agents and serological tests are available for diagnosis of the parasite in blood samples, lymph node aspirations, or spinal fluid. The diagnosis follows a 3-step approach: screening, parasitological confirmation and staging. The staging step is essential because the treatment of the first and second stage of the disease are very different.[5] However, these tests are costly and require complicated instrumentation. Therefore, it is a huge problem in rural areas in Africa.

3.1.1. Treatment of Human African Trypanosomiasis

Different medication has been used depending on the type and stage of African trypanosomiasis. Suramin and pentamidine are the recommended drugs during the acute hemolymphatic stage.[6] However, melarsoprol or eflornithine are recommended if the CNS is involved.[7] Nifurtimox, in combination with eflornithine, is used for late stage treatment.[8]

3.1.2. Drugs Used in Hemolymphatic Stage

Suramin

Suramin is a polysulfonated naphthylamine derivative of urea that was synthesized in 1916 and marketed in 1922 as an antiparasitic agent. It is the drug used for early-stage African

trypanosomiasis and onchocerciasis.[9] Suramin is trypanocidal and works by inhibiting parasitic enzymes and growth factors.[10, 11] A number of negative charges on the drug increases the electrostatic interaction and the ligand binds to many enzymes with a high affinity. Suramin is highly bound to serum proteins, therefore the drug can not cross the blood-brain barrier.[12] Suramin is more effective and less toxic than pentamidine.

Pentamidine isethionate

This antiprotozoal diarylamidine agent was first developed in 1941 and is typically used for the early stage of African trypanosomiasis. It is also used for *Pneumocystis carinii* pneumonia and leishmaniasis.[13-17] The mitochondrion appears to be a target for pentamidine in various species including yeast.[18] The dicationic property of pentamidine facilitates electrostatic interaction with cellular polyanions such as circular DNA molecules. Pentamidine has been suggested to inhibit the dihydrofolate reductase enzyme and thereby interfere with parasite aerobic glycolysis.[19] Pentamidine is administered by injection due to poor gastro-intestinal (GI) absorption, and is strongly bound to tissues, including the spleen, liver, and kidney. Pentamidine does not penetrate the blood-brain barrier effectively and, therefore, it is not used to treat CNS infection.[20, 21]

3.1.3. Drugs Used in the Neurological Stage

Melarsoprol

This trivalent arsenical compound was synthesized in 1949 and is used in the late stage of African trypanosomiasis, despite its extremely toxic side effects.[22, 23] Melarsoprol kills trypanosomes rapidly by inhibiting parasitic glycolysis which causes ATP loss.[24] The drug is administered by direct injection, and can penetrate the blood brain barrier to levels of only around 1–2% of the maximum plasma levels.[25] The therapy often has a 90-95% success rate in

clearing the parasitemia. However, the drug is highly toxic and may cause fatal complications in 5 to 10% of patients.

Eflornithine

α-Difluoromethylornithine was developed in the early 1980s as a cancer treatment. However, the drug was found to be highly effective for treatment of only the West African form (**T.b.g.)** of trypanosomiasis.[26] This drug has been used for treatment of patients in the late stages of the disease. The drug is a selective and irreversible inhibitor of ornithine decarboxylase, which is a critical enzyme for DNA and RNA synthesis.[27, 28] Eflornithine is generally tolerated better and is less toxic than arsenic drugs and it is used for patients who are infected with ***T.b.r.*** and cannot tolerate melarsoprol.

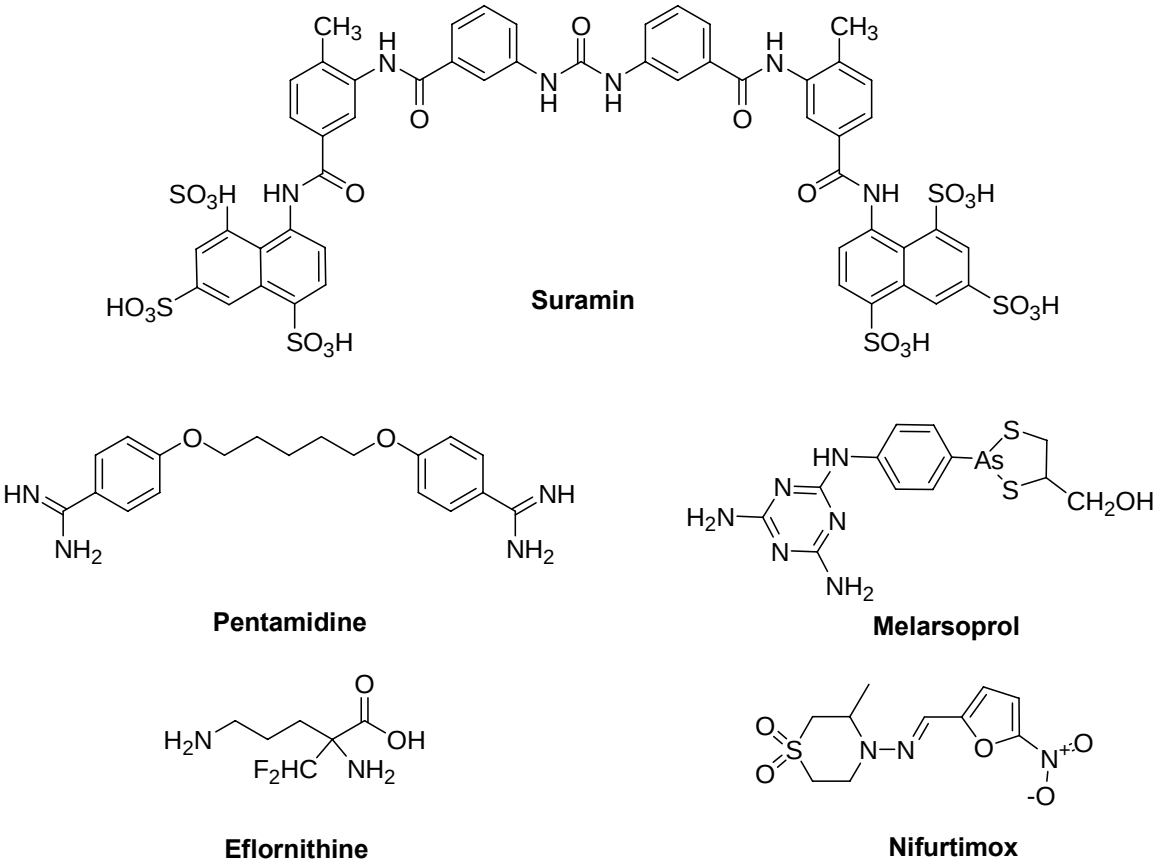

Figure 3.1. Structure of clinically used antitrypanosomal drugs.

3.1.4. Drugs Entered into Clinical Trials

Pafuramidine maleate (DB 289)

The usage of the furamidine (**DB 75)** has been limited due to its toxicity and bioavailability. **DB 75** was chemically modified to form the prodrug pafuramidine maleate (**DB 289)**.[29] The prodrug is metabolized to furamidine after cellular uptake. Studies showed that the prodrug strategy was successful in the terms of reducing toxicity and increasing efficacy. In addition, **DB 289** can be administered orally.[30] **DB 289** successfully cleared parasitical infections in animal models. While the mechanism of action is not fully understood, it is known that **DB 289** is metabolized to **DB 75** which causes mitochondrial damage in the parasite.[31] The compound was removed from trials due to renal toxicity.

Diminazene

Diminazene, a diamidine product also known as **Bernil,** was first registered as a veterinary trypanocide.[32] However, human trials also resulted in promising trypanocidal activity.[33] The drug enters the trypanosomes via the P2 transporter and binds to the DNA.[34-36]

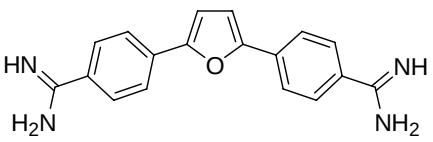

Furamidine, DB 75

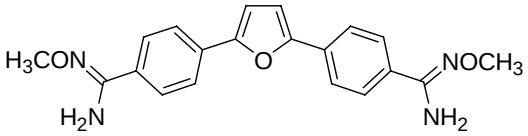

Pafuramidine maleate, DB 289

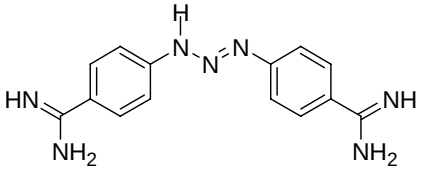

Berenil

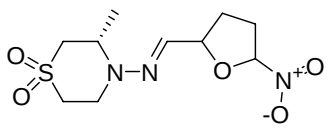

Nifurtimox

Figure 3.2. Drugs entered into clinical trails for treatment of trypanosomoasis.

Nifurtimox

Nifurtimox is a 5-nitrofuran compound that was produced by Bayer and the drug is currently in trials for HAT therapy. It is an alternative treatment agent for cases that are resistant to melarsoprol. Nifurtimox is usually administered in combination with other antiparasitical agents used against *T. brucei gambiense*[37, 38] The suggested mode of action involves the reduction of the nitro group to yield a radical species, which, by unknown mechanisms, ultimately leads to parasite death.[39]

3.1.5. Combination Chemotherapy

Combination chemotherapy is becoming the preferred methodology in today's medicine. Combination drug therapy can lower dosage use when synergy exists. In some cases, this methodology is more effective for treatment in cases of drug resistance. For example, administration of suramin 15 minutes before administration of melarsoprol results in good cure rates in the Stage 2 mouse model. Suramin also altered the volume of distribution and pharmacokinetics of the experimental trypanocide megazol in mice.[40] Recent clinical trials using a combination of eflornithine and nifurtimox have yielded cure rates as high as 98%.[38] These studies also showed that the combinations of melarsoprol and eflornithine, or melarsoprol and nifurtimox were considered too toxic to pursue. However, the nifurtimox–eflornithine combination is currently in trials due to the increasing failure rate of melarsoprol mono therapy.[38]

3.2. Leismaniasis

Leishmaniasis is a parasitic disease transmitted by the bite of the sand fly. According to the WHO report in January 2009, an estimated 12 million people are currently infected and around 2 million new infections occur each year. The disease is prevalent in four continents and is

endemic in 88 countries, ranging from rainforests in Central and South America to deserts in West Asia. Up to 350 million people are at risk in these highly populated areas. The infection occurs in humans from the bite of an infected insect. However, parasites can be transferred among humans via blood transfusions or after sharing a needle from an infected human.[41] There are more than 20 species and subspecies of parasites that cause leismaniasis. Patients with leishmaniasis demonstrate a wide range of clinical symptoms. The disease seen in humans has three different clinical forms; cutaneous, mucocutaneous and visceral.

Cutaneous leishmaniasis is the most common form of the disease.[42] It causes ulcers on the face, arms and legs. Although, the ulcers can heal spontaneously, they can also cause serious disability and leave severe permanent skin damage.

In contrast, visceral leishmaniasis is the most severe form of the disease and attacks the internal organs. If the patient remains untreated, this form of leishmaniasis causes death in about two years.[43]

In mucocutaneous leishmaniasis, the patient develops partial or total destruction of the mucous membranes of the nose, mouth, throat cavities and surrounding tissues.[44] Infections from the parasite occur during a blood meal on the mammalian host. The female phlebotomine sandfly injects the promastigotes during blood transferal from the host. Promastigotes invade host cells that are involved in immunity. The promastigotes transform into amastigotes and multiply by binary fission. In the host, amastigotes spread throughout the body and invade new cells and new tissues, which can cause lesions and tissue destruction. Sand flies become infected by receiving blood from the infected host. Amastigotes transform into promastigotes and develop in the gut of the insect by binary fission while subsequently migrating to the proboscis. Infection is transmitted to the host with another insect bite.[45]

3.2.1. Treatment of Leishmaniasis

The development of the chemotherapeutic agents for leishmaniasis often targets the intracellular amastigote form of the parasite that survives in the host and multiplies in the tissue macrophages.[46] In many cases, patients with leishmaniasis are also co-infected with HIV. Treatment of these patients is often complicated and challenging.

3.2.2. Drugs Used for Treatment of Leishmaniasis

Pentavalent antimonial

In 1937, a pentavalent antimonial complex, sodium stibogluconate, was the first pentavalent antimonial agent reported as active against leishmaniasis. These pentavalent drugs are still in use for chemotherapy against various forms of leishmaniasis, including visceral leishmaniasis.[47] The mechanism of drug action is not fully known. However, it is known that antimony inhibits the parasite's glycotic and fatty acid oxidation activity. Thus, these drugs decrease the antioxidant defense mechanism and decrease energy for metabolism.[48] Antimony treatment induces activation of important components of the intracellular signaling pathway. This action produces an early wave of reactive oxygen species. The reactive species are assumed to cause the parasite toxicity.[47] Antimonials have several disadvantages that limit their usage, including the requirement for up to 28 days of consecutive administration, toxicity, high cost and the development of significant drug resistance. [49]

Pentamidine

Recent interest in the development of antileishmanial drugs has focused on the reduction of parasite drug resistance and lowering the cost. In 1952, pentamidine was shown to be effective against visceral and cutaneous leishmaniasis. Pentamidine is a relatively safe and effective first-line treatment for cutaneous leishmaniasis. Nonetheless, pentamidine was given up as a

second-line treatment for visceral leishmaniasis, due to toxicity. [50] However, in view of promising results in HIV infected leishmania patients, pentamidine might again become an alternative drug for treatment of co-infected patients. Studies indicate that the drug interferes with the mechanism of the synthesis of DNA, RNA, phospholipids and proteins.[51]

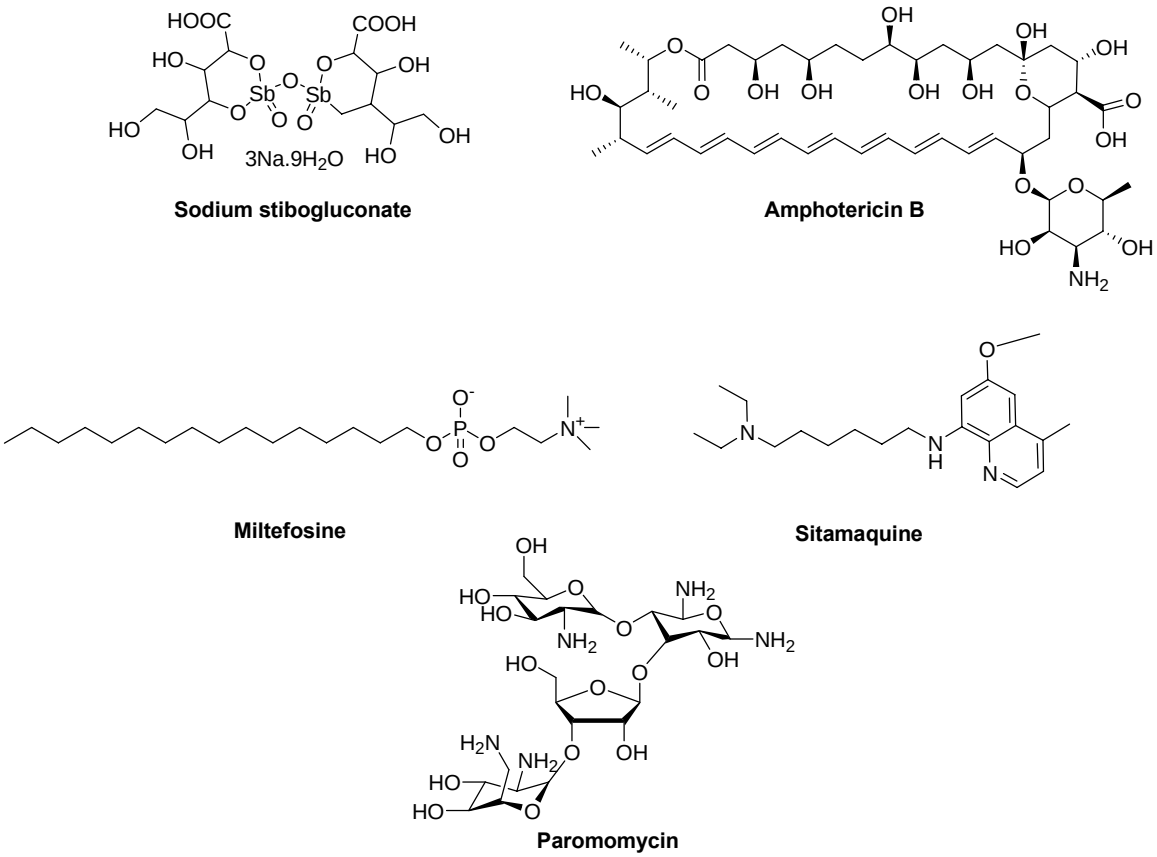

Figure 3.3. Structure of clinically used antileishmanial drugs.

Amphotericin B

Amphotericin B, a polyene antibiotic, has been found to be highly effective for the treatment of antimonial resistant *L. donovani* and for cases of mucocutaneous leishmaniasis that have not responded to antimonials.[52] The drug is given by *i.v.* infusion and has a high toxicity. The drug must be administered by slow infusion over four hours. The high cost of the drug is another

limiting factor for use in developing countries.[53] The Amphotericin B mechanism of action has been suggested to involve binding to the parasite surface membrane, leading to modulation of immune functions.[54]

Miltefosine

Miltefosine is an alkylphosphocholine that was originally developed as an anticancer drug. However, the drug was found to be active against leishmaniasis in the mid-1980s. The drug was registered in India after a Phase III trial. A high cure rate was reported in patients with visceral leishmaniasis by administrating the drug orally for 28 days.[55] The major limitation of miltefosine is teratogenicity and this excludes its use in women of childbearing age. The mode of action of Miltefosine is not fully understood yet. *In vitro* studies found that miltefosine induces apoptosis-like death in the parasite.[55]

Paromomycin

Paromomycin, an aminoglycoside antibiotic, was found to be an effective antileishmanial product in the 1960s and the drug has been in clinical trials for both visceral leishmaniasis and mucocutaneous leishmaniasis.[56] Phase I, II, and III studies in both visceral leishmaniasis and mucocutaneous leishmaniasis were successfully completed.[57, 58] In bacteria, paromomycin inhibits protein synthesis by binding to 30S subunit ribosomes, causing misreading and premature termination of mRNA translation. In leishmania, paromomycin has been found to affect the mitochondrion.[57] With the excellent efficacy, low cost, shorter duration of administration period and good safety profile, the drug has the potential to be a first-line drug.[59]

3.2.3. Drugs Entered into Clinical Trials

Sitamaquine

Sitamaquine is an orally active 8-aminoquinoline analog. The antileishmanial activity of this compound was first identified in the 1970s. Phase III trials for the treatment of visceral leishmaniasis were initiated in March 2002. Phase I and II clinical trials were completed with varying levels of success. Sitamaquine has been found effective for patients also infected with HIV.[60, 61] The drug is rapidly metabolized to form desethyl and 4-CH_2OH derivatives. The metabolized products of the drug are assumed responsible for the activity. In general, toxicity appears to be relatively mild, however, serious side effects such as methemglobinaemia, are noted in some patients.[61]

3.3. Malaria

Malaria is another parasitic, life-threatening, mosquito borne disease. According to the 2008 World Health Organization Malaria report; there are an estimated 247 million malaria cases annually, and 3.3 billion people at risk of infection. Annually, malaria causes nearly a million deaths, the majority of whom are children under 5 years of age. The disease is endemic in 109 countries.[62] Malaria is caused by protozoan parasites of the genus *Plasmodium*. There are more than 100 species of *Plasmodium* known to infect animals and humans. Only five species of the plasmodium parasite infect humans. The most serious form of the disease is caused by *Plasmadium falciparum*. Human malaria is also caused by *Plasmodium vivax*, *Plasmodium ovale*, and *Plasmodium malariae* species, and *Plasmodium knowlesi*. The *Anopheles gambiae* mosquito transmits the malaria causing parasite, *Plasmodium,* to the host during a blood meal. In humans, parasites invade the liver cells where they grow and multiply, and then subsequently invade red blood cells. The parasite grows inside the red blood cells and destroys

them, releasing daughter parasites, merozoites, that continue the cycle by invading other red blood cells. Some parasites differentiate into sexual erythrocytic stages to male microgametocytes and female macrogametocytes in the blood stage. An Anopheles mosquito ingests the gametocytes, male (microgametocytes) and female (macrogametocytes), during a blood meal from an infected person. The parasites multiply in the mosquito which is known as the sporogonic cycle. The microgametes penetrate the macrogametes generating zygotes while in the mosquito's stomach. The zygotes turn into motile and elongated ookinetes and invade the midgut wall of the mosquito where they develop into oocysts. The oocysts grow, rupture, and release sporozoites and move to the mosquito's salivary glands. The sporozoites transfer to the new host with a mosquito bite.[63]

The blood stage parasites are responsible for the clinical symptoms of the disease such as fever, shaking chills, headache and muscle pain. Patients who do not receive medication develop anemia, kidney failure, coma, and respiratory stress.

3.3.1. Treatment of Malaria

Most malaria symptoms are observed during the erythrocytic stage of the infection. Nearly all available drugs are active in the erythrocytic stage of the disease except primaquine, which is active in the hepatic stage of the infection. The therapy for the infected patient varies, depending on the infecting species. The cost of the therapy, drug resistant parasites, and the toxicity of the medication are the still biggest challenges remaining in the fight against the disease.

3.3.2. Drugs Used in Malaria

Chloroquine

A 4-aminoquinoline analog, chloroquine, is commonly used and has been an important drug for the treatment and the prevention of malaria for more than 50 years. This drug accumulates in intraerythrocytic trophozoites and prevents hemoglobin degradation.[64] In addition, chloroquine was found to cause specific inhibition of a novel heme polymerase enzyme. However, the clinical usage of the drug is now limited due to the evolution and spread of chloroquine resistant malaria parasites. Resistance occurs by reducing the accumulation of the drug via an unidentified transmembrane protein pump in the parasite.[65]

Sulfadoxine-pyrimethamine

The sulfadoxine-pyrimethamine combination is an alternative first-line antimalarial treatment for use against chloroquine resistant *Plasmodium falciparum*.[66] It is known that sulphadoxine competitively inhibits dihydrofolic acid synthesis by inhibiting dihydropteroate synthetase.[67] In addition, pyrimethamine is a folic acid antagonist by binding to and reversibly inhibiting dihydrofolate reductase.[68] The sulphadoxine and pyrimethamine combination inhibits the two enzymes that are involved in the biosynthesis of folinic acid in the parasite.

Mefloquine

The oral bioavailability and high efficacy of mefloquine make the drug an attractive alternative treatment for malaria.[69] Mefloquine is active against the erythrocytic stages of the Plasmodium species. However, the drug has no effect against the exoerythrocytic stages of the parasite. The mechanism of the action is not fully understand though it is thought that the drug works by blocking the polymerization of a toxic heme released during hemoglobin proteolysis in the

intraerythrocytic stage of *Plasmodium falciparum*, causing accumulation to a level that kills the parasite.[70]

Atovaquone-proguanil

Atovaquone-proguanil is a fixed-dose combination tablet of two antimalarial agents and is highly effective for the prevention of malaria caused by *Plasmodium falciparum*.[71] Both atovaquone and proguanil are active against the pre-erythrocytic stage of *P. falciparum*, as well as the erythrocytic stage of *P. falciparum*. The combination increases the existing inhibition effect of atovaquone on parasitic mitochondrial electron transport. In addition, the drug has been found to be active against drug resistant strains of *P. falciparum*. Studies show that the efficacy of the atovaquone-proguanil combination is higher than mefloquine, chloroquine or proguanil monotherapy. Atovaquone-proguanil is generally well tolerated by both adults and children. The drug also showed fewer side effects than many other antimalarial agents. [72]

Primaquinine

Primaquine has been used for preventing relapse of *Plasmodium vivax* and *P. ovale* malaria since the early 1950s.[73] It is the only available drug for the treatment of liver stages of *Plasmodium vivax*.[74] Primaquinine can be administered orally and is rapidly absorbed from the GI tract. Its exact mechanism of action is not fully known, although it is believed to cause interference with the function of the plasmodial DNA. The major concern about the drug is that, if administered to glucose-6-phosphatedehydrogenase deficient patients, these patients can develop severe methemoglobinemia.[75]

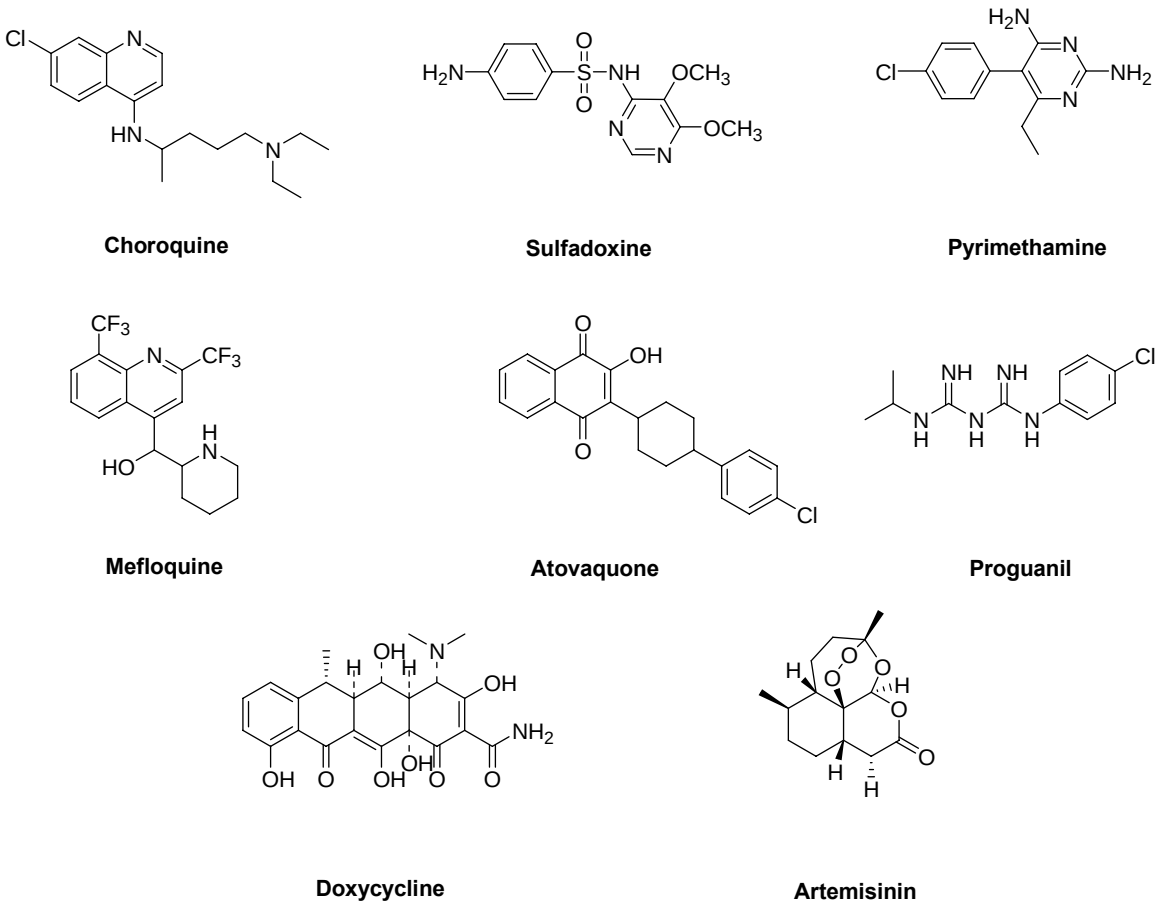

Figure 3.4. Structure of clinically used antimalarial drugs.

Doxycycline

Doxycycline is a tetracycline antibiotic. It has been used against many bacterial infections over the years. Tetracyclines are effective but slow acting antimalarial drugs. The drug is used as a prophylactic agent rather than as a treatment for malaria. The medication is not recommended in pediatric (under 8 years) or pregnant patients. Its mechanism of action remains uncertain. Tetracyclines specifically block expression of the apicoplast genome, resulting in the distribution of nonfunctional apicoplasts into daughter merozoites. The loss of apicoplast function in the progeny of treated parasites leads to a slow but potent antimalarial effect.[76]

Artemisin

Artemisin was isolated from sweet wormwood (*Artemisia annua*) in 1972 by Chinese scientists, and it has a potent activity against *Plasmodium falciparum*.[77] Artemisin is a sesquiterpene lactone and widely used to treat multidrug resistant malaria.[78] Studies showed that the mechanism of action of the drug appears to involve heme mediated decomposition. The endoperoxide bridge can produce carbon-centered highly reactive free radicals. The resulting carbon-centered free radicals may cause alkylation of heme proteins. High doses of artemisinin were found to be neurotoxic. The mechanism of neurotoxicity may be similar to the mechanism of action.[79] Using the drug as a monotherapy is not recommended because parasitic resistance seems to be developing against artemisin. Therefore, the drug is preferred for use in combination therapies for malaria treatment.

4. Genomics Based Drug Design

Current chemotherapies to treat parasitical diseases are expensive and many have undesirable side effects. In addition, many drugs used for parasitic diseases require long treatment times. Because of the side effects and poor bioavailability, the patients need to be under surveillance in an advanced health care system. It can easily be seen that this is impossible for patients who live in developing countries. Under these circumstances, it is urgent to develop new therapeutic agents against parasitical diseases.

4.1. The Code of Life

Deoxyribonucleic acid (**DNA**) exists in a variety of sizes and forms in all known living organisms as well as some viruses. DNA is a double stranded polymer of nucleotides, responsible for storing and monitoring all biological living functions. The polymer contains two purine bases, adenine (**A**), and guanine (**G**), and two pyrimidine bases cytosine (**C**), thymine (**T**). Nucleotides are linked to each other with stable phosphoester bonds. The 5'-phosphate group of one nucleotide is joined to the 3'-hyroxyl group on the sugar to obtain 3', 5'-phosphodiester linkages.[80] Chargaff discovered that the ratio of adenine and thymine (**A/T**) and the ratio of guanine and cytosine (**G/C)** are always equal in any DNA.[81] Watson and Crick analyzed all of the existing DNA findings and subsequently proposed that DNA intertwined to form a helical duplex. As such, strong hydrogen bonding between the base pairs of adenine with thymine and guanine with cytosine holds the two strands together. Purine and pyrimidine bases are stacked along the inside of the helix almost perpendicular to the sugar phosphate backbone which winds in an anti-parallel direction through the helix. The base pairs are stacked with 3.4 Å of space between each other and rotate 36^{o} per base. Therefore, every ten base pairs produce one helical turn. Glycosidic bonds of the sugar rings link the bases in the helix. As

such, the space of the sugar-phosphate backbone results in two different grooves along the helix. The wide and shallow groove is called the major groove, and the narrow, deeper groove is called the minor groove.

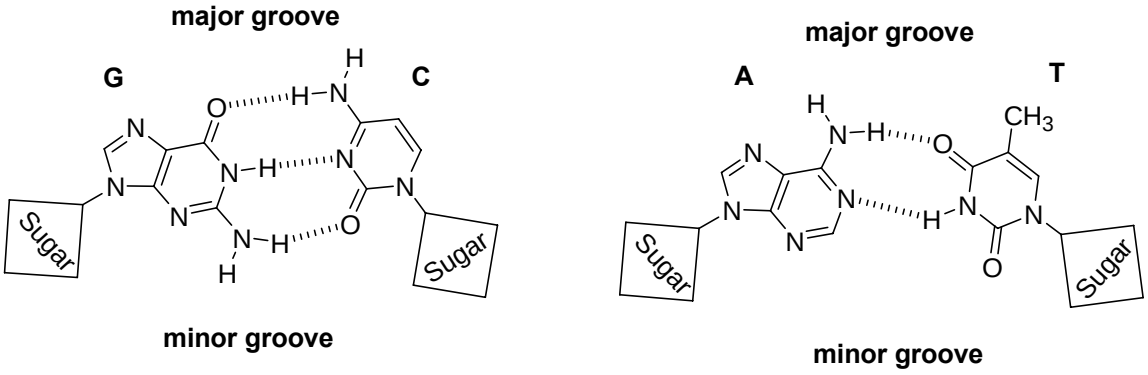

Figure 4.1. Watson and Crick proposed DNA complementary base pairs.

These two grooves twist around the surface of the double helix. The major groove is 22 Å wide, filled with base pair nitrogen and oxygen atoms. The base pairs are positioned inward from the sugar phosphate backbone, facing the center of the double helix. In contrast, the minor groove is 12 Å wide and the base pairs of the minor groove are positioned outward from the sugar phosphate backbone towards the edges of the helix. Therefore, the edges of the bases in the major groove are more accessible than in the minor groove.

Specific proteins such as transcription factors and single stranded oligonucleotides can recognize the specific sequences in double-stranded B-DNA.[82-84] Proteins and many DNA intercalators use major groove interaction because major grooves have richer donor acceptor sites for hydrogen bonding than minor grooves. However, many ligands, small natural products, and even some proteins prefer to bind to the minor groove of the B-DNA.[85]

There are two major types of interactions that occur between DNA and ligands; reversible and irreversible. Both interactions have been commonly used in therapeutic developments in

today`s medicine. Generally, irreversible interaction causes permanent damage to the DNA. In contrast, reversible ligand and DNA interactions do not cause permanent DNA damage. However, complex formation temporarily disturbs essential biological functions.

4.2. DNA Groove Binders

There are three common classes of DNA interactive agents that have been used for therapeutic purposes. Alkylators, in which small molecules react covalently with DNA bases, in most cases, the bond formation happens at guanine and adenine. Reversible binders result from noncovalent interactions with DNA. Strand breakers arise by reactive radical generation by a ligand and cause cleavage of a DNA strand. The ideal DNA interactive agent should be a nonpeptide, as well as sequence and site size specific.[86] The design of major groove binders is challenging because the size of the helical gap requires large complex molecules. Some of the major drawbacks to consider when designing major groove binders are the synthetic process, delivery of the relatively large molecules, cellular transportation and cellular uptake. One such approach involves the use of the antisense strategy. Despite much research, antisense approaches for sequence specific recognition of major grooves still have a long way to before achieving practical use. Therefore, many research efforts currently focus on targeting the DNA minor groove.

4.2.1. DNA Minor Groove Targeted Therapeutic Agents

Over the past decades of research, X-ray crystallography, high field NMR, computational chemistry, and new techniques in molecular biology have provided detailed and extensive information about oligonucleotides, as well as their interactions. Oligonucleotides interact with a variety of small molecules, including; bioinorganic species including water, and metal cations, small organic molecules and proteins.[87] Minor groove binders generally have several

characteristic features, such as a curved shape, which optimizes the best fit in the helical twist, favorable van der Waals interactions, hydrophobic forces, and hydrogen bonding. Minor groove binding molecules mostly contain aromatic rings, which are connected with a single bond. These single bonds allow for torsional rotation of the ring systems in order to fit into the helical curve. The minor groove is generally narrower in the A-T rich region as opposed to the G-C rich region. As a result, the A-T region provides a snugger fit for small and flat molecules. The location of hydrogen donors and acceptors between the base pairs plays a significant role in determining if minor groove binders favor the A-T region or the G-C region. In the minor groove of A-T regions, C2 oxygen and N3 nitrogen atoms are accessible and available for small molecule interaction. However, the similar location of the minor groove at G-C sequences is more sterically hindered, due to the additional amino group in G and the hydrogen bonding with C2 carbonyl oxygen. Theoretical studies of DNA showed that the negative electrostatic potential of poly(dA)-poly(dT) is much higher than the minor groove of poly(dG)-poly(dC), particularly due to the amino group on C2 of guanine.[88] Therefore, cationic molecules can show higher selectivity for the A-T rich sequence as a result of their electrostatic potential interactions.

In contrast to intercalators, minor groove binding molecules generally do not induce any significant structural changes in the DNA nor do they significantly unwind the double helix.[89]

4.2.1.1. DNA Binding Antibiotics

a) *Pyrrole-Amidine Antibiotics*

Netropsin and distamycin A are two of the well known DNA binding antibiotics which target the A-T sequence in double stranded DNA. Netropsin was isolated from *Streptomyces netropsis*. Distamycin A, distamycin B and C are major fermentation products of *Streptomyces*

distallicus. Both antibiotic structures contain *N*-methylpyrrole groups linked with amide bonds, which show antibacterial and antiviral activity.

The binding of pyrrole-amidine antibiotics to DNA has been investigated using several physical techniques, including; UV absorption, CD, NMR, thermal melting and hydrodynamic measurements. Studies performed with different sequences of DNA clearly suggest that netropsin shows a high binding specificity to A-T base pairs, whereas no significant binding has been detected for G-C rich DNA .[90-92]

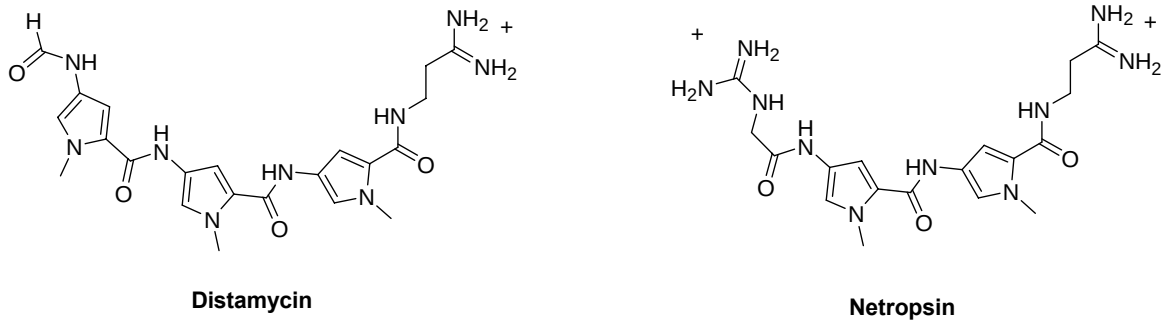

Figure 4.2. Chemical structure of Pyrrole-Amidine Antibiotics; Distamycin and Netropsin.

J. W. Lown et al. successfully synthesized new derivatives of pyrrole amidine antibiotics. Their modification, the replacement of methylpyrrole rings with imidazole rings, changed the binding specificity of netropsin. Imidazole derivatives of netropsin, called lexitropsins, showed reduced A-T binding affinity, but increased G-C binding.

Comparative binding experiments of distamycin A with nucleic acids in solution indicated that the binding results are very similar to those of netropsin. Distamycin A shows a high preference for A-T base pairs while almost no affinity was found for RNAs. In contrast to netropsin, distamycin A showed a small induced CD with G-C containing polymers.[93-95] Studies

concluded that netropsin may act as an extended flat molecule that bridges the two strands of duplex DNA along the minor groove. [96]

The crystal structure analysis of netropsin suggested that bowed shape molecules provide an inherent geometrical fit for insertion into the minor groove.[97] In addition, ^{1}H-NMR data suggested that the methylpyrrole carboxamide system of distamycin adapted the same preferred conformation. The rotations around the bonds between pyrrole carbons and peptides provide a twisted shape allowing an excellent fit in the minor groove of the helix.[98] Derivatives of distamycin were synthesized by replacing N-methylpyrrole rings with phenyl groups. The modification of the phenyl derivatives exhibited a reduction in binding affinity and a preference of A-T over G-C sequences compared to distamycin.[99]

The common conclusion of molecular modeling studies was that the A-T specificity of the interaction is due to hydrogen bond formation by hydrogen donating groups of the carboxamide system with O2 atom of thymine and N3 atoms of the adenine bases in the sequence of four to five A-T pairs within the minor groove. In addition, the sequence specificity of netropsin and distamycin are facilitated by steric inhibition of binding created by the amino group of guanine residues. [96, 100]

4.2.1.2. Synthetic DNA Binding Compounds

In addition to the natural antibiotics, many chemically synthesized organic agents have shown promising affinity against tumors, bacterial and protozoal infections through inhibition of nucleic acid synthesis or by effects on the chromosomal structure.

a) *Diarylamidines*

Diarylamidines have been used for the treatment of protozoal diseases such as trypanosomiasis and leishmaniasis since the 1930s. In the early 1970s, a large number of diarylamidine

derivatives were synthesized in an effort to find more efficient antiparasitic drugs, especially against trypanosomes. Compounds such as 4'-6-diamidino-2-phenylindole (**DAPI**), berenil, pentamidine and furamidine were found to be therapeutically useful agents against several parasitical diseases.

DAPI showed very promising results against *Trypanosome congolese*.[101] However, clinical use of **DAPI** has been limited due to the cyclotoxicity of the drug. The drug binds specifically to the AT-rich regions of double stranded DNA and has shown inhibition of DNA and RNA polymerase.[102, 103] **DAPI** binding with the minor groove occurs at the ATT sequence with the phenyl and indole rings parallel to the groove walls. The terminal amidinium groups make a close interaction with C2 and N3 atoms of adenine and O2 of thymine at the A-T region on the helix.[104] The terminal amidine groups of **DAPI** contribute complex stability between the cations and the bases through hydrogen bonds and electrostatic interactions. [105]

Another synthetic diarylamididine product, berenil, shows trypanocidal, babesicidal, and bactericidal activity and the drug has been used in veterinary medicine for the treatment of *trypanosomiasis*. Spectrophotometric and hydrodynamic binding studies of berenil have indicated that the binding affinity was selective for the minor groove in AT regions. The interaction of berenil with the DNA template affects the replication process. The drug's biological activity has been correlated with a selective interaction with A-T regions of kinetoplasts within the mitochondrion.[106, 107] Berenil most likely interacts in the minor groove by hydrogen bonding with two of the thymidine acceptor sites and by electrostatic interaction forces of the terminal diamidine groups.[108]

Pentamidine is an aromatic dicationic analog that has been clinically used for treatment of infections caused by *Trypanosoma brucei gambiense*, *Leismania donovani*, and *Pneumocystis*

carinii.[109] Pentamidine has been used in the treatment of *P. carinii pneumonia* patients who are HIV-positive and cannot tolerate co-trimoxazole.[110] The mechanism of pentamidine action against *P. carinii* has not been elucidated. However, studies have shown that this compound inhibits DNA, RNA, and protein synthesis. Footprinting analysis indicated the pentamidine binding preference is at the A-T rich region of the DNA minor groove, it recognizes sequences containing at least five consecutive A-T base pairs.[111] According to one molecular modeling study, researchers suggested that the terminal cationic ends of the drug could form hydrogen bond interactions with acceptor atoms of either adenine or thymine bases in the minor groove.[112]

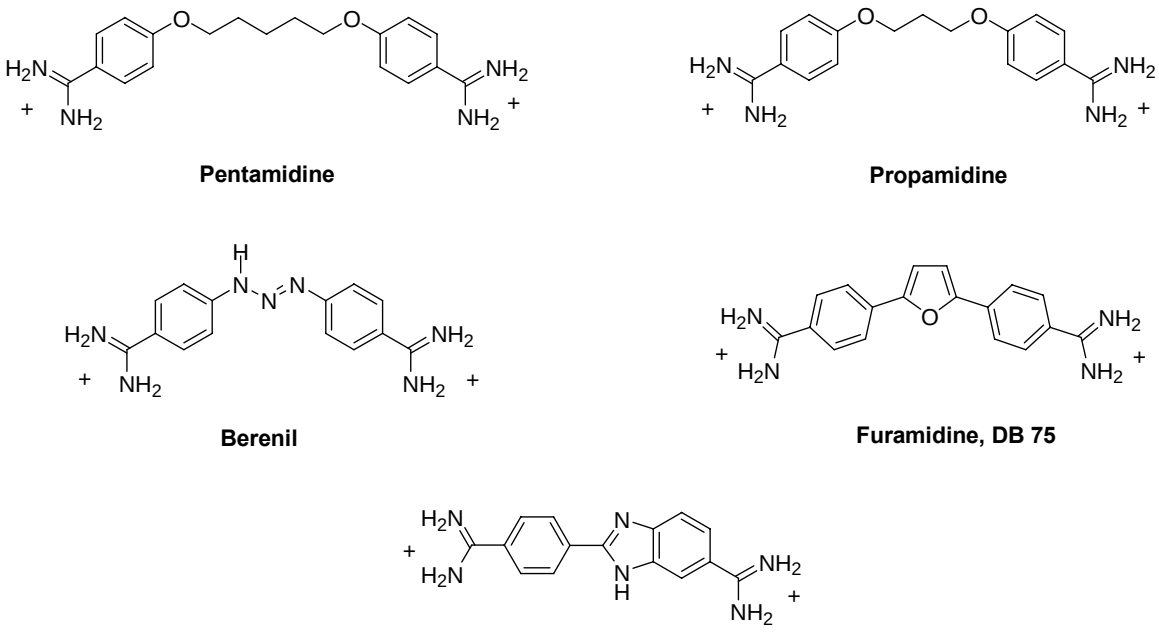

Figure 4.3. Chemical structure of synthetic diarylamidines.

These findings suggested that the mechanism of pentamidine is probably involved with direct interaction with the pathogenic genome of *P. carini.* Even though pentamidine is used for treatment of *P. carinii pneumonia*, the toxicity of the drug is not desirable. Therefore, usage of

the drug is limited to fatal infections of AIDS patients. However, the promising activity of pentamidine has led to the development of analogs to achieve less toxic congeners. Chemical modification of pentamidine has been done with different linkers and different cationic terminal groups. A conformationally locked derivative of pentamidine, *cis*-butamidine, was synthesized by replacement of the pentyl bridge of pentamidine with a 2-butene. The new analog showed increased *in vitro* and *in vivo* activity in treating *P. carinii pneumonia* in immunosuppressed rats.[113] Replacement of the amidine groups of pentamidine with imidazoline moieties increased the anti *P. carinii pneumonia* activity and reduced toxicity.[114] The replacement of the triazene linker of berenil with the five membered heterocycle furan gave the dicationic 2,5-diaryl furan derivative (**DB 75**) which is reported to be highly effective in *in vivo* studies against *P. carinii* in the immunosuppressed rat model.[115] In addition, **DB 75** was found to be active against highly infectious parasites such as *Giardia lamblia*, *Plasmodium falciparum*, and *Trypanosoma rhodesience*.[116, 117] An X-ray structure of the complex between DNA and **DB 75** has shown that the crescent shape of the molecule matches the curvature of the minor groove at A-T sequences.[118] The compound fits snugly to the AATT minor groove binding site and forms hydrogen bonds to A-T base pairs at the floor of the minor groove.[115] In addition, biophysical examination of **DB 75** also demonstrated that the drug strongly binds to the minor groove of DNA at A-T rich sites and weakly binds by intercalation to G-C sites of DNA.[119] Biophysical evidence suggests a model for the biological action of **DB 75** in which the drug binds in the DNA minor groove at A-T rich region and forms a stable complex. The complex formation is most likely responsible for the inhibition of one or more DNA dependant enzymes such as the topoisomerases. A series of **DB 75** derivatives has been synthesized by replacing or modifying both the heterocyclic portions and the phenyl groups, as well as the

cationic groups. The resulting derivatives were evaluated against *P. carinii* infections. The replacement of terminal groups by cyclic amidines did not show better inhibition of topoisomerase isolated from *G. lamblia*.[115] However, the introduction of different sizes of alkyl groups on both terminal amidino groups has shown promising activity and no overt toxicity at the screening dose of 10 mmol/kg/day against the immunosuppressed rat model of *P.carinii*. The X-ray structures for the derivatives, 2,5-bis[4-(*N*-isopropylamindino) phenyl]furan and 2,5-bis[4-(*N*-cyclopropyl amidino) phenyl] furan, demonstrated the excellent fit of this class of compounds in the minor groove at the AATT site.[115, 120, 121] In addition, studies have shown that these derivatives of furan amidines tend to bind to RNA by intercalation.[122] The efficiency of these derivatives provided a lead candidate for development of more effective agents against *P. carinii* infections.

b) Bis-benzimidazoles

The synthetic bisbenzimidazole derivative Hoechst 33258, Pibenzimol, has been used as an effective DNA binding fluorophore in chromosomal banding patterns. Hoechst 33258 shows a fluorescence enhancement upon interaction with both A-T and G-C rich DNA. However, fluorescence enhancement is greater at A-T rich DNA than enhancement with G-C rich DNA. Hoechst 33258 is a useful tool to identify A-T regions in specific chromosome regions.[123] Hoechst 33258 has been found to be A-T selective and binds in the minor groove at four or five consecutive A-T base pairs. Binding was suggested to involve two bisbenzimidazole NHs forming a bridge with three central A-T base pairs on the floor of the minor groove between adjacent adenine N3 and thymine O2 atoms on opposite strands.[124] Hoechst 33258 shows antihelmintic activity but its low potency and high toxicity have limited usage in clinical

treatment.[125, 126] The mechanism of cytotoxicity is not known. Hoechst 33258 easily penetrates cells and binds in a reversible manner to DNA and inhibits topoisomerase.[127-129]

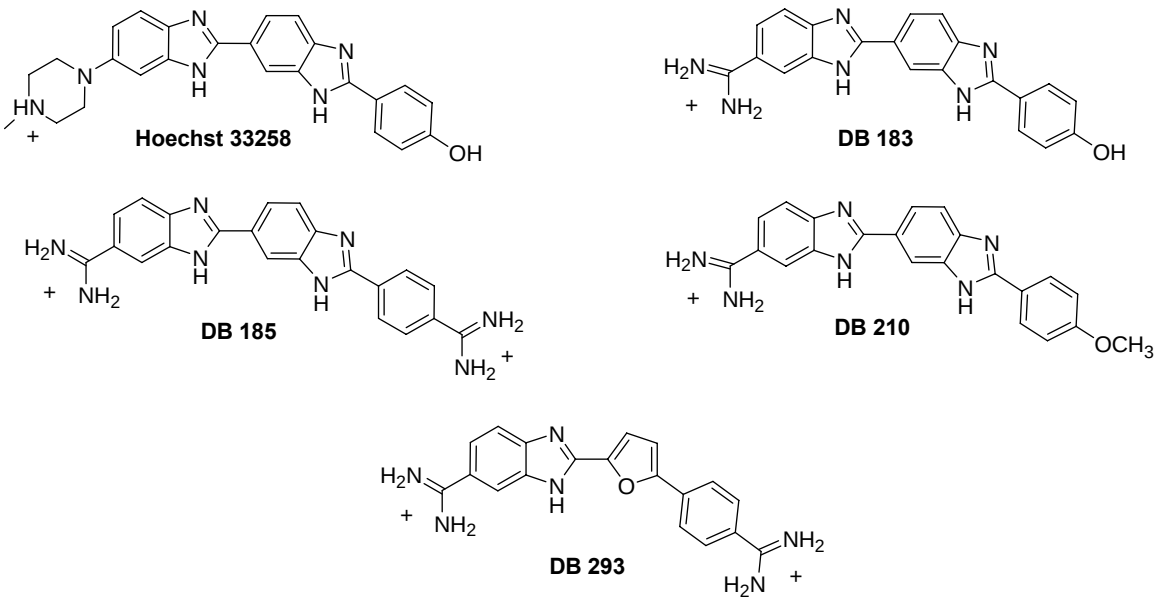

Figure 4.4. Chemical structure of bis-benzimidazole derivatives.

Switching the phenolic hydroxyl group of Hoechst 33258 from the para to the meta position lowers the cytotoxicity. It is assumed that the para position of the hydroxyl plays a key role for penetration through cell membranes.[130] Derivatives have been synthesized by alkylation of the phenolic hydroxyl group. These modifications produced enhanced cytotoxicity. The ready uptake of these compounds by the cytoplasmic and nuclear membranes, is assumed to lead to accumulation in the nucleus followed by inhibition of the binding of regulatory proteins.[131] Converting the cationic bulky end on Hoechst 33258 to a planer amidine group significantly changes the DNA interaction affinity. Monoamidines **DB 183** and **DB 210,** and diamidine **DB 185** was synthesized by Boykin *et al.* and are related to the well-known minor groove binding agents. Footprinting studies indicated that the synthetic compounds bind at A-T sequences in

the minor groove. Circular dichroism spectroscopy also showed that the compounds bind in the DNA minor groove. Biosensor-surface Plasmon resonance (**SPR**) studies clearly showed that the monoamidine compounds bind to TTAA sequence in a 2:1 complex as a dimer but bind as a monomer to AATT. The dication, **DB 185** binds to both DNA sequences as monomer complexes. The binding of **DB 185** at AATT is significantly stronger than binding to TTAA. The reason for the different binding motif at the different sequences is apparent from molecular dynamics simulations. These studies showed that the AATT sequence has a narrow time average minor groove width that is a very good receptor site for the bisbenzimidazole compounds. The groove is widened at the TTAA sequence and the width must be reduced to form a favorable monomer complex. Therefore, the monocation analogs form an antiparallel dimer stack and closely fits the structure of the TTAA minor groove. Another hybrid analog of the original Hoechst 33258 is the benzimidazole furan diamidine compound **DB 293**.[132] The hybrid molecule showed a dimeric antiparallel stacking and binding motif. The stacking occurs preferentially at ATGA sites.[127] **DB 293** analogs with either two phenyls, **DB 75** or two benzimidazoles, **DB 270** did not show any tendency to form the stacked dimer.[133] Dimer stacking molecules are excellent candidates for the design of gene specific targeting at minor groove.

4.3. Optimal Fit to Minor Groove

The classical approach for designing minor groove binders consists of optimizing the shape of the ligand to match the helical curve and twist of the groove. Any shape of the ligand that does not fit the curvature requirement was considered unlikely to bind. Specifically, a natural product, distamycin, has shown great binding affinity to the A-T minor groove of the helix. The natural shape of distamycin is twisted and the ligand provides a snug fit into the minor groove.

Replacing the *N*-methylpyrrole rings with phenyl groups results in a more the linear shape which did not bind as strongly. It was found that the naturally curved shape of distamycin shows strong binding affinity to the helix. This evidence strongly supports the classical approach for DNA binders. Tidwell *et. al.* examined the DNA binding properties of a series of bisbenzamidines, including pentamidine, by measuring changes in the thermal denaturation temperature.

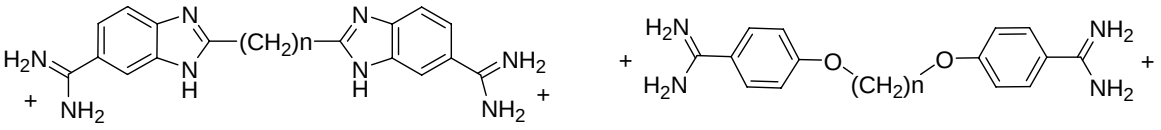

Figure 4.5. Structure of DNA binding compounds; bis-bezimidazole and bis-phenyl diamidines.

The studies showed that all the analogs of bisbenzamidine compounds have a significant affinity for DNA and moderate specificity for AT base pairs without intercalation. The derivatives of pentamidine, with an odd number of methylene linkages between the benzamidine rings, had a stronger binding affinity for the minor groove than derivatives with an even number linkage. Switching the cationic ends to the meta position resulted in lower polynucleotide affinity. All these findings suggested that the shape of the molecules is important for DNA binding affinity. Modeling studies demonstrated the correlation between the DNA binding and the radius of the curvature of molecular mechanic models of the molecules. Later, similar studies of a series of bis-amidinobenzimidazo1es and bis-amidinoindo1es with varied linking chains reported similar results. The analysis of the shape of the molecules is consistent with this mode of nucleic acid binding. Analogs, with an even number of methylene linkages with the benzimidazole rings have a higher affinity for DNA than those with an odd

numbers. Molecular modeling studies suggested that the shape of the molecule, as a function of chain length, affects the strength of nucleic acid binding. In addition, hydrogen bonding from the imidazole nitrogens and electronic effects from the cationic substituents contribute to the nucleic acid affinity.[134]

Another interesting example of the crescent shape ligands are furamidine derivatives. Furamidine (**DB 75**) has significantly better activity against a number of parasites with lower toxicity than pentamidine. Modification of the parent phenyl-furan phenyl diamidine to a phenyl-thiophene-benzimidazole derivative yielded an analogue which showed a 10-fold increase in affinity for the minor groove at AT region. An X-ray investigation of the derivatives indicated a small bond angle difference between the C-S-C angle of thiophene and the C-O-C angle of furan leads to a better fit for the terminal ends of the benzimidazole compounds at the floor of the groove. This effect is thought to cause the significant difference in binding affinity.[135]

All of these examples, in addition to other studies not summarized in this chapter, have confirmed that the shape of the ligand is an important factor in strong binding.

4.4. Non-Classical DNA Minor Groove Binders

Synthetic compounds, which fit into a classic isohelical approach, have shown strong binding to the DNA minor groove. Compounds that are too curved, or too linear have shown poor minor groove binding affinity. The crescent shape of the ligands has been viewed as important in the design of new therapeutic agents, but it is not the only factor for strong binding. Several compounds that do not fit into the classical concept have showed unexpected DNA binding results. Several synthetic dicationic linear, or close to linear shaped ligands have been shown to bind extremely strongly to the minor groove in A-T rich regions. In a contrast, the highly

curved molecule, bisamidino diphenylether benzimidazole **RT 29,** was shown to bind to the DNA minor groove stronger than many ligands that were designed following the isohelical binding criteria.[136, 137] The linear shaped compound, **CGP40215A** is not complementary to the curve of the DNA groove. However, the ligand exhibited a high binding affinity in comparison to curved diamidine molecules.

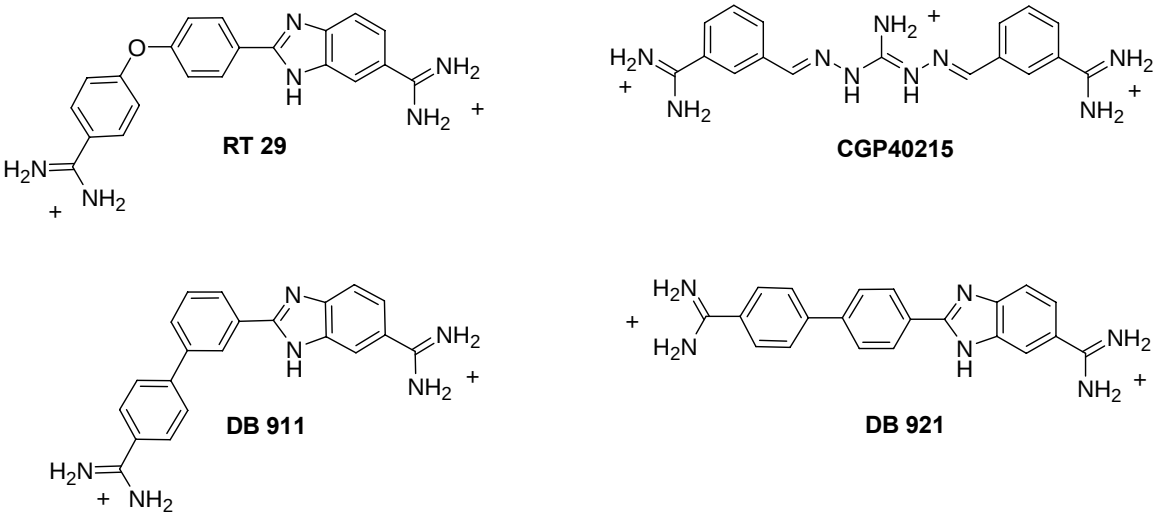

Figure 4.6. The structure of the compounds which shown unusual DNA binding affinity.

The positively charged amidine groups at the ends of the **CGP40215A** and the proton donor amino groups on the linker interact with the DNA bases. Both the X-ray and molecular dynamics studies indicated that water molecules act like a mediator to form hydrogen bonds between the ligand and the DNA.[111] Complementary results were obtained by investigating the linear **DB 921** and its curved derivative **DB 911. DB 921** is a near linear dicationic benzimidazole-biphenyl molecule while **DB 911** has the classical crescent shape. The central meta substituted phenyl gives the compound a shape similar to known crescent shaped minor groove binding compounds. The experimental results were surprising; **DB 921** is a dicationic near linear compound that does not have the appropriate radius of curvature to match the

groove shape. Therefore, it was expected that **DB 911** should be a more effective minor groove binder than **DB 921**. However, studies indicated that **DB 921** not only binds in the groove but that it also has a significantly higher binding constant (2.9×10^8 M^{-1}, vs 2.1×10^7 M^{-1} for **DB 911)**. The X-ray structure of the **DB 921** complex shows that an induced fit structural change in **DB 921** reduces the twist of the biphenyl to complement the groove. This change places the functional groups in position to interact with DNA bases at the floor of the minor groove. A water molecule forms hydrogen bonds between the phenylamidine and the groove bases. **DB 921** and a water molecule complete a curved binding module that is complementary to the minor groove and provides a number of strong hydrogen bonding interactions that are not possible with **DB 911**.[138]

The crescent shape of the ligand is important for the optimal fit of many natural and synthetic compounds within the minor groove of the helix. However, new findings also suggest that the traditional requirement of a compound's curvature shape for DNA minor groove complex formation needs to be reevaluated. As such, the role of water should be considered in the development of the new DNA binders.

4.5. Conclusions

The genetic diversity of all living forms is a very attractive target for the development of new therapeutic agents. In addition, more in depth understanding of DNA and its interactions are being utilized to develop methodologies to design and develop future therapeutics agents. For many biological and biophysical reasons, the DNA minor groove provides a useful target for ligand interactions. Therefore, the minor groove of the helix is a potential target for many drugs in modern medicine. Even though gene targeting methodology is a powerful approach for finding a cure at the molecular level, researchers still have many challenges to overcome,

including; gene sequence specificity, cytotoxicity, and delivering the drug to the genes. In this review, we have only summarized results for a few of the important natural and synthetic DNA minor groove binding compounds. Of these, the majority noncovalently bind to the DNA minor groove at AT rich sequences without intercalation. Because of their sequence specific recognition in the minor groove of the helix, these ligands hold potential for developing new gene specific reagents. Studies with these compounds indicate that the binding affinity for the ligand and nucleic acid complexes depend on several factors, including a complementary shape of the ligand for minor groove. In many cases, the crescent shape of the drug is extremely important for fit within the minor groove. However, recent results have shown that high binding affinity is not limited to crescent shape molecules. In fact, water can join with linear molecules to bind strongly to the DNA minor groove. Extensive efforts are still underway in hopes of developing gene specific agents, or the "magic bullet," to cure existing diseases.

References

1. Smith, D. H.; Pepin, J.; Stich, A. H. R. Human African trypanosomiasis: an emerging public health crisis. *Br Med Bull* **1998,** 54, 341-355.

2. Report of a WHO expert committee. Epidemiology and control of African trypanosomiasis. *Technical Report Series. World Health Organization. Geneva, Switzerland.* **1986,** 739, 126.

3. Williams, B. I. *African trypanosomiasis. In The Wellcome Trust illustrated history of tropical diseases.* The Wellcome Trust: London, United Kingdom, 1996.

4. Vickerman, K. DEVELOPMENTAL CYCLES AND BIOLOGY OF PATHOGENIC TRYPANOSOMES. *Br Med Bull* **1985,** 41, 105-114.

5. Chappuis, F. o. Editorial Commentary: Melarsoprolâ€Free Drug Combinations for Secondâ€Stage Gambian Sleeping Sickness: The Way to Go. *Clinical Infectious Diseases* **2007,** 45, 1443-1445.

6. Pépin, J.; Milord, F. The treatment of human African trypanosomiasis. *Adv. Parasitol* **1994,** 33, 1-47.

7. Abramowicz, M. *Drugs For Parasitic Infections*. The Medical Letter, Inc.: New Rochelle,NY, 2000.

8. Priotto, G.; Kasparian, S.; Ngouama, D.; Ghorashian, S.; Arnold, U.; Ghabri, S.; Karunakara, U. Nifurtimoxâ€Eflornithine Combination Therapy for Secondâ€Stage Trypanosoma brucei gambiense Sleeping Sickness: A Randomized Clinical Trial in Congo. *Clinical Infectious Diseases* **2007,** 45, 1435-1442.

9. Voogd, T.; Vansterkenburg, E.; Wilting, J.; Janssen, L. Recent research on the biological activity of suramin. *Pharmacol Rev* **1993,** 45, 177-203.

10. Darsaud, A.; Chevrier, C.; Bourdon, L.; Dumas, M.; Buguet, A.; Bouteille, B. Megazol combined with suramin improves a new diagnosis index of the early meningo-encephalitic phase of experimental African trypanosomiasis. *Tropical Medicine & International Health: TM & IH* **2004,** 9, 83-91.

11. Scott, A. G.; Tait, A.; Turner, C. M. Characterisation of cloned lines of Trypanosoma brucei expressing stable resistance to MelCy and suramin. *Acta Trop* **1996** 60, 251-262.

12. Vansterkenburg, E. L.; Coppens, I.; Wilting, J.; Bos, O. J.; Fischer, M. J.; Janssen, L. H.; Opperdoes, F. R. The uptake of the trypanocidal drug suramin in combination with low-density lipoproteins by Trypanosoma brucei and its possible mode of action. *Acta Trop* **1993,** 54, 237-250.

13. Damper, D.; C.L., P. entamidine transport and sensitivity in brucei-group trypanosomes. *J.Protozool.* **1976,** 23, 349-56.

14. Berger, B. J.; Carter, N. S.; Fairlamb, A. H. Characterisation of pentamidine-resistant Trypanosoma brucei brucei. *Molecular and Biochemical Parasitology* **1995,** 69, 289-298.

15. Carter, N. S.; Berger, B. J.; Fairlamb, A. H. Uptake of Diamidine Drugs by the P2 Nucleoside Transporter in Melarsen-sensitive and -resistant Trypanosoma brucei brucei. *J. Biol. Chem.* **1995,** 270, 28153-28157.

16. De Koning, H. P. Uptake of Pentamidine in Trypanosoma brucei brucei is Mediated by Three Distinct Transporters: Implications for Cross-Resistance with Arsenicals. *Mol Pharmacol* **2001,** 59, 586-592.

17. Bray, P. G.; Barrett, M. P.; Ward, S. A.; de Koning, H. P. Pentamidine uptake and resistance in pathogenic protozoa: past, present and future. *Trends in Parasitology* **2003,** 19, 232-239.

18. Ludewig, G.; Williams, J. M.; Li, Y.; Staben, C. Effects of pentamidine isethionate on Saccharomyces cerevisiae. *Antimicrob. Agents Chemother.* **1994,** 38, 1123-1128.

19. Simpson, L. Kinetoplast DNA in trypanosomid flagellates. *Int. Rev. Cytol.* **1986,** 99, 119-179.

20. Doua, F.; Miezan, T. W.; Singaro, J. R. S.; Yapo, F. B.; Baltz, T. The Efficacy of Pentamidine in the Treatment of Early-Late Stage Trypanosoma brucei gambiense Trypanosomiasis. *Am J Trop Med Hyg* **1996,** 55, 586-588.

21. Bronner, U.; Doua, F.; Ericsson, O.; Gustafsson, L. L.; Miézan, T. W.; Rais, M.; L., R. Pentamidine concentrations in plasma, whole blood and cerebrospinal fluid during treatment of Trypanosoma gambiense infection in Côte d'Ivoire. *Trans R. Soc. Trop. Med. Hyg.* **1991,** 85, 608-611.

22. J. Blum, S. N., C. Burri,. Clinical description of encephalopathic syndromes and risk factors for their occurrence and outcome during melarsoprol treatment of human African trypanosomiasis. *Tropical Medicine & International Health* **2001,** 6, 390-400.

23. Blum, J.; Schmid, C.; Burri, C. Clinical aspects of 2541 patients with second stage human African trypanosomiasis. *Acta Tropica* **2006,** 97, 55-64.

24. Emile SCHAFTINGEN, F. R. O., Henry-Géry HERS,. Effects of various metabolic conditions and of the trivalent arsenical melarsen oxide on the intracellular levels of fructose 2,6-bisphosphate and of glycolytic intermediates in Trypanosoma brucei. *European Journal of Biochemistry* **1987,** 166, 653-661.

25. C. Burri, J. K. Pharmacokinetic investigations in patients from northern Angola refractory to melarsoprol treatment. *Tropical Medicine & International Health* **2001,** 6, 412-420.

26. Pepin, J.; Guern, C.; Milord, F.; Schechter, P. J. DIFLUOROMETHYLORNITHINE FOR ARSENO-RESISTANT TRYPANOSOMA BRUCEI GAMBIENSE SLEEPING SICKNESS. *The Lancet* **1987,** 330, 1431-1433.

27. Yarlett, N.; Bacchi, C. J. Effect of -[alpha]-difluoromethylornithine on methionine cycle intermediates in Trypanosoma brucei brucei. *Molecular and Biochemical Parasitology* **1988,** 27, 1-10.

28. Fairlamb, A. H.; Henderson, G. B.; Bacchi, C. J.; Cerami, A. In vivo effects of difluoromethylornithine on trypanothione and polyamine levels in bloodstream forms of Trypanosoma brucei. *Molecular and Biochemical Parasitology* **1987,** 24, 185-191.

29. Crowell, A. L.; Stephens, C. E.; Kumar, A.; Boykin, D. W.; Secor, W. E. Activities of Dicationic Compounds against Trichomonas vaginalis. *Antimicrob. Agents Chemother.* **2004,** 48, 3602-3605.

30. Thuita, J. K.; Karanja, S. M.; Wenzler, T.; Mdachi, R. E.; Ngotho, J. M.; Kagira, J. M.; Tidwell, R.; Brun, R. Efficacy of the diamidine DB75 and its prodrug DB289, against murine models of human African trypanosomiasis. *Acta Tropica* **2008,** 108, 6-10.

31. Lanteri, C. A.; Trumpower, B. L.; Tidwell, R. R.; Meshnick, S. R. DB75, a Novel Trypanocidal Agent, Disrupts Mitochondrial Function in Saccharomyces cerevisiae. *Antimicrob. Agents Chemother.* **2004,** 48, 3968-3974.

32. Peregrine, A. S.; Mamman, M. Pharmacology of diminazene: a review. *Acta Trop.* **1993,** 54.

33. Pépin, J.; Milord, F. The treatment of human African trypanosomiasis. *Adv Parasitol.* **1994,** 33, 1-47.

34. de Koning, H. P.; Anderson, L. F.; Stewart, M.; Burchmore, R. J. S.; Wallace, L. J. M.; Barrett, M. P. The Trypanocide Diminazene Aceturate Is Accumulated Predominantly through the TbAT1 Purine Transporter: Additional Insights on Diamidine Resistance in African Trypanosomes. *Antimicrob. Agents Chemother.* **2004,** 48, 1515-1519.

35. Witola, W. H.; Inoue, N.; Ohashi, K.; Onuma, M. RNA-interference silencing of the adenosine transporter-1 gene in Trypanosoma evansi confers resistance to diminazene aceturate. *Experimental Parasitology* **2004,** 107, 47-57.

36. Matovu, E.; Stewart, M. L.; Geiser, F.; Brun, R.; Maser, P.; Wallace, L. J. M.; Burchmore, R. J.; Enyaru, J. C. K.; Barrett, M. P.; Kaminsky, R.; Seebeck, T.; de Koning, H. P. Mechanisms of Arsenical and Diamidine Uptake and Resistance in Trypanosoma brucei. *Eukaryotic Cell* **2003,** 2, 1003-1008.

37. Jennings, F. W. Chemotherapy of CNS-trypanosomiasis: the combined use of the arsenicals and nitro-compounds. *Trop. Med. Parasito.* **1991,** 42, 139-142.

38. Priotto, G.; Fogg, C.; Balasegaram, M.; Erphas, O.; Louga, A.; Checchi, F.; Ghabri, S.; Piola, P. Three Drug Combinations for Late-Stage <italic>Trypanosoma brucei gambiense</italic> Sleeping Sickness: A Randomized Clinical Trial in Uganda. *PLOS Clin Trial* **2006,** 1, e39.

39. Enanga, B.; Ariyanayagam, M. R.; Stewart, M. L.; Barrett, M. P. Activity of Megazol, a Trypanocidal Nitroimidazole, Is Associated with DNA Damage. *Antimicrob. Agents Chemother.* **2003,** 47, 3368-3370.

40. Bernard Bouteille, O. O., Sylvie Bisser, Michel Dumas,. Treatment perspectives for human African trypanosomiasis. *Fundamental & Clinical Pharmacology* **2003,** 17, 171-181.

41. MOLINA, R.; GRADONI, L.; ALVAR, J. HIV and the transmission of *Leishmania*. *Annals of TropicalMedicine & Parasitology* **2003,** 97, 29-45.

42. Belkaid, Y.; Kamhawi, S.; Modi, G.; Valenzuela, J.; Noben-Trauth, N.; Rowton, E.; Ribeiro, J.; Sacks, D. L. Development of a Natural Model of Cutaneous Leishmaniasis: Powerful Effects of Vector Saliva and Saliva Preexposure on the Long-Term Outcome of Leishmania major Infection in the Mouse Ear Dermis. *J. Exp. Med.* **1998,** 188, 1941-1953.

43. Desjeux, P. The increase in risk factors for leishmaniasis worldwide. *Transactions of the Royal Society of Tropical Medicine and Hygiene* **2001,** 95, 239-243.

44. Ahluwalia, S.; Lawn, S. D.; Kanagalingam, J.; Grant, H.; Lockwood, D. N. J. Mucocutaneous leishmaniasis: an imported infection among travellers to central and South America. *BMJ* **2004,** 329, 842-844.

45. Roberts, L. S.; Janovy Jr, J.; Schmidt, G. *Foundations of Parasitology*. 6th ed.; McGraw Hill: Boston, 2000.

46. Zilberstein, D.; Baker, J. R.; Muller, R. Transport of Nutrients and Ions across Membranes of Trypanosomatid Parasites. In *Advances in Parasitology*, Academic Press: 1993; Vol. Volume 32, pp 261-291.

47. Mookerjee Basu, J.; Mookerjee, A.; Sen, P.; Bhaumik, S.; Sen, P.; Banerjee, S.; Naskar, K.; Choudhuri, S. K.; Saha, B.; Raha, S.; Roy, S. Sodium Antimony Gluconate Induces Generation of Reactive Oxygen Species and Nitric Oxide via Phosphoinositide 3-Kinase and Mitogen-Activated Protein Kinase Activation in Leishmania donovani-Infected Macrophages. *Antimicrob. Agents Chemother.* **2006,** 50, 1788-1797.

48. Abdi, Y. A.; Gustafsson, L. L.; Ericsson, O.; Hellgren, U. *Handbook of Drugs for Tropical Parasitic Infections*. 2th ed.; CRC Press: 1995.

49. Moore, E.; O'Flaherty, D.; Heuvelmans, H.; Seaman, J.; Veeken, H.; Wit, S. d.; Davidson5, R. N. Comparison of generic and proprietary sodium stibogluconate for the treatment of visceral leishmaniasis in Kenya. *Bulletin of the World Health Organization* **2001,** 9, 388-393.

50. Hellier, I.; Dereure, O.; Tournillac, I.; Pratlong, F.; Guillot, B.; Dedet, J. P.; Guilhou, J. J. Treatment of Old World Cutaneous Leishmaniasis by Pentamidine Isethionate. *Dermatology* **2000,** 200, 120-123.

51. de Koning, H. P. Transporters in African trypanosomes: role in drug action and resistance. *International Journal for Parasitology* **2001,** 31, 511-521.

52. Thakur, C. P.; Singh, R. K.; Hassan, S. M.; Kumar, R.; Narain, S.; Kumar, A. Amphotericin B deoxycholate treatment of visceral leishmaniasis with newer modes of administration and precautions: a study of 938 cases. *Transactions of the Royal Society of Tropical Medicine and Hygiene* **1999,** 93, 319-323.

53. Jha, T. K.; Giri, Y. N.; Singh, T. K.; Jha, S. Use of Amphotericin B in Drug-Resistant Cases of Visceral Leishmaniasis in North Bihar, India. *Am J Trop Med Hyg* **1995,** 52, 536-538.

54. Ehrenfreund-Kleinman, T.; Domb, A. J.; Jaffe, C. L.; Nasereddin, A.; Leshem, B.; Golenser, J. THE EFFECT OF AMPHOTERICIN B DERIVATIVES ON LEISHMANIA AND IMMUNE FUNCTIONS. *Journal of Parasitology* **2005,** 91, 158-163.

55. Sundar, S.; Jha, T. K.; Thakur, C. P.; Engel, J.; Sindermann, H.; Fischer, C.; Junge, K.; Bryceson, A.; Berman, J. Oral Miltefosine for Indian Visceral Leishmaniasis. *N Engl J Med* **2002,** 347, 1739-1746.

56. Thakur, C. P.; Kanyok, T. P.; Pandey, A. K.; Sinha, G. P.; Messick, C.; Olliaro, P. Treatment of visceral leishmaniasis with injectable paromomycin (aminosidine). An open-label

randomized phase-II clinical study. *Transactions of the Royal Society of Tropical Medicine and Hygiene* **2000,** 94, 432-433.

57. El-On, J.; Halevy, S.; Grunwald, M. H.; Weinrauch, L. Topical treatment of Old World cutaneous leishmaniasis caused by Leishmania major: A double-blind control study. *Journal of the American Academy of Dermatology* **1992,** 27, 227-231.

58. Sundar, S.; Jha, T. K.; Thakur, C. P.; Sinha, P. K.; Bhattacharya, S. K. Injectable Paromomycin for Visceral Leishmaniasis in India. *N Engl J Med* **2007,** 356, 2571-2581.

59. Sundar, S.; Chakravarty, J. Paromomycin in the treatment of leishmaniasis. *Expert Opinion on Investigational Drugs* **2008,** 17, 787-794.

60. Dietze, R.; Carvalho, S.; Valli, L.; Berman, J.; Brewer, T.; Milhous, W.; Sanchez, J.; Schuster, B.; Grogl, M. Phase 2 trial of WR6026, an orally administered 8-aminoquinoline, in the treatment of visceral leishmaniasis caused by Leishmania chagasi. *Am J Trop Med Hyg* **2001,** 65, 685-689.

61. Yeates, C. Sitamaquine (GlaxoSmithKline/Walter Reed Army Institute). *Curr. Opin. Investig. Drugs.* **2002,** 3, 1446-1452.

62. Snow, R. W.; Guerra, C. A.; Noor, A. M.; Myint, H. Y.; Hay, S. I. The global distribution of clinical episodes of Plasmodium falciparum malaria. *Nature* **2005,** 434, 214-217.

63. Murder, M. J. *Magic and Medicine*. 2nd ed.; Oxford University Press: Oxford, 2000.

64. Orjih, A. U. Heme Polymerase Activity and the Stage Specificity of Antimalarial Action of Chloroquine. *J Pharmacol Exp Ther* **1997,** 282, 108-112.

65. Slater. *Pharmacology & therapeutics* **1993,** 57, 203.

66. Deloron, P.; Mayombo, J.; Le Cardinal, A.; Mezui-Me-Ndong, J.; Bruzi-Baert, C.; Lekoulou, F.; Elissa, N. Sulfadoxine-pyrimethamine for the treatment of Plasmodium

falciparum malaria in Gabonese children. *Transactions of the Royal Society of Tropical Medicine and Hygiene* **2000,** 94, 188-190.

67. J. J. Platteeuw. Resistance to sulphadrug-based antifolate therapy in malaria: are we looking in the right place? *Tropical Medicine & International Health* **2006,** 11, 804-808.

68. Rollo, I. M.; Bushby, S. R. M. Dihydrofolate reductase inhibitors as antimicrobial agents and their potentiation by sulfonamides. *Critical Reviews in Clinical Laboratory Sciences* **1970,** 1, 565 - 583.

69. Maguire, J. D.; Krisin; Marwoto, H.; Richie, T. L.; Fryauff, D. J.; Baird, J. K. Mefloquine is highly efficacious against chloroquine-resistant Plasmodium vivax malaria and Plasmodium falciparum malaria in Papua, Indonesia. *Clinical Infectious Diseases: An Official Publication Of The Infectious Diseases Society Of America* **2006,** 42, 1067-1072.

70. Sullivan Jr., D. J.; Matile, H.; Ridley, R. G.; Goldberg, D. E. A Common Mechanism for Blockade of Heme Polymerization by Antimalarial Quinolines. *J. Biol. Chem.* **1998,** 273, 31103-31107.

71. Camus, D.; Djossou, F. l.; Schilthuis, HerbertÂ J.; HÃ¸gh, B.; Dutoit, E.; Malvy, D.; Roskell, NeilÂ S.; Hedgley, C.; De Boever, ErikaÂ H.; Miller, GerriÂ B. Atovaquoneâ€Proguanil versus Chloroquineâ€Proguanil for Malaria Prophylaxis in Nonimmune Pediatric Travelers: Results of an International, Randomized, Openâ€Label Study. *Clinical Infectious Diseases* **2004,** 38, 1716-1723.

72. McKeage, K.; Scott, L. Atovaquone/proguanil: a review of its use for the prophylaxis of Plasmodium falciparum malaria. *Drugs* **2003,** 63, 597-623.

73. HILL, D. R.; BAIRD, J. K.; PARISE, M. E.; LEWIS, L. S.; RYAN, E. T.; MAGILL, A. J. PRIMAQUINE: REPORT FROM CDC EXPERT MEETING ON MALARIA CHEMOPROPHYLAXIS I. *Am J Trop Med Hyg* **2006,** 75, 402-415.

74. Oliver, M.; Simon, F.; de Monbrison, F.; Beavogui, A. H.; Pradines, B.; Ragot, C.; Moalic, J. L.; Rapp, C.; Picot, S. Le nouvel âge de la primaquine contre le paludisme. *Médecine et Maladies Infectieuses* **2008,** 38, 169-179.

75. Caicedo, O.; Ramirez, O.; Mourao, M. P. G.; Ziadec, J.; Perez, P.; Santos, J. B.; Quinones, F.; Alecrim, M. G. C.; Arevalo-Herrera, M.; Lacerda, M. V. G.; Herrera, S. Comparative Hematologic Analysis of Uncomplicated Malaria in Uniquely Different Regions of Unstable Transmission in Brazil and Colombia. *Am J Trop Med Hyg* **2009,** 80, 146-151.

76. Dahl, E. L.; Shock, J. L.; Shenai, B. R.; Gut, J.; DeRisi, J. L.; Rosenthal, P. J. Tetracyclines Specifically Target the Apicoplast of the Malaria Parasite Plasmodium falciparum. *Antimicrob. Agents Chemother.* **2006,** 50, 3124-3131.

77. Haynes, R. K. Artemisinin and derivatives: the future for malaria treatment? *Current Opinion in Infectious Diseases* **2001,** 14, 719-726.

78. Eckstein-Ludwig, U.; Webb, R. J.; van Goethem, I. D. A.; East, J. M.; Lee, A. G.; Kimura, M.; O'Neill, P. M.; Bray, P. G.; Ward, S. A.; Krishna, S. Artemisinins target the SERCA of Plasmodium falciparum. *Nature* **2003,** 424, 957-961.

79. Meshnick, S. R. Artemisinin: mechanisms of action, resistance and toxicity. *International Journal for Parasitology* **2002,** 32, 1655-1660.

80. Dekker, C. A.; Michelson, A. M.; Todd, A. R. Nucleotides. Part XIX. Pyrimidine deoxyribonucleoside diphosphates. *Journal of the Chemical Society* **1953**, 947 - 951.

81. Zamenhof, S.; Brawerman, G.; Chargaff, E. On the desoxypentose nucleic acids from several microorganisms. *Biochim Biophys Acta* **1952,** 4, 402-405.

82. Seeman, N. C.; Rosenberg, J. M.; Rich, A. Sequence-specific recognition of double helical nucleic acids by proteins. *Proceedings of the National Academy of Sciences of the United States of America* **1976,** 73, 804-808.

83. Pabo, C. O.; Sauer, R. T. Protein-DNA Recognition. *Annual Review of Biochemistry* **1984,** 53, 293-321.

84. Jones, S.; Heyningen, P. v.; Berma, H. M.; Thornton, J. M. Protein-DNA interactions: a structural analysis. *Journal of Molecular Biology* **1999,** 287, 877-896

85. Huth, J. R.; Bewley, C. A.; Nissen, M. S.; Evans, J. N. S.; Reeves, R.; Gronenborn, A. M.; Clore, G. M. The solution structure of an HMG-I(Y)−DNA complex defines a new architectural minor groove binding motif. *Nature Structural Biology* **1997,** 4, 657 - 665.

86. Hurley, L. H. DNA and associated targets for drug design. *Journal of Medicinal Chemistry* **1989,** 32, 2027-2033.

87. Haq, I. Thermodynamics of drug-DNA interactions. *Archives of Biochemistry and Biophysics* **2002,** 403, 1-15.

88. Burridge, J. M.; Quarendon, P.; Reynolds, C. A.; Goodford, P. J. Electrostatic potential and binding of drugs to the minor groove of DNA. *Journal of Molecular Graphics* **1987,** 5, 165-166.

89. Zimmer, C.; Wähnert, U. Nonintercalating DNA-binding ligands: Specificity of the interaction and their use as tools in biophysical, biochemical and biological investigations of the genetic material. *Progress in Biophysics and Molecular Biology* **1986,** 47, 31-112.

90. Luck, G.; Zimmer, C. Interaction of netropsin with DNA in the course of the B-A transition. *Studia Biophys*

1973, 40, 9-12.

91. Zasedatelev, A. S.; Gursky, G. V.; Zimmer, C.; Thrum, H. Binding of netropsin to DNA and synthetic polynucleotides. *Molec. Biol. Rep.* **1974,** 1, 337-342.

92. Zimmer, C.; Lang, H.; Reinert, K. E. Interaction of netropsin with ultraviolet-light irradiated DNA

and poly(dA)- poly(dT). *Studia Biophysica* **1979,** 3, 153-162.

93. Luck, G.; Zimmer, C. On the specificity of the interaction of distamycins with DNA and synthetic duplex polydeoxyribonucleotides. *Studia Biophys* **1976,** 58, 241-244.

94. Zimmer, C.; Luck, G.; Birch-Hirschfeld, E.; Weiss, R.; Arcamone, F.; Guschlbauer, W. Chain length-dependent association of distamycin-type oligopeptides with A- T and G" D pairs in polynucleotide duplexesduplexes. *Biochim. biophys. Acta* **1983,** 741, 15-22.

95. Luck, G.; Zimmer, C.; Reinert, K.-E.; Arcamone, F. Specific interactions of distamycin A and its analogs with (A-T) rich and (G-C) rich duplex regions of DNA and deoxypolynucleotides. *Nucl. Acids Res.* **1977,** 4, 2655-2670.

96. Wartell, R. M.; Larson, J. E.; Wells, R. D. Netropsin. A SPECIFIC PROBE FOR A-T REGIONS OF DUPLEX DEOXYRIBONUCLEIC ACID. *J. Biol. Chem.* **1974,** 249, 6719-6731.

97. Berman, H. M.; Neidle, S.; Zimmer, C.; Thrum, H. Netropsin, a DNA-binding oligopeptide structural and binding studies. *Biochimica et Biophysica Acta (BBA) - Nucleic Acids and Protein Synthesis* **1979,** 561, 124-131.

98. Turchin, K. F.; Grokhovsky, S. L.; Zi-Iuze, A. L.; Gottikrt, B. P. DNA base pair specific ligands. II. Studies of distamycin A chromophore stereochemistry by 1H-NMR spectroscopy. *Bioorean. Khim.* **1977,** 4, 1065-1077.

99. Rao, K. E.; Dasgupta, D.; Sasisekharan, V. Interaction of synthetic analogs of distamycin and netropsin with nucleic acids. Does curvature of ligand play a role in distamycin-DNA interactions? *Biochemistry* **1988,** 27, 3018-3024.

100. Luck, G.; Triebel, H.; Waring, M.; Zimmer, C. Conformation dependent binding of netropsin and distamycin to DNA and DNA model polymers. *Nucl. Acids Res.* **1974,** 1, 503-530.

101. Dann, O.; Fernbach, R.; Pfeifer, W.; Demant, E.; Bergen, G.; Lang, S.; Lurding, G. Trypanocidal diamidines with three ring in two isolated ring systems. *Just Lieb Ann Chem* **1972,** 760, 37-87.

102. Chandra, P.; Mildner, B.; Dann, O.; Metz, A. Influence of 4-6-diamidino-2-phenylindole on the secondary structure and template activities of DNA and polydeoxynucleotides. *Mol Cel Biochem* **1977,** 18, 81-86.

103. Mildner, B.; Metz, A.; Chandra, P. Interaction of 4'-6-diamidino-2-phenylindole to nucleic acids, and its implication to their template activity in RNA-polymerase reaction of E. coli bacteria and of friend-virus infected mouse spleen. *Cancer Letters* **1978,** 4, 89-98.

104. Larsen, T.; Goodsell, D. S.; Cascio, D.; Grzeskowiak, K.; RE, D. The structure of DAPI bound to DNA. *J Biol Struct Dyn* **1989,** 7, 477-491.

105. Pier Giovanni Baraldi, A. B., Francesca Fruttarolo, Delia Preti, Mojgan Aghazadeh Tabrizi, Maria Giovanna Pavani, Romeo Romagnoli,. DNA minor groove binders as potential antitumor and antimicrobial agents. *Medicinal Research Reviews* **2004,** 24, 475-528.

106. Newton, B. A. Interaction of berenil with DNA and some characteristics of the berenil-DNA complex. *Biochemical Journal* **1967,** 105, 50P-51P.

107. Yoshida, M.; Banville, D. L.; Shafer, R. H. Structural analysis of d(GCAATTGC)2 and its complex with berenil by nuclear magnetic resonance spectroscopy. *Biochemistry* **1990,** 29, 6585-6592.

108. Gresh, N.; Pullman, B. A theoretical study of the nonintercalative binding of berenil and stilbamidine to double-stranded (dA-dT)n oligomers. *Mol Pharmacol* **1984,** 25, 452-458.

109. Richard R. Tidwell, D. D. W. B. Dicationic DNA Minor Groove Binders as Antimicrobial Agents. In *Small Molecule DNA and RNA Binders*, Dr. Martine Demeunynck, D. C. B. P. D. W. D. W., Ed. 2004; pp 414-460.

110. Queener, S. F. New Drug Developments for Opportunistic Infections in Immunosuppressed Patients: Pneumocystis carinii. *Journal of Medicinal Chemistry* **1995,** 38, 4739-4759.

111. Nguyen, B.; Lee, M. P. H.; Hamelberg, D.; Joubert, A.; Bailly, C.; Brun, R.; Neidle, S.; Wilson, W. D. Strong Binding in the DNA Minor Groove by an Aromatic Diamidine with a Shape That Does Not Match the Curvature of the Groove. *Journal of the American Chemical Society* **2002,** 124, 13680-13681.

112. Edwards, K. J.; Jenkins, T. C.; Neidle, S. Crystal structure of a pentamidine-oligonucleotide complex: implications for DNA-binding properties. *Biochemistry* **1992,** 31, 7104-7109.

113. Donkor, I. O.; Tidwell, R. R.; Jones, S. K. Pentamidine Congeners. 2. 2-Butene-Bridged Aromatic Diamidines and Diimidazolines as Potential Anti-Pneumocystis carinii Pneumonia Agents. *Journal of Medicinal Chemistry* **1994,** 37, 4554-4557.

114. Tidwell, R. R.; Jones, S. K.; Geratz, J. D.; Ohemeng, K. A.; Cory, M.; Hall, J. E. Analogs of 1,5-bis(4-amidinophenoxy)pentane (pentamidine) in the treatment of experimental Pneumocystis carinii pneumonia. *Journal of Medicinal Chemistry* **1990,** 33, 1252-1257.

115. Boykin, D. W.; Kumar, A.; Spychala, J.; Zhou, M.; Lombardy, R. J.; Wilson, W. D.; Dykstra, C. C.; Jones, S. K.; Hall, J. E. Dicationic Diarylfurans as Anti-Pneumocystis carinii Agents. *Journal of Medicinal Chemistry* **1995,** 38, 912-916.

116. Das, B. P.; Boykin, D. W. Synthesis and antiprotozoal activity of 2,5-bis(4-guanylphenyl)furans. *Journal of Medicinal Chemistry* **1977,** 20, 531-536.

117. Steck, E. A.; Kinnamon, K. E.; Davidson, D. E.; Duxbury, R. E.; Johnson, A. J.; Masters, R. E. Trypanosoma rhodesiense: Evaluation of the antitrypanosomal action of 2,5-bis(4-guanylphenyl)furan dihydrochloride. *Experimental Parasitology* **1982,** 53, 133-144.

118. Chaires, J. B.; Ren, J.; Hamelberg, D.; Kumar, A.; Pandya, V.; Boykin, D. W.; Wilson, W. D. Structural Selectivity of Aromatic Diamidines. *Journal of Medicinal Chemistry* **2004,** 47, 5729-5742.

119. Boykin, D. W.; Kumar, A.; Xiao, G.; Wilson, W. D.; Bender, B. C.; McCurdy, D. R.; Hall, J. E.; Tidwell, R. R. 2,5-Bis[4-(N-alkylamidino)phenyl]furans as Anti-Pneumocystis carinii Agents. *Journal of Medicinal Chemistry* **1998,** 41, 124-129.

120. Trent, J. O.; Clark, G. R.; Kumar, A.; Wilson, W. D.; Boykin, D. W.; Hall, J. E.; Tidwell, R. R.; Blagburn, B. L.; Neidle, S. Targeting the Minor Groove of DNA: Crystal Structures of Two Complexes between Furan Derivatives of Berenil and the DNA Dodecamer d(CGCGAATTCGCG)2. *Journal of Medicinal Chemistry* **1996,** 39, 4554-4562.

121. Laughton, C. A.; Tanious, F.; Nunn, C. M.; Boykin, D. W.; Wilson, W. D.; Neidle, S. A Crystallographic and Spectroscopic Study of the Complex between d(CGCGAATTCGCG)2

and 2,5-Bis(4-guanylphenyl)furan, an Analogue of Berenil. Structural Origins of Enhanced DNA-Binding Affinity&#x2020. *Biochemistry* **1996,** 35, 5655-5661.

122. Wilson, W. D.; Ratmeyer, L.; Zhao, M.; Strekowski, L.; Boykin, D. The search for structure-specific nucleic acid-interactive drugs: Effects of compound structure on RNA versus DNA interaction strength. *Biochemistry* **1993,** 32, 4098-4104.

123. Weisblum, B.; Haenssler, E. Fluorometric properties of the bibenzimidazole derivative hoechst 33258, a fluorescent probe specific for AT concentration in chromosomal DNA *Chromosoma* **1974,** 46, 255-260.

124. Harshman, K. D.; Dervan, P. B. Molecular recognition of B-DNA by Hoechst 33258. *Nucl. Acids Res.* **1985,** 13, 4825-4835.

125. Lammler, G.; Herzog, H.; Saupe, E.; Schutze, H. Chemoterapeutic studies of Litomosodoides carini infection of Mastomys nataleusis 1. The filaricidal action of 2,6-bis-benzimidazoles. *WHO Bull* **1971,** 44, 751-756.

126. Kraut, E.; Fleming, T.; Segal, M.; Neidhart, J.; Beherens, B.; Mac Donald, J. Phase II study of Pibenzimol in pancreatic cancer - A southwest oncology group study. *Invest New Drugs* **1999,** 9, 95-96.

127. Czarny, A.; Boykin, D. W.; Wood, A. A.; Nunn, C. M.; Neidle, S.; Zhao, M.; Wilson, W. D. Analysis of van der Waals and Electrostatic Contributions in the Interactions of Minor Groove Binding Benzimidazoles with DNA. *Journal of the American Chemical Society* **1995,** 117, 4716-4717.

128. Bontemps, J.; Houssier, C.; Fredericq, E. Physico-chemical study of the complexes of '33258 Hoechst' with DNA and nucleohistone. *Nucl. Acids Res.* **1975,** 2, 971-984.

129. Loontiens, F. G.; Regenfuss, P.; Zechel, A.; Dumortier, L.; Clegg, R. M. Binding characteristics of Hoechst 33258 with calf thymus DNA, poly[d(A-T)] and d(CCGGAATTCCGG): multiple stoichiometries and determination of tight binding with a wide spectrum of site affinities. *Biochemistry* **1990,** 29, 9029-9039.

130. Ebrahimi, S. E. S.; Bibby, M. C.; Fox, K. R.; Douglas, K. T. Synthesis, DNA binding, footprinting and in vitro antitumor studies of a meta-hydroxy analog of Hoechst 33258. *Anti-Cancer Drug Design* **1995,** 10, 463-479.

131. Finlay, G. J.; Baguley, B. C. Potentiation by phenylbisbenzimidazoles of cytotoxicity of anticancer drugs directed against topoisomerase II. *European Journal of Cancer and Clinical Oncology* **1990,** 26, 586-589.

132. Tanious, F. A.; Hamelberg, D.; Bailly, C.; Czarny, A.; Boykin, D. W.; Wilson, W. D. DNA Sequence Dependent Monomer−Dimer Binding Modulation of Asymmetric Benzimidazole Derivatives. *Journal of the American Chemical Society* **2004,** 126, 143-153.

133. Wang, L.; Carrasco, C.; Kumar, A.; Stephens, C. E.; Bailly, C.; Boykin, D. W.; Wilson, W. D. Evaluation of the Influence of Compound Structure on Stacked-Dimer Formation in the DNA Minor Groove&#x2020. *Biochemistry* **2001,** 40, 2511-2521.

134. Fairley, T. A.; Tidwell, R. R.; Donkor, I.; Naiman, N. A.; Ohemeng, K. A.; Lombardy, R. J.; Bentley, J. A.; Cory, M. Structure, DNA minor groove binding, and base pair specificity of alkyl- and aryl-linked bis(amidinobenzimidazoles) and bis(amidinoindoles). *Journal of Medicinal Chemistry* **1993,** 36, 1746-1753.

135. Mallena, S.; Lee, M. P. H.; Bailly, C.; Neidle, S.; Kumar, A.; Boykin, D. W.; Wilson, W. D. Thiophene-Based Diamidine Forms a “Super” AT Binding Minor Groove Agent. *Journal of the American Chemical Society* **2004,** 126, 13659-13669.

136. Tanious, F. A.; Laine, W.; Peixoto, P.; Bailly, C.; Goodwin, K. D.; Lewis, M. A.; Long, E. C.; Georgiadis, M. M.; Tidwell, R. R.; Wilson, W. D. Unusually Strong Binding to the DNA Minor Groove by a Highly Twisted Benzimidazole Diphenylether: Induced Fit and Bound Water&#x2020. *Biochemistry* **2007,** 46, 6944-6956.

137. Goodwin, K. D.; Lewis, M. A.; Tanious, F. A.; Tidwell, R. R.; Wilson, W. D.; Georgiadis, M. M.; Long, E. C. A High-Throughput, High-Resolution Strategy for the Study of Site-Selective DNA Binding Agents: Analysis of a “Highly Twisted” Benzimidazole-Diamidine. *Journal of the American Chemical Society* **2006,** 128, 7846-7854.

138. Miao, Y.; Lee, M. P. H.; Parkinson, G. N.; Batista-Parra, A.; Ismail, M. A.; Neidle, S.; Boykin, D. W.; Wilson, W. D. Out-of-Shape DNA Minor Groove Binders: Induced Fit Interactions of Heterocyclic Dications with the DNA Minor Groove&#x2020. *Biochemistry* **2005,** 44, 14701-14708.

5. Design and Synthesis of Linear Diamidine Molecules as Antiparasitic Agents

Abstract

Diamidine compounds, DNA minor groove binders, have been used as treatment for many different diseases for over half a century. Typically, DNA minor groove binders need to be crescent shaped to create a complimentary fit in the groove. However, recent studies indicate that linear dicationic molecules can show a strong binding affinity with DNA and show promising antiparasitic activity in *in vivo*. These linear molecules can bind as strongly to DNA as crescent shaped dicationic compounds. To further evaluate the linear dicationic molecules, a small series of diamidine arylacetylene derivatives were synthesized and two of them were tested against *Trypanosoma brucei rhodesiense* and *Plasmodium falciparum*. However, the examined diamidine derivatives were found to have only moderate *in vitro* activity.

5.1. Introduction

DNA carries the genetic information about living organisms and is intricately involved in many essential biological and pathological processes. The clarification of the DNA structure by Watson and Crick in 1953 opened a new era in molecular biology. As DNA studies have progressed, increased understanding of its structure and role in living cells has made oligonucelotides a promising target for design of therapeutic reagents.

Proteins, natural products, and synthetic cationic products can show strong reversible and irreversible interactions with double helix grooves. [1] Aromatic cations have shown strong and reversible binding affinities at DNA minor grooves. [2] These interactions can be used to develop new therapies. Diamidine compounds such as pentamidine, propamidine, and berenil have been successfully used to treat infections caused by parasites and fungi. [3] Pentamidine is used in the initial stage of HAT, as well as a secondary treatment for AIDS related *P. jiroveci*

pneumonia. [4] Studies show that biological activities of aromatic diamidine compounds have been correlated with their interaction with the DNA minor groove at AT sequences. [1]

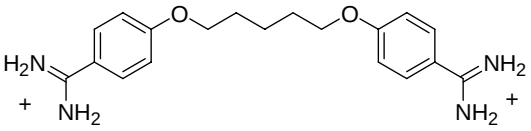

Pentamidine

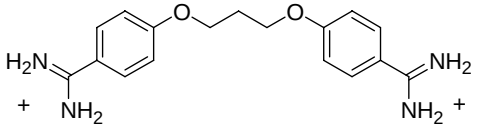

Propamidine

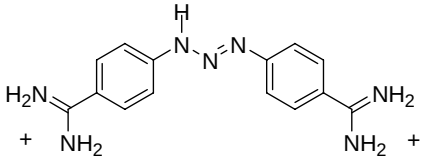

Berenil

Figure 5.1. Structure of diamidine compounds that have been successfully used to treat infections caused by parasites and fungi.

The typical interactions of molecules which exhibit strong DNA minor groove binding, are as follows: H-bonding, van der Walls interactions, complementary charge and complementary shape. A curved shaped molecule provides the optimal fit to the helical curve in DNA. In support of the optimal fit theory, many crescent shaped diamidine compounds show strong binding affinity in A-T rich sequences such as pentamidine, furamidine and their analogs. However, recent studies indicate that near linear diamidine compounds also can show quite a strong interaction with minor groove at A-T sites. [5]

Unexpectedly, DNA binding studies with the linear diamidine compound **CGP 40215** showed that it binds quite strongly to A-T sequences. However, it was commonly believed that the ligand should have a curved shape to create a perfect match to the helical turn in the minor grove. The crystal structure of the complex of **CGP 40215** at a AATT binding site provided an explanation for the unexpected binding capability of the linear compound.

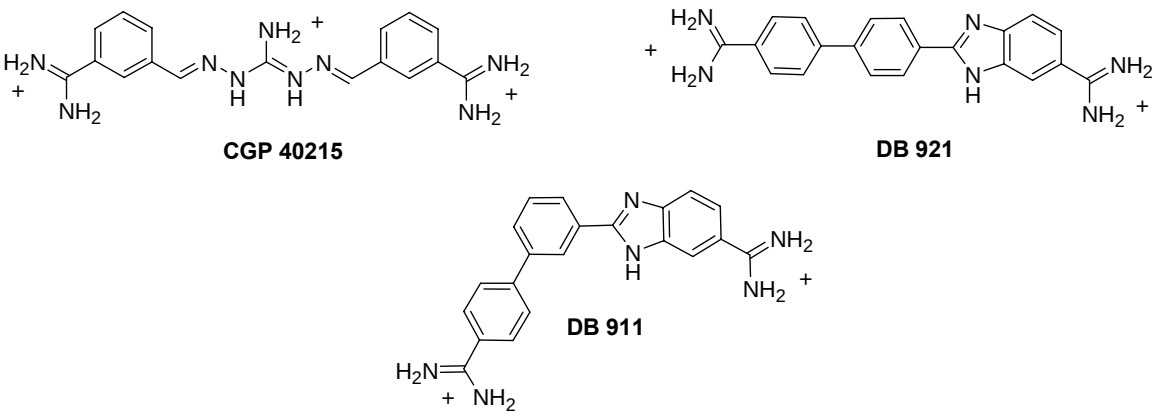

Figure 5.2. Structure of dicationic aryldiamidines which shown unusual binding affinity with duble helix.

A single water molecule is able to form a direct contact between the cationic amidine ends of the compound and the A-T base pair groups at the floor of the minor groove. **CGP 40215** completes the curved shape by interaction with water in the DNA-ligand complex. A similar observation was recorded during the investigation of biphenylbenzimidazole derivatives. **DB 911** has a central meta-substituted phenyl that gives it a classical curved shape that binds to the DNA minor groove with a strong affinity. On the other hand, **DB 921** has a central para-substituted phenyl that has a much more linear shape, which obviously does not match the curvature of the DNA minor groove. However, binding studies have shown that **DB 921**, even though it is near linear, has an almost 10 fold higher binding affinity to the DNA minor groove at A-T sequences. Compound to **CGP 40215** and **DB 921** interact with a water molecule in the complex to form a complementary module.[6] In addition to the strong binding affinity, many other linear shaped dicationic compounds show promising *in vivo* activity against parasites in animal models.[7]

Based on this previous knowledge, we have designed derivatives of linear diamidine compounds that may target the AT rich minor groove and may serve as a therapeutic agents, Figure 5.3. We decided to make linear diamidines which are symmetric, These molecules may be viewed as a a simplification of **DB 921,** in which the benzimidazole group is removed. The designed molecules (Figure 5.3) are some what longer than DB 921, and are devoid of hydrogen bond donors other than the amidine units. In this line, a small series of dicationic amidinophenylethynyl benzene derivatives were synthesized in order to evaluate their DNA binding and biological activities.

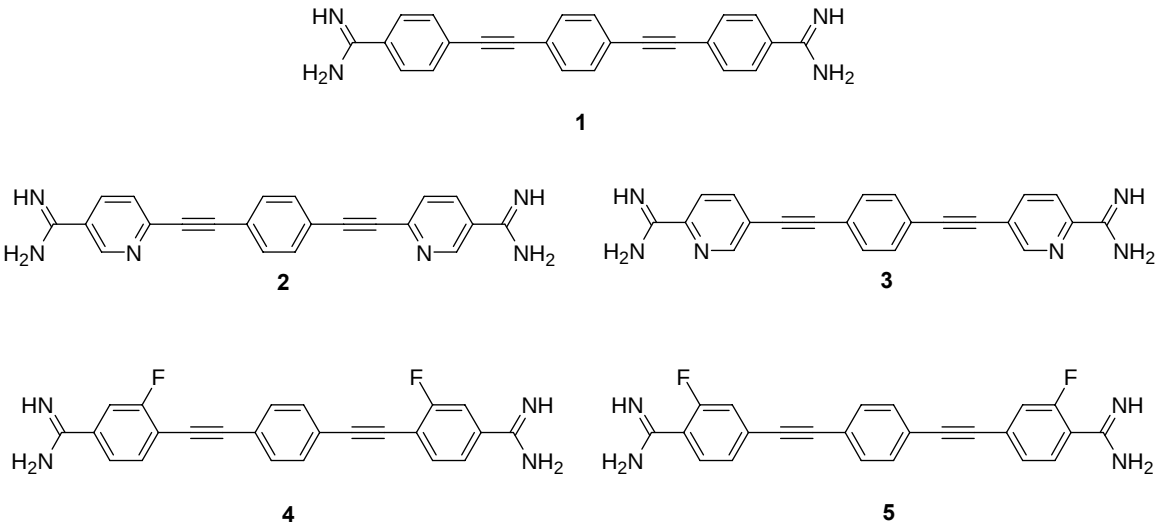

Figure 5.3. Chemical structures of bis-amidinophenylethynyl benzene derivatives.

5.2. Result and Discussion

5.2.1. Chemistry

The target diamidino arylacetylenes **1-5** were obtained from the respective bis-nitriles **14-18** by direct reaction using lithium trimethylsilylamide, Scheme 5.1. The bis-nitriles intermediates were synthesized by palladium catalyzed Sonogashira coupling reactions of the respective bromo arylnitriles **9-13** and diethynylbenzene **8**. The syntheses of the bis-nitriles **14-18**

require diethynylbenzene **8** as a common precursor. Diethynylbenzene **8** was conveniently achieved in two steps; starting with a Sonogashira coupling between diiodobenzene **6** and trimethylsilylacetylene followed by deprotection of trimethylsilyl- under basic conditions to furnish diethynylbenzene **8.**

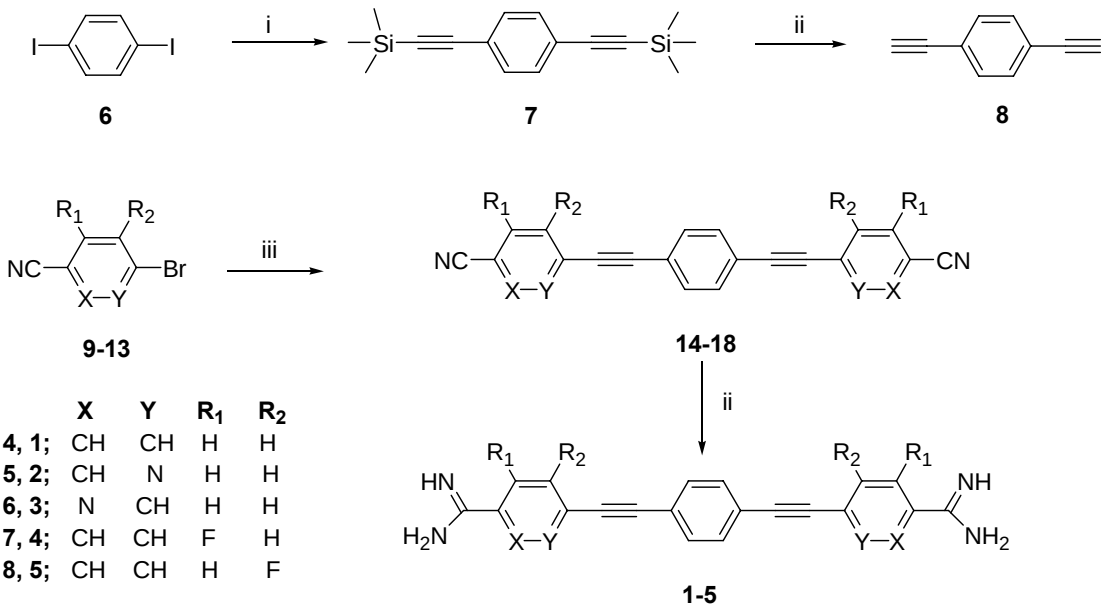

	X	Y	R_1	R_2
9, 14, 1;	CH	CH	H	H
10, 15, 2;	CH	N	H	H
11, 16, 3;	N	CH	H	H
12, 17, 4;	CH	CH	F	H
13, 18, 5;	CH	CH	H	F

Scheme 5.1. Synthesis of biamidino arylacetylene derivatives.

Reagents and conditions: i) $(CH_3)_3SiCCH$, $Pd(PPh_3)_3Cl_2$, CuI, PPh_3, diethylamine, DMF, 120 ^{o} C, 68%; ii) LiOH, MeOH, 90%; iii) **9-13**, 1,4-diethynylbenzene **8,** $Pd(PPh_3)_4$, CuI, diethylamine, DMF, 120 ^{o} C, 24-38%; iv) $LiN(TMS)_2$, THF, rt., MeOH, HCl, 75-92%.

The bis-nitrile synthesis route was quite straightforward. However, the coupling reactions gave undesired mono, homo, and self-coupling products and poor yields of the desired compounds, eventhough the reactions were carefully conducted in an inert atmosphere, using a well-dried apparatus, reagents, and solvents. Despite many experimental trials with different conditions, the best yield of the desired products was 38%.

Under these circumstances, we designed a different synthetic approach for obtaining the bis-nitriles by Sonogashira coupling between arylacetylene and diiodoarene, Scheme 5.2. First, 4-ethynylbenzonitrile **20** was synthesized from 4-bromobenzonitrile **9** with similar reaction sequences as described above for synthesis of **8**. Sonogashira coupling of **20** and 1,4-diiodobenzene **6** gave the desired product 1,4-bis-(4-cyanophenylethynyl)benzene **14,** however, only in a 42% yield.

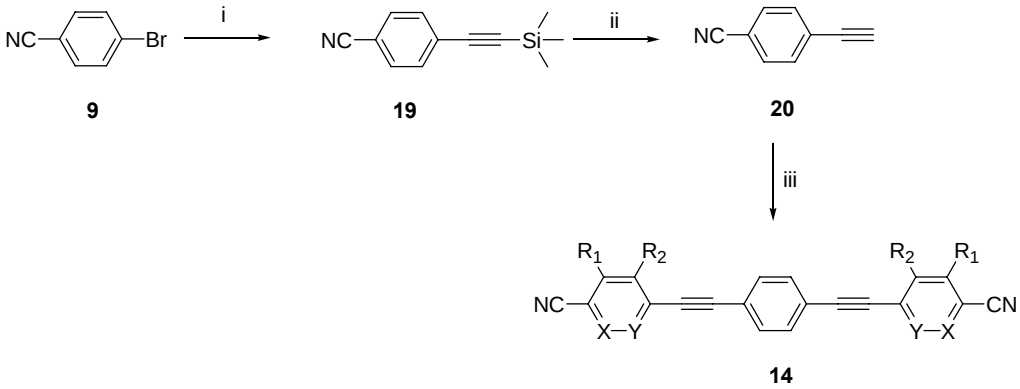

Scheme 5.2. An alternative synthesis route of bis-nitrile.

Reagents and conditions**:** i) $(CH_3)_3SiCCH$, $Pd(PPh_3)_3Cl_2$, CuI, PPh_3, diethylamine, DMF, 120 ^{o} C, 68%; ii) LiOH, MeOH, 89%; iii) 4-ethynylbenzonitrile **20**, 1,4-diiodobenzene, CuI, PPh_3, diethylamine, DMF, 120 ^{o} C, 42%.

The yield was only slightly improved compared to first synthesis approach. The convenience of direct use of commercially available bromo arylnitriles in Sonogashira coupling with diethynylbenzene lead us to use the first route, Scheme 5.1.

5.2.2. Biology

Aromatic diamidines are well known cationic molecules that have a strong and reversible interaction with DNA. Recent work has shown that linear and near linear molecules exhibit excellent biological activity against trypanosomes.[8] The mechanism of action for antitrypanosomal activity has been suggested to involve the inhibition of DNA dependent enzymes or direct inhibition of transcription.[9, 10]

Table 5.1. DNA affinities and *in vitro* antiprotozoan data for linear dications.

Compound	ΔTm^a (^{o} C)	*T.b.r.*[b] IC_{50} (μM)	*P.f.*[b] IC_{50} (μM)	cytotoxicity[c] IC_{50} (μM)
Pentamidine	12.6	0.0022	NA	2.1
Furamidine	25.0	0.0045	0.0155	6.4
DB 921	28.0	0.0077	0.0005	17.0
DB 1762 (1)	4.0	0.812	0.166	7.4
DB 1914 (2)	NA	0.441	0.22	99.6

[a] Poly(d(A-T)$_2$ in MES10 buffer; ratio compound/DNA is 0.3. [b] The *T.b.r.*(*Trypanosoma brucei rhodesiense*) strain was STIB900, and the *P. f.* (*Plasmodiumfalciparum*) strain was K1. [c]Cytotoxicity was evaluated using cultured L6 rat myoblast cells using the same assay procedure for *T. b. r.*

The biological activity of newly synthesized linear dicationic compounds; **DB 1762**, **1** and **DB 1914**, **2** was evaluated against *T.b.r.* and *P.f.* However, the new compounds were much less active than standard compounds in Table 5.1. **DB 1762** and **DB 1914** gave IC_{50} values against *T.b.r* of 0.812 and 0.441 μM, respectively, compared to values of the standards at 2 to 7 nM,

Table 5.1. The activity of **DB 1762** and **DB 1914** agaist *P.f.* (IC_{50} value of 0.666 and 0.221 μM) was also much less than the standard (0.0155 μM). The ΔTm value of **DB 1762** was found significanly less than standard compounds. Most likely, **DB 1762** does not bind to the DNA with a strong affinity. The moderate bioactivity maybe due to low DNA affinity, poor cellular up take or a combination of both. We are awaiting data on the remaining analogs which are structurally quite similar. Nevertheless, it is unlikely that further studies on these analogues will be performed.

5.3. Conclusions

Diarylamidines have been used as chemotherapeutic agents for infections caused by parasites since the middle of the 20^{th} century. Their mechanisms of action against the microbes are not well understood. Along with the great activity of these dicationic compounds, they also exhibit toxic effects. Studies to overcome these major drawbacks are continuing.

5.4. Methods and Materials

5.4.1. Synthesis

All moisture and air sensitive reactions were carried out in glassware that was oven dried overnight and under dry nitrogen (passed through drying agents). Commercially supplied chemicals and reagents were used without additional purification. Ether and THF were distilled from Na and benzophenone. Triethylamine (CaH_2) and ethanol (Mg/I_2) were distilled from the indicated drying agents. Ethanolic HCl solutions were prepared from fresh distilled dry ethanol that was treated with dry HCl gas for 10-15 min at ice bath temperature. Anhydrous DMF was purchased from Aldrich. TLC analysis was carried out on silica gel 60 F_{254} coated aluminum sheets and detection was with two wavelengths of UV light. Column chromatography was performed with silica gel (flash 32-63 nm), from Dynamic Adsorbents Inc, in Norcross, GA.

Melting points were recorded using a Mel-Temp 3.0 capillary melting point apparatus and are uncorrected. Mass spectrometry analyses were performed by the Mass Spectrometry Facilities of Georgia State University by chemical ionization under conditions which gave the protonated species M+1. Elemental analyses were performed by Atlantic Microlab, Atlanta, GA. ^{1}H and ^{13}C NMR spectra were recorded a Bruker 400 MHz instrument. Chemical shifts (δ) are given in ppm relative to TMS (0 ppm), DMSO (2.49 ppm), $CHCl_3$ (7.24 ppm) or MeOH (3.31 ppm) for ^{1}H spectra and TMS (0 ppm), DMSO (39.52 ppm), $CHCl_3$ (77.16 ppm) or MeOH (49.00 ppm) for ^{13}C spectra.

5.4.2. In Vitro Assays

In vitro efficacy and cyctotoxcity studies were performed at the Swiss Tropical Institute in Basel, Switzerland under the direction of Professor Reto Brun according to published procedures (*T.b.r.*,[11] *P.f.*[12, 13] and cyctotoxcity[14]). *Tm* measurments were performed at Georgia State University, under the direction of Professor David Wilson. We are grateful for being provided these data by Professor Brun and Professor Wilson.

5.4.3. Synthetic Procedures

1,4-Bis-trimethylsilanylethynylbenzene (**7**).

A mixture of 1,4-diiodobenzene **6** (2 g, 6.0 mmol), $Pd(PPh_3)Cl_2$ (420 mg, 0. 6 mmol), CuI (40 mg, 0. 6 mmol), triphenylphosphine (630 mg, 2.4 mmol) was degassed and flushed three times with dry nitrogen. Trimethylsilylacetylene (2.5 mL, 18 mmol), dry diethylamine (3 mL), and dry DMF (3 mL) was injected into a pressure glass vial and sealed with a Teflon septum. The mixture was stirred at 120 ºC for 2 hours. The solvent was removed under reduced pressure to give a residue, which was dissolved in ethyl acetate (50 mL) and washed with 5% $NaHCO_3$ (2 × 20 mL). The organic layer was dried over Na_2SO_4. The organic layer was filtered, the filtrate

was concentrated under reduced pressure and the residue was purified with column chromatography eluting with hexenes /ethylacetate (5:1) to give **7** as a white solid (1.1 g, 68%); mp: 120-121 ^{o}C; (lit[15] mp: 117-119 ^{o}C). ^{1}H NMR ($CDCl_3$): δ 7.38 (s, 4H), 0.24 (s, 18H). ^{13}C NMR (100 MHz, $CDCl_3$): δ 131.9, 123.4, 104.81, 96.5, 0.25 ppm.

1,4-Diethynylbenzene (**8**).

1,4-Bis-(trimethylsilanylethynyl)benzene **7** (1.0 g, 3.7 mmol) and LiOH (0.2 g 8.3 mmol) were dissolved in methanol (5 mL) and dicholoromethane (5 mL), and the mixture was stirred at room temperature overnight. The solvent was removed under reduced pressure and the residue was dissolved in ethyl acetate (150 mL) and washed with 5% $NaHCO_3$ (3 ×20 mL). The organic layer was dried over Na_2SO_4, filtrered and the filtrate was concentrated under reduced pressure. The solid was purified with column chromatography by eluting with hexanes/ethyl acetate (7:1) to give **8** as a white solid (420 mg, 90%); mp: 97-98 ^{o}C; (lit[16] mp: 96-97 ^{o}C). ^{1}H NMR ($CDCl_3$): δ 7.42 (s, 4H), 3.16 (s, 2H). ^{13}C NMR (100 MHz, $CDCl_3$): δ 132.1, 122.7, 83.22, 79.33 ppm.

4-[(Trimethylsilyl)ethynyl]benzonitrile (19).

19 was synthesized by following a similar procedure as that used for the synthesis of **7**, starting with 4-bromobenzonitrile **9**. The crude product was purified with column chromatography by eluting with hexanes/ethyl acetate (4:1) to give **10** as a white solid **(**62%); mp: 96-97 ^{o}C; (lit[17] mp: 96-98 ^{o}C). ^{1}H NMR ($CDCl_3$): δ 7.58 (d, *J*= 8.4, 2H), 7.52 (d, *J*= 8.4, 2H) 0.26 (s, 9H). ^{13}C NMR (100 MHz, $CDCl_3$): δ 132.4, 131.9, 127.9,118.3, 102.9, 99.5, -0.27 ppm.

4-Ethynylbenzonitrile (20).

20 was synthesized by following a similar procedure as that used for the synthesis of 1,4-diethynylbenzene **8**, starting with compound **19**. The crude product was purified with column chromatography by eluting with hexanes/ethyl acetate (3:1) to give **20** as a white solid **(**89%); mp: 96-97 ^{o}C; (lit[17] mp: 96-98 ^{o}C). ^{1}H NMR ($CDCl_3$): δ 7.62 (d, *J*= 8.4, 2H), 7.57 (d, *J*= 8.4, 2H), 3.30 (s, 1H). ^{13}C NMR (100 MHz, $CDCl_3$): δ 132.6, 132.0, 127.9,118.2, 112.3, 81.87, 81.57 ppm.

1,4-Bis-(4-cyanophenylethynyl)benzene (14).

A mixture of 4-bromobenzonitrile **9** (2 g, 10.9 mmol), $Pd(PPh_3)Cl_2$ (379 mg, 0.54 mmol), CuI (140 mg, 2.17 mmol), triphenylphosphine (141 mg, 0.54 mmol), 1,4-diethynylbenzene **8** (688 mg, 5.4 mmol) was degased in a round bottom flask and flushed with dry nitrogen three times. Dry triethylamine (5 mL) and dimethylformamide (10 mL) was injected into the mixture. The reaction mixture was stirred at 110-120 ºC overnight in a nitrogen atmosphere. The solvent was removed *in vacuo* to give a residue, which was dissolved in dichloromethane (250 mL) and the organic layer was washed with 1 N NH_4Cl (3×50 mL). The organic layer was dried over $MgSO_4$ and filtered. The filtrate was treated with charcoal and was allowed to heat at reflux for an hour. The solvent was filtered through celite while hot. The filtrate was concentrated under reduced pressure and the residue was crystallized in DMF (3 mL), the solid was washed with dry ether to give a white solid in (680 mg, 37%); mp: 278-280 ^{o}C . ^{1}H NMR (400 MHz, $CDCl_3$): δ 7.65 (d, *J*= 8.8, 4H), 7.61 (d, *J*= 8.8, 4H), 7.54 (s, 4H).

Alternative synthesis of 1,4-bis-(4-cyanophenylethynyl)benzene (**14**).

A mixture of 4-ethynylbenzonitrile **20** (2 g, 15.7 mmol), $Pd(PPh_3)Cl_2$ (273 mg, 0.4 mmol), CuI (25 mg, 0.4 mmol), 1,4-diiodobenzene **6** (2.6 g, 7.8 mmol) was degased in a round bottom flask

and flushed with dry nitrogen three times. Dry triethylamine (7 mL) and anhydrous dimethylformamide (15 mL) was injected into the mixture. The reaction mixture was bubbled with nitrogen for 15 min, then stirred at 110-120 ºC for 32 hours in a nitrogen atmosphere. The solvent was removed under reduced pressure, and the yellow residue was dissolved in dichloromethane (400 mL) and the organic layer was washed with 1 N NH_4Cl (4×100 mL). The organic layer was dried over $MgSO_4$ and filtered. The filtrate was treated with charcoal and was allowed to heat at reflux for an hour. The organic solvent was filtered through celite while hot. The filtrate was concentrated under reduced pressure and the residue was crystallized from DMF (2 mL) and ether (2 mL) mixture. The solid was washed with dry ether to give a white solid in (1.5 g, 42%); mp: 278-281 ^oC . ^1H NMR (400 MHz, d_6-DMSO): δ 7.90 (d, J= 8.4, 4H), 7.76 (d, J= 8.4, 4H), 7.67 (s, 4H). Analysis calculated for $C_{24}H_{12}N_2$-0.5H_2O: C, 85.44; H, 3.88; N, 8.30; found: C, 85.90; H, 3.68; N, 8.30.

1,4-Bis-(5-cyanopyridyl-2ylethynyl) benzene (**15**).

15 was synthesized by following a similar procedure as that used for the synthesis of 1,4-bis-(4-cyanophenylethynyl)benzene **14** starting with 6-bromonicotinonitrile **10** to yield **15** as a pale yellow solid (35%); mp: 344-347 ^oC. ^1H NMR (400 MHz, d_6-DMSO): δ 9. 04 (d, J= 1.2, 2H), 8.36 (dd, J_1= 2.0, J_2= 8.0, 2H), 7.87 (d, J= 8.4, 2H), 7.76 (s, 4H). Analysis calculated for $C_{22}H_{10}N_4$-0.25H_2O: C, 78.91; H, 3.16; N, 16.73; found: C, 78.95; H, 3.11; N, 16.75.

1,4-Bis-(2-cyanopyridyl-5ylethynyl)benzene (**16**).

16 was synthesized by following a similar procedure as that used for the synthesis of 1,4-bis-(4-cyanophenylethynyl)benzene **14** starting with 5-bromo-2-cyanopyridine **11** to yield **16** as a pale yellow solid (25%) ; mp: 344-347 ^oC. ^1H NMR (400 MHz, d_6-DMSO): δ 8.94 (d, J= 2,

2H), 8.24 (dd, J_1= 2.0, J_2= 8.0, 2H), 8.10 (d, J= 8.0, 2H), 7.73 (s, 4H). Analysis calculated for $C_{22}H_{10}N_4$-0.9H_2O: C, 76.24; H, 3.32; N, 16.16; found: C, 76.55; H, 3.32; N, 15.94.

1,4-Bis-(2-fluoro-4-cyanophenylethynyl)benzene (**17**).

17 was synthesized by following a similar procedure as that used for the synthesis of 1,4-bis-(4-cyanophenylethynyl)benzene **14** starting with 4-bromo-3-fluorobenzonitrile **12** to yield **17** as a pale yellow solid (28%) ; mp: 240-243 ^oC. ^1H NMR (400 MHz, $CDCl_3$): δ 7.66-7.56 . (m, 6H), 7.48-7.43 (m, 4H). Analysis calculated for $C_{24}H_{10}F_2N_2$-0.8$C_4H_{10}O$: C, 77.11; H, 4.28; N, 6.61; found: C, 78.54; H, 4.24; N, 5.98.

1,4-Bis-(3-fluoro-4-cyanophenylethynyl)benzene (**18**).

18 was synthesized by following a similar procedure as that used for the synthesis of 1,4-bis-(4-cyanophenylethynyl)benzene **14** starting with 4-bromo-2-fluorobenzonitrile **13**to yield **13e** as a pale yellow solid (24%) ; mp: 237-239 ^oC. ^1H NMR (400 MHz, $CDCl_3$): δ 7.65-7.52 . (m, 6H), 7.43-7.28 (m, 4H). Analysis calculated for $C_{24}H_{10}F_2N_2$: C, 79.12; H, 2.77; N, 7.69; found: C, 79.86; H, 2.80; N, 6.95.

1,4-Bis-(4-amidinophenylethynyl)benzene hydrochloride salt (1).

1,4-Bis-(4-cyanophenylethynyl)benzene **14** (100 mg, 0.3 mmol) was placed in an oven dried 50 mL round bottom flask and sealed with a rubber septum. The flask was degassed and flushed with dry nitrogen. Then, fresh distilled THF (3 mL) was injected into the flask with a syringe under a nitrogen atmosphere. The solution was cooled to 0 ^oC in an ice bath and then was treated with lithium trimethylsilyamide (1 M in THF) (2 mL). The reaction mixture was stirred at room temperature overnight. The mixture was cooled in an ice bath and was treated with ethanol-HCl (1 mL). The mixture was stirred for 2 hours and diluted with ether. The precipitate was filtered and washed with generous amounts of ether to yield a white solid. The solid was

suspended in a methanol and water mixture. A 10% NaOH solution was added to the suspension until pH of 10 was reached and then stirred for an hour. The precipitate was filtered and dried under reduced pressure overnight. The solid was suspended in dry MeOH (10 mL) and cooled to 0 ^{o}C in an ice bath and ethanol-HCl (1 mL) was added. The mixture was stirred overnight, diluted with dry ether and filtered. Next, it was washed with dry ether to produce a white solid (80 mg, 61%); mp: 314-317 ^{o}C. ^{1}H NMR (400 MHz, d_6-DMSO): δ 9.33 (br, 8H, NH), 7.91 (d, *J*= 8.0 Hz, 4H), 7.83 (d, *J*= 8.0 Hz, 4H), 7.70 (s. 4H). ESI-MS: m/z calculated for $C_{24}H_{18}N_4$:362.4; found: 363.3 (M+1). Analysis calculated for $C_{24}H_{18}N_4$-2HCl-2H_2O: C, 61.15; H, 4.88; N, 11.89; found: C, 61.21; H, 4.63; N, 11.52.

1,4-Bis-(5-amidinopyridyl-2ylethynyl)benzene hydrochloride salt (**2**).

1,4-Bis-(5-amidinopyridyl-2ylethynyl)benzene hydrochloride salt **2** was synthesized by following a similar procedure as that used for the synthesis of 1,4-bis-(4-amidinophenyl ethynyl) benzene hydrochloride salt **1** starting with 1,4-Bis-(5-cyanopyridyl-2ylethynyl) benzene **15** to yield **2** as a white solid (64%) ; mp: 324-326 ^{o}C. ^{1}H NMR (400 MHz, d_6-DMSO): δ 9.66-9.39 (br d, 8H, NH), 9.03(s, 2H), 8.31 (d, *J*= 8.4 Hz, 2H), 7.95 (d, *J*= 8.0 Hz, 2H), 7.78 (s, 4H). ESI-MS: m/z calculated for $C_{22}H_{16}N_6$: 364.1; found: 365.2 (M+1).Analysis calculated for $C_{22}H_{16}N_6$-4HCl-1.3H_2O-$C_4H_{10}O$: C, 49.92; H, 4.52; N, 15.32; found: C, 49.77; H, 4.11; N, 15.09.

1,4-Bis-(2-amidinopyridyl-5ylethynyl)-benzene hydrochloride salt (**3**).

1,4-Bis-(2-amidinopyridyl-5ylethynyl)-benzene hydrochloride salt **3** was synthesized by following a similar procedure as that used for the synthesis of **1** starting with 1,4-Bis-(2-cyanopyridyl-5ylethynyl)benzene **16** to yield **3** as a white solid (61%) ; mp: >350 ^{o}C. ^{1}H NMR (400 MHz, d_6-DMSO): δ 9.70-9.52 (br d, 8H, NH), 9.02 (s, 2H), 8.40 (s, 4H), 7.76 (s, 4H).

ESI-MS: m/z calculated for $C_{22}H_{16}N_6$: 364.1; found: 365.2 (M+1). Analysis calculated for $C_{22}H_{16}N_6$-4HCl-0.2H_2O-1.3$C_4H_{10}O$: C, 53.53; H, 5.51; N, 13.77; found: C, 53.34; H, 5.29; N, 13.74.

1,4-Bis-(4-amidino-2-fluorophenylethynyl)benzene hydrochloride salt (**4**).

4 was synthesized by following a similar procedure as that used for the synthesis of 1,4-bis-(4-amidinophenylethynyl)benzene hydrochloride salt **1** starting with 1,4-bis-(2-fluoro-4-cyanophenylethynyl)benzene **17** to yield **4** as a white solid (58%) ; mp: >350 ^oC. ^1H NMR (400 MHz, d_6-DMSO): δ 9.57-9.42 (br d, 8H, NH), 7.78-7.74 (m, 4H), 7.71 (s, 4H), 7.70-7.63 (m, 2H). ESI-MS: m/z calculated for $C_{24}H_{16}F_2N_4$: 398.4; found: 399.3 (M+1). Analysis calculated for $C_{24}H_{16}F_2N_4$-2HCl-0.5H_2O: C, 60.01; H, 3.98; N, 11.66; found: C, 60.08; H, 3.97; N, 10.04.

1,4-Bis-(4-amidino-3-fluorophenylethynyl)benzene hydrochloride salt (**5**).

1,4-Bis-(4-amidino-3-fluorophenylethynyl)benzene hydrochloride salt **5** was synthesized by following a similar procedure used for the synthesis of **1** starting with 1,4-bis-(3-fluoro-4-cyanophenylethynyl)benzene **18** to yield **5** as a white solid (52%) ; mp: >350 ^oC. ^1H NMR (400 MHz, d_6-DMSO): δ 9.57-9.42 (br d, 8H, NH), 7.79-7.76 (m, 4H), 7.71 (s, 4H), 7.65-7.63 (m, 2H). ESI-MS: m/z calculated for $C_{24}H_{16}F_2N_4$: 398.4; found: 399.3 (M+1). Analysis calculated for $C_{24}H_{16}F_2N_4$-2HCl-0.25H_2O-0.41$C_4H_{10}O$: C, 60.83; H, 4.48; N, 11.06; found: C, 61.15; H, 3.98; N, 10.61.

References

1. Chaires, J. B.; Ren, J.; Hamelberg, D.; Kumar, A.; Pandya, V.; Boykin, D. W.; Wilson, W. D. Structural Selectivity of Aromatic Diamidines. *J. Med. Chem.* **2004,** 47, 5729-5742.

2. Wang, L.; Bailly, C.; Kumar, A.; Ding, D.; Bajic, M.; Boykin, D. W.; Wilson, W. D. Specific molecular recognition of mixed nucleic acid sequences: An aromatic dication that binds in the DNA minor groove as a dimer. *Proceedings of the National Academy of Sciences* **2000,** 97, 12-16.

3. Crowell, A. L.; Stephens, C. E.; Kumar, A.; Boykin, D. W.; Secor, W. E. Activities of Dicationic Compounds against Trichomonas vaginalis. *Antimicrob. Agents Chemother.* **2004,** 48, 3602-3605.

4. Soeiro, M. N.; De Souza, E. M.; Stephens, C. E.; Boykin, D. W. Aromatic diamidines as antiparasitic agents. *Expert Opinion on Investigational Drugs* **2005,** 14, 957-972.

5. Nguyen, B.; Lee, M. P. H.; Hamelberg, D.; Joubert, A.; Bailly, C.; Brun, R.; Neidle, S.; Wilson, W. D. Strong Binding in the DNA Minor Groove by an Aromatic Diamidine with a Shape That Does Not Match the Curvature of the Groove. *J. Am. Chem. Soc.* **2002,** 124, 13680-13681.

6. Miao, Y.; Lee, M. P. H.; Parkinson, G. N.; Batista-Parra, A.; Ismail, M. A.; Neidle, S.; Boykin, D. W.; Wilson, W. D. Out-of-Shape DNA Minor Groove Binders: Induced Fit Interactions of Heterocyclic Dications with the DNA Minor Groove&#x2020. *Biochemistry* **2005,** 44, 14701-14708.

7. Ismail, M. A.; Arafa, R. K.; Brun, R.; Wenzler, T.; Miao, Y.; Wilson, W. D.; Generaux, C.; Bridges, A.; Hall, J. E.; Boykin, D. W. Synthesis, DNA Affinity, and Antiprotozoal Activity

of Linear Dications: Terphenyl Diamidines and Analogues. *J. Med. Chem.* **2006,** 49, 5324-5332.

8. Ismail, M. A.; Brun, R.; Wenzler, T.; Tanious, F. A.; Wilson, W. D.; Boykin, D. W. Dicationic biphenyl benzimidazole derivatives as antiprotozoal agents. *Bioorganic & Medicinal Chemistry* **2004,** 12, 5405-5413.

9. Wilson, W. D.; Nguyen, B.; Tanious, F. A.; Mathis, A.; Hall, J. E.; Stephens, C. E.; Boykin, D. W. Dications That Target the DNA Minor Groove: Compound Design and Preparation, DNA Interactions, Cellular Distribution and Biological Activity. *Current Medicinal Chemistry - Anti-Cancer Agents* **2005,** 5, 389-408.

10. Fitzgerald, D. J.; Anderson, J. N. Selective Nucleosome Disruption by Drugs That Bind in the Minor Groove of DNA. *J. Biol. Chem.* **1999,** 274, 27128-27138.

11. Baltz, T.; Baltz, D. G., C.; Crockett, J. Cultivation in a semi-defined medium of animal infective forms of Trypanosoma brucei, T. equiperdum, T. evansi, T. rhodesiense and T.gambiense.

. *EMBO Journal,* **1985,** 4, 1273-1277.

12. Räz, B.; Iten, M.; Grether-Bühler, Y.; Kaminsky, R.; Brun, R. The Alamar Blue® assay to determine drug sensitivity of African trypanosomes (T.b. rhodesiense and T.b. gambiense) in vitro. *Acta Tropica* **1997,** 68, 139-147.

13. Matile, H.; Pink, J. R. L. *Plasmodium falciparum malaria parasite cultures and their use in immunology. In Immunological Methods*. Academic Press San Diego, 1990; p 221−234.

14. Nguyen, C.; Kasinathan, G.; Leal-Cortijo, I.; Musso-Buendia, A.; Kaiser, M.; Brun, R.; Ruiz-Perez, L. M.; Johansson, N. G.; Gonzalez-Pacanowska, D.; Gilbert, I. H. Deoxyuridine

Triphosphate Nucleotidohydrolase as a Potential Antiparasitic Drug Target. *Journal of Medicinal Chemistry* **2005,** 48, 5942-5954.

15. Takahashi, S.; Kuroyama, Y.; Sonogashira, K.; Hagihara, N. A Convenient Synthesis of Ethynylarenes and Diethynylarenes

Synthesis **1980**, 627-630.

16. Hay, A. Notes- Preparation of m- and p-Diethynylbenzenes. *The Journal of Organic Chemistry* **1960,** 25, 637-638.

17. Blackburn, B. K.; Lee, A.; Baier, M.; Kohl, B.; Olivero, A. G.; Matamoros, R.; Robarge, K. D.; McDowell, R. S. From Peptide to Non-Peptide. 3. Atropisomeric GPIIbIIIa Antagonists Containing the 3,4-Dihydro-1H-1,4-benzodiazepine-2,5-dione Nucleus. *Journal of Medicinal Chemistry* **1997,** 40, 717-729.

6. Synthesis of Arylimidamides as Potential Leishmanisis Treatment Agents

Abstract

The dicationic 2,5-diaryl furan furamidine and its derivatives have shown promising activities against a variety of protozoans with low toxicity. Our previous work with arylguanidines and arylimidamides analogs of 2,5-diaryl furan have shown exciting *in vitro* results. In this study, a series of new arylimidamides were synthesized by modification of 2,5-diaryl furan framework and were evaluated against *Leishmania amazonensis, Plasmodium falciparum*, *Trypanosoma brucei rhodesiense.* **DB 1852**, **DB 1853**, **DB 1890**, and **DB 1920** were found to be highly active against *L.a.* **DB 1890** showed almost two fold higher activity whereas **DB 1852** showed almost the same activity compared to a current medication, Amphotericin B**. DB 1953** and **DB 1920** were found to be highly effective against *Plasmodium falciparum* and the tolerable cytotoxicity of these compounds make them promising for candidates for further development.

6.1. Introduction

The antimicrobial properties of diarylamidines in the treatment of protozoal diseases such as trypanosomiasis and leishmaniasis were discovered in the 1930s. In the 1970s, diarylamidine derivatives additional attention because of their activities against a number of pathogens, particularly *Trypanosoma*. [1] A large number of the diarylamidine derivatives were synthesized for evaluation. One diarylamidine analog, pentamidine, was found to be active against a variety of protozoa, including *Trypanosoma* brucei gambiense, *Leismania donovani*, and *Pneumocystis carinii*. Pentamidine became a widely used drug for infections caused by these micro-organisms, especially in AIDS patients.[2] A number of diarylamidine cationic derivatives have been shown to bind to the minor-groove of DNA at A-T sequences. This unique interaction of diarylamidines with the minor groove of DNA has been intensely investigated.[3-5] While the

biological effects of these compounds are not fully understood, it is believed that initially the ligands bind to the minor groove and then inhibit DNA dependent enzymes such as topoisomerases, nucleases, etc.[4, 6, 7]

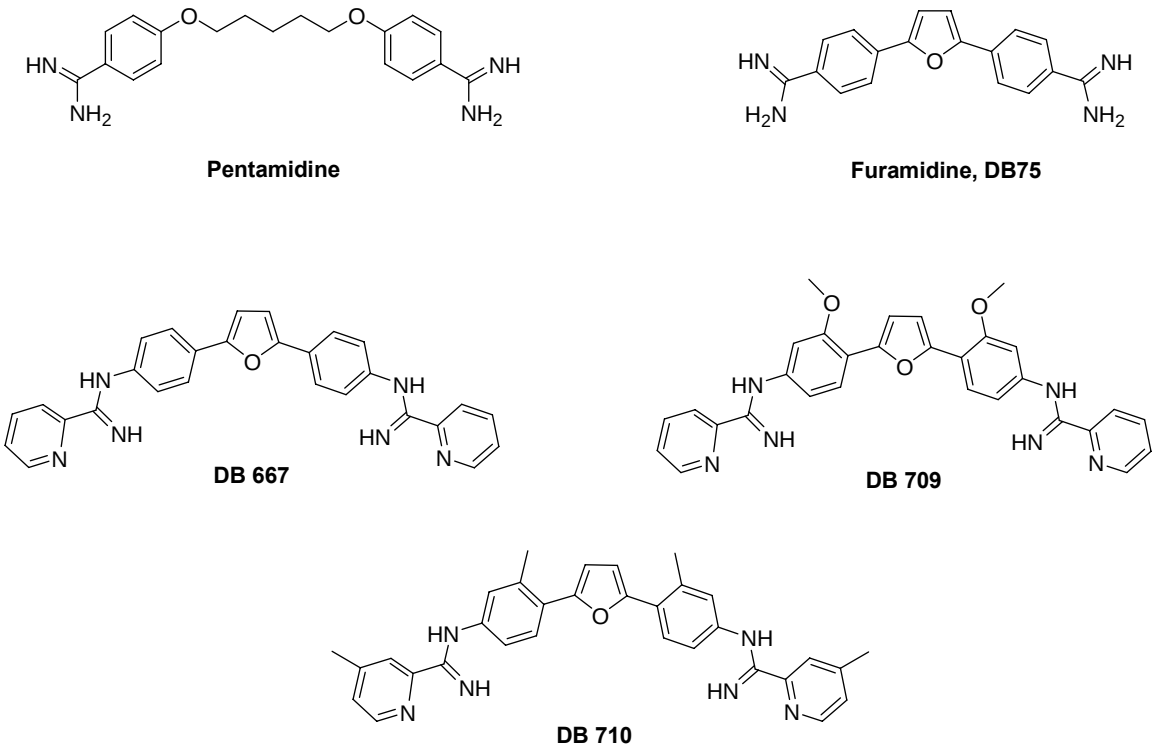

Figure 6.1. Structure of pentamidine, furamidine and previously synthesized arylimidamides.

The dicationic 2,5-diaryl furan furamidine was found to be an effective agent on intravenous administration, in rat model, against *P. carinii*.[8] Studies showed that **DB 75** is more effective and less toxic than pentamidine upon intravenous administration. The *N*-alkyl derivatives of **DB 75** gave similar results, however their toxicity was not as acceptable as **DB 75**.[8] Moreover, additional evaluation with different parasitical species such as *Giardia lamblia*, *Plasmodium falcifarum*, and *Trypanosoma rhodesience* **DB 75** showed promising results as well.[1, 9]

Recent work focused on the furamidine framework in which the amidine groups were replaced with guanidine groups. A series of 2,5-bis-(4-guanidinophenyl) furan analogs were evaluated

against microbial activity. These guanidino derivatives have shown promising *in vitro* activity against both *C. albicans* and *M. tuberculosis.*[12] The conversion of guanidino phenyl moiety to arylimidamides gave compounds which showed both antifungal and antimycobacterial activity. Biophysical results also indicated that both the diguanidines and the arylimidamides in the 2,5-diarylfuran system bind strongly to DNA. The arylimidamide analogs with terminal phenyl- and 2-prydyl- (**DB 667**) were found to be active against *M. tuberculosis* and antifungal species. In addition, the arylimidamide analogues **DB 709**, **DB 710**, and **DB 667**, were found to be more active than pentamidine against *L.a.* (0.37-0.53 μM).[13] Therefore, arylimidamides have great potential for development for Leishmania infections.

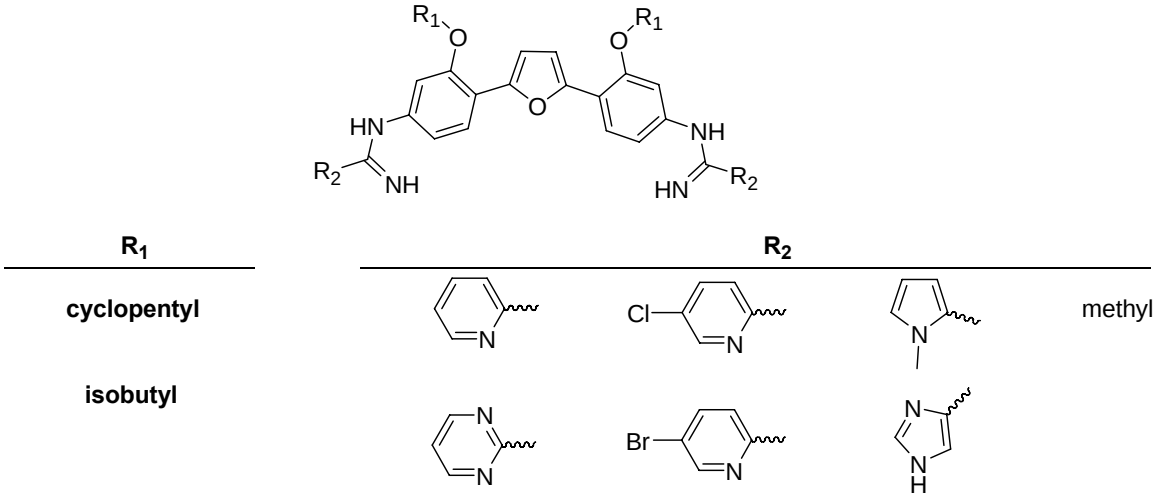

Figure 6.2. The structure of synthesized arylimidamidines.

Our previous work showed that modification of the phenyl units of **DB 667** significantly affected the DNA binding affinity.[12] To further these studies, a new series of arylimidamides was synthesized. The cyclopentyloxy and isobutoxy groups were substituted on the central phenyl rings. In addition, a small study investigated the variation of the terminal *N*-heterocyclic group.

6.2. Results and Discussion

6.2.1. Synthesis

The structure of arylimidamides can be viewed as composed of three different units; the central furan ring, modified phenyl groups on either side of the furan, and the terminal *N*-heterocycles. Our synthetic plan for the preparation of arylimidamides diamino compounds (**22, 23**) as the key precursor is shown in Figure 6.3. The diamino moieties can be achieved in two ways; reduction of the bis-nitrophenyl furans (**20, 21**) by catalytic hydrogenation or by the action of stannous chloride. The preparation of the bis-nitrophenyl furan analogs can be achieved starting with the appropriate substituted bromonitrobenzene and bis-alkylstannyl furan.[14, 15]

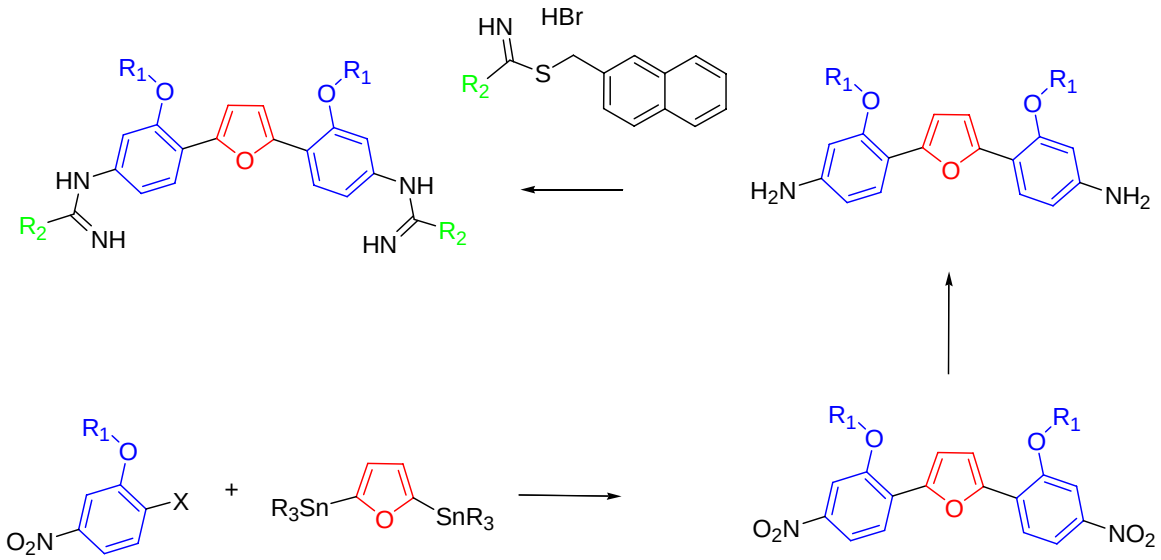

Figure 6.3. Retro synthetic approach for synthesizing arylimidamides.

The synthesis began with the preparation of *o*-alkylbromonitrobenzene analogs **14-16** in two steps, substitution of the aminogroup via a Sandmayer reaction followed by the alkylation of the phenolic hydroxyl group.[16, 17]

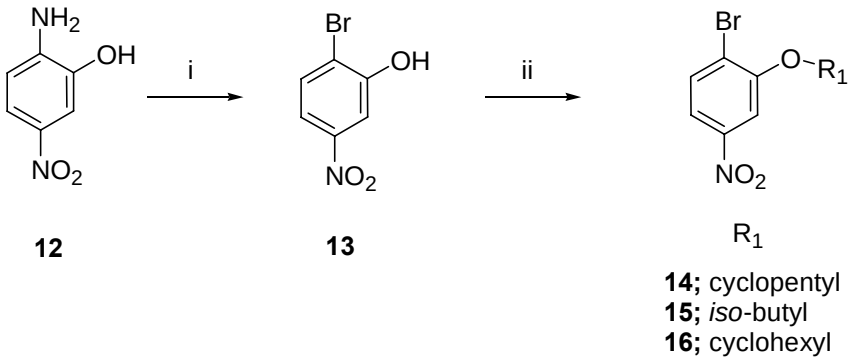

Scheme 6.1. The synthesis of *o*-alkylbromonitrobenzene derivatives.

Reagents and conditions**:** i) $NaNO_2$, NH_2SO_3H, CuBr, HBr, 58%; ii) KOtBu, THF/DMF, reflux **14)** iodocyclopentyl, 67%; **15**) iodo-*iso*-butyl, 53%; **16**) iodocyclohexyl, 10%.

The commercially available 2-amino-5-nitro-phenol (**12)** was converted into 2-bromo-5-nitrophenol (**18**) via Sandmayer reaction in a 58% yield. 2-Bromo-5-nitrophenol **12** was alkylated with iodocyclopentyl, iodo-*iso*-butane, and iodocyclohexane under basic conditions to give compounds **14-16** in 67, 53, 10% yield, respectively. The cyclohexyl analogue was not investigated further due to the low yield obtained for synthesis of **16.**

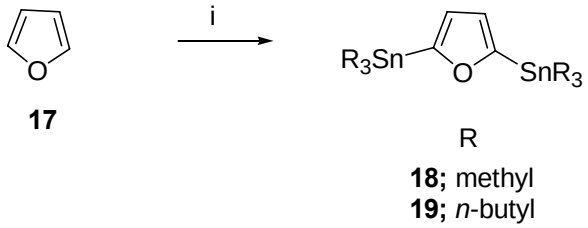

Scheme 6.2. Synthesis of 2,5 bis(trimethylstannyl)furan, **18** and 2,5 bis(tri-*n*-butylstannyl) furan,**19.**

Reagents and conditions**: 18;** i) TMEDA, *sec*-BuLi, Me_3SnCl, hexane, 0-10 ^oC, 27%.

19; i) TMEDA, *sec*-BuLi*, n*-Bu_3SnCl, hexane, 0-10 ^oC, 38%.

To provide the cenral furan core, furan was reacted with *sec*-butyllithium to generate 2,5 bis-lithiofuran, which was treated with trimethyltin chloride to yield compound **18,** (27% yield)**.** A similar procedure was repeated using tri-*n*-butyltin choloride to yield the compound **19** (38% yield).

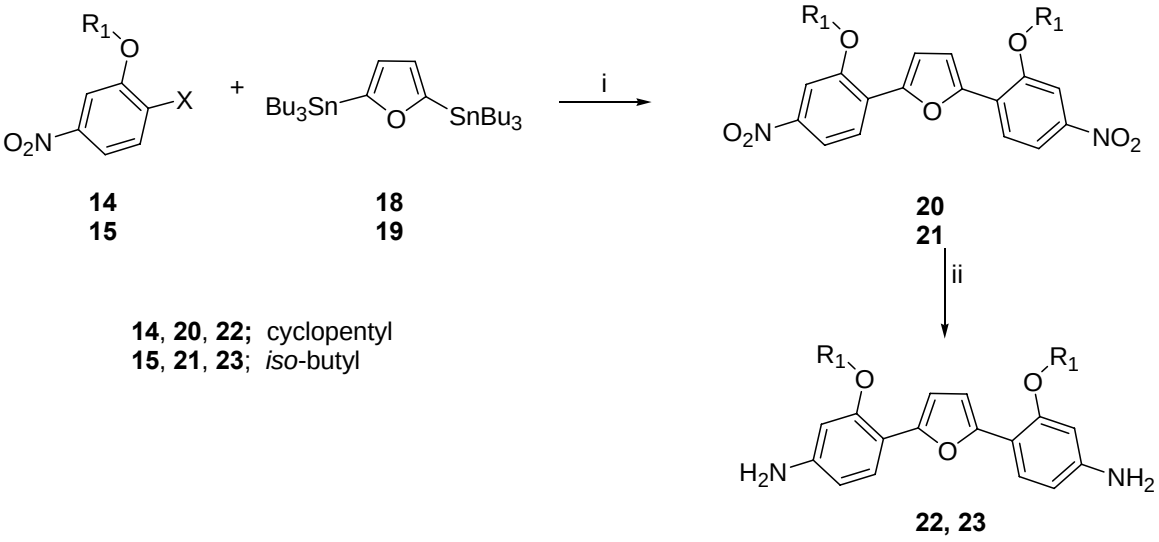

Scheme 6.3. Synthesis of bis-aminophenyl furan derivatives, **22, 23**.

Reagents and conditions**: 20;** i) **14**, **18**, Pd(Ph_3P), 1,4 dioxane, 80 ^oC., 74%. **21**; i) **15**, **19**, Pd(Ph_3P), 1,4 dioxane, 80 ^oC., 72%. ii) H_2, Pd/C, EtAc, EtOH, (**22**, 68%; **23,** 76%).

The synthesis of **22** begins with a palladium (0) catalyzed Stille coupling reaction with 2,5-bis(trimethylstannyl) furan with compound **14** to yield 2,5-bis-(nitrophenyl)furan **20** (74% yield). Reduction of **20** was achieved by palladium-catalyzed hydrogenation to yield **22** (68% yield). A similar procedure was followed to prepare **23** by starting with 1-bromo-2-*iso*-butoxy-4-nitrobenzene **15** with 2, 5-bis(tri-*n*-butyllstannyl) furan. Hydrogenation of **15** gave **23.**

n order to prepare the target arylimidamides the diamines **22** and **23** were arylated using the appropriate napthylmethylthioamides (**38-44**). The thioamides were prepared in two steps from

arylnitriles as show in Scheme 6.4.[18-20] Two of the heterocyclic nitriles were not commercially available and were made in a two-step process from the appropriate heterocyclic aldehydes as shown in Scheme 6.5.

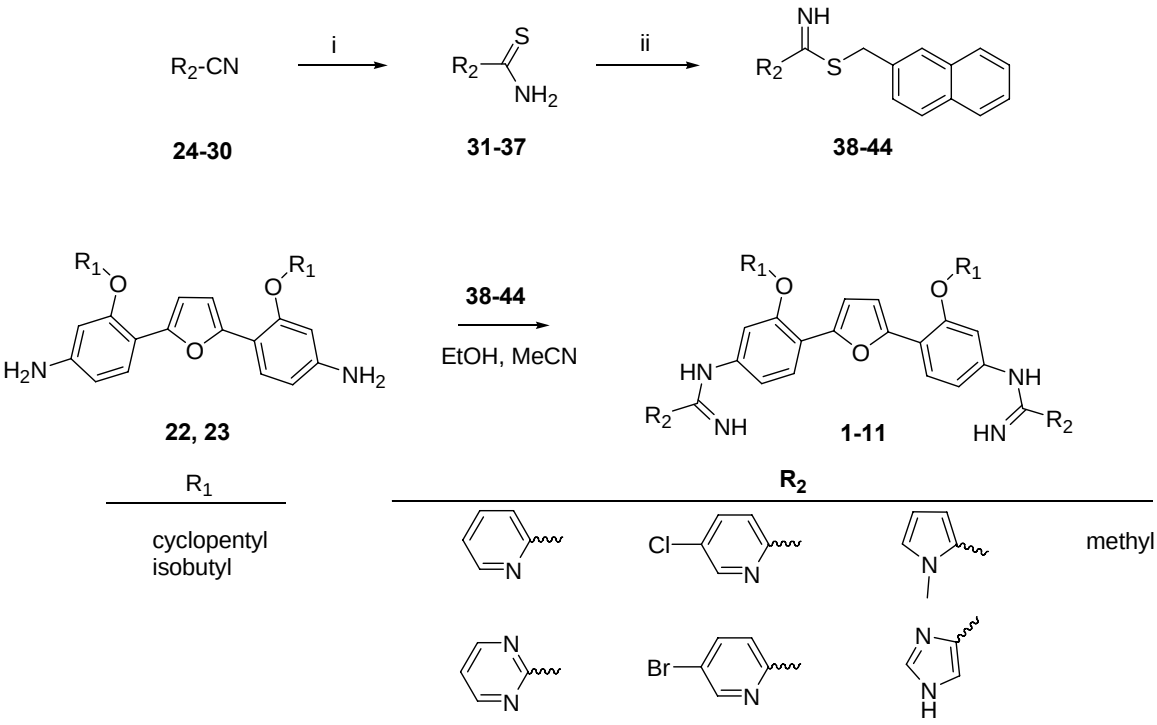

Scheme 6.4. Preparation of arylimidamides**.**

Reagents and conditions**:** i**)** NaSH, $MgCl_2.6H_2O$, DMF. ii) 2-bromo methylnaphthalene, $CHCl_3$, reflux.

I*N*-Methyl-2-pyrrolecarbonitrile **29** was synthesized from *N*-Methyl-2-pyrrolealdehyde **45** in two steps by oxime formation followed by dehydration.[21] A similar approach was used for synthesis of 1*H*-imidazole-4-carbonitrile **30**, without isolation of oxime intermediate. Briefly, a solution of 1*H*-imidazole-4-carbaldehyde **47** in pyridine was treated with hydroxylamine

hydrochloride at room temperature followed by to addition of acetic anhydride to give the nitrile compound with a good yield, 72%.[22]

It has been reported that arylimidamides exhibit antileishmanial and antimicrobial activity.[12, 13] In fact, some of the previously synthesized arylimidamide analogs have been found to be more active *in vitro* than current drugs used for Leishmaniasis treatment. The activities of the newly synthesized arylimidamides (**1-11)** against *L. amazonensis* (M), *T. brucei rhodesiense* (STIB900), *P. falciparum* (K1) in vitro, as well as their toxicities to L6 cell (rat myoblasts) are shown in Table 6.1.

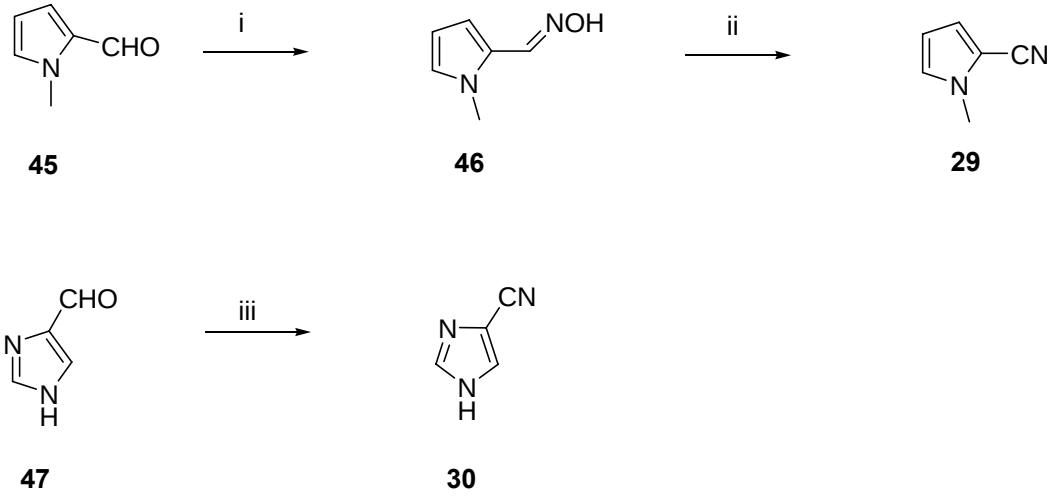

Scheme 6.5. Synthesis of arylnitriles**.**

Reagents and conditions**:** i**)** $NH_2OH.HCl$, NaOAc, reflux, 77%. ii) Ac_2O, reflux, 79%. iii) $NH_2OH.HCl$, NaOAc, Ac_2O, pyridine, 72%.

6.2.2. Biology

The activities of Mitefosine and Amphotericin B, which are two current medicines used to treat visceral leishmaniasis are included as controls in Table 6.1.As the table shows, these *in vitro* results are both promising and exciting as potential treatments for Leishmania. Five of the

Table 6. 1. *In vitro* antiprozoan activity and cytotoxicity data for arylimidamides **1-11**.

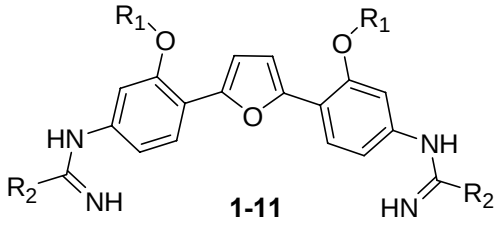

1-11

Compound	R_1	R_2	*L.a.* [a] IC_{50} (µM)	*T.b.r.* [a] IC_{50} (µM)	*P.f.* [a] IC_{50} (µM)	Cytotoxicity[b] IC_{50} (µM)
DB 1852, 1	cyclopentyl	pyridyl-	0.175	4.6	0.218	6.3
DB 1853, 2		prymidyl-	0.208	0.215	0.024	5.0
DB 1888, 3		cloropryl-	>10	>113.1	76.2	>113.1
DB 1889, 4		bromopyridyl-	>10	>101.0	0.166	>101.0
DB 1908, 5		1-H imidazyl-	>10	3.21	0.292	7.5
DB 1921, 6		methyl-	4.680	4.12	0.378	2.2
DB 1890, 7	isobuthyl	pyridyl-	0.095	6.25	0.094	7.6
DB 1920, 8		prymidyl-	0.493	0.192	0.022	6.0
DB 1912, 9		cloropryl-	>10	95.44	6.5	117.7
DB 1913, 10		bromopyridyl-	>10	>106.0	>5.0	>106.0
DB 1909, 11		1-H imidazyl-	>10	4.08	0.163	6.9
Miltefosine			15.0	ND	ND	ND
AmB			0.16	ND	ND	ND

[a] The *L.a.* (*L. amazonensis)*, *T.b.r.*(*Trypanosoma brucei rhodesiense*) strain was STIB900, and the *P. f.* (*Plasmodium falciparum*) strain was K1. [b]Cytotoxicity was evaluated using cultured L6 rat myoblast cells using the same assay procedure for *T. b. r*.

eleven arylimidamides were found to be more active than one of the current drugs (Miltefosine) against *L. amazonensis* (M). **DB 1852**, **DB 1853**, **DB 1890**, **DB 1920** were found to be highly active against *L.a.* **DB 1852** activity is almost as good as the other current medication, Amphotericin B. **DB 1890** showed almost two fold better activity than Amphotericin B. And, in addition to promising activity**,** the cytotoxicity of these compounds are tolerable. **DB 1853** and **DB 1920** were found to be highly active *in vitro* against *Plasmodium falciparum.* These two derivatives have terminal prymidyl groups. It appears that the structure of the terminal group plays an important role in *P. f.* activity. Over all, the prymidyl and pyridyl terminal units provide the best activity. There is not a significant difference in *in vito* activity between the *o*-cyclopentyl and *o-iso*butyl analogs. These studies show that the arylimidamide derivatives merit further evaluation for use against protozoan diseases. In vivo investigations against leishmania with **DB 1852** and **DB 1850** are underway.

6.3. Conclusions

A small series of arylimidamides compounds were synthesized. Their activity was evaluated *in vitro* against *L. amazonensis*, *T. brucei rhodesiense*, *P. falciparum*. **DB 1852**, **DB 1853**, **DB 1890**, and **DB 1920** were found to be highly active and had low cytotoxicities. These compounds are candidates for further evaluation against animal models of the diseases.

6.4. Methods and Materials

6.4.1. General Information

All moisture and air sensitive reactions were carried out in glassware that was oven dried overnight and under dry nitrogen (passed through drying agents). Commercially supplied chemicals and reagents were used without additional purification. Ether and THF were distilled from Na and benzophenone. Triethylamine (CaH_2) and ethanol (Mg/I_2) were distilled from the

indicated drying agents. Ethanolic HCl solutions were prepared from fresh distilled dry ethanol that was treated with dry HCl gas for 10-15 min at ice bath temperature. Anhydrous DMF was purchased from Aldrich. TLC analysis was carried out on silica gel 60 F_{254} coated aluminum sheets and detection was with two wavelengths of UV light. Column chromatography was performed with silica gel (flash 32-63 nm), from Dynamic Adsorbents Inc, in Norcross, GA. Melting points were recorded using a Mel-Temp 3.0 capillary melting point apparatus and are uncorrected. Mass spectrometry analyses were performed by the Mass Spectrometry Facilities of Georgia State University by chemical ionization under conditions which gave the protonated species M+1. Elemental analyses were performed by Atlantic Microlab, Atlanta, GA. ^{1}H and ^{13}C NMR spectra were recorded a Bruker 400 MHz instrument. Chemical shifts (δ) are given in ppm relative to TMS (0 ppm), DMSO (2.49 ppm), $CHCl_3$ (7.24 ppm) or MeOH (3.31 ppm) for ^{1}H spectra and TMS (0 ppm), DMSO (39.52 ppm), $CHCl_3$ (77.16 ppm) or MeOH (49.00 ppm) for ^{13}C spectra.

6.4.2. In Vitro Assay

In vitro efficacy and cyctotoxcity studies were performed at the Swiss Tropical Institute in Basel, Switzerland under the direction of Professor Reto Brun according to published procedures (T.b.r,[23] P.f.[24, 25] and cyctotoxcity[26]). The *in vitro L.a.* data was provide by Karl Webovets at Ohio State University. We are grateful for being provided these data by Professor Brun and Professor Werbovetz.

6.4.3. Synthetic Prosedures

2-Bromo-5-nitrophenol (13).

Concentrated hydrobromic acid (200 mL) was added slowly to a mixture of 2-amino-5-nitrophenol **12** (15 g, 97.4 mmol) and sulfamic acid (1.13g, 11.7 mmol) in water (300 mL)

while cooling in an ice cold-water bath. A solution of sodium nitrite (8.1 g, 116.8 mmol) in water (150 mL) was added dropwise while the reaction mixture was cooled with an ice-water mixture. After the addition of the sodium nitrite solution, the reaction mixture was stirred for an hour, and then CuBr (27.8 g, 194.8 mmol) in water (400 mL) was carefully added portionwise into the reaction mixture. The brown colored mixture was stirred for 4 h in a cold-water bath. The solid was collected by filtration. The residue was washed with water, dissolved in ethyl acetate (250 mL), and extracted three times with water (50 mL), and the organic layer was dried over $MgSO_4$. After filtration and evaporation of the solvent, the crude product was purified by column chromatography on 50 g of silica gel and eluting with hexanes/ethyl acetate (20:1) to give compound **18** as a pale yellow solid (11.2 g, 53%), mp: 120-121 ^oC; (lit[27] mp: 119-120 ^oC). ^1H NMR (CD_3OD): δ 12.10 (s, 1H), 8.58 (d, J = 8.8 Hz, 1H), 8.52 (d, J = 2.4 Hz, 1H), 8.38 (dd, J_1 = 2.4 Hz, J_2 = 9.0 Hz, 1H); ^{13}C NMR (CD_3OD): δ 164.5, 157.1, 143.1, 127.1, 124.5, 119.7.

1-Bromo-2-cyclopentyloxy-4-nitrobenzene (14).

Potassium tert-butoxide (0.6 g, 5.5 mmol) was added to a solution of 2-bromo-5-nitrophenol **13** (1 g, 4.6 mmol) in anhydrous THF (10 mL) and anhydrous DMF (2 mL) at 0 ^oC in an ice bath. The reaction mixture was stirred at 0 ^oC for 15 min. Then, iodocyclopentane (1.1 mL, 9.2 mmol) was injected into the flask dropwise. The mixture was stirred for 30 min. at room temperature. Then, a condensor was attached to the flask and the reaction mixture was allowed to reflux overnight. The solvent was removed under a vacuum. The red residue was dissolved in ethyl acetate (150 mL) and washed with 5% $NaHCO_3$ (2 × 50 mL). The organic layer was dried over Na_2SO_4, filtered and solvent was removed under reduced pressure to yield a dark yellow solid. The crude material was purified by column chromatography with 30 g silica gel,

eluting with hexanes/ethyl acetate (20:1) to give a white solid (880 mg, 67%), mp: 46-47 ^{o}C. ^{1}H NMR ($CDCl_3$): δ 7.70-7.02 (m, 1H), 7.67-7.66 (m, 2H), 4.91 (q, *J*=2.4 Hz, 1H), 1.99-1.66 (m, 8H);); ^{13}C NMR ($CDCl_3$): δ 154.9, 147.8, 133.4, 120.7, 155.8, 108.3, 81.6, 32.6, 23.9. ESI-MS: m/z calculated for $C_{11}H_{12}BrNO_3$: 286.1; found: 286.1 (M). Analysis calculated for $C_{11}H_{12}BrNO_3$: C, 46.17; H, 4.22; N, 4.89; found: C, 46.15; H, 4.25; N, 4.77

1-Bromo-2-*iso*-butoxy-4-nitrobenzene (15).

1-Bromo-2-isobutoxy-4-nitrobenzene **15** was synthesized by alkylation of 2-bromo-5-nitrophenol **13** with 1-iodo-2-methylpropane by following a similar procedure to that used for the synthesis of **14**, resulting in **15** as a pale yellow solid (53%), mp: 59-60 ^{o}C. ^{1}H NMR ($CDCl_3$): δ 7.64 (s, 3H), 3.85 (d, *J*=6.4 Hz, 2H), 2.18 (m, 1H), 1.08 (d, *J* = 6.8 Hz, 6H); ^{13}C NMR ($CDCl_3$): δ155.9, 147.9, 133.3, 119.9, 116.1, 107.1, 75.8, 28.2, 19.1; ESI-MS: m/z calculated for $C_{10}H_{12}BrNO_3$: 273.0; found: 272.3 (M - H). Analysis calculated for $C_{10}H_{12}BrNO_3$: C, 43.81; H, 4.41, N,5.10; found: C, 43.90; H, 4.35; N, 5.04.

Alternative preparation of 1-bromo-2-*iso*-butoxy-4-nitrobenzene (15).

NaH (60% in mineral oil) (330 mg, 5.5 mmol) was added portionwise into a solution of **13** (1g**,** 4.5 mmol) in anhydrous DMF (10 mL) at 0 ^{o}C. The reaction mixture was stirred for 20 min. at 0 ^{o}C, and 1-iodo-2-methylpropane (1.3 g, 6.8 mmol) was injected dropwise into the mixture with a syringe. The mixture was allowed to reflux for 24 h DMF was evaporated *in vacuo* and the resulting residue was dissolved in ethyl acetate (100 mL). The solution was washed with NaOH 10% solution (3 × 30 mL), water (2 × 30 mL), and dried over Na_2SO_4. After filtration and evaporation of the solvent, the crude product was purified by column chromatography with 15 g of silica gel, eluting with hexanes/ethyl acetate (20:1) to give a pale yellow solid (660 mg,

54%), mp: 60 °C. ^{1}H NMR ($CDCl_3$): δ 7.72 (s, 1H), 7.71 (d, *J*=0.8 Hz, 2H), 3.90 (d, *J*=6.4 Hz, 2H), 2.22 (m, 1H), 1.12 (d, *J* = 6.8 Hz, 6H).

1-Bromo-2-cyclohexyloxy-4-nitrobenzene (16).

1-Bromo-2-cyclohexyloxy-4-nitrobenzene **16** was synthesized by alkylation of 2-bromo-5-nitrophenol **13** with iodocyclohexane, following a similar procedure to that used for the synthesis of **14**, to give **16** as a pale yellow solid (10%), mp: 31-32 °C. ^{1}H NMR ($CDCl_3$): δ 7.74-7.73 (m, 1H), 7.71-7.70 (m, 2H), 4.50 (q, *J* = 3.2 Hz, 1H), 2.00-1.45 (m, 11H); ^{13}C NMR ($CDCl_3$): δ 154.8, 147.9, 133.7, 121.3, 116.2, 109.0, 77.2, 31,1, 25.4, 23.1; EI-MS: m/z calculated for $C_{12}H_{14}BrNO_3$: 299.0; found: 299.0 (M). Analysis calculated for $C_{12}H_{14}BrNO_3$: C, 48.02 ; H, 4.70; N, 4.66; found: C,47.96; H, 4.70; N, 4.57.

2,5-Bis(trimethylstannyl)furan (18).[28]

A solution of 1.4 M *sec*-butyllithium (550 mL, 0.77 mol) in cyclohexane was added dropwise at 0 °C to a mixture of furan (22.4 mL, 0.31 mol), TMEDA (116 mL, 0.77 mol) in fresh distilled hexanes (150 mL). After 2 hr stirring at 0 °C, the mixture was allowed to warm to room temperature. After stirring for 6 hr, the reaction mixture cooled to 0 °C and a solution of trimethyltin chloride (99g, 2.7 mol) in distilled hexanes (150 mL) was added dropwise. After addition, the reaction mixture was allowed to warm to room temperature. The reaction mixture was stirred for 36 h. A water solution of 1 N ammonium chloride (200 mL) was added at 0 °C dropwise. The organic layer was extracted with the ethyl acetate (200 mL). The organic layer was washed multiple times with an aqueous copper sulfate solution. The organic layer was dried over Na_2SO_4 and filtered. The solvent was removed under reduced pressure to give a yellow oil. Distillation of the crude product gave a pale yellow oil **13a** (33 g, 27%), bp: 115-

117 ^{o}C / 1.5 mmHg, lit[28] bp 90-91 ^{o}C / 0.5 torr. ^{1}H NMR ($CDCl_3$): δ 6.61 (d, *J*= 4.0 Hz, 2H), 0.31 (s, 18 H); ^{13}C NMR ($CDCl_3$): δ 165.2, 120.5, -0.45.

2,5-Bis(tri-*n*-butylstannyl)furan (19).

2,5-Bis(tri-*n*-butylstannyl)furan **19** was synthesized by following a similar procedure to that used for the synthesis of **18** by using tri-*n*-butyltin chloride, to give **19** as a pale yellow oil (38%), bp: 175-177 ^{o}C/ 0.015 mmHg, lit[29] bp: 222-224 ^{o}C / 0.6 mmHg. ^{1}H NMR ($CDCl_3$): δ 6.58 (d, *J*= 2.0 Hz, 2H), 1.66-1.05 (m, 54H); ^{13}C NMR ($CDCl_3$): δ 164.3, 120.4, 29.1, 27.3, 18.3, 16.4.

2,5-Bis-(2-cyclopentyloxy-4-nitrophenyl)furan (20).

2,5-Bis(trimethylstannyl)furan **18** (606 mg, 1.5 mmol) was injected into a **s**olution of 1-bromo-2-cyclopentyloxy-4-nitrobenzene **14** (880 mg, 3.1 mmol) and tetrakis-(triphenylphosphine)palladium(0) (54 mg, 0.04 mmol) in anhydrous 1,4-dioxane (10 mL) at room temperature under nitrogen. The mixture was allowed to reflux under nitrogen overnight. The orange colored suspension was diluted with hexanes (8mL) and cooled to room temperature. The residue was filtered and washed with hexanes. The orange fluffy residue was recrystallized from toluene (25 mL) to give yellow fluffy solid (1.1 g, 74%), mp : 271-273 ^{o}C. ^{1}H NMR ($CDCl_3$): δ 8.08 (d, *J*=8.8 Hz, 2H), 7.91 (dd, J_1=2.0 Hz, J_2= 9.0 Hz, 2H), 7.27 (d, *J*= 2.0 Hz, 2H), 7.29 (s, 2H), 5.08-5.04 (m, 2H), 2.12-1.74 (m, 16H) ; ^{13}C NMR ($CDCl_3$): δ 153.9, 148.9, 147.0, 125.9, 125.5. 116.1, 115.8, 107.9, 80.9, 32.9, 24.1; ESI-MS: m/z calculated for $C_{26}H_{26}N_2O_7$: 478.1; found: 479.0 (M+1). Analysis calculated for $C_{12}H_{14}BrNO_3$: C, 65.20; H,5.47; N, 5.85; found: C, 64.90; H, 5,76; N, 5.85.

2,5-Bis(2-*iso*-butoxy-4-nitrophenyl)furan (21).

2,5-Bis(2-isobutoxy-4-nitrophenyl)furan **21** was synthesized by following a similar procedure to that used for the synthesis of **20** using 2,5-bis-tri-*n*-butylstannanyl furan **19**, to give **21** as a yellow fluffy solid (72%), mp: 230-232 ^{o}C. ^{1}H NMR ($CDCl_3$): δ 8.10 (d, *J*= 8.8 Hz, 2H), 7.94 (d, *J*=8.4 Hz, 2H), 7.82 (s, 2H), 7.36 (s, 2H), 4.01 (d, *J*=6 Hz, 4H), 2.35-2.28 (m, 2H), 1.16 (d, *J*= 6.8 Hz, 12H); ^{13}C NMR ($CDCl_3$): δ155.1, 148.9, 147.1, 125.9, 124,9, 116.2, 116.1, 106.9, 75.8, 28.3, 19.5. ESI-MS: m/z calculated for: $C_{24}H_{26}N_2O_7$: 454.1; found: 455.2 (M+1). Analysis was calculated for $C_{24}H_{26}N_2O_7$-0.7H_2O: C, 61.71; H, 5.91; N, 5.99; found: C, 61.61; H,5.65 ; N, 5.59.

2,5-Bis-(2-cyclopentyloxy-4-aminophenyl)furan (22).

To a suspension of 2,5-bis(2-cyclopentyloxy-4-nitrophenyl)furan **20** (2.5 g**,** 5.21 mmol) in a mixture of ethyl acetate (50 mL) and anhydrous ethanol (20 mL), Pd/C (500 mg, 10%) was added. The suspension was bubbled with dry nitrogen for 15 min. and hydrogenated overnight using a Parr apparatus with a starting pressure of 50 psi. The consumption of hydrogen gave a clear solution. The solution was filtrated over well-packed celite, and the filtrate was removed under reduced pressure to give a light brown fluffy solid (1.4 g, 64%), mp : 114-116 ^{o}C. ^{1}H NMR (d_6-DMSO): δ 7.51 (d, *J*= 8.0 Hz, 2H), 6.60 (br s, 2H), 6.35 (s, 2H), 6.30 (d, *J*= 1.6 Hz, 2H), 6.23 (d, *J*= 6.8 Hz, 2H), 5.40 (br s, 3H), 4.82-4.79 (m, 2H), 3.57 (s, 2H), 1.97-1.61 (m, 16H), 1.69-1.63 (m, 16 H); ^{13}C NMR (d_6-DMSO): δ;154.3, 148.8, 148.0, 125.9, 108.6, 107.7, 106.2, 99.0, 78.6, 32.5, 23.7. ESI-MS: m/z calculated for $C_{26}H_{30}N_2O_3$: 418.2; found: 419.1 (M+1). Analysis calculated for $C_{26}H_{30}N_2O_3$: C, 74.61; H, 7.22; N, 6.69; found: C, 74.55; H, 7.19; N, 6.99.

2,5-Bis-(2-*iso*-butyloxy-4-aminophenyl)furan (23).

2,5-Bis(2-isobutoxy-4-aminophenyl)furan **23** was synthesized by following a similar procedure to that used for the synthesis of **22**, to give a fluffy light orange-solid (76 %), mp: 91-92 ^{o}C. ^{1}H NMR ($CDCl_3$): δ 7.78 (d, *J*= 8.0 Hz, 2H), 6.88 (s, 2H), 6.38 (d, *J*= 8.0 Hz, 2H), 6.29 (s, 2H), 3.82 (d, *J*=6 Hz, 4H), 3.71(br s, 2H), 2.26-2.24 (m, 2H), 1.14 (d, *J*= 6.8 Hz, 12H); ^{13}C NMR ($CDCl_3$): δ 156.1, 148.3, 146.3, 126.8, 111.7, 109.4, 107.2, 99.1, 74.7, 28.4, 19,6. ESI-MS: m/z calculated for $C_{24}H_{30}N_2O_3$: 394.2; found: 395.2 (M+1). Analysis calculated for $C_{24}H_{30}N_2O_3$: C, 73.07; H, 7.66; N, 7.10; found: C, 73.29; H, 7.92; N, 7.07.

1-Methyl-1*H*-pyrrole-2-carbaldehyde oxime (46).[21]

1-Methyl-2-pyrrolecarboxaldehyde **45** (25 g, 0.23 mol) was added portionwise in a solution of hydroxylamine hydrochloride (24 g, 0.34 mol) and sodium acetate (28 g, 0.34 mol) at 0 ^{o}C. The reaction mixture was allowed to warm to room temperature and stirred overnight. The reaction mixture was poured into (500 mL) water and filtered. The residue was washed with water and crystallized from ethanol to give a pale pink solid (22 g, 77%), mp: 154-156 ^{o}C; (lit[30] mp: 148.5-149.5 ^{o}C). ^{1}H NMR ($CDCl_3$): δ 8.90 (br s, 1H), 7.44 (s, 1H), 7.33 (dd, J_1= 1.6 Hz, J_2= 4.0 Hz, 1H), 6.72 (t, *J*=2.4 Hz, 1H), 6.26-6.24 (m, 1H), 3.76 (s, 3H); ^{13}C NMR ($CDCl_3$): δ 136.1, 125.5, 123.1, 118.5, 108.8, 34.4.

1-Methyl-1*H*-pyrrole-2-carbonitrile (29).[21]

1-Methyl-1*H*-pyrrole-2-carbaldehyde oxime **46** (20 g, 0.16 mol) was heated at refluxed in an acetic anhydride (150 mL) for 3 hr and was extracted with dichloromethane (3×300 mL) and dried over $MgSO_4$. After filtration, the organic layer was removed under reduced pressure to give a yellow oil. The crude product was purified by column chromatography with 50 g of silica gel, eluting with hexanes/ethyl acetate (50:1) to give the compound **29** as a pale yellow

oil (13.5 g, 79%), (lit[30] bp: 89-90 ^{o}C/ 1.5 mmHg). ^{1}H NMR ($CDCl_3$): δ 6.80 (t, J= 2.0 Hz, 1H), 6.72 (dd, J_1= 1.6 Hz, J_2= 4.0 Hz, 1H), 6.13-6.11 (m, 1H), 3.72 (s, 3H); ^{13}C NMR ($CDCl_3$): δ 127.7, 119.7, 113.8, 109.3, 104.2, 35.2.

1*H*-imidazole-4-carbonitrile (30).[22]

Hydroxylamine hydrochloride (5.4 g, 78 mmol) was added to a solution of 1*H*-imidazole-4-carbaldehyde **47** (5 g, 52 mmol) in pyridine (15 mL). After stirring for 2 h at room temperature, the reaction mixture was heated at 80 ^{o}C and acetic anhydride (40mL) was added dropwise over 2 h. Then, the mixture was allowed to cool to room temperature and was stirred overnight. The pH of the reaction mixture was adjusted to 8.0 with 10% NaOH solution and extracted with ethyl acetate (3 ×300 mL). The organic layers were combined, washed three times with brine and dried over K_2CO_3. After filtration, the organic solvent was removed under reduced pressure to give a white solid. The crude material was further washed with ether to give **30** as a white solid (3.5 g, 72%), mp: 141.0-143.0 (lit[31] mp: 143.5-144.5). ^{1}H NMR (d_6-DMSO): δ 13.00 (br s, 1H), 8.08 (s, 1H), 7.89 (s, 1H); ^{13}C NMR (d_6-DMSO): δ 138.5, 127.3, 116.4, 112.2.

Pyrimidine-2-carbothioamide (31).

Pyrimidine-2-carbonitrile (500 mg, 4.76 mmol) was added to a mixture of slurry of sodium hydrosulfide hydrate (704 mg, 9.52 mmol) and magnesium chloride hexahydrate in DMF (15 mL) at room temperature. The resulting green slurry mixture was stirred overnight at room temperature. The mixture was poured into water (200 mL). The yellow precipitate was collected by filtration and washed with water. The crude product was dissolved in DCM (250 mL) and dried on K_2CO_3. The organic layer was filtered through celite, concentrated under reduced pressure The yellow crude product was crystallized with DCM and gave a yellow solid

(550 mg, 83%), mp: 203-204 ^{o}C. ^{1}H NMR (MeOD): δ 8.89 (d, *J*= 4.8 Hz, 2H), 7.59 (t, *J*= 4.8 Hz, 1H); ^{13}C NMR ($CDCl_3$): δ 194.8, 158.5, 157.2, 122.2. ESI-MS: m/z calculated for $C_5H_5N_3S$: 139.0; found: 140 (M+1). Analysis calculated for $C_5H_5N_3S$: C, 43.14; H, 3.62; N, 30.19; found: C, 43.37; H, 3.64; N, 29.98.

Pyridine-2-carbothioamide (32).

32 was synthesized by following a similar procedure to that used for the synthesis of **31**, starting with pyridine-2-carbonitrile to yield a yellow solid (86%), mp: 138-140 ^{o}C, (lit[12] mp: 136-137 ^{o}C). ^{1}H NMR (*d_6*-DMSO*)*: δ 9.93-9.74 (br d, 2H, NH), 8.58-8.49 (m, 2H), 7.95 (t, *J*= 7.6 Hz, 1H), 7.57 (t, *J*= 6.8 Hz, 1H); ^{13}C NMR (*d_6*-DMSO): δ 194.7, 151.6, 147.2, 136.9, 125.9, 124.1. ESI-MS: m/z calculated for $C_6H_6N_2S$: 138.0; found: 139.0 (M+1).

5-Chloropyridine-2-carbothioamide (33).

33 was synthesized by following a similar procedure to that used for the synthesis of **31**, starting with 5-chloropyridine-2-carbonitrile to give yellow solid (67%), mp: 130-131 ^{o}C. ^{1}H NMR ($CDCl_3$): δ 9.34 (br s, 1H, NH), 8.67 (d, *J*= 8.8 Hz, 1H), 7.78 (br s, 1H, NH), 7.81 (dd, J_1= 2.4 Hz, J_2= 9.0 Hz, 1H); ^{13}C NMR ($CDCl_3$): δ 194.5, 148.6, 146.1, 136.7, 135.5, 126.3. ESI-MS: m/z calculated for $C_6H_5ClN_2S$: 171.9; found: 173.0 (M+1). Analysis calculated for $C_6H_5ClN_2S$: C, 41.74; H, 2.92; N, 16.22; found: C, 41.67; H, 2.90; N, 15.99.

5-Bromopyridine-2-carbothioamide (**34**).

34 was synthesized by following a similar procedure to that used for the synthesis of **31**, starting with 5-bromopyridine-2-carbonitrile to give a yellow solid (73%), mp: 138-139 ^{o}C. ^{1}H NMR ($CDCl_3$): δ 9.33 (br s, 1H, NH), 8.64-8.56 (m, 2H), 7.97 (dd, J_1= 2.4 Hz, J_2= 8.0 Hz, 1H), 7.79 (br s;1H); ^{13}C NMR ($CDCl_3$): δ 194.7, 148.9, 148.3, 139.6, 126.6, 124.7. ESI-MS:

m/z calculated for $C_6H_5BrN_2S$: 217.1; found: 217.0 (M). Analysis calculated for $C_6H_5BrN_2S$: C, 33.19; H, 2.32; N, 12.90; found: C, 33.60; H, 2.32; N, 13.09.

1*H*-Imidazole-4-carbothioamide (35).

35 was synthesized by following a similar procedure to that used for the synthesis of **31**, starting with 1H-imidazole-4-carbonitrile **30** and yielded a yellow solid (71%), mp: 209-211 ^oC. ^1H NMR (d_6-DMSO*)*: δ 9.33-9.03 (br d, 2H, NH), 7.78 (s, 1H), 7.75 (s, 1H), 2.40 (br s, 1H, NH); ^{13}C NMR (d_6-DMSO): δ 194.8, 145.4, 141.2, 128.4. ESI-MS: m/z calculated for $C_6H_8N_2S$: 127.1; found: 128.1 (M+1). Analysis calculated for $C_4H_5N_3S$: C, 37.77; H, 3.96; N, 33.04; found: C, 37.84; H, 3.98; N, 32.95.

1-Methyl-1*H*-pyrrole-2-carbothioamide (36).

36 was synthesized by following a similar procedure to that used for the synthesis of **31**, starting with 1-methyl-1*H*-pyrrole-2-carbonitrile **29** to yield a yellow solid (75%), mp: 87-88 ^oC. ^1H NMR (d_6-DMSO*)*: δ 9.93-9.74 (br d, 2H, NH), 6.99 (s, 1H), 6.68 (q, *J*= 2.0 Hz, 1H), 6.02 (t, *J*= 2.8 Hz, 1H), 3.95 (s, 3H) ; ^{13}C NMR (d_6-DMSO): δ 189.4, 132.6, 130.6, 112.6, 106.9, 37.5. ESI-MS: m/z calculated for $C_6H_8N_2S$: 140.0; found: 141.0 (M+1). Analysis calculated for $C_5H_5N_3S$: C, 51.39; H, 5.75; N, 19.98; found: C, 51.27; H, 5.92; N, 20.06.

***S*-(2-naphthylmethyl)-2-pyridylthioimidate hydrobromide (38).[12]**

2-Bromomethylnaphthalene (19 g, 86.9 mol) was added to a solution of pyrimidine-2-carbothioamide **32** (10 g, 72.4 mol) in dry chloroform (350 mL). The reaction mixture was heated at reflux for 36 h. The reaction mixture was allowed to cool to room temperature and the white participate was filtered. The white fluffy solid was washed with dry ether and dry dichloromethane, dried under reduced pressure to yield a white fluffy solid (15.3 g, 59%), mp: 187-188 ^oC, (lit[12] mp: 192 ^oC). ^1H NMR (d_6-DMSO*)*: δ 11.20 (s, 1H, NH), 8.92 (d, *J*= 5.4 Hz,

2H), 8.25 (d, *J*=8.0 Hz, 1H), 7.89 (s, 1H), 7.83-7.81 (m, 3H), 7.63-7.59 (m, 1H), 7.54 (d, *J*=8.4 Hz, 1H), 7.45-7.43 (m, 2H), 4.48 (s, 2H).

***S*-(2-naphthylmethyl)-2-pyrimidylthioimidate hydrobromide (39).**

39 was synthesized by following a similar procedure to that used for the synthesis of **38**, starting with **31** to give a white fluffy solid (53%), mp: 175-176 ^{o}C. ^{1}H NMR (d_6-DMSO): δ 11.30 (br s, 1H, NH), 8.97 (d, *J*= 5.4 Hz, 2H), 7.95 (s, 1H), 7.89-7.85 (m, 3H), 7.66 (t, *J*=5.2 Hz, 1H), 7.57 (dd, J_1=1.6, J_2=8.0 Hz, 1H), 7.45-7.43 (m, 2H), 4.48 (s, 2H). ESI-MS: m/z calculated for $C_{16}H_{13}N_3S$: 279.3; found: 280.2 (M+1). Analysis calculated for $C_{16}H_{13}N_3S$-2HBr-0.2H_2O: C, 43.03; H, 3.52; N, 9.40; found: C, 43.20; H, 3.78; N, 9.17.

***S*-(2-Naphthylmethyl)-5-chloro-2-pyridylthioimidate hydrobromide (40).**

40 was synthesized by following a similar procedure to that used for the synthesis of **38**, starting with **32** and resulted in a white fluffy solid (58%), mp: 201-202 ^{o}C. ^{1}H NMR (MeOD): δ 8.84 (t, *J*=1.2 Hz, 1H), 8.20 (d, *J*=1.6 Hz, 2H), 7.82-7.76 (m, 4H), 7.50-7.42 (m, 3H), 3.90 (s, 2H). ESI-MS: m/z calculated for $C_{17}H_{13}ClN_2S$: 312.0; found: 313.1 (M+1). Analysis calculated for $C_{17}H_{14}BrClN_2S$: C, 51.86; H, 3.58; N, 7.11; found: C, 51.59; H, 3.53; N, 7.00.

***S*-(2-Naphthylmethyl)-5-bromo-2-pyridylthioimidate hyrobromide (41).**

41 was synthesized following a similar procedure to that used for the synthesis of **38**, starting with **33** and resulted in a white fluffy solid (66 %), mp: 204-205 ^{o}C. ^{1}H NMR (MeOD): δ 8.96 (s, 1H), 8.36 (dd, J_1= 2.0 Hz, J_2= 8.0 Hz 1H), 8.13 (d, *J*= 8.4 Hz, 1H), 7.83-7.77 (m, 4H), 7.51-7.45 (m, 3H), 3.91 (s, 2H). ESI-MS: m/z calculated for $C_{17}H_{13}BrN_2S$: 357.0; found: 357.3 (M+1). Analysis calculated for $C_{17}H_{14}Br_2N_2S$-0.4H_2O: C, 45.84; H, 3.34; N, 6.28; found: C, 45.85; H, 3.13; N, 6.69.

***S*-(2-Naphthylmethyl)-4-1*H*-imidazylthioimidate hyrobromide (42).**

42 was synthesized by following a similar procedure to that used for the synthesis of **38**, starting with **36** and resulted in a white fluffy solid (53%), mp: 175-176 ^{o}C. ^{1}H NMR (d_6-DMSO): δ 11.30 (br s, 1H, NH), 8.97 (d, J= 5.4 Hz, 2H), 7.95 (s, 1H), 7.89-7.85 (m, 3H), 7.66 (t, J=5.2 Hz, 1H), 7.57 (dd, J_1=1.6, J_2=8.0 Hz, 1H), 7.45-7.43 (m, 2H), 4.48 (s, 2H). ESI-MS: m/z calculated for $C_{16}H_{13}N_3S$: 280.3; found: 280.2 (M). Analysis calculated for $C_{16}H_{13}N_3S$-2HBr-0.2H_2O: C, 43.03; H, 3.52; N, 9.40; found: C, 43.20; H, 3.78; N, 9.17.

***S*-(2-Naphthylmethyl)-4-1-methyl-1*H*-pyrrolethioimidate hyrobromide (43).**

43 was synthesized by following a similar procedure to that used for the synthesis of **38**, starting with **35** and resulted in a white fluffy solid (64%), mp: 187-190 ^{o}C. ^{1}H NMR (MeOD): δ 8.33 (s, 1H), 8.02 (s, 1H), 7.98 (s, 1H), 7.94-7.88 (m, 3H), 7.59-7.52 (m, 3H), 4.84 (s, 2H). ESI-MS: m/z calculated for $C_{15}H_{13}N_3S$: 267.3; found: 268.1 (M+1). Analysis calculated for $C_{15}H_{13}N_3S$-HBr: C, 51.73; H, 4.05; N, 12.06; found: C, 51.04; H, 3.83; N, 12.76

2,5-Bis[2-cyclopentoxyl-4-(2-pyridylimino)aminophenyl]furan.HCl (1).

38 (371 mg, 1.03 mmol) was added into a cooled solution of 2,5-bis-(2-cyclopentyloxy-4-aminophenyl)furan **22** (200 mg, 0.47 mmol) in mixture of dry ethanol (10 mL) and dry acetonitrile (5 mL) in an ice bath. The reaction mixture was stirred at room temperature overnight. After the disappearance of the starting material, the organic solvent was removed under reduced pressure to yield a crude oil product. Dry ether (20 mL) was added to the crude material and the mixture was stirred at room temperature for 4 h. The red participate was filtered and washed with dry ether. The solid was dissolved in water, the solution was cooled to 0 ^{o}C in a ice bath and 10% NaOH was added until pH reached approximately 10. The free base was participated, and then extracted into dichloromethane (2 ×200 mL). The organic layer was

washed with distilled water, dried over K_2CO_3, filtered and removed under reduced pressure. The resulting yellow solid was crystallized from dichloromethane/hexane mixture and filtrated. The free base yellow solid was characterized with NMR. Then the free base was suspended in dry ethanol (10 mL) and cooled to 0 ^oC in a ice bath. Freshly prepared hydrochloric ethanol (2 mL) was added into the suspension and the mixture was stirred at room temperature overnight. The resulting red solution was concentrated under vacuo. The red crude solid was crystallized with dry ethanol and dry ether and filtered to yield an red-orange solid (120 mg, 36%), mp: 208-210 ^oC. ^1H NMR (d_6-DMSO): δ 11.90 (br s, 2H, NH), 10.08 (s, 2H, NH), 9.32 (s, 2H, NH), 8.90 (s, 2H), 8.42 (s, 2H), 8.23-8.13 (m, 4H), 7.86 (s, 2H), 7.28-7.13 (m, 6H), 5.05 (s, 2H), 2.01-1.68 (m, 16H) ; ^{13}C NMR (d_6-DMSO): δ 159.9, 154.6, 150.3, 148.5, 144.9, 138.8, 134.6, 129.0, 127.0, 124.4, 119.4, 118.1, 113.3, 111.5, 80.4, 32.7, 24.1; ESI-MS: m/z calculated for $C_{38}H_{38}N_6O_3$: 626.3; found: 627.2 (M+1). Analysis calculated for $C_{38}H_{38}N_6O_3$-3.5HCl-0.6$C_4H_{10}O$: C, 60.74; H, 5.99; N, 10.52; found: C, 60.75; H, 6.02; N, 10.47.

2,5-Bis[2-cyclopentoxyl-4-(2-pyrimidylimino)aminophenyl]furan.HCl (2).

2 was synthesized by following a similar procedure to that used for the synthesis of **1**, starting with **39** and resulted in a dark red solid (48%), mp: 210-212 ^oC. ^1H NMR (d_6-DMSO): δ 12.00 (br s, 2H, NH), 10.15 (s, 2H, NH), 9.66 (s, 2H, NH), 9.21 (d, *J*=4.8 Hz, 4H), 8.12 (d, *J*=8.4 Hz, 2H), 7.97 (t, *J*=4.8 Hz, 2H), 7.27 (s, 2H), 7.15-7.12 (m, 4H), 5.03 (s, 2H), 2.07-1.68 (m, 16H) ; ^{13}C NMR (d_6-DMSO): δ 158.8, 157.4, 154.5, 148.5, 134.9, 126.9, 125.4, 119.5, 118.1, 113.4, 111.6, 80.3, 32.7, 24.1; ESI-MS: m/z calculated for $C_{36}H_{36}N_8O_3$:700.2; found: 701.1 (M+1). Analysis calculated for $C_{36}H_{36}N_8O_3$-4HCl-0.3$C_4H_{10}O$: C, 56.07; H, 5.44; N, 14.06; found: C, 56.06; H, 5.72; N, 14.10.

2,5-Bis[2-cyclopentoxyl-4-(5-chloro-2-pyridylimino)aminophenyl]-furan.HCl (3).

3 was synthesized by following a similar procedure to thats used for the synthesis of **1**, starting with **40** and resulted in a bright red solid (52%), mp: 247-249 ^{o}C. ^{1}H NMR (MeOD): δ 8.92 (d, *J*=1.6 Hz, 2H), 8.33-8.19 (m, 6H), 7.24-7.18 (m, 6H), 5.11 (s, 2H), 2.09-1.78 (m, 16H) ; ^{13}C NMR (MeOD): δ 159.8, 154.9, 149.0, 148.5, 142.5, 137.8, 137.1, 133.1, 126.8, 124.0, 120.7, 116.9, 113.1, 110.4, 80.4, 32.4, 23.6; ESI-MS: m/z calculated for $C_{38}H_{36}Cl_2N_6O_3$: 795.3; found: 695.3 (M). Analysis calculated for $C_{38}H_{36}Cl_2N_6O_3$-2HCl-1.5H_2O: C, 57.36; H, 5.19; N, 10.56; found: C, 57.55; H, 5.19; N, 10.18.

2,5-Bis[2-cyclopentoxyl-4-(5-bromo-2-pyridylimino)aminophenyl]furan.HCl (4).

4 was synthesized by following a similar procedure to that used for the synthesis of **1**, starting with **41** and resulted in a bright red solid (57%), mp: 256-257 ^{o}C. ^{1}H NMR (MeOD): δ 9.02 (d, *J*=1.6 Hz, 2H), 8.44 (dd, J_1=2.0, J_2=8.0 Hz, 2H), 7.25-7.19 (m, 4H), 7.24-7.18 (m, 6H), 5.10 (s, 2H), 2.07-1.78 (m, 16H) ; ^{13}C NMR (MeOD): δ 159.8, 154.9, 151.3, 148.4, 142.9, 140.8, 133.1, 126.7, 124.2, 120.7, 116.9, 113.1, 110.4, 80.4, 32.4, 23.6; ESI-MS: m/z calculated for $C_{38}H_{36}Br_2N_6O_3$: 782.1; found: 783.3 (M+1). Analysis calculated for $C_{38}H_{36}Br_2N_6O_3$-2HCl - 1.8H_2O: C, 51.23; H, 4.71; N, 9.43; found: C, 50.90; H, 4.69; N, 9.26.

2,5-Bis[2-cyclopentoxyl-4-(4-1*H*-imidylimino)aminophenyl]-furan.HCl (5).

5 was synthesized by following a similar procedure to that used for the synthesis of **1**, starting with **42** and resulted in an orange solid (55%), mp: 255-258 ^{o}C. ^{1}H NMR (MeOD): δ 8.26 (s, 2H), 8.19 (s, 2H), 8.14 (d, 8.4 Hz, 2H), 7.16-7.11 (m, 6H), 5.07 (d, *J*=2.8 Hz, 2H), 2.05-1.74 (m, 16H); ^{13}C NMR (MeOD): δ 157.4, 156.3, 149.9, 139.3, 134.5, 128.9, 128.1, 124.3, 121.8, 118.2, 114.4, 111.7, 81.8, 33.9, 25.1; ESI-MS: m/z calculated for $C_{32}H_{36}N_8O_3$ -2HCl: 604.2;

found: 605.3 (M-2HCl). Analysis calculated for $C_{34}H_{36}N_8O_3$-4HCl-5H_2O: C, 48.57; H, 5.99; N, 13.33; found: C, 48.61; H, 5.34; N, 13.02.

2,5-Bis[2-cyclopentoxyl-4-(methyl)aminophenyl]-furan.HCl (6).

6 was synthesized by following a similar procedure to that used for the synthesis of **1**, starting with *S*-(2-naphthylmethyl)methylthioimidate.HBr salt **44** which was previously prepared in our lab, resulted in an orange solid (57%), mp: 225-228 ^oC. ^1H NMR (MeOD): δ 8.11 (d, 8.4 Hz, 2H), 7.14 (s, 2H), 7.06-7.02 (m, 4H), 5.08-5.05 (m, 2H), 2.46 (s, 6H), 2.05-1.74 (m, 16H); ^{13}C NMR (MeOD): δ 165.2, 154.8, 148.3, 133.1, 126.7, 120,4, 116.5, 112.8, 110.0, 80.3, 32,4, 23.6, 17.7; ESI-MS: m/z calculated for $C_{30}H_{36}N_4O_3$: 500.2; found: 501.2 (M+1). Analysis calculated for $C_{30}H_{36}N_4O_3$-2HCl-0.4CH_2Cl_2-0.7$C_4H_{10}O$: C, 60.47; H, 7.00; N, 8.49; found: C, 60.79; H, 6.61; N, 8.24.

2,5-Bis[2-isobutoxyl-4-(2-pyridylimino)aminophenyl]-furan.HCl (7).

7 was synthesized by following a similar procedure to that used for the synthesis of **1**, starting with **38** and 2,5-bis(2-isobutyloxy-4-aminophenyl)furan **23** and resulted in a orange-red solid (60%), mp: 201-203 ^oC. ^1H NMR (MeOD): δ 8.92 (d, *J*=4.8 Hz, 2H), 8.32 (d, *J*=8.0 Hz, 2H), 8.23-8.18 (m, 4H), 7.85-7.83 (m, 2H), 7.27-7.21 (m, 6H), 4.04 (d, *J*=6.4 Hz, 4H) 2.32-2.30 (m, 2H), 1.19 (d, *J*=6.8 Hz, 12H); ^{13}C NMR (MeOD): δ160.3, 156.1, 150.0, 148.4, 144.1, 138.2, 133.4, 128.4, 126.7, 122.9, 120.1, 117.2, 113.1, 109.3, 75.2, 28.1, 18.4; ESI-MS: m/z calculated for $C_{36}H_{38}N_6O_3$-2HCl: 602.3; found: 603.4 (M+1). Analysis calculated for $C_{36}H_{38}N_6O_3$-2HCl -2.85H_2O: C, 59.47; H, 6.33; N, 11.56; found: C, 59.45; H, 6.36; N, 11.19

2,5-Bis[2- *iso*-butoxyl -4-(2-pyrimidylimino)aminophenyl]furan.HCl (8).

8 was synthesized by following a similar procedure to that used for the synthesis of **7**, starting with **39** and resulted in a red solid (55%), mp: 200-201 ^oC. ^1H NMR (MeOD): δ 9.17 (d, *J*=4.8

Hz, 4H), 8.23 (d, *J*=8.4 Hz, 2H), 7.89 (t, *J*=5.2 Hz, 2H), 7.29-7.23 (m, 6H), 4.05 (d, *J*=6.0 Hz, 4H) 2.36-2.29 (m, 2H), 1.19 (d, *J*=6.4 Hz, 12H); ^{13}C NMR (MeOD): δ171.6, 158.1, 157.4, 156.1, 152.8, 148.4, 133.2, 126.6, 124.6, 120.1, 117.2, 113.2, 109.3, 75.2, 28.1, 18.4; ESI-MS: m/z calculated for $C_{34}H_{36}N_8O_3$: 604.3; found: 605.3 (M+1). Analysis calculated for $C_{34}H_{36}N_8O_3$-2HCl -0.8CH_2Cl_2-0.8$C_4H_{10}O$: C, 56.07; H, 6.01; N, 13.76; found: C, 56.07; H, 5.69; N, 13.86

2,5-Bis[2- *iso*-butoxyl -4-(5-choloro-2-pyridylimino)aminophenyl]furan.HCl (9).

9 was synthesized by following a similar procedure to that used for the synthesis of **7**, starting with **40** and resulted in a bright red solid (61%), mp: 275 ^{o}C. ^{1}H NMR (MeOD): δ 8.92 (d, *J*=0.8 Hz, 2H), 8.32-8.20 (m, 6H), 7.27-7.20 (m, 6H), 4.04 (d, *J*=6.4 Hz, 4H), 2.33-2.29 (m, 2H), 1.18 (d, *J*=6.8 Hz, 6H) ; ^{13}C NMR (MeOD): δ 161.0, 157.6, 150.5,149.9, 144.0, 139.3, 138.6, 134.7, 128.1, 125.4, 121.6, 118.6, 114.6, 110.7, 76.7, 29.6, 19.8; ESI-MS: m/z calculated for $C_{36}H_{36}Cl_2N_6O_3$: 670.2; found: 671.3 (M+1). Analysis calculated for $C_{36}H_{36}Cl_2N_6O_3$-2HCl-1.1H_2O: C, 56.56; H, 5.30; N, 10.99; found: C, 56.36; H, 5.27; N, 10.83.

2,5-Bis[2-*iso*-butoxyl-4-(5-bromo-2-pyridylimino)aminophenyl]furan.HCl (10).

10 was synthesized by following a similar procedure to that used for the synthesis of **7**, starting with **41** and resulted in a red solid (52%), mp: 2-271-272 ^{o}C. ^{1}H NMR (MeOD): δ 9.00 (d, *J*=2.0 Hz, 2H), 8.40 (dd, J_1=2.4, J_2=8.0 Hz, 2H), 8.20 (t, *J*=9.6, 4H), 7.24-7.18 (m, 6H), 4.02 (d, *J*=6.4 Hz, 4H), 2.31-2.28 (m, 2H), 1.16 (d, *J*=6.8 Hz, 6H); ^{13}C NMR (MeOD): δ 159.8, 156.2, 151.3, 148.4, 142.9, 140.8, 133.3, 126.7, 126.1, 124.2, 120.1, 117.2, 113.2, 109.3, 75.2, 28.1, 18.4; ESI-MS: m/z calculated for $C_{36}H_{36}Br_2N_6O_3$: 758.1; found: 759.3 (M+1). Analysis calculated for $C_{36}H_{36}Br_2N_6O_3$-2HCl -0.85H_2O: C, 50.94; H, 4.71; N, 9.90; found: C, 50.61; H, 4.68; N, 9.74.

2,5-Bis[2-*iso*-butoxyl-4-(4-1*H*-imidazylimino)aminophenyl]furan.HCl (11).

11 was synthesized by following a similar procedure to that used for the synthesis of **7**, starting with **42** and resulted in a orange solid (56%), mp: 235-237 ^{o}C. ^{1}H NMR (MeOD): δ 8.48 (s, 2H), 8.36 (s, 2H), 8.19 (d, 8.0 Hz, 2H), 7.24-7.18 (m, 6H), 4.04 (d, *J*=4.0 Hz, 4H), 2.34-2.28 (m, 2H), 1.18 (d, *J*=6.8 Hz, 6H); ^{13}C NMR (MeOD): δ 157.5, 156.6, 149.8, 139.2, 134.6, 128.1, 127.8, 124.7, 121.3, 118.4, 114.5, 110.5, 76.7, 29.6, 18.8; ESI-MS: m/z calculated for $C_{32}H_{36}N_8O_3$: 580.3; found: 581.3 (M+1). Analysis calculated for $C_{32}H_{36}N_8O_3$-4HCl-1.5H_2O-0.5$C_4H_{10}O$: C, 51.65; H, 6.11; N, 14.17; found: C, 51.84; H, 5.89; N, 14.17.

References

1. Das, B. P.; Boykin, D. W. Synthesis and antiprotozoal activity of 2,5-bis(4-guanylphenyl)furans. *Journal of Medicinal Chemistry* **1977,** 20, 531-536.

2. Queener, S. F. New Drug Developments for Opportunistic Infections in Immunosuppressed Patients: Pneumocystis carinii. *Journal of Medicinal Chemistry* **1995,** 38, 4739-4759.

3. Wilson, W. D.; Tanious, F. A.; Ding, D.; Kumar, A.; Boykin, D. W.; Colson, P.; Houssier, C.; Bailly, C. Nucleic Acid Interactions of Unfused Aromatic Cations: Evaluation of Proposed Minor-Groove, Major-Groove, and Intercalation Binding Modes. *Journal of the American Chemical Society* **1998,** 120, 10310-10321.

4. Bailly, C.; Dassonneville, L.; Carrasco, C.; Lucas, D.; Kumar, A.; Boykin, D.; Wilson, W. *Relationship between topoisomerase II inhibition, sequence-specificity and DNA binding mode of dicationic diphenylfuran derivatives*. 1999; Vol. 14., p 47-60.

5. Mazur, S.; Tanious, F. A.; Ding, D.; Kumar, A.; Boykin, D. W.; Simpson, I. J.; Neidle, S.; Wilson, W. D. A thermodynamic and structural analysis of DNA minor-groove complex formation. *Journal of Molecular Biology* **2000,** 300, 321-337.

6. Bell, C. A.; Dykstra, C. C.; Naiman, N. A.; Cory, M.; Fairley, T. A.; Tidwell, R. R. Structure-activity studies of dicationically substituted bis-benzimidazoles against Giardia lamblia: correlation of antigiardial activity with DNA binding affinity and giardial topoisomerase II inhibition. *Antimicrob. Agents Chemother.* **1993,** 37, 2668-2673.

7. Dykstra, C. C.; McClernon, D. R.; Elwell, L. P.; Tidwell, R. R. Selective inhibition of topoisomerases from Pneumocystis carinii compared with that of topoisomerases from mammalian cells. *Antimicrob. Agents Chemother.* **1994,** 38, 1890-1898.

8. Boykin, D. W.; Kumar, A.; Xiao, G.; Wilson, W. D.; Bender, B. C.; McCurdy, D. R.; Hall, J. E.; Tidwell, R. R. 2,5-Bis[4-(N-alkylamidino)phenyl]furans as Anti-Pneumocystis carinii Agents. *Journal of Medicinal Chemistry* **1998,** 41, 124-129.

9. Boykin, D. W.; Kumar, A.; Spychala, J.; Zhou, M.; Lombardy, R. J.; Wilson, W. D.; Dykstra, C. C.; Jones, S. K.; Hall, J. E. Dicationic Diarylfurans as Anti-Pneumocystis carinii Agents. *Journal of Medicinal Chemistry* **1995,** 38, 912-916.

10. Francesconi, I.; Wilson, W. D.; Tanious, F. A.; Hall, J. E.; Bender, B. C.; Tidwell, R. R.; McCurdy, D.; Boykin, D. W. 2,4-Diphenyl Furan Diamidines as Novel Anti-Pneumocystis carinii Pneumonia Agents. *Journal of Medicinal Chemistry* **1999,** 42, 2260-2265.

11. Pier Giovanni Baraldi, A. B., Francesca Fruttarolo, Delia Preti, Mojgan Aghazadeh Tabrizi, Maria Giovanna Pavani, Romeo Romagnoli,. DNA minor groove binders as potential antitumor and antimicrobial agents. *Medicinal Research Reviews* **2004,** 24, 475-528.

12. Stephens, C. E.; Tanious, F.; Kim, S.; Wilson, W. D.; Schell, W. A.; Perfect, J. R.; Franzblau, S. G.; Boykin, D. W. Diguanidino and "Reversed" Diamidino 2,5-Diarylfurans as Antimicrobial Agents. *Journal of Medicinal Chemistry* **2001,** 44, 1741-1748.

13. Werbovetz, K. A.; Brendle, J. J.; Boykin, D. W.; Stephens, C. E. Reversed amidines and methods of using for treating, preventing, or inhibiting leishmaniasis 2004

14. Kumar, A.; Stephens, C. E.; Boykin, D. W. Palladium catalyzed cross-coupling reactions for the synthesis of 2,5-disubstitutedfurans. *Heterocyclic Comm* **1999**, 301−304.

15. Bajic, M.; Kumar, A.; Boykin, D. W. Synthesis of 2,5-bis(4-cyanophenyl)furan. *Heterocyclic Comm.* **1996,** 2, 135.

16. Wang, M.; Funabiki, K. Synthesis and properties of bis(hetaryl)azo dyes. *Dyes and Pigments* **2003,** 57.

17. Ruiz-Caro, J.; Basavapathruni, A.; Kim, J. T.; Bailey, C. M.; Wang, L.; Anderson, K. S.; Hamilton, A. D.; Jorgensen, W. L. Optimization of diarylamines as non-nucleoside inhibitors of HIV-1 reverse transcriptase. *Bioorganic & Medicinal Chemistry Letters* **2006,** 16, 668-671.

18. Manaka, A.; Sato, M. Synthesis of Aromatic Thioamide from Nitrile Without Handling of Gaseous Hydrogen Sulfide *Synthetic Communications* **2005,** 35, 761-764.

19. Shearer, B. G.; Oplinger, J. A.; Lee, S. S-2-Naphthylmethyl thioacetimidate hydrobromide: A new odorless reagent for the mild synthesis of substituted acetamidines. *Tetrahedron Letters* **1997,** 38, 179-182.

20. Collins, J. L.; Shearer, B. G.; Oplinger, J. A.; Lee, S.; Garvey, E. P.; Salter, M.; Duffy, C.; Burnette, T. C.; Furfine, E. S. N-Phenylamidines as Selective Inhibitors of Human Neuronal Nitric Oxide Synthase: Structure−Activity Studies and Demonstration of in Vivo Activity. *Journal of Medicinal Chemistry* **1998,** 41, 2858-2871.

21. Liang, Z.; Zhao, L.; Xie, Y.; Zhu, Y.; Yuan, S. Synthesis and characterization of N-methyl-2-pyrrolecarbonitrile. *Henan Huagong* **2003,** 11, 10-11.

22. Kawakami, J.-I.; Kimura, K.; Yamaoka, M. A convenient synthesis of 4(5)-alkylacyl-1H-imidazoles from 4(5)-imidazolecarboxaldehyde. *Synthesis* **2003,** 5, 677-680.

23. Baltz, T.; Baltz, D. G., C.; Crockett, J. Cultivation in a semi-defined medium of animal infective forms of Trypanosoma brucei, T. equiperdum, T. evansi, T. rhodesiense and T.gambiense.

. *EMBO Journal,* **1985,** 4, 1273-1277.

24. Räz, B.; Iten, M.; Grether-Bühler, Y.; Kaminsky, R.; Brun, R. The Alamar Blue® assay to determine drug sensitivity of African trypanosomes (T.b. rhodesiense and T.b. gambiense) in vitro. *Acta Tropica* **1997,** 68, 139-147.

25. Matile, H.; Pink, J. R. L. *Plasmodium falciparum malaria parasite cultures and their use in immunology. In Immunological Methods*. Academic Press San Diego, 1990; p 221−234.

26. Nguyen, C.; Kasinathan, G.; Leal-Cortijo, I.; Musso-Buendia, A.; Kaiser, M.; Brun, R.; Ruiz-Perez, L. M.; Johansson, N. G.; Gonzalez-Pacanowska, D.; Gilbert, I. H. Deoxyuridine Triphosphate Nucleotidohydrolase as a Potential Antiparasitic Drug Target. *Journal of Medicinal Chemistry* **2005,** 48, 5942-5954.

27. Bonilha, J. B. S.; Tedesco, A. C.; Nogueira, L. C.; Diamantino, M. T. R. S.; Carreiro, J. C. Further Evidence for the Triplet Mechanism in the Photosubstitution of Nitroaryl Ethers in Alkaline Medium. *Tetrahedron* **1993,** 49, 3053-3064.

28. Seitz, D. E.; Lee, S.; Hanson, R. N.; Bottaro, J. C. Synthesis and Reactivity of the 2,5-Bis(trimethylstannyl) Derivatives of Thiophene and Furan *Synthetic Communications* **1983,** 13, 121-128.

29. Saadeh, H.; Goodson, T.; Yu, L. Synthesis of a Polyphenylene-co-furan and Polyphenylene-co-thiophene and Comparison of Their Electroluminescent Properties. *Macromolecules* **1997,** 30, 4608-4612.

30. Anderson, H. J. PYRROLE CHEMISTRY: II. 2-PYRROLECARBONITRILE, 1-METHYL-2-PYRROLECARBONITRILE, AND THEIR NITRATION PRODUCTS. *Canadian Journal of Chemistry* **1959,** 37, 2053-2058.

31. Mitsuhashi, K.; Itho, E.-i.; Kawahara, T.; Tanaka, K. 4-Cyano- and 4-Methylimidazoles with Isocyanates. *Journal of Heterocyclic Chemistry* **1983,** 20, 1103 - 1106.

APPENDIX A

Supporting Information:

Synthesis and Evaluation of Dual Wavelength Fluorescent Benzo[b]thiophene Boronic Acid Derivatives for Sugar Sensing

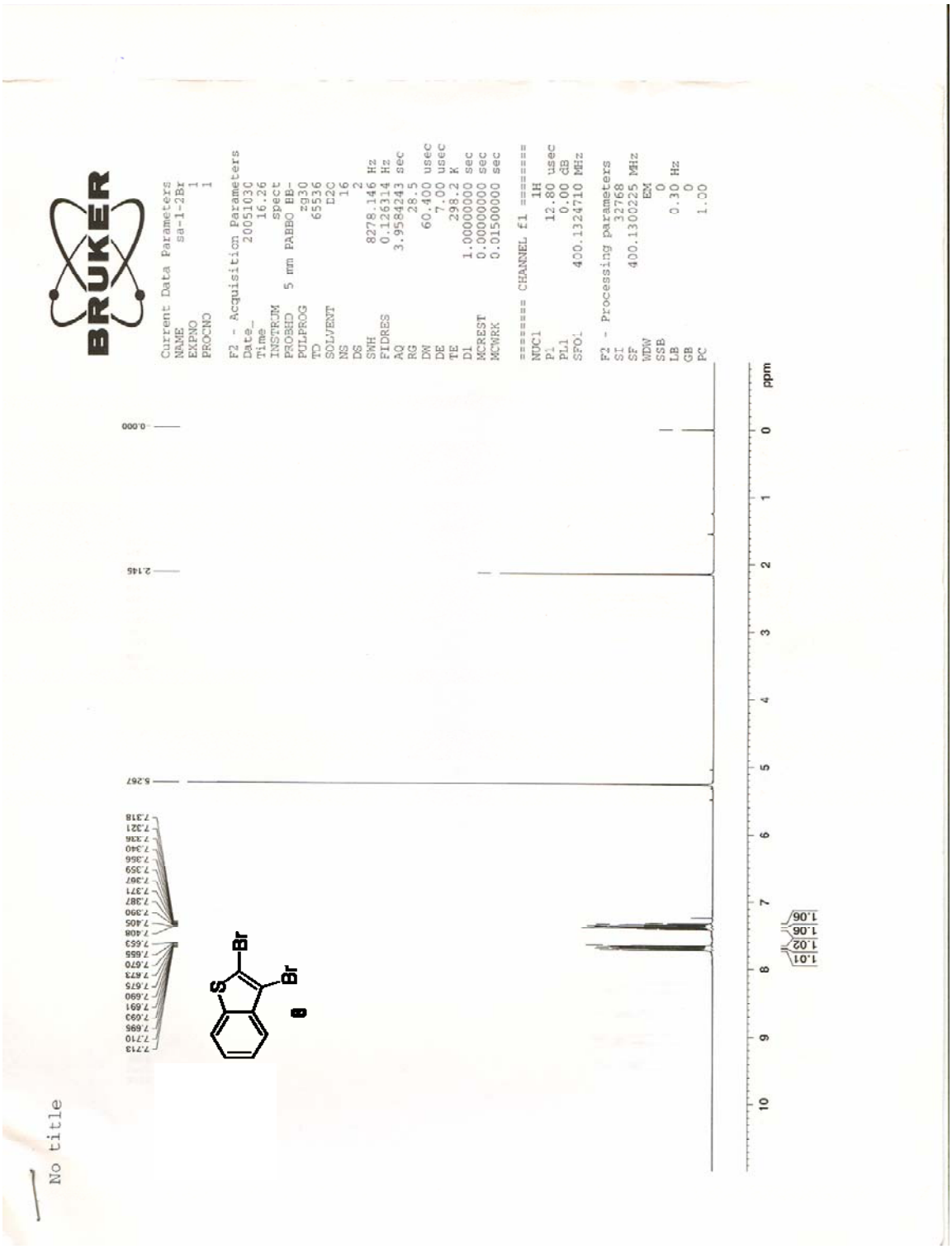
No title
BRUKER
Current Data Parameters
NAME sa-1-2Br
EXPNO 1
PROCNO 1
F2 - Acquisition Parameters
Date_ 20051030
Time 16.26
INSTRUM spect
PROBHD 5 mm PABBO BB-
PULPROG zg30
TD 65536
SOLVENT D2O
NS 16
DS 2
SWH 8278.146 Hz
FIDRES 0.126314 Hz
AQ 3.9584243 sec
RG 28.5
DW 60.400 usec
DE 7.00 usec
TE 298.2 K
D1 1.00000000 sec
MCREST 0.00000000 sec
MCWRK 0.01500000 sec
======== CHANNEL f1 ========
NUC1 1H
P1 12.80 usec
PL1 0.00 dB
SFO1 400.1324710 MHz
F2 - Processing parameters
SI 32768
SF 400.1300225 MHz
WDW EM
SSB 0
LB 0.30 Hz
GB 0
PC 1.00
0.000
2.145
5.267
7.318
7.321
7.336
7.340
7.356
7.359
7.387
7.390
7.405
7.408
7.653
7.656
7.670
7.673
7.675
7.690
7.691
7.693
7.696
7.710
7.713
Br
S
Br
1
1.01
1.02
1.06
1.06
ppm

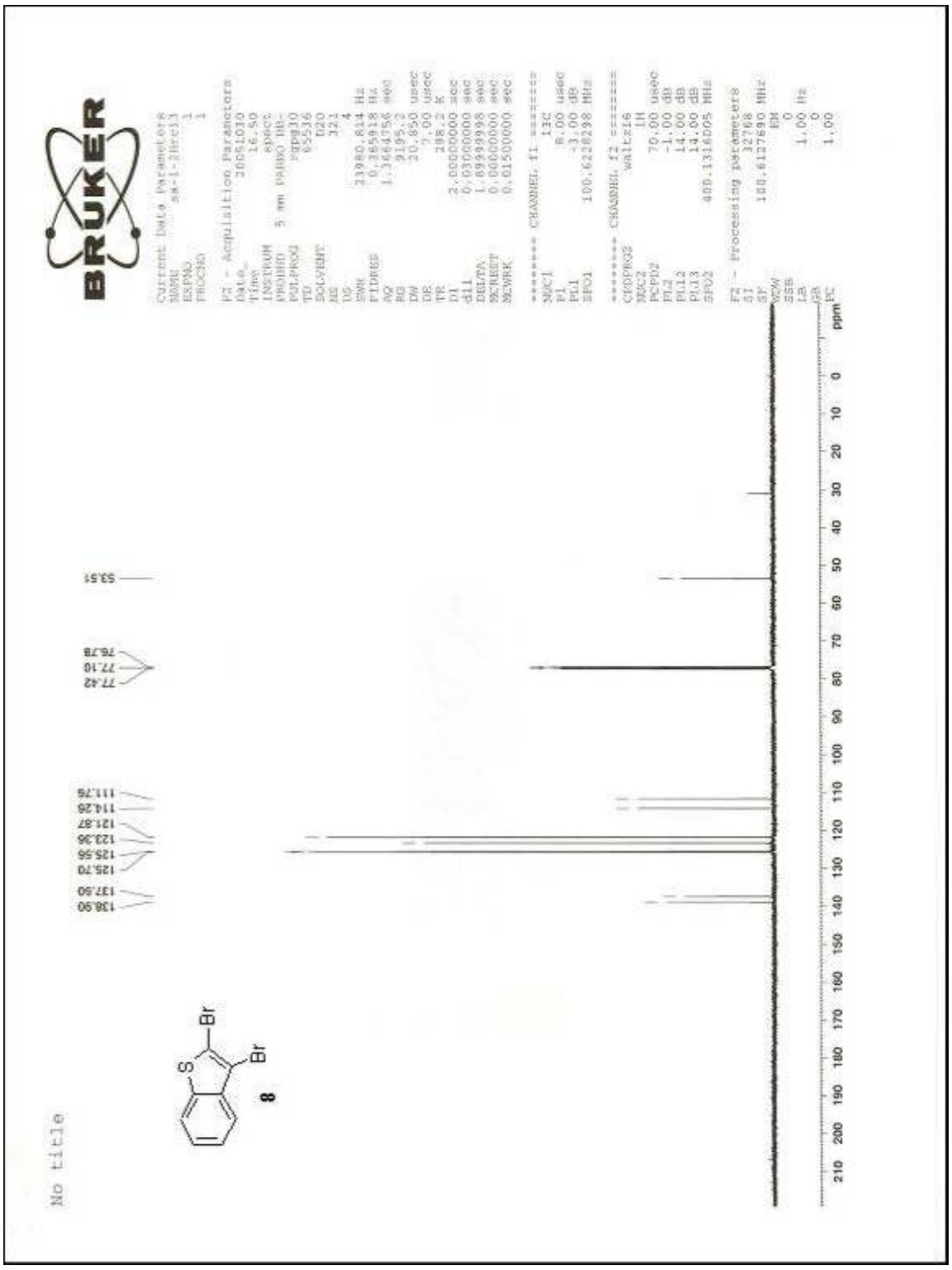
No title
8
Br
Br
S
53.51
76.78
77.10
77.42
111.76
114.26
121.87
123.36
125.56
125.70
137.50
138.90
ppm

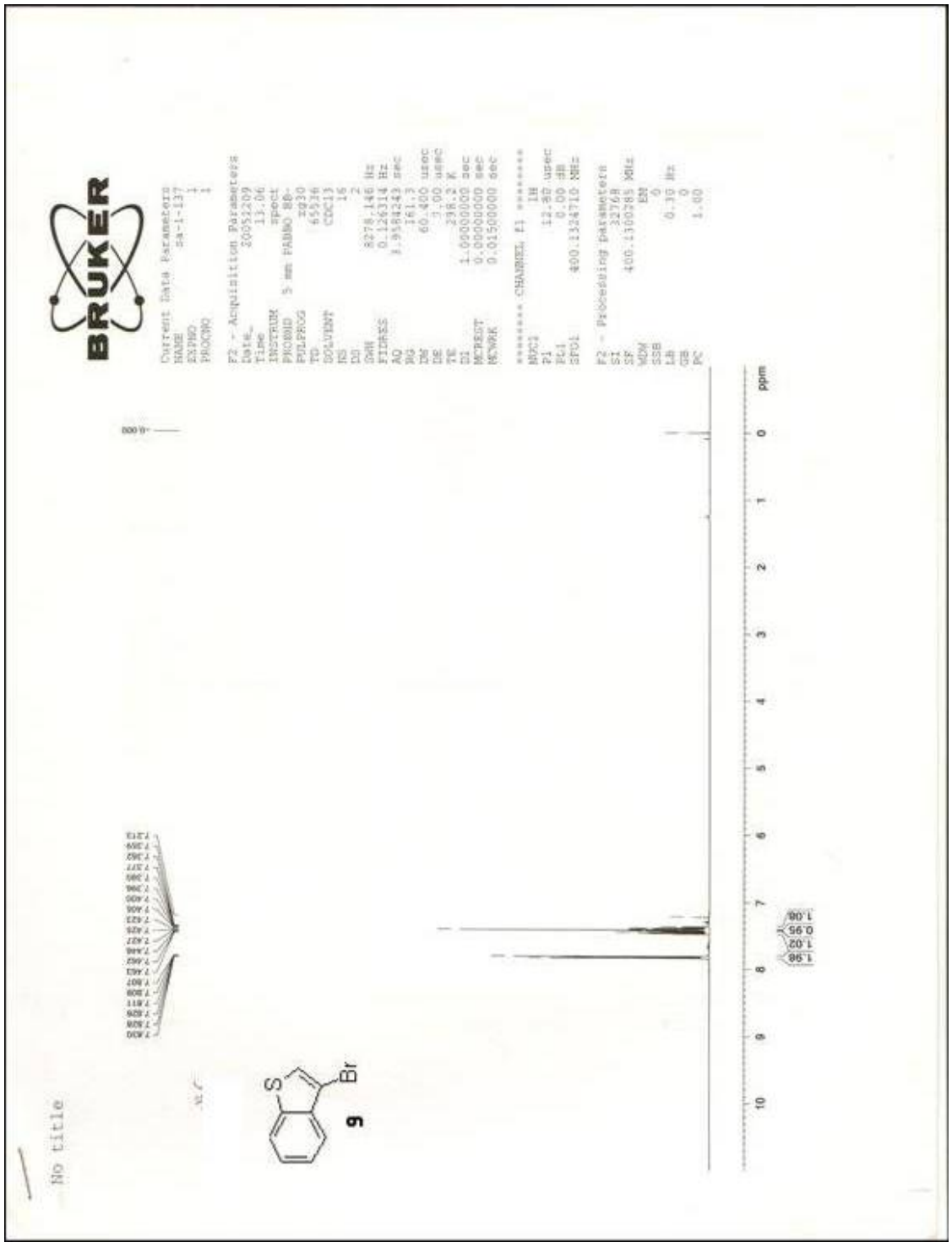
No title
BRUKER
Current Data Parameters
NAME sa-1-137
EXPNO 1
PROCNO 1
F2 - Acquisition Parameters
Date_ 20052209
Time 13.06
INSTRUM spect
PROBHD 5 mm PABBO BB-
PULPROG zg30
TD 65536
SOLVENT CDCl3
NS 16
DS 2
SWH 8278.146 Hz
FIDRES 0.126314 Hz
AQ 3.9584243 sec
RG 161.3
DW 60.400 usec
DE 7.00 usec
TE 298.2 K
D1 1.00000000 sec
MCREST 0.00000000 sec
MCWRK 0.01500000 sec
======== CHANNEL f1 ========
NUC1 1H
P1 12.90 usec
PL1 0.00 dB
SFO1 400.1324710 MHz
F2 - Processing parameters
SI 32768
SF 400.1300285 MHz
WDW EM
SSB 0
LB 0.30 Hz
GB 0
PC 1.00
S
Br
9
1.98
1.02
0.95
1.08
ppm

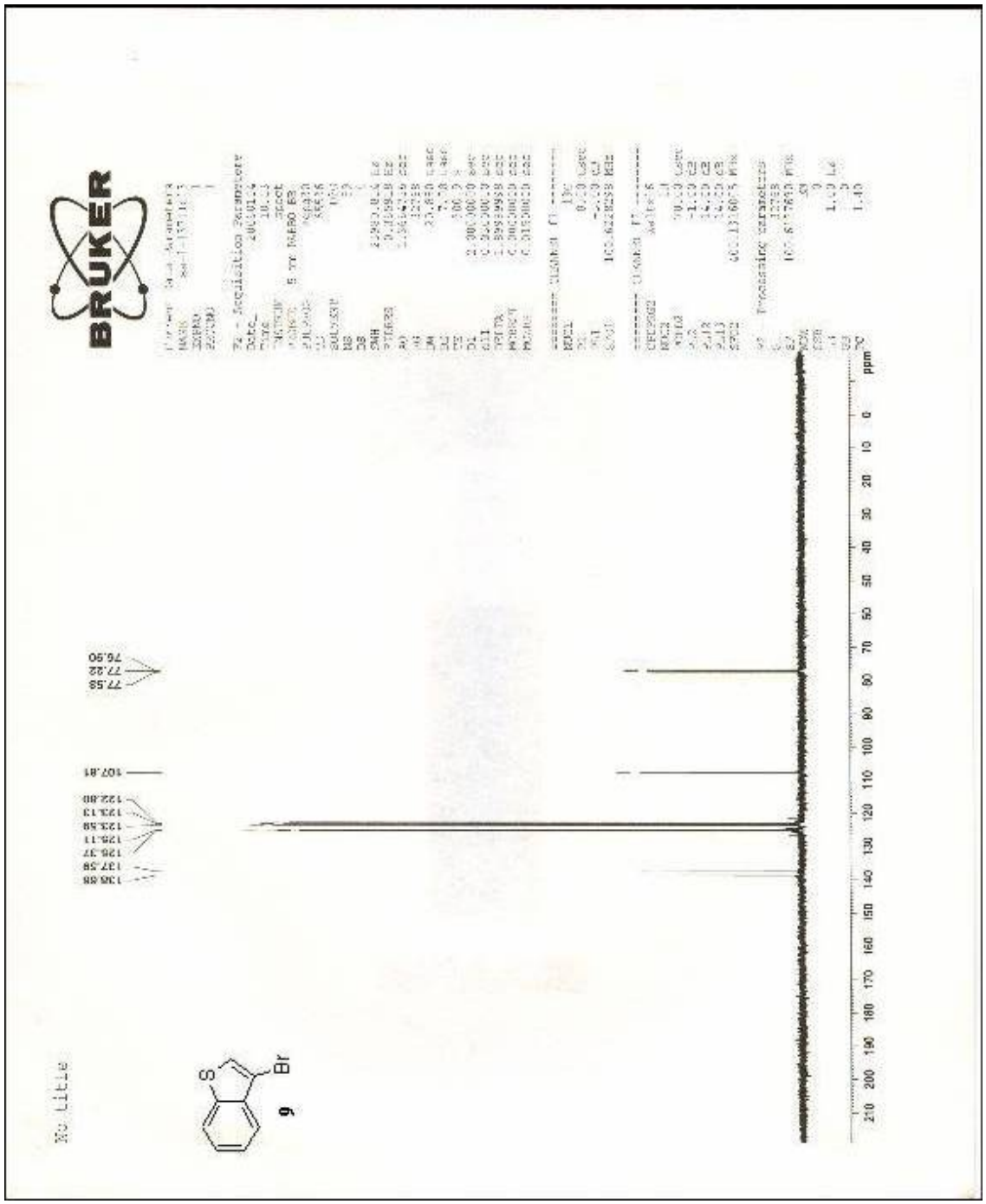
BRUKER
Xu Little
S
Br
9
77.58
77.22
76.50
107.81
132.80
133.13
133.58
135.11
136.37
137.58
138.88
ppm

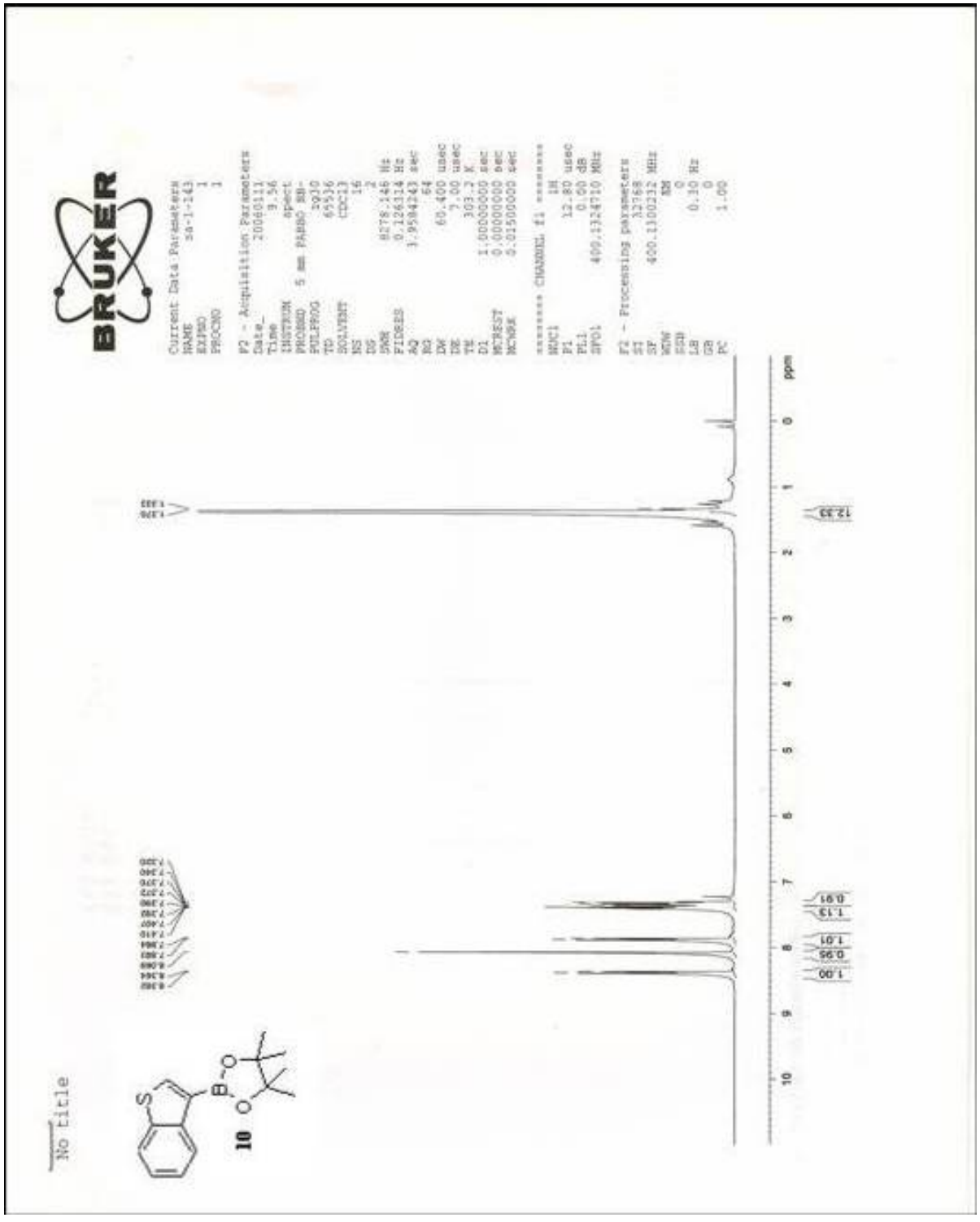
No title
10
BRUKER
Current Data Parameters
NAME 36-1-143
EXPNO 1
PROCNO 1
F2 - Acquisition Parameters
Date_ 20060111
Time 9.56
INSTRUM spect
PROBHD 5 mm PABBO BB-
PULPROG zg30
TD 65536
SOLVENT CDCl3
NS 16
DS 2
SWH 8278.146 Hz
FIDRES 0.126314 Hz
AQ 3.9584243 sec
RG 64
DW 60.400 usec
DE 7.00 usec
TE 303.2 K
D1 1.00000000 sec
MCREST 0.00000000 sec
MCWRK 0.01500000 sec
======== CHANNEL f1 ========
NUC1 1H
P1 12.80 usec
PL1 0.00 dB
SFO1 400.1324710 MHz
F2 - Processing parameters
SI 32768
SF 400.1300232 MHz
WDW EM
SSB 0
LB 0.30 Hz
GB 0
PC 1.00
12.33
1.00
0.95
1.01
1.13
0.91
ppm

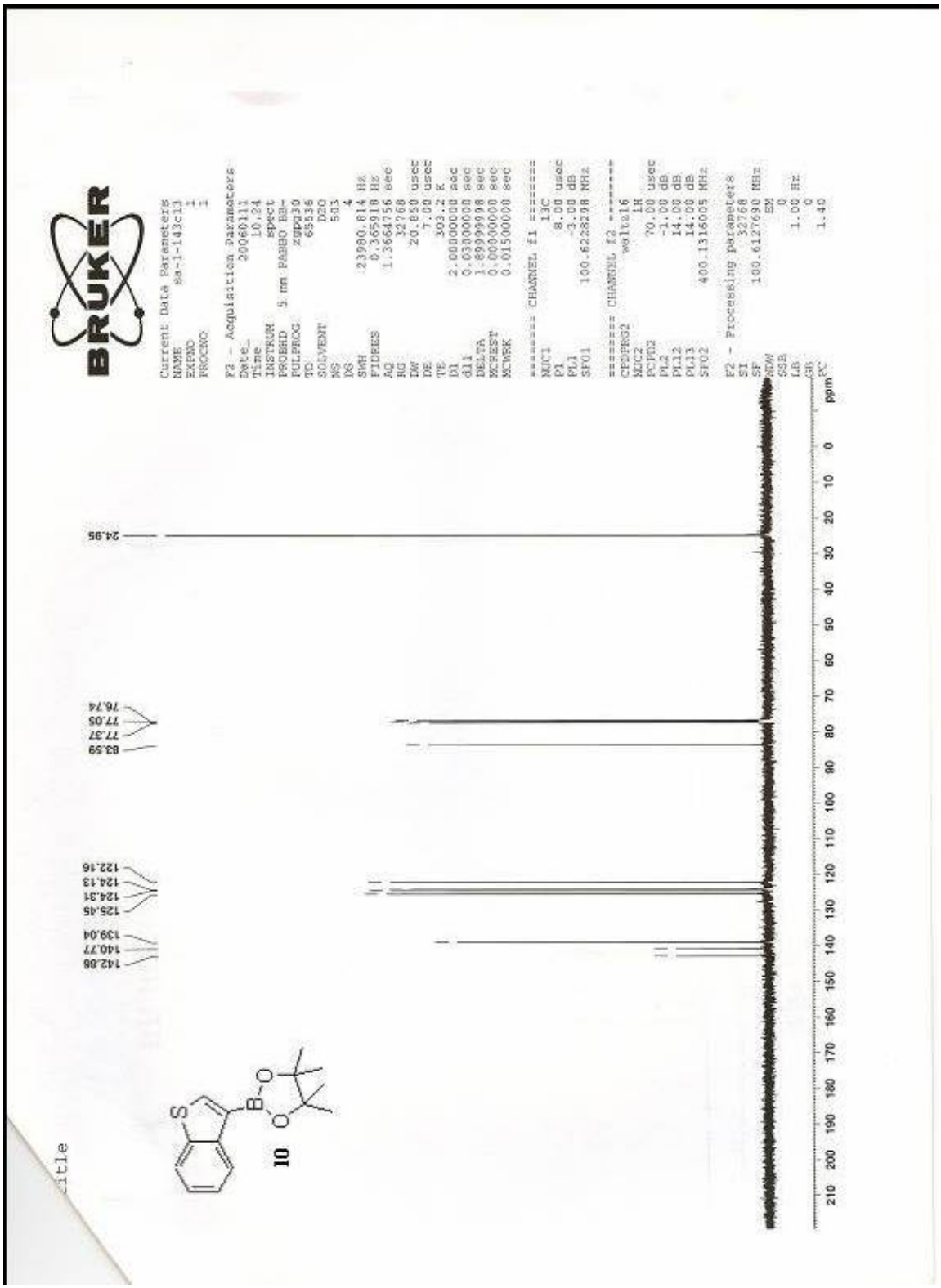
BRUKER
Current Data Parameters
NAME sa-1-143c13
EXPNO 1
PROCNO 1
F2 - Acquisition Parameters
Date_ 20060111
Time 10.24
INSTRUM spect
PROBHD 5 mm PABBO BB-
PULPROG zgpg30
TD 65536
SOLVENT D2O
NS 503
DS 4
SWH 23980.814 Hz
FIDRES 0.365918 Hz
AQ 1.3664756 sec
RG 32768
DW 20.850 usec
DE 7.00 usec
TE 303.2 K
D1 2.00000000 sec
d11 0.03000000 sec
DELTA 1.89999998 sec
MCREST 0.00000000 sec
MCWRK 0.01500000 sec
======== CHANNEL f1 ========
NUC1 13C
P1 8.00 usec
PL1 -3.00 dB
SFO1 100.6228298 MHz
======== CHANNEL f2 ========
CPDPRG2 waltz16
NUC2 1H
PCPD2 70.00 usec
PL2 -1.00 dB
PL12 14.00 dB
PL13 14.00 dB
SFO2 400.1316005 MHz
F2 - Processing parameters
SI 32768
SF 100.6127690 MHz
WDW EM
SSB 0
LB 1.00 Hz
GB 0
PC 1.40
24.95
76.74
77.05
77.37
83.59
122.16
124.13
124.31
125.45
139.04
140.77
142.86
ppm
10

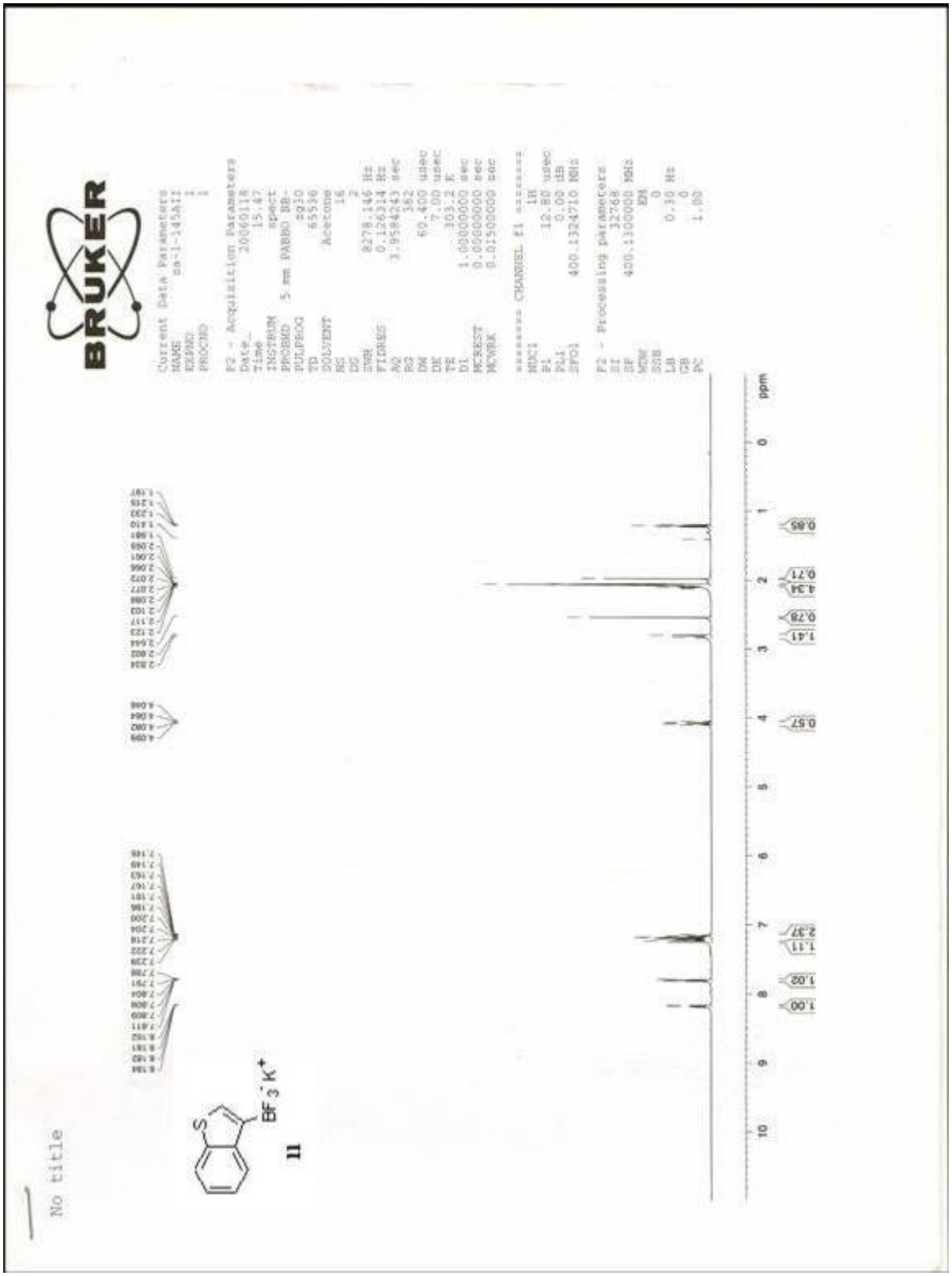
No title
BRUKER
Current Data Parameters
NAME ea-1-145a11
EXPNO 1
PROCNO 1
F2 - Acquisition Parameters
Date_ 20060118
Time 15.47
INSTRUM spect
PROBHD 5 mm PABBO BB-
PULPROG zg30
TD 65536
SOLVENT Acetone
NS 16
DS 2
SWH 8278.146 Hz
FIDRES 0.126314 Hz
AQ 3.9584243 sec
RG 362
DW 60.400 usec
DE 7.00 usec
TE 303.2 K
D1 1.00000000 sec
MCREST 0.00000000 sec
MCWRK 0.01500000 sec
======== CHANNEL f1 ========
NUC1 1H
P1 12.80 usec
PL1 0.00 dB
SFO1 400.1324710 MHz
F2 - Processing parameters
SI 32768
SF 400.1300000 MHz
WDW EM
SSB 0
LB 0.30 Hz
GB 0
PC 1.00
ppm
0.85
4.34
0.71
0.78
1.41
0.57
1.11
2.37
1.02
1.00
BF3 K+
11

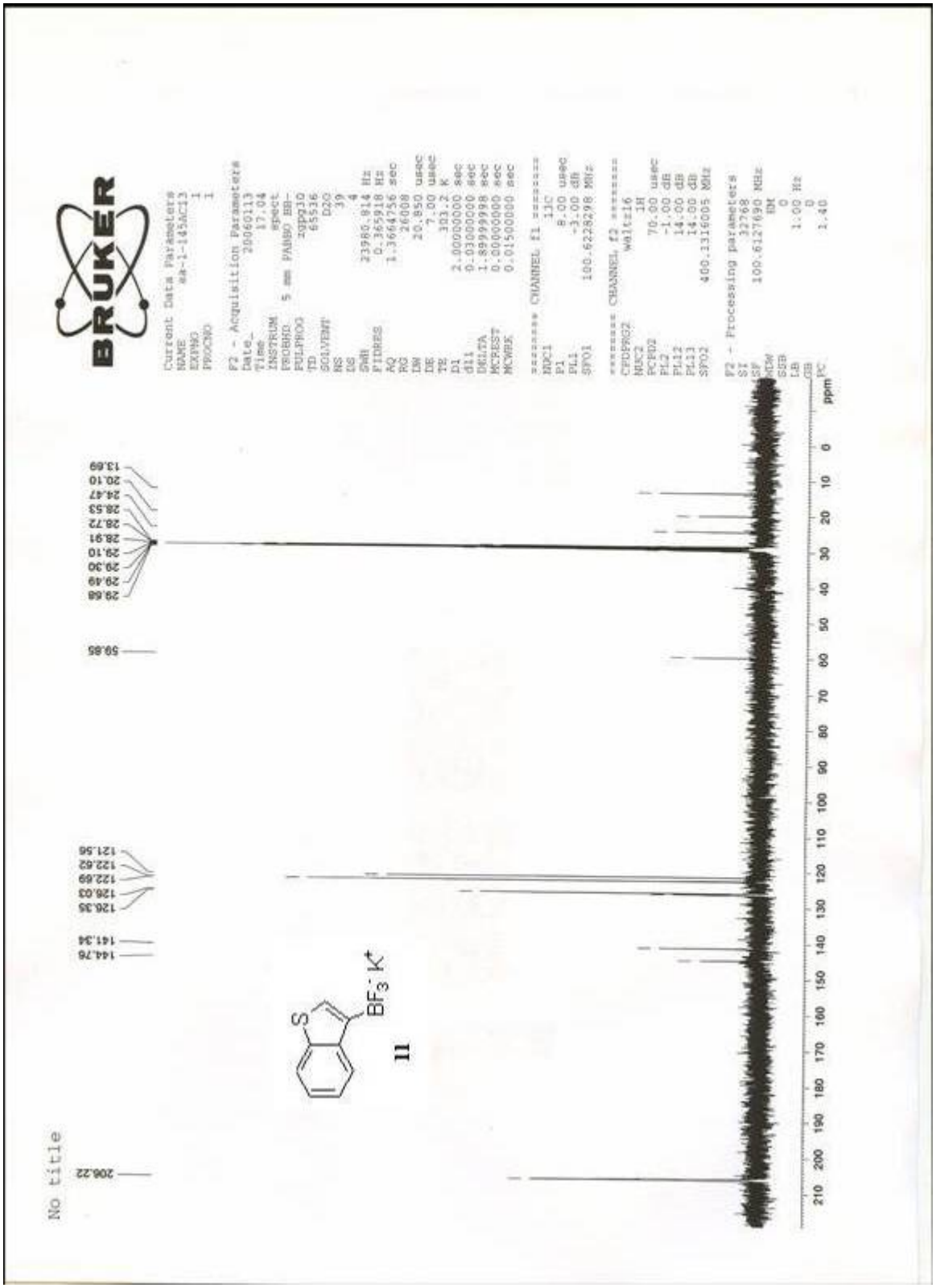
No title
BRUKER
Current Data Parameters
NAME ka-1-145AC13
EXPNO 1
PROCNO 1
F2 - Acquisition Parameters
Date_ 20060113
Time 17.04
INSTRUM spect
PROBHD 5 mm PABBO BB-
PULPROG zgpg30
TD 65536
SOLVENT D2O
NS 39
DS 4
SWH 23980.814 Hz
FIDRES 0.365918 Hz
AQ 1.3664756 sec
RG 26008
DW 20.850 usec
DE 7.00 usec
TE 301.2 K
D1 2.00000000 sec
D11 0.03000000 sec
DELTA 1.89999998 sec
MCREST 0.00000000 sec
MCWRK 0.01500000 sec
======== CHANNEL f1 ========
NUC1 11C
P1 8.00 usec
PL1 -3.00 dB
SFO1 100.6228298 MHz
======== CHANNEL f2 ========
CPDPRG2 waltz16
NUC2 1H
PCPD2 70.00 usec
PL2 -1.00 dB
PL12 14.00 dB
PL13 14.00 dB
SFO2 400.1316005 MHz
F2 - Processing parameters
SI 32768
SF 100.6127690 MHz
WDW EM
SSB 0
LB 1.00 Hz
GB 0
PC 1.40
ppm
13.69
20.10
24.47
28.53
28.72
28.91
29.10
29.30
29.49
29.68
50.85
121.56
122.62
122.69
126.03
126.35
141.34
144.76
206.22
S
BF3 K+
11

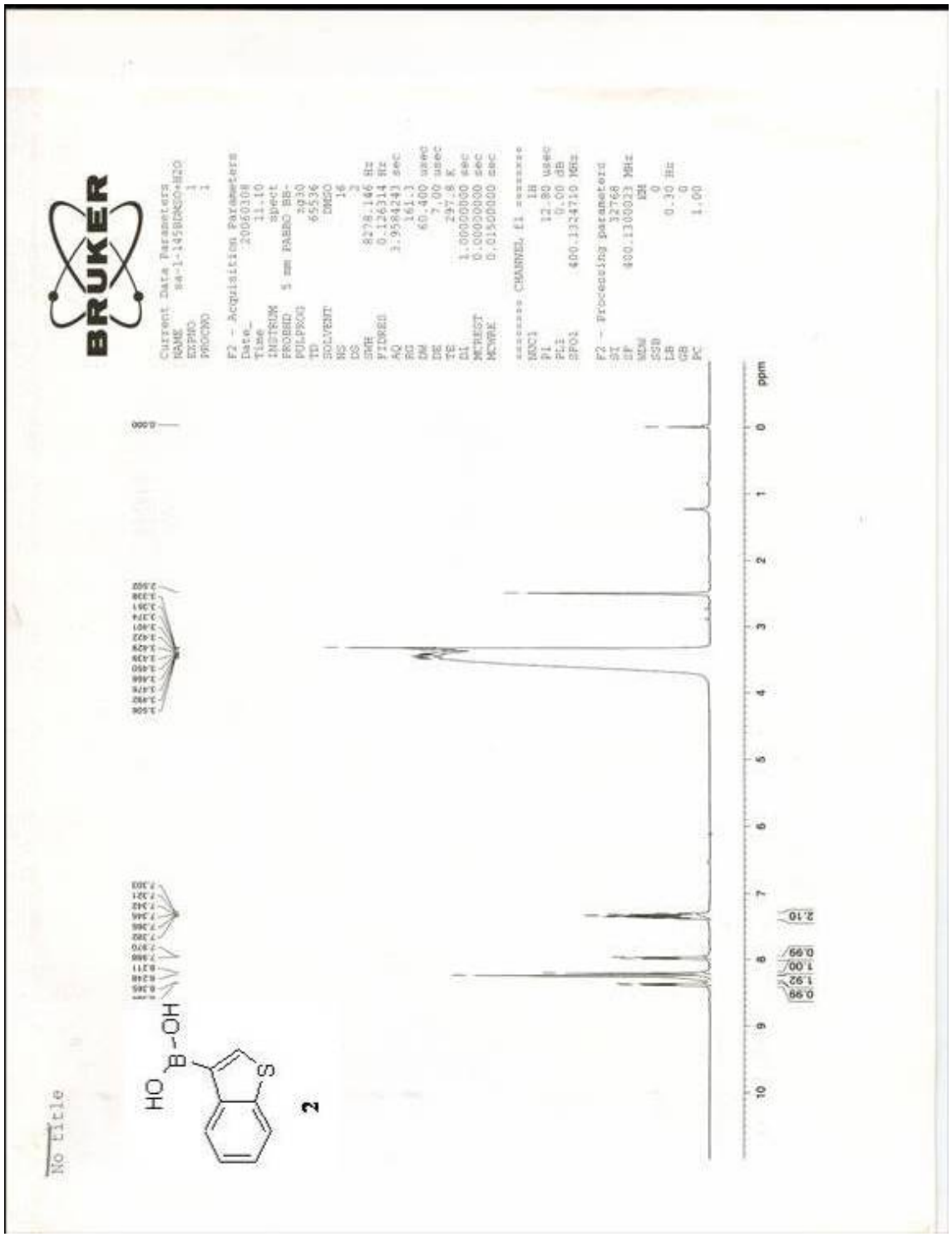
BRUKER
No Title
HO
B
OH
S
2
ppm

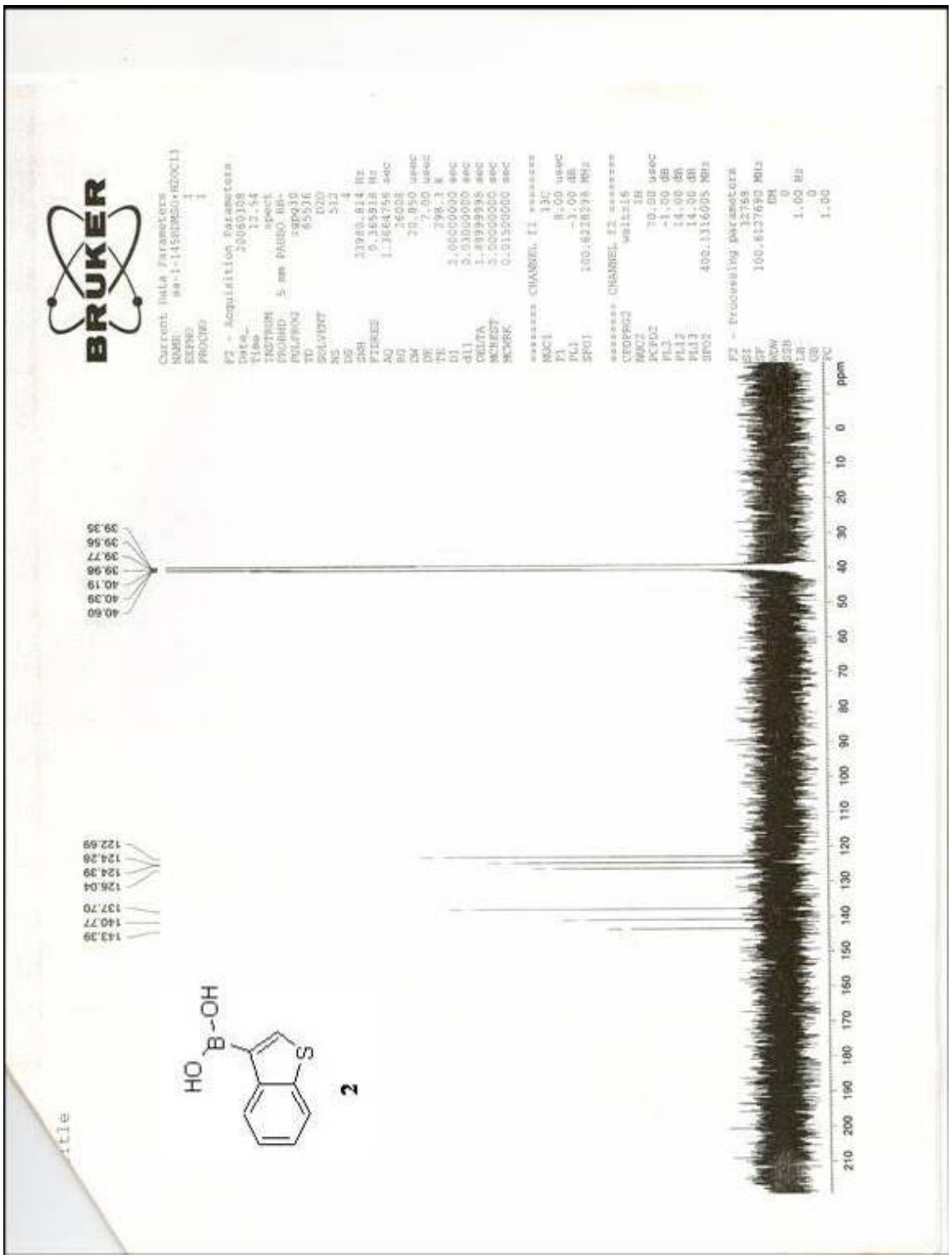
BRUKER
HO
B
OH
S
2
143.39
140.77
137.70
126.04
124.39
124.26
122.69
40.60
40.39
40.19
39.96
39.77
39.56
39.35
ppm

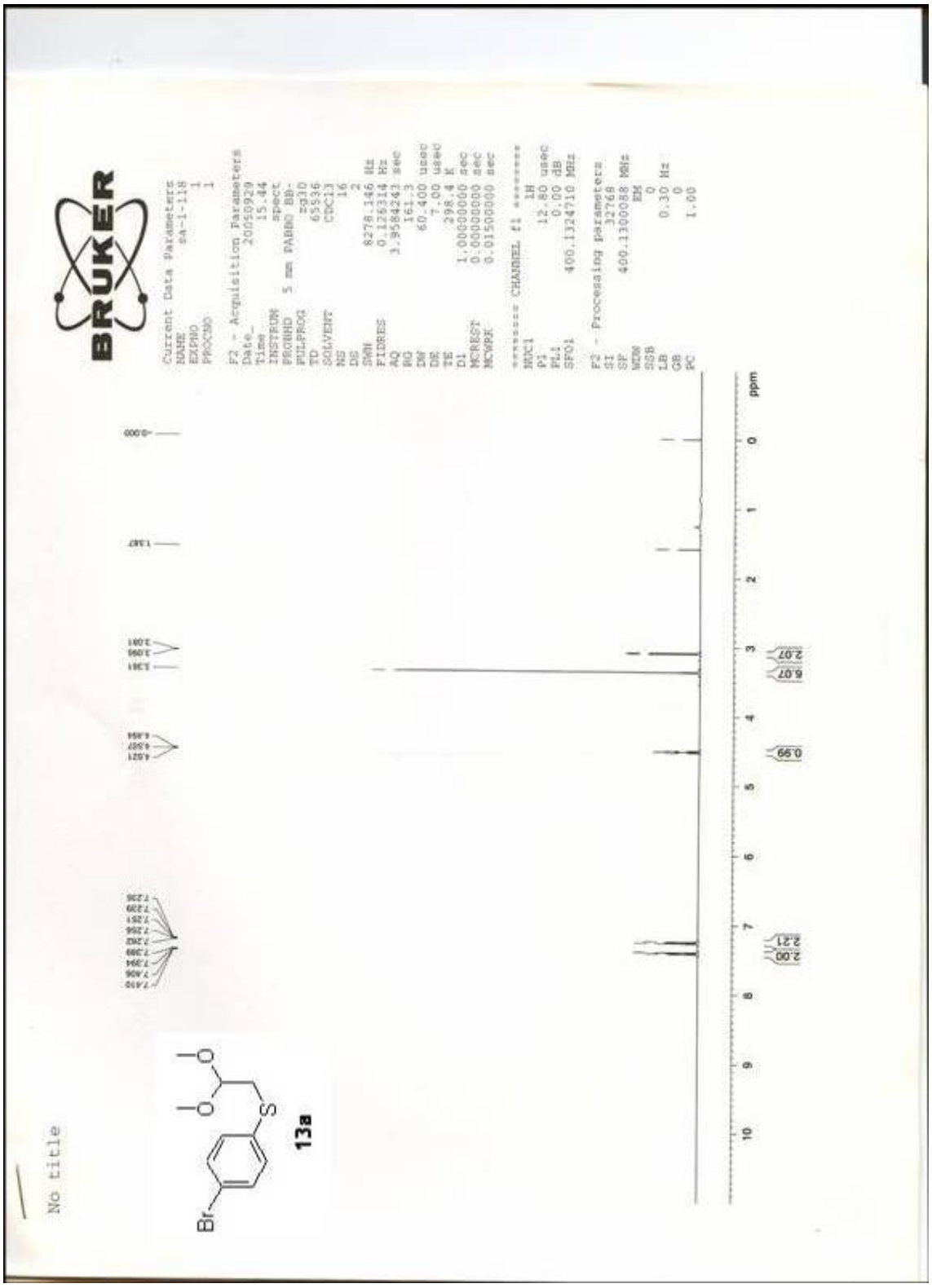
No title
13a
Br
O
O
S
BRUKER
Current Data Parameters
NAME sa-1-118
EXPNO 1
PROCNO 1
F2 - Acquisition Parameters
Date_ 20050929
Time 15.44
INSTRUM spect
PROBHD 5 mm PABBO BB-
PULPROG zg30
TD 65536
SOLVENT CDCl3
NS 16
DS 2
SWH 8278.146 Hz
FIDRES 0.126314 Hz
AQ 3.9584243 sec
RG 161.3
DW 60.400 usec
DE 7.00 usec
TE 298.4 K
D1 1.00000000 sec
MCREST 0.00000000 sec
MCWRK 0.01500000 sec
======== CHANNEL f1 ========
NUC1 1H
P1 12.80 usec
PL1 0.00 dB
SFO1 400.1324710 MHz
F2 - Processing parameters
SI 32768
SF 400.1300088 MHz
WDW EM
SSB 0
LB 0.30 Hz
GB 0
PC 1.00
7.496
7.406
7.394
7.399
7.392
7.386
7.381
7.329
7.236
6.021
6.007
6.004
3.981
3.096
3.081
1.587
0.000
ppm
2.07
6.07
0.99
2.00
2.21

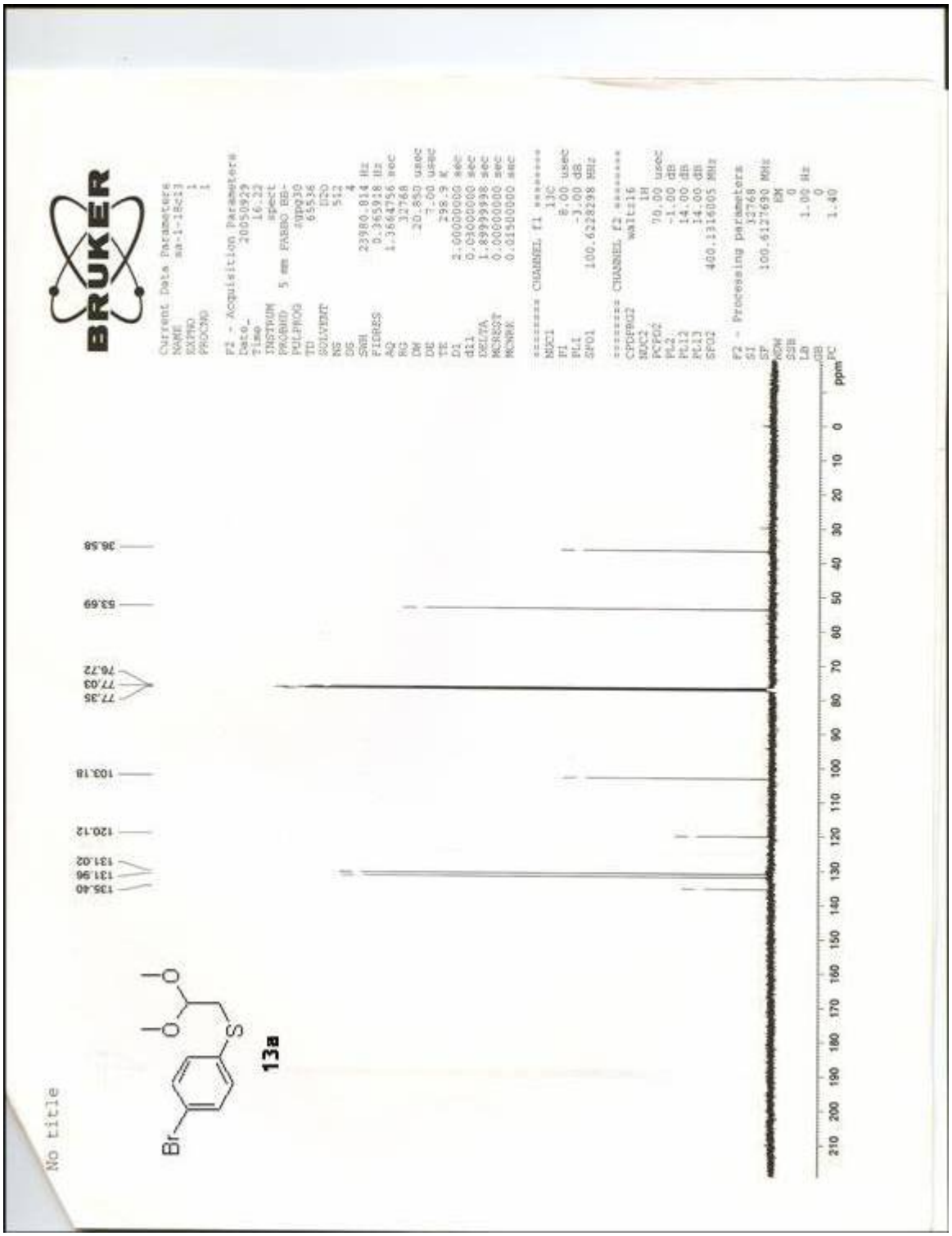
No title
BRUKER
13a
Br
O
O
S
135.40
131.96
131.02
120.12
103.18
77.35
77.03
76.72
53.69
36.58
ppm

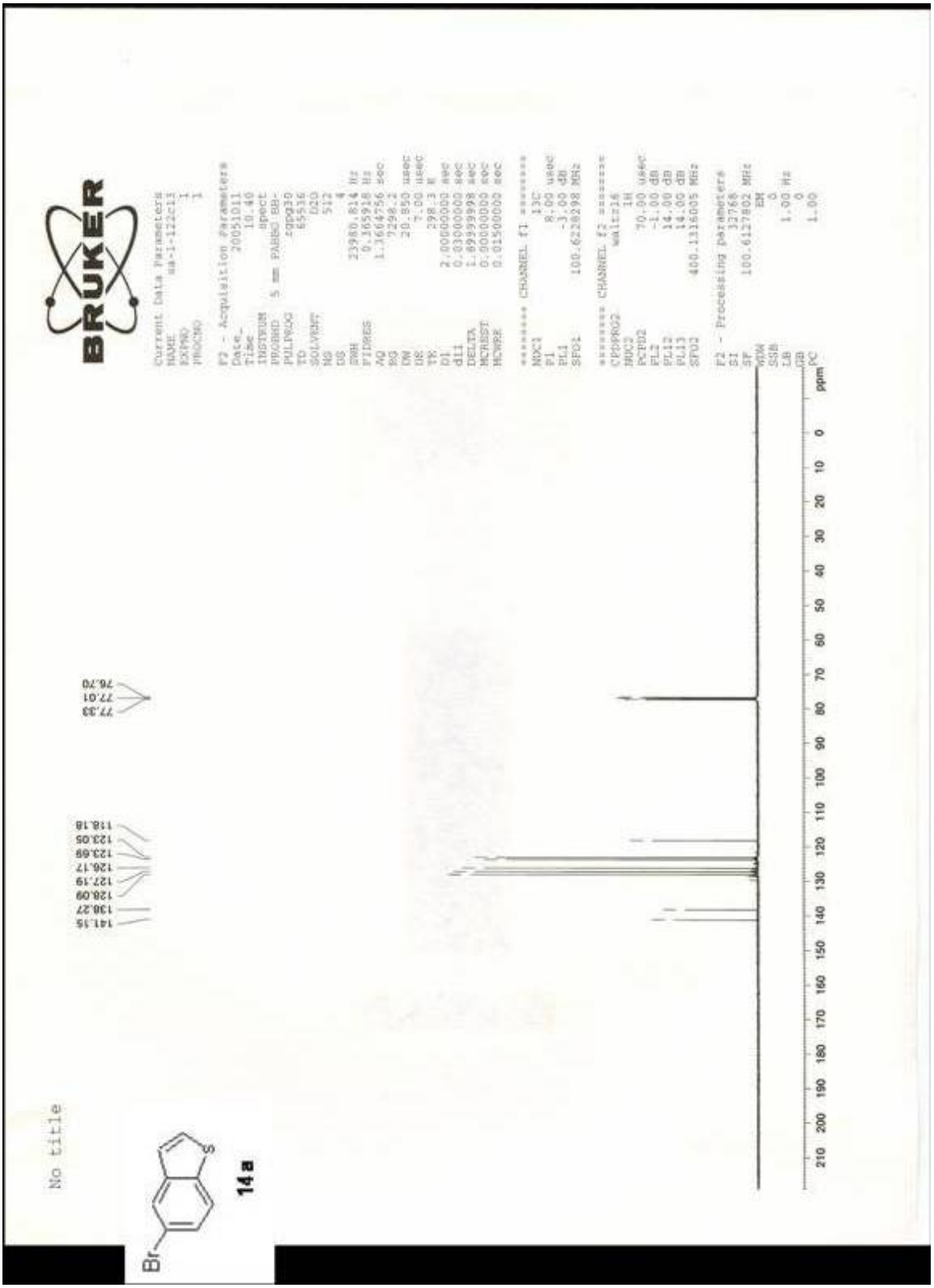
No title
14 a
Br
141.15
138.27
128.09
127.19
126.17
123.89
123.05
118.18
77.33
77.01
76.70
BRUKER
Current Data Parameters
NAME wa-1-122c13
EXPNO 1
PROCNO 1
F2 - Acquisition Parameters
Date_ 20051011
Time 10.40
INSTRUM spect
PROBHD 5 mm PABBO BB-
PULPROG zgpg30
TD 65536
SOLVENT CDCl3
NS 512
DS 4
SWH 23980.814 Hz
FIDRES 0.365918 Hz
AQ 1.3664756 sec
RG 7298.2
DW 20.850 usec
DE 7.00 usec
TE 298.3 K
D1 2.00000000 sec
d11 0.03000000 sec
DELTA 1.89999998 sec
MCREST 0.00000000 sec
MCWRK 0.01500000 sec
======== CHANNEL f1 ========
NUC1 13C
P1 8.00 usec
PL1 -3.00 dB
SFO1 100.6228298 MHz
======== CHANNEL f2 ========
CPDPRG2 waltz16
NUC2 1H
PCPD2 70.00 usec
PL2 -1.00 dB
PL12 14.00 dB
PL13 14.00 dB
SFO2 400.1316005 MHz
F2 - Processing parameters
SI 32768
SF 100.6127802 MHz
WDW EM
SSB 0
LB 1.00 Hz
GB 0
PC 1.00
ppm

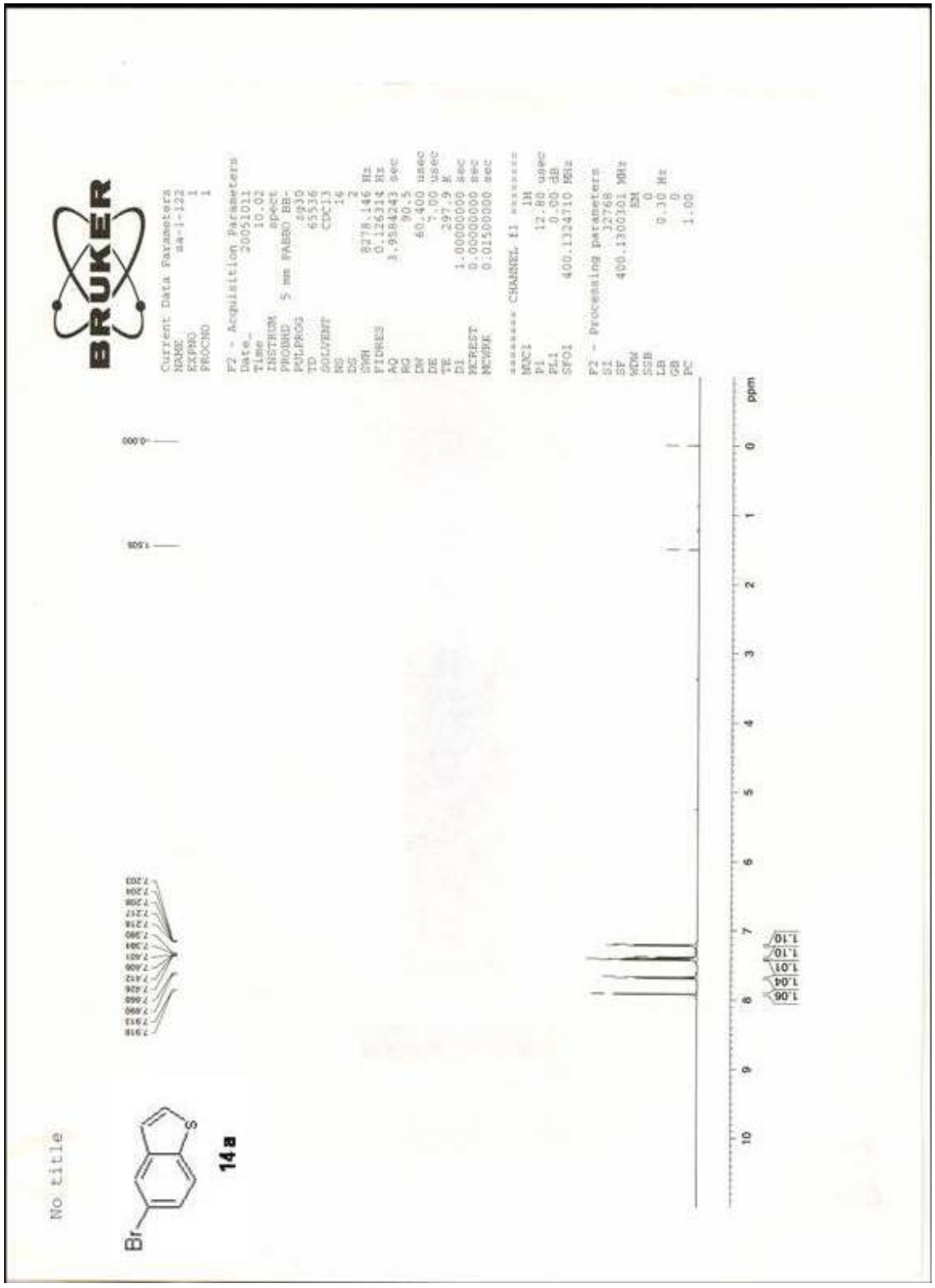
No title
14a
Br
BRUKER
Current Data Parameters
NAME sa-1-122
EXPNO 1
PROCNO 1
F2 - Acquisition Parameters
Date_ 20051011
Time 10.02
INSTRUM spect
PROBHD 5 mm PABBO BB-
PULPROG zg30
TD 65536
SOLVENT CDCl3
NS 16
DS 2
SWH 8278.146 Hz
FIDRES 0.126314 Hz
AQ 3.9584243 sec
RG 90.5
DW 60.400 usec
DE 7.00 usec
TE 297.9 K
D1 1.00000000 sec
MCREST 0.00000000 sec
MCWRK 0.01500000 sec
======== CHANNEL f1 ========
NUC1 1H
P1 12.80 usec
PL1 0.00 dB
SFO1 400.1324710 MHz
F2 - Processing parameters
SI 32768
SF 400.1300301 MHz
WDW EM
SSB 0
LB 0.30 Hz
GB 0
PC 1.00
1.06
1.04
1.01
1.10
1.10
ppm

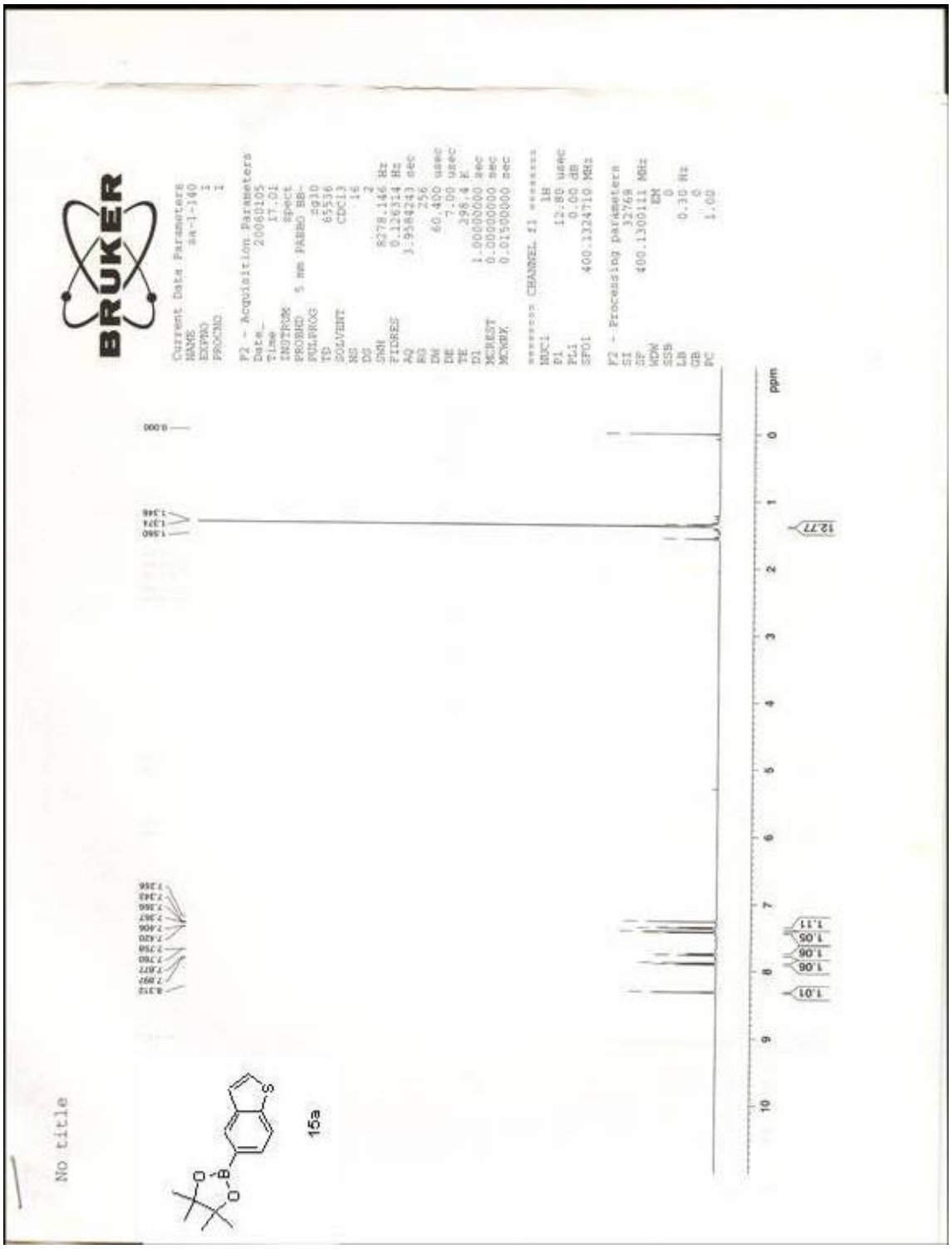
No title
15a
BRUKER
ppm

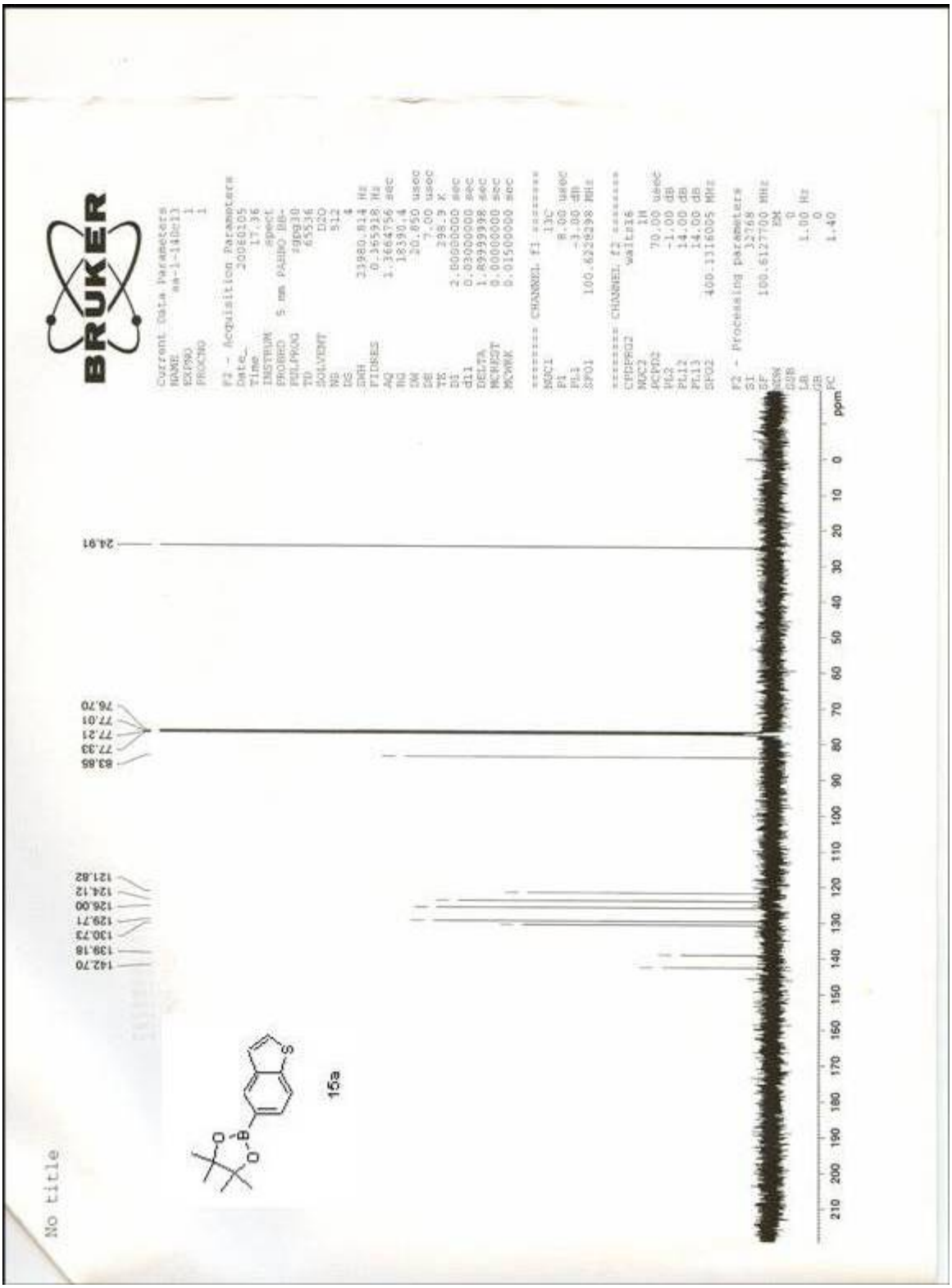
No title
BRUKER
15a
24.91
76.70
77.01
77.21
77.33
83.85
121.82
124.12
126.00
129.71
130.73
139.18
142.70
ppm

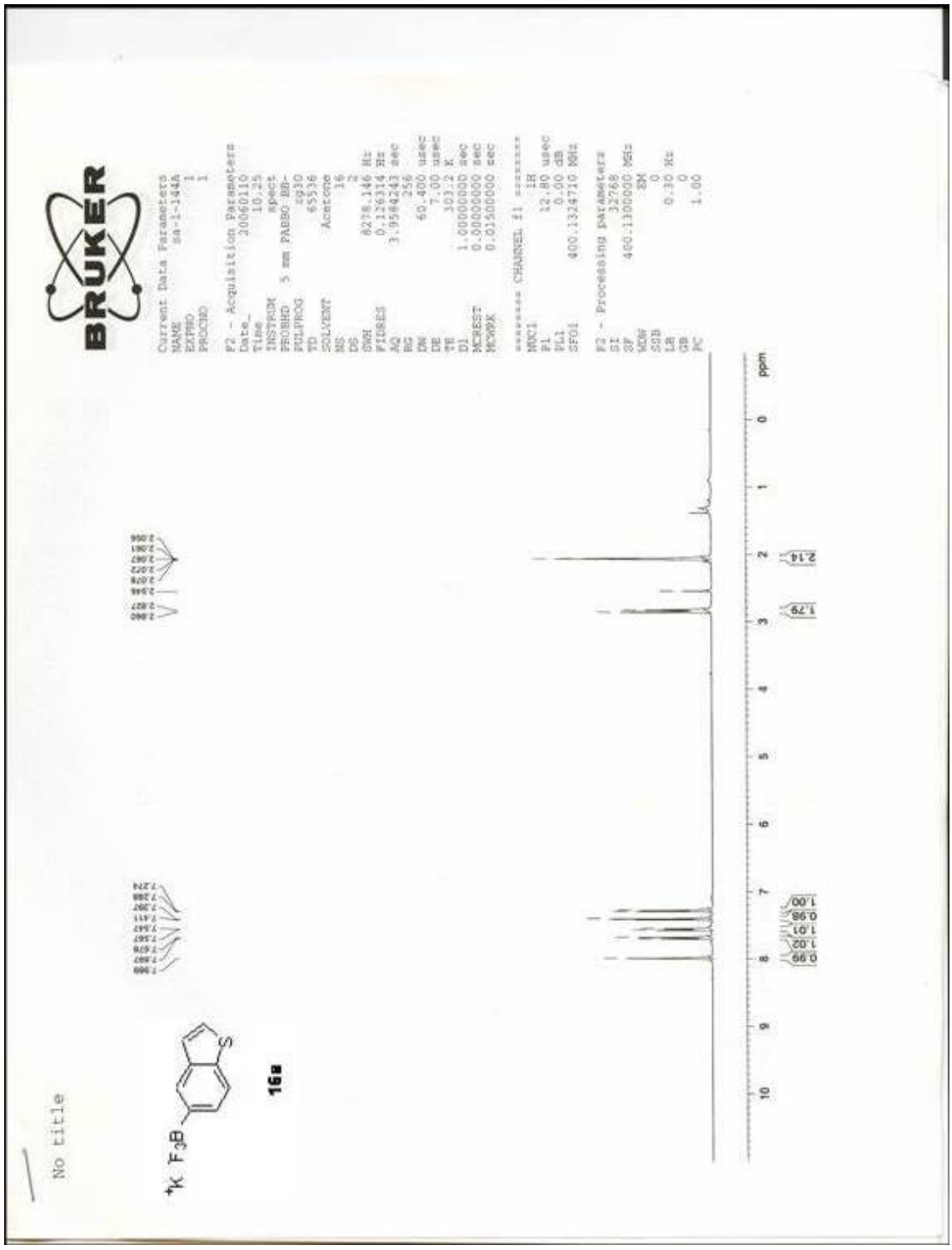
No title
16a
BRUKER
Current Data Parameters
NAME sa-1-144A
EXPNO 1
PROCNO 1
F2 - Acquisition Parameters
Date_ 20060110
Time 10.25
INSTRUM spect
PROBHD 5 mm PABBO BB-
PULPROG zg30
TD 65536
SOLVENT Acetone
NS 16
DS 2
SWH 8278.146 Hz
FIDRES 0.126314 Hz
AQ 3.9584243 sec
RG 256
DW 60.400 usec
DE 7.00 usec
TE 103.2 K
D1 1.00000000 sec
MCREST 0.00000000 sec
MCWRK 0.01500000 sec
======== CHANNEL f1 ========
NUC1 1H
P1 12.80 usec
PL1 0.00 dB
SFO1 400.1324710 MHz
F2 - Processing parameters
SI 32768
SF 400.1300000 MHz
WDW EM
SSB 0
LB 0.30 Hz
GB 0
PC 1.00
ppm
2.14
1.79
0.99
1.02
1.01
0.98
1.00

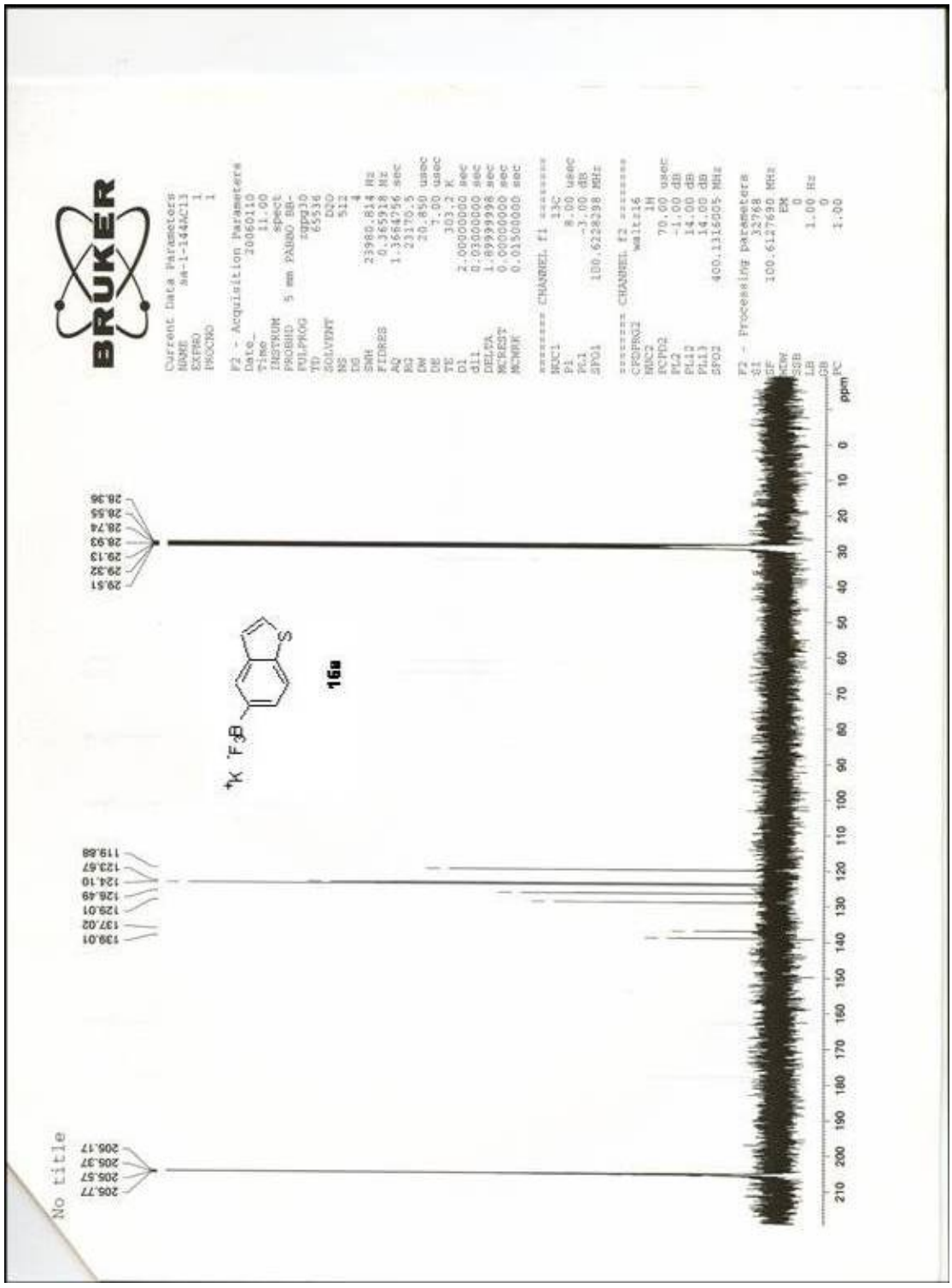
No title
BRUKER
16a
ppm

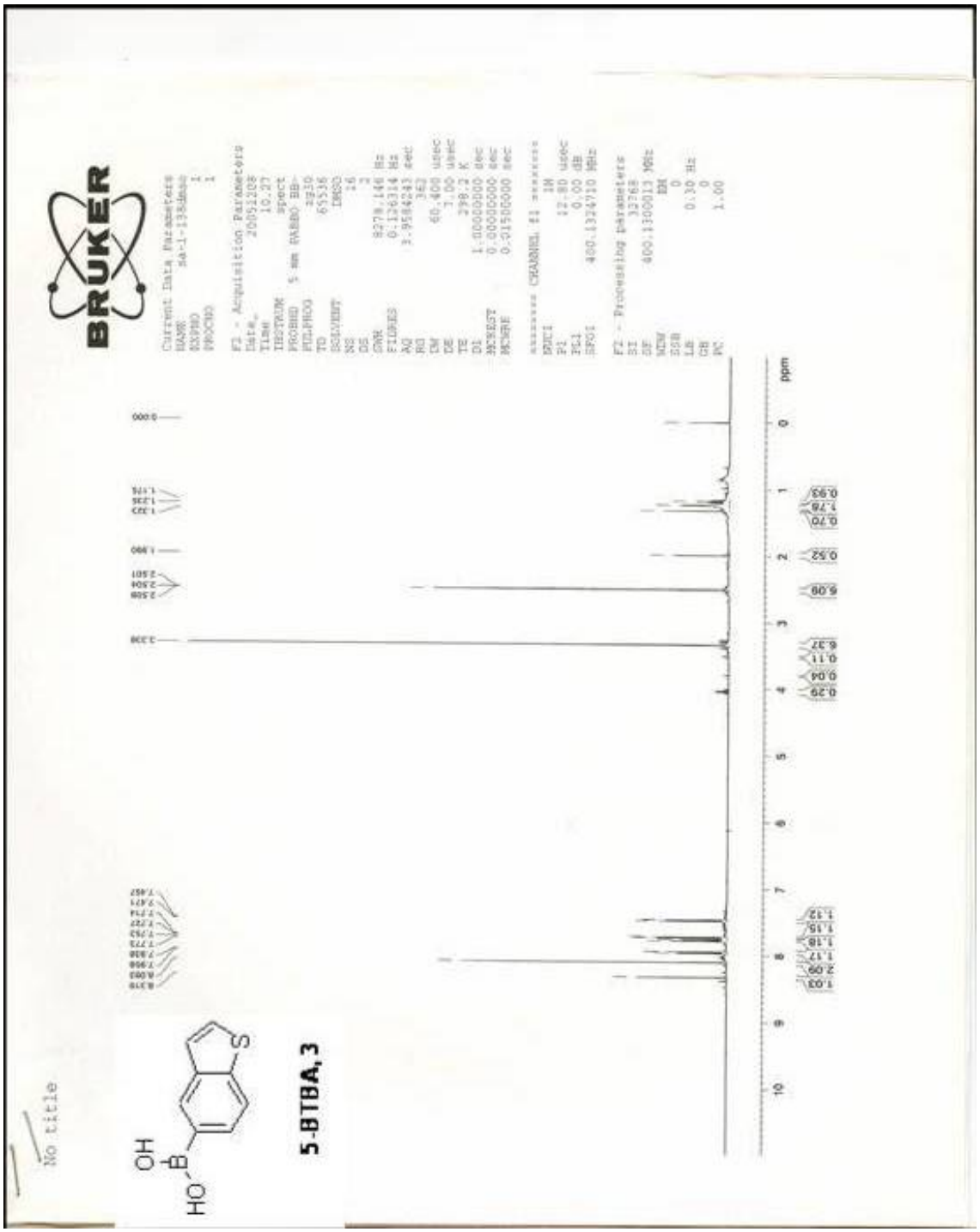
No title
BRUKER
5-BTBA,3
OH
B
HO
S
ppm

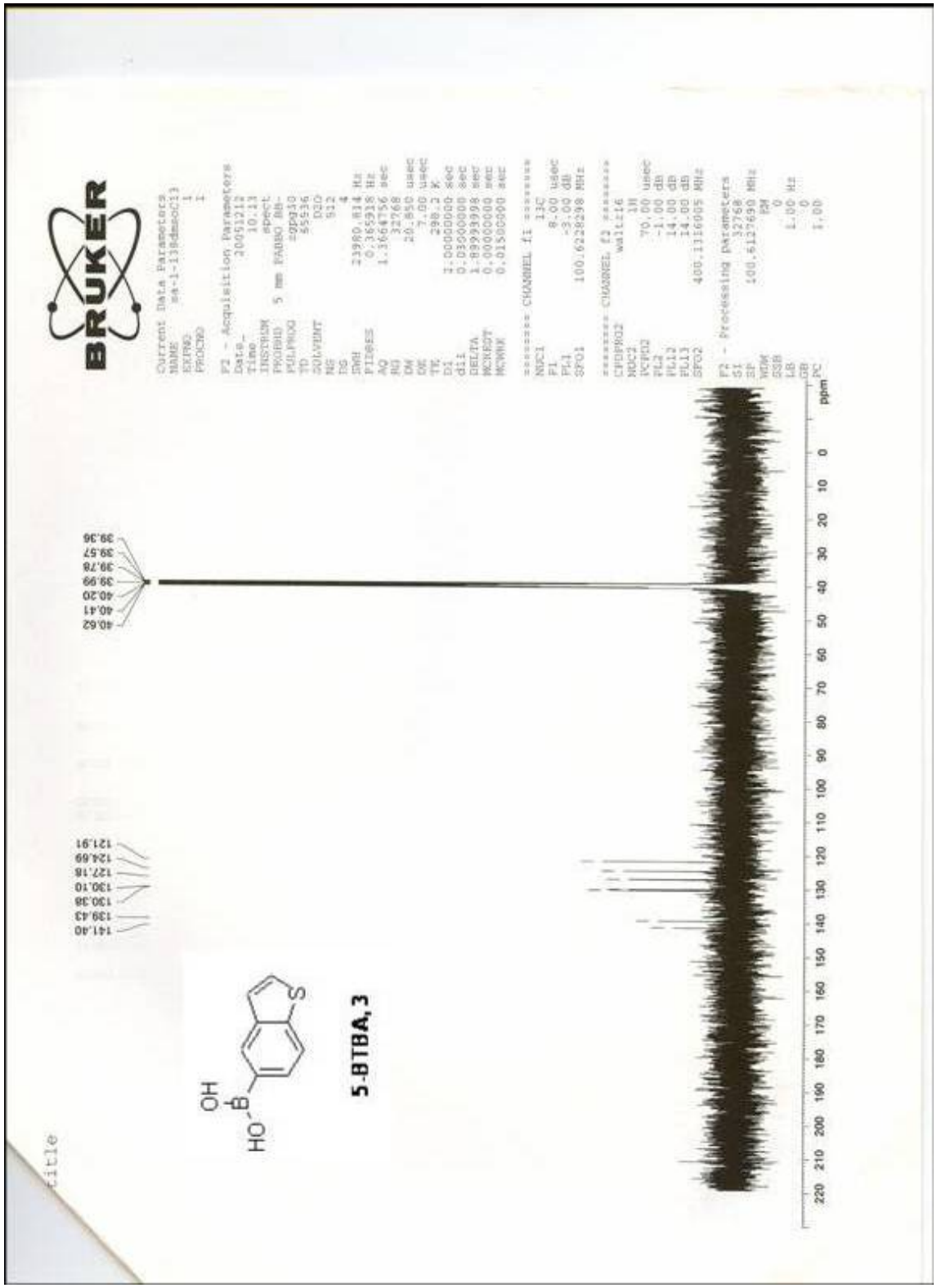
BRUKER
5-BTBA,3
OH
B
HO
S
141.40
139.43
130.38
130.10
127.18
124.69
121.91
40.62
40.41
40.20
39.99
39.78
39.57
39.36
ppm

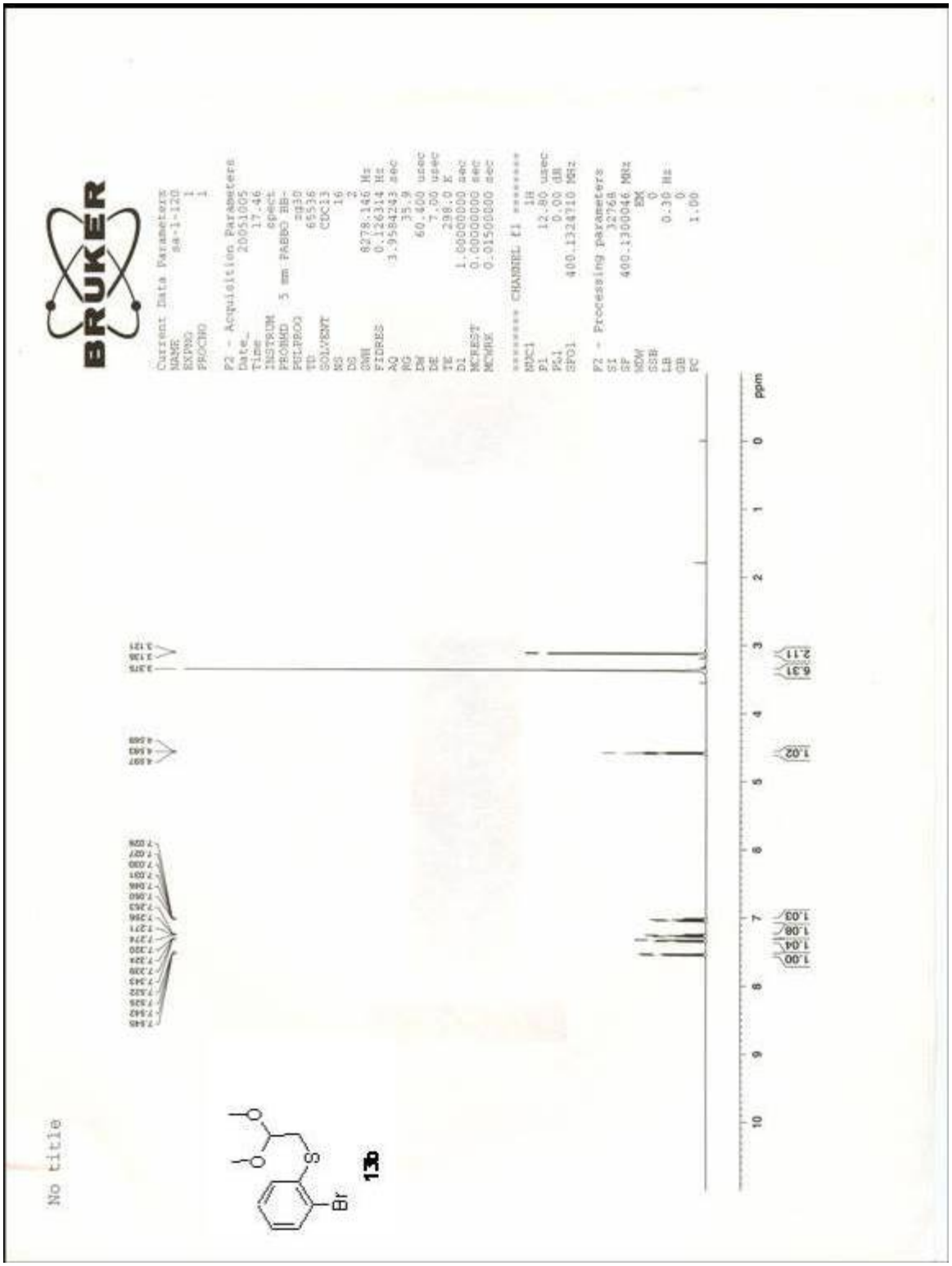
No title
13b
Br
BRUKER
ppm
6.31
2.11
1.02
1.00
1.03
1.06
1.04
1.00

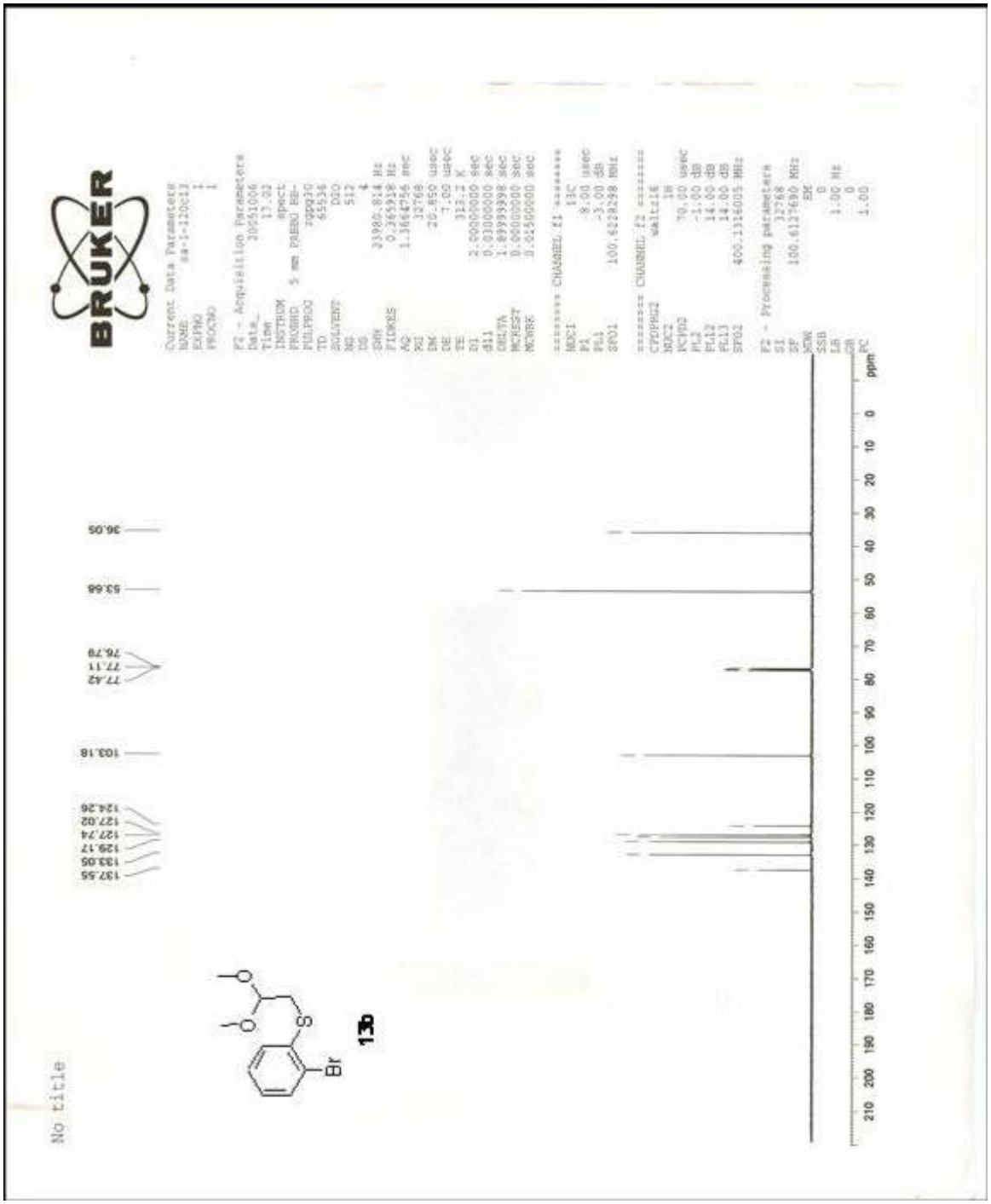
No title
13b
Br
36.05
53.66
76.79
77.11
77.42
103.18
124.26
127.02
127.74
129.17
133.05
137.55
ppm

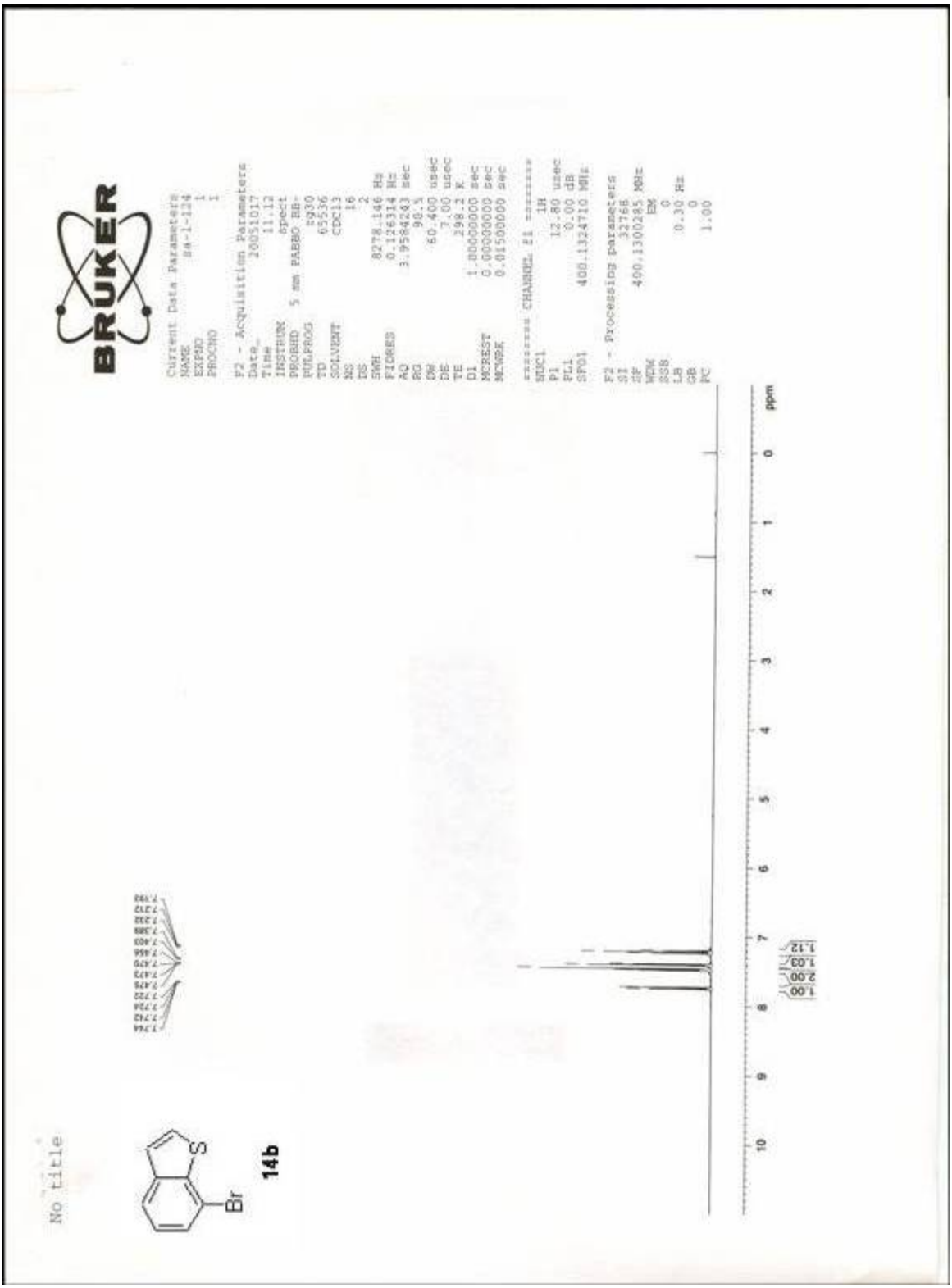
No title
14b
Br
S
BRUKER
Current Data Parameters
NAME 04-1-124
EXPNO 1
PROCNO 1
F2 - Acquisition Parameters
Date_ 20051017
Time 11.12
INSTRUM spect
PROBHD 5 mm PABBO BB-
PULPROG s930
TD 65536
SOLVENT CDCl3
NS 16
DS 2
SWH 8278.146 Hz
FIDRES 0.126314 Hz
AQ 3.9584243 sec
RG 90.5
DW 60.400 usec
DE 7.00 usec
TE 298.2 K
D1 1.00000000 sec
MCREST 0.00000000 sec
MCWRK 0.01500000 sec
======== CHANNEL f1 ========
SDC1 1H
P1 12.80 usec
PL1 0.00 dB
SFO1 400.1324710 MHz
F2 - Processing parameters
SI 32768
SF 400.1300285 MHz
WDW EM
SSB 0
LB 0.30 Hz
GB 0
PC 1.00
1.00
2.00
1.03
1.12
ppm

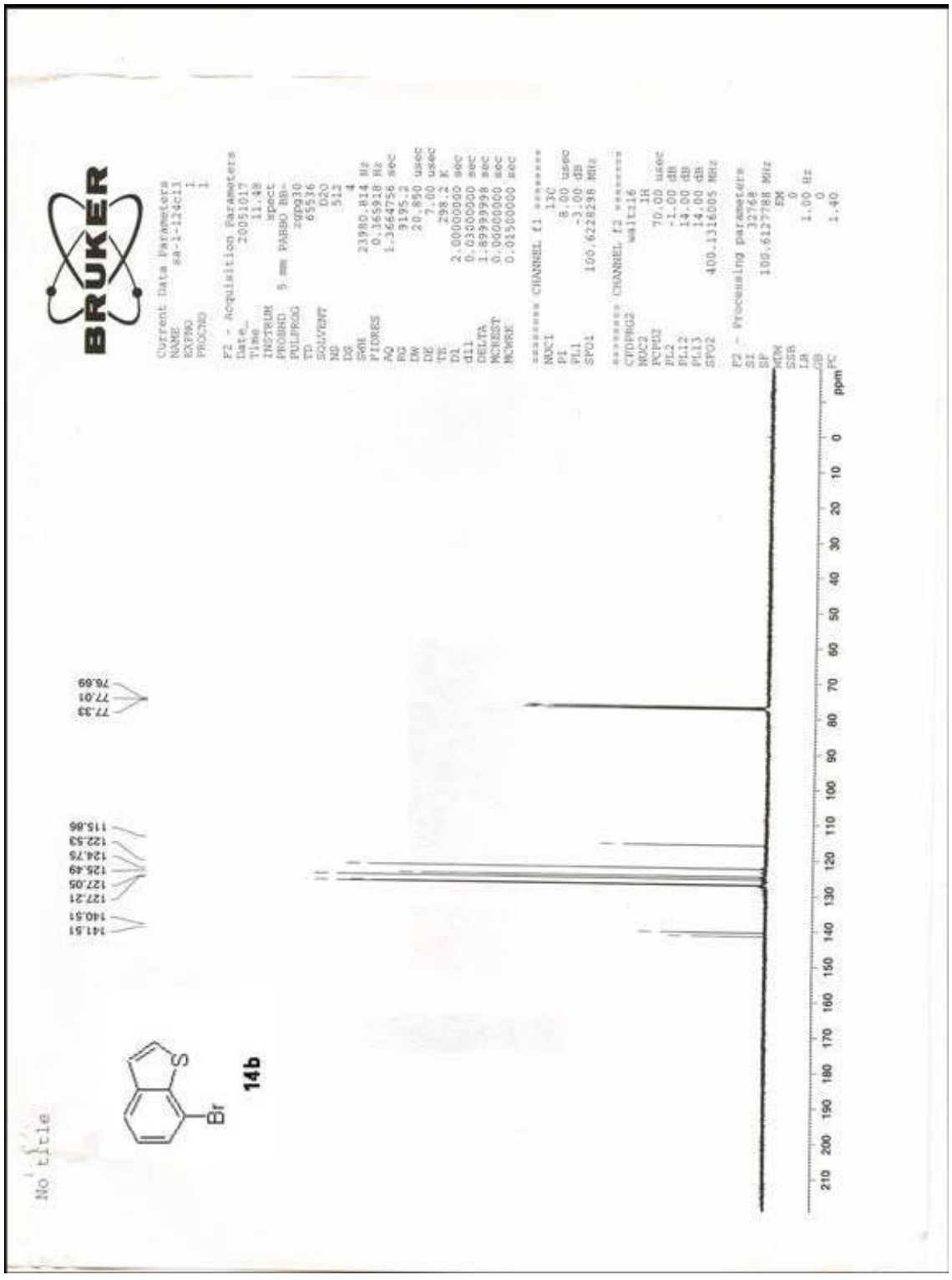
BRUKER
Current Data Parameters
NAME sa-1-124c11
EXPNO 1
PROCNO 1
F2 - Acquisition Parameters
Date_ 20051017
Time 11.48
INSTRUM spect
PROBHD 5 mm PABBO BB-
PULPROG zgpg30
TD 65536
SOLVENT CDCl3
NS 512
DS 4
SWH 23980.814 Hz
FIDRES 0.365918 Hz
AQ 1.3664756 sec
RG 3195.2
DW 20.850 usec
DE 7.00 usec
TE 298.2 K
D1 2.00000000 sec
d11 0.03000000 sec
DELTA 1.89999998 sec
MCWEGT 0.00000000 sec
MCWBK 0.01500000 sec
======== CHANNEL f1 ========
NUC1 13C
PL1 8.00 dBm
PL1 -3.00 dB
SFO1 100.6228298 MHz
======== CHANNEL f2 ========
CPDPRG2 waltz16
NUC2 1H
PCPD2 70.00 usec
PL2 -1.00 dB
PL12 14.00 dB
PL13 14.00 dB
SFO2 400.1316005 MHz
F2 - Processing parameters
SI 32768
SF 100.6127788 MHz
WDW EM
SSB 0
LB 1.00 Hz
GB 0
PC 1.40
77.33
77.01
76.69
141.51
140.51
127.21
127.05
125.49
124.75
122.53
115.86
ppm
14b
Br
S
No title

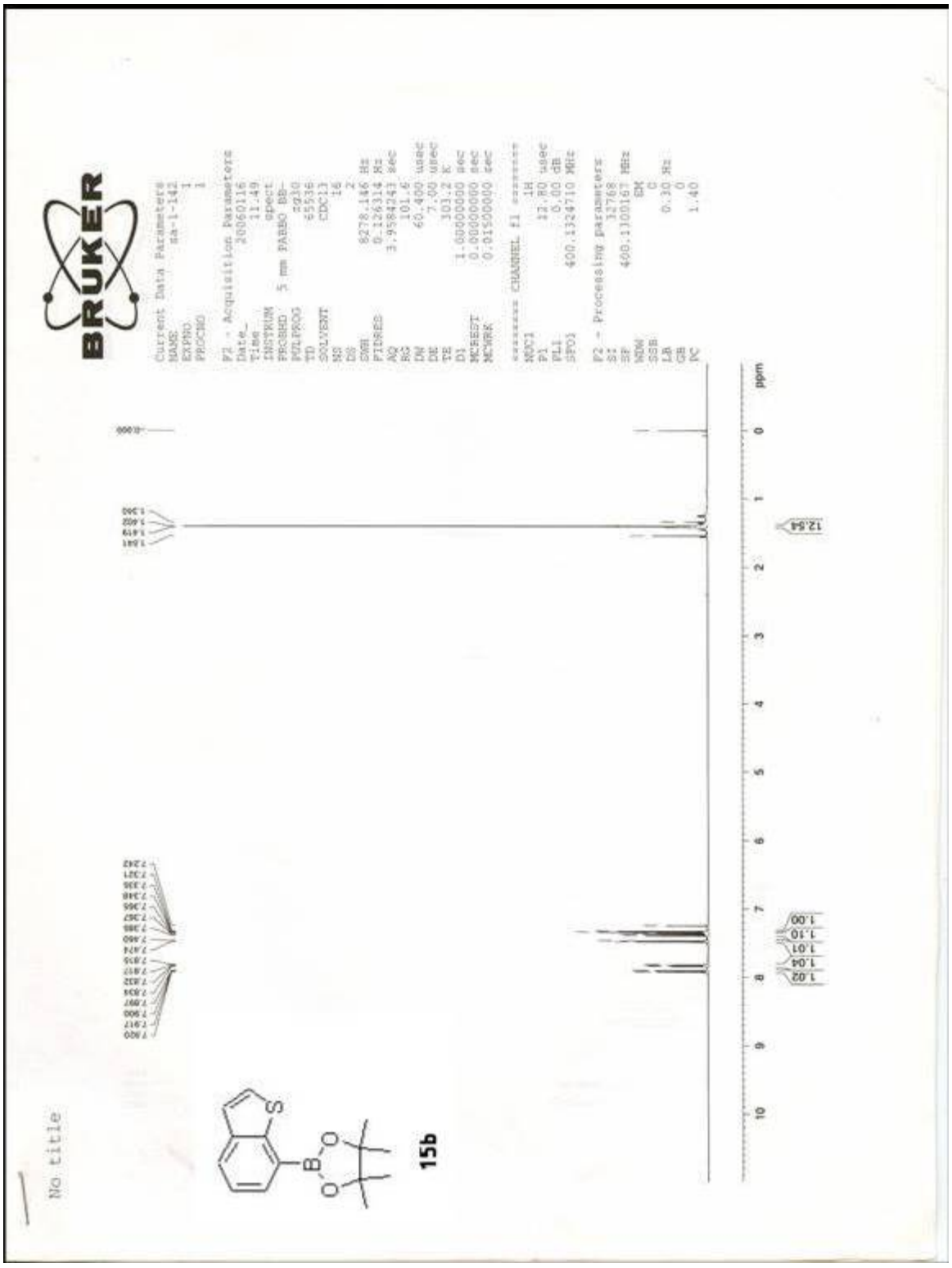
No title
BRUKER
Current Data Parameters
NAME sa-1-142
EXPNO 1
PROCNO 1
F2 - Acquisition Parameters
Date_ 20060116
Time 11.49
INSTRUM spect
PROBHD 5 mm PABBO BB-
PULPROG zg30
TD 65536
SOLVENT CDCl3
NS 16
DS 2
SWH 8278.146 Hz
FIDRES 0.126314 Hz
AQ 3.9584243 sec
RG 101.6
DW 60.400 usec
DE 7.00 usec
TE 303.2 K
D1 1.00000000 sec
MCREST 0.00000000 sec
MCWRK 0.01500000 sec
======== CHANNEL f1 ========
NUC1 1H
P1 12.80 usec
PL1 0.00 dB
SFO1 400.1324710 MHz
F2 - Processing parameters
SI 32768
SF 400.1100167 MHz
WDW EM
SSB 0
LB 0.30 Hz
GB 0
PC 1.40
12.54
1.02
1.04
1.01
1.10
1.00
ppm
15b

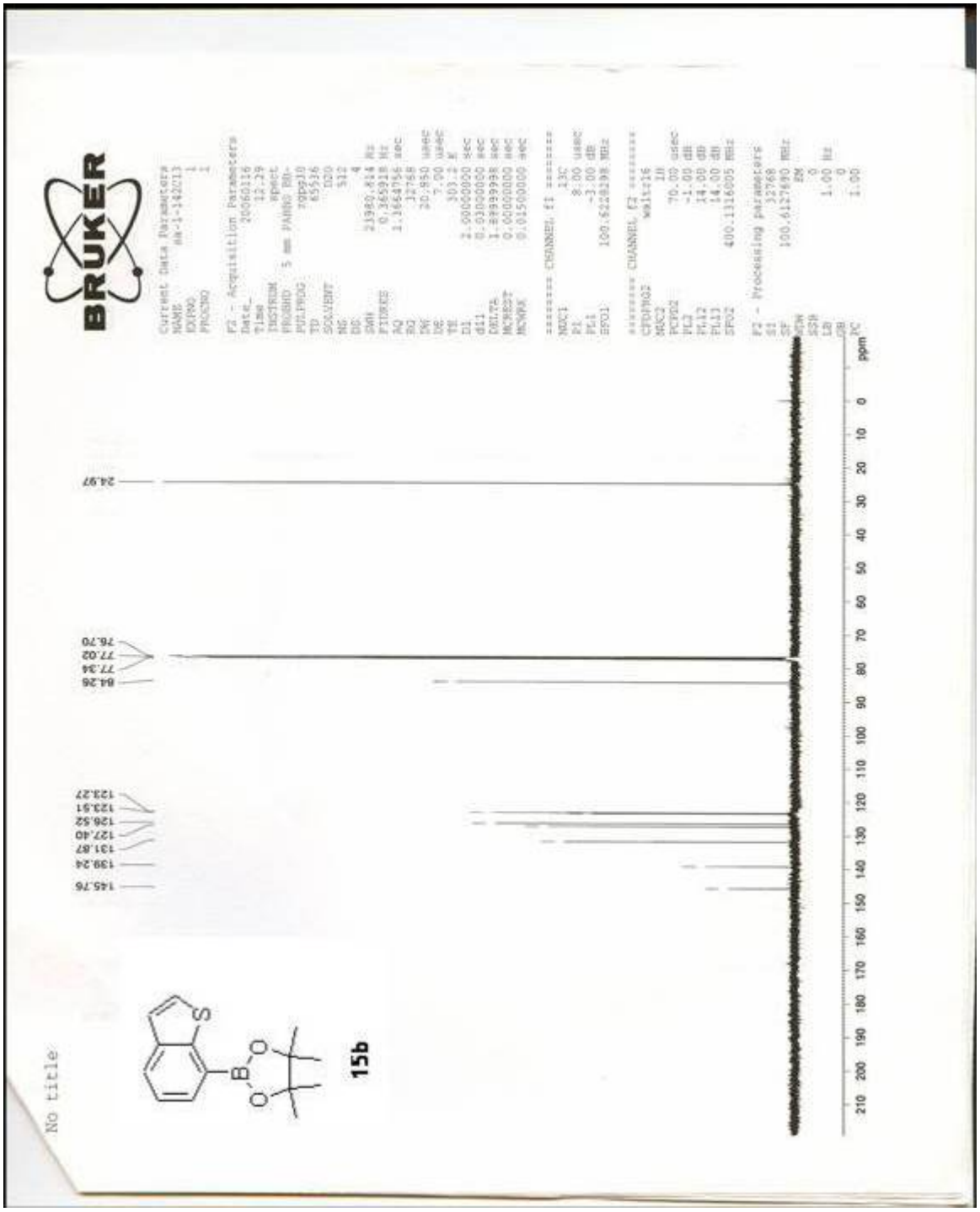
No title
15b
24.97
76.70
77.02
77.34
84.26
123.27
123.51
126.52
127.40
131.87
139.24
145.76
ppm

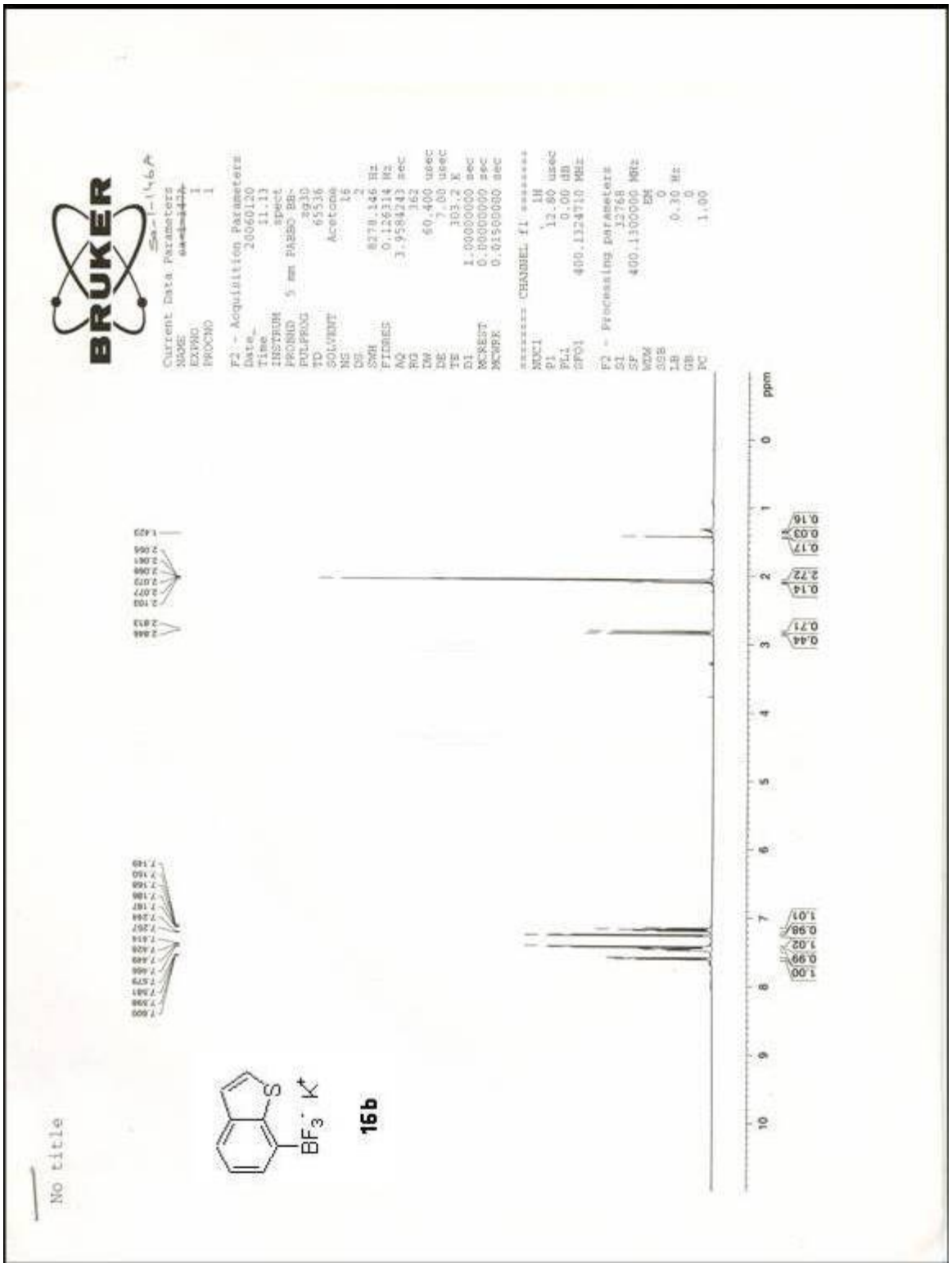
BRUKER
Current Data Parameters
F2 - Acquisition Parameters
F2 - Processing parameters
No title
16b
BF3 K+
S
ppm

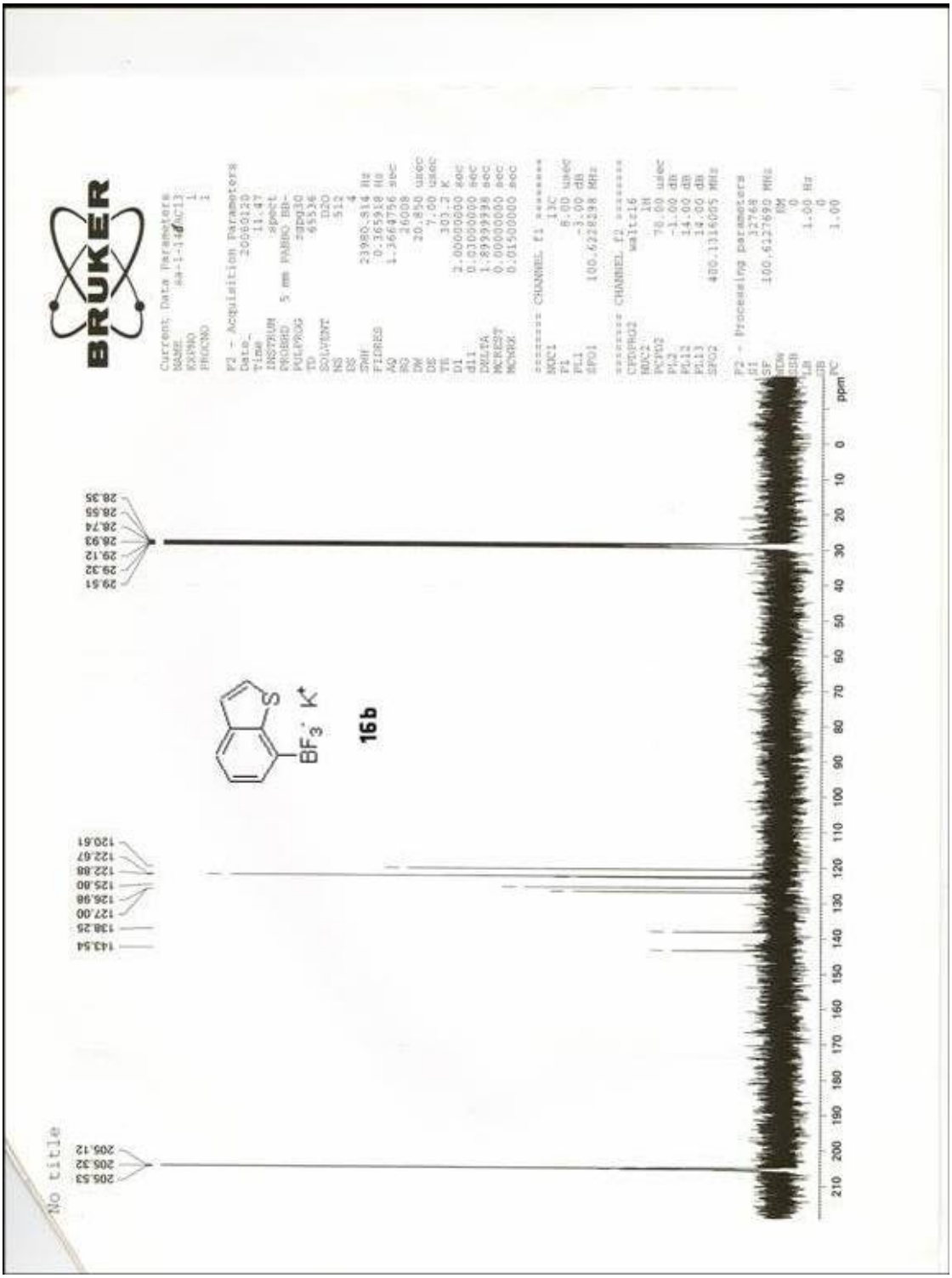
No title
BRUKER
16b
BF3 K+
S
205.53
205.32
205.12
143.54
138.25
127.00
126.98
125.80
122.88
122.67
120.61
29.51
29.32
29.12
28.93
28.74
28.55
28.35
ppm

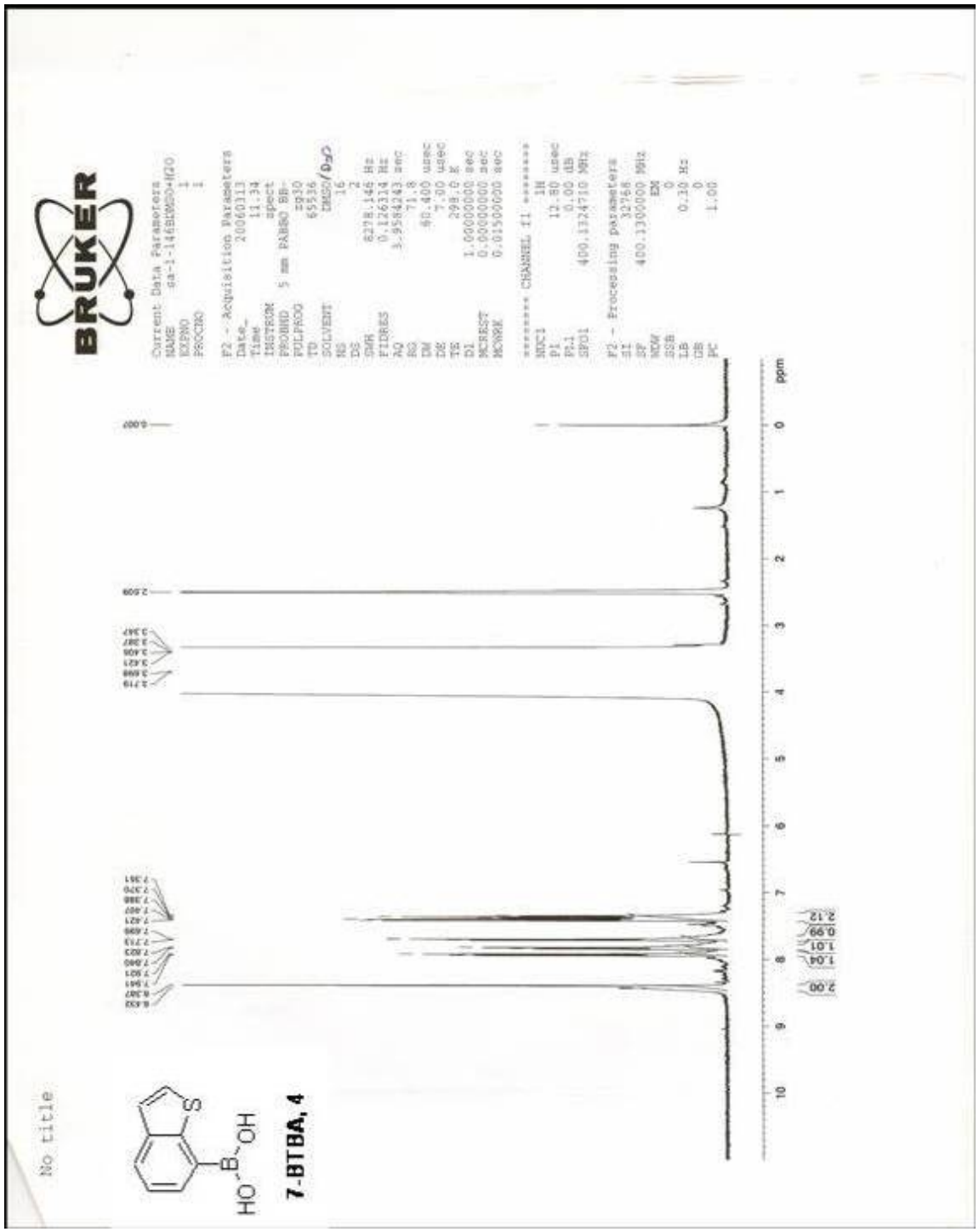
No title
BRUKER
Current Data Parameters
NAME ca-1-146BOMSO-H2O
EXPNO 1
PROCNO 1
F2 - Acquisition Parameters
Date_ 20060313
Time 11.34
INSTRUM spect
PROBHD 5 mm PABBO BB-
PULPROG zg30
TD 65536
SOLVENT DMSO
NS 16
DS 2
SWH 8278.146 Hz
FIDRES 0.126314 Hz
AQ 3.9584243 sec
RG 71.8
DW 60.400 usec
DE 7.00 usec
TE 298.0 K
D1 1.00000000 sec
MCREST 0.00000000 sec
MCWRK 0.01500000 sec
======== CHANNEL f1 ========
NUC1 1H
P1 12.80 usec
PL1 0.00 dB
SFO1 400.1324710 MHz
F2 - Processing parameters
SI 32768
SF 400.1300000 MHz
WDW EM
SSB 0
LB 0.10 Hz
GB 0
PC 1.00
2.509
3.719
3.899
3.421
3.406
3.387
3.367
6.432
6.387
7.341
7.361
7.379
7.388
7.407
7.427
7.698
7.713
7.723
7.860
7.901
2.00
1.04
1.01
0.99
2.12
ppm
HO
B
OH
S
7-BTBA, 4

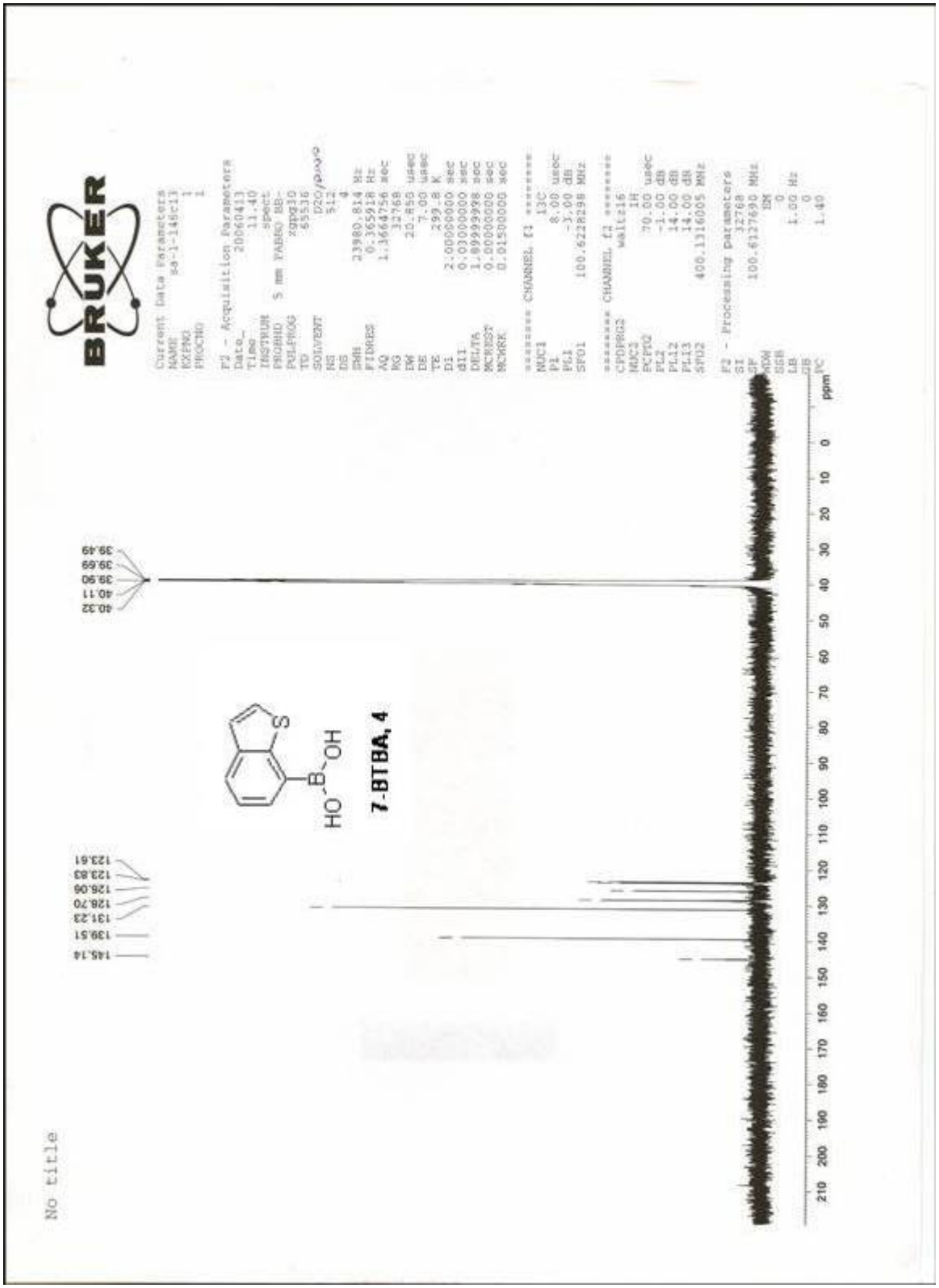
No title
BRUKER
Current Data Parameters
NAME xa-1-146c13
EXPNO 1
PROCNO 1
F2 - Acquisition Parameters
Date_ 20060413
Time 11.40
INSTRUM spect
PROBHD 5 mm PABBO BB-
PULPROG zgpg30
TD 65536
SOLVENT D2O/pyro
NS 512
DS 4
SWH 23980.814 Hz
FIDRES 0.365918 Hz
AQ 1.3664756 sec
RG 32768
DW 20.850 usec
DE 7.00 usec
TE 299.8 K
D1 2.00000000 sec
d11 0.03000000 sec
DELTA 1.89999998 sec
MCREST 0.00000000 sec
MCWRK 0.01500000 sec
======== CHANNEL f1 ========
NUC1 13C
P1 8.00 usec
PL1 -3.00 dB
SFO1 100.6228298 MHz
======== CHANNEL f2 ========
CPDPRG2 waltz16
NUC2 1H
PCPD2 70.00 usec
PL2 -1.00 dB
PL12 14.00 dB
PL13 14.00 dB
SFO2 400.1316005 MHz
F2 - Processing parameters
SI 32768
SF 100.6127690 MHz
WDW EM
SSB 0
LB 1.00 Hz
GB 0
PC 1.40
ppm
40.32
40.11
39.90
39.69
39.49
145.14
139.51
131.23
128.70
128.06
123.83
123.61
S
HO
B
OH
7-BTBA, 4

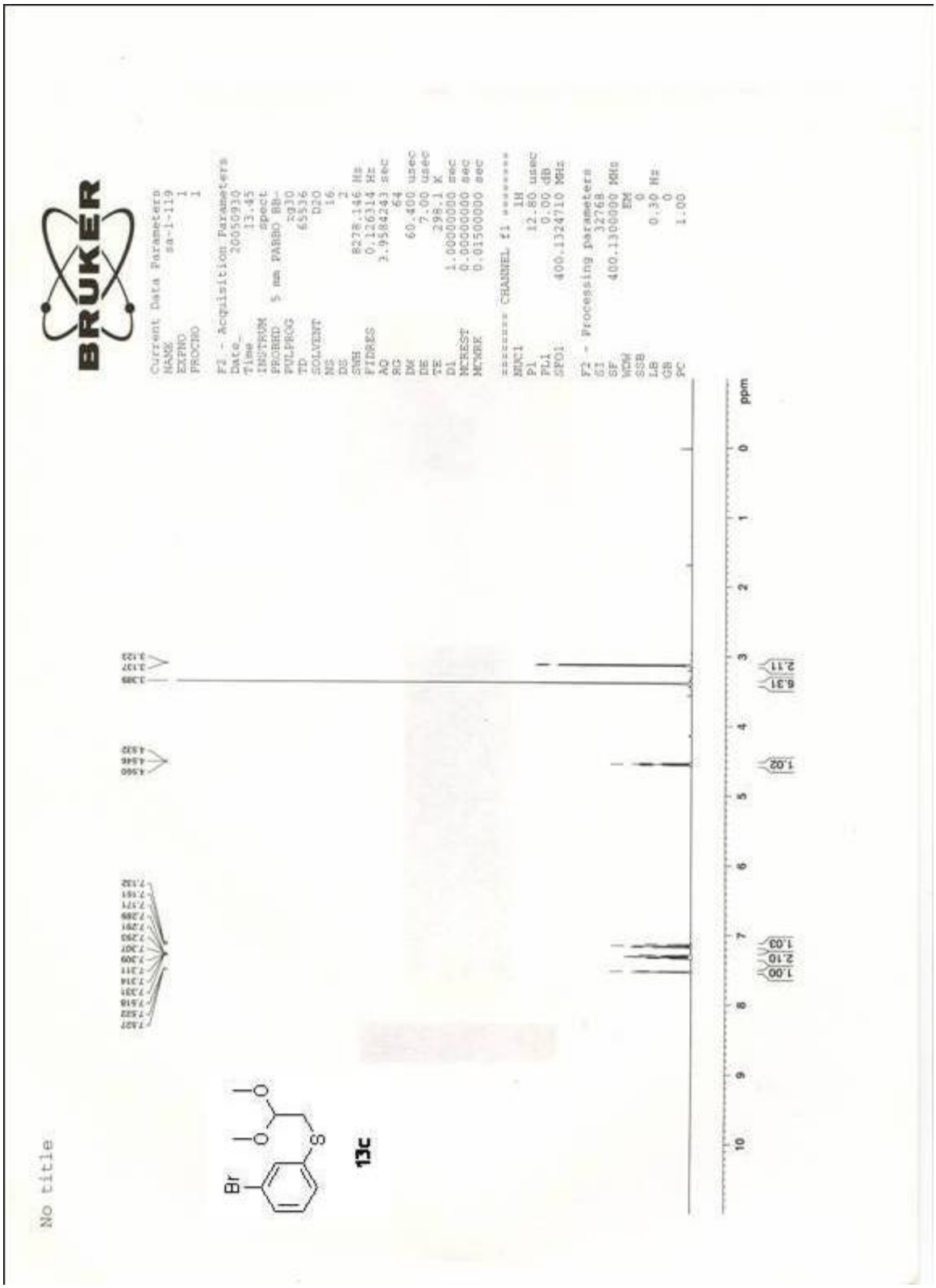
BRUKER
Current Data Parameters
NAME sa-1-119
EXPNO 1
PROCNO 1
F2 - Acquisition Parameters
Date_ 20050930
Time 13.45
INSTRUM spect
PROBHD 5 mm PABBO BB-
PULPROG zg30
TD 65536
SOLVENT D2O
NS 16
DS 2
SWH 8278.146 Hz
FIDRES 0.126314 Hz
AQ 3.9584243 sec
RG 64
DW 60.400 usec
DE 7.00 usec
TE 298.1 K
D1 1.00000000 sec
MCREST 0.00000000 sec
MCWRK 0.01500000 sec
======== CHANNEL f1 ========
NUC1 1H
P1 12.80 usec
PL1 0.00 dB
SFO1 400.1324710 MHz
F2 - Processing parameters
SI 32768
SF 400.1300000 MHz
WDW EM
SSB 0
LB 0.30 Hz
GB 0
PC 1.00
13c
No title
ppm

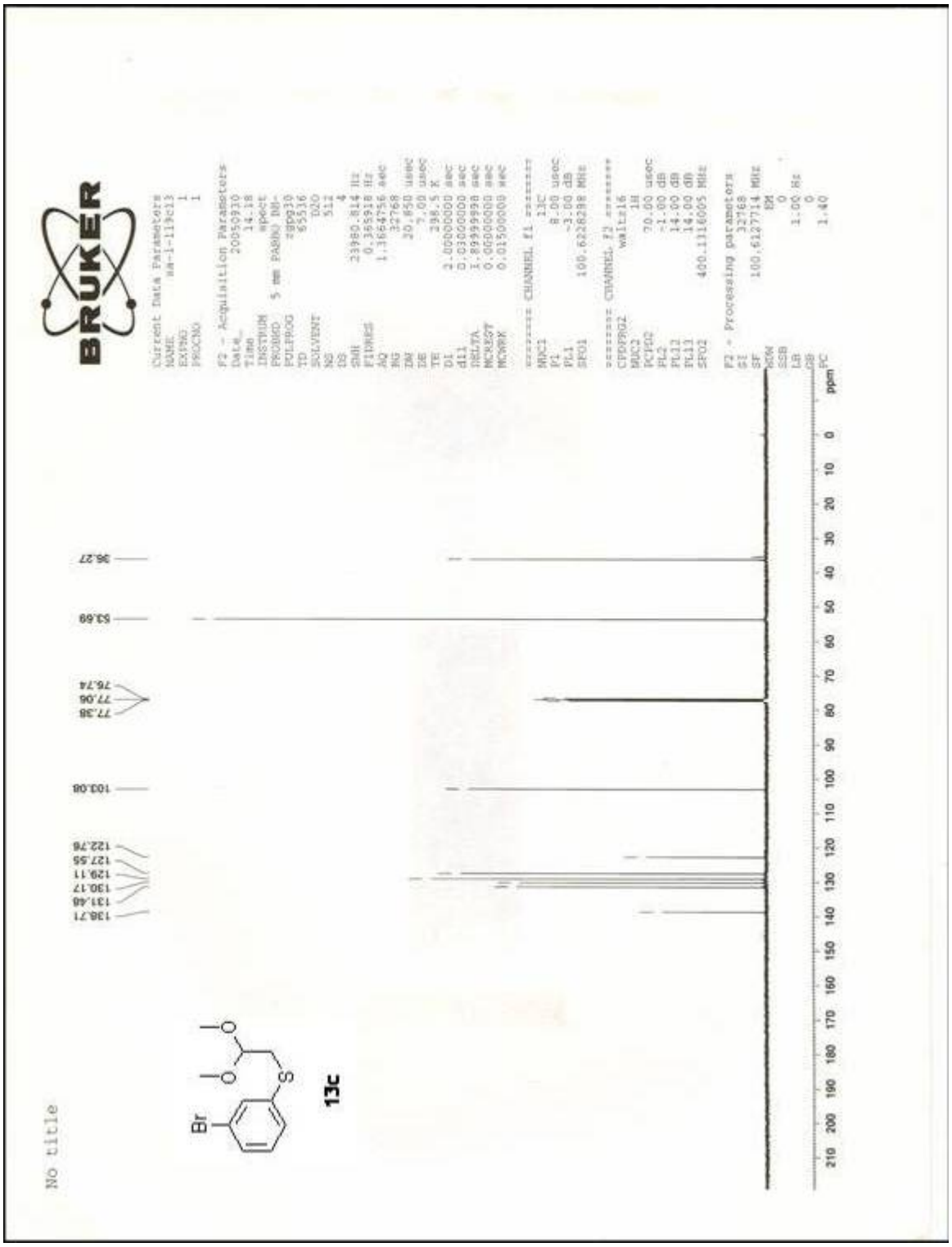
No title
13c
Br
O
O
S
136.71
131.46
130.17
129.11
127.55
122.76
103.08
77.38
77.06
76.74
53.69
36.27
ppm

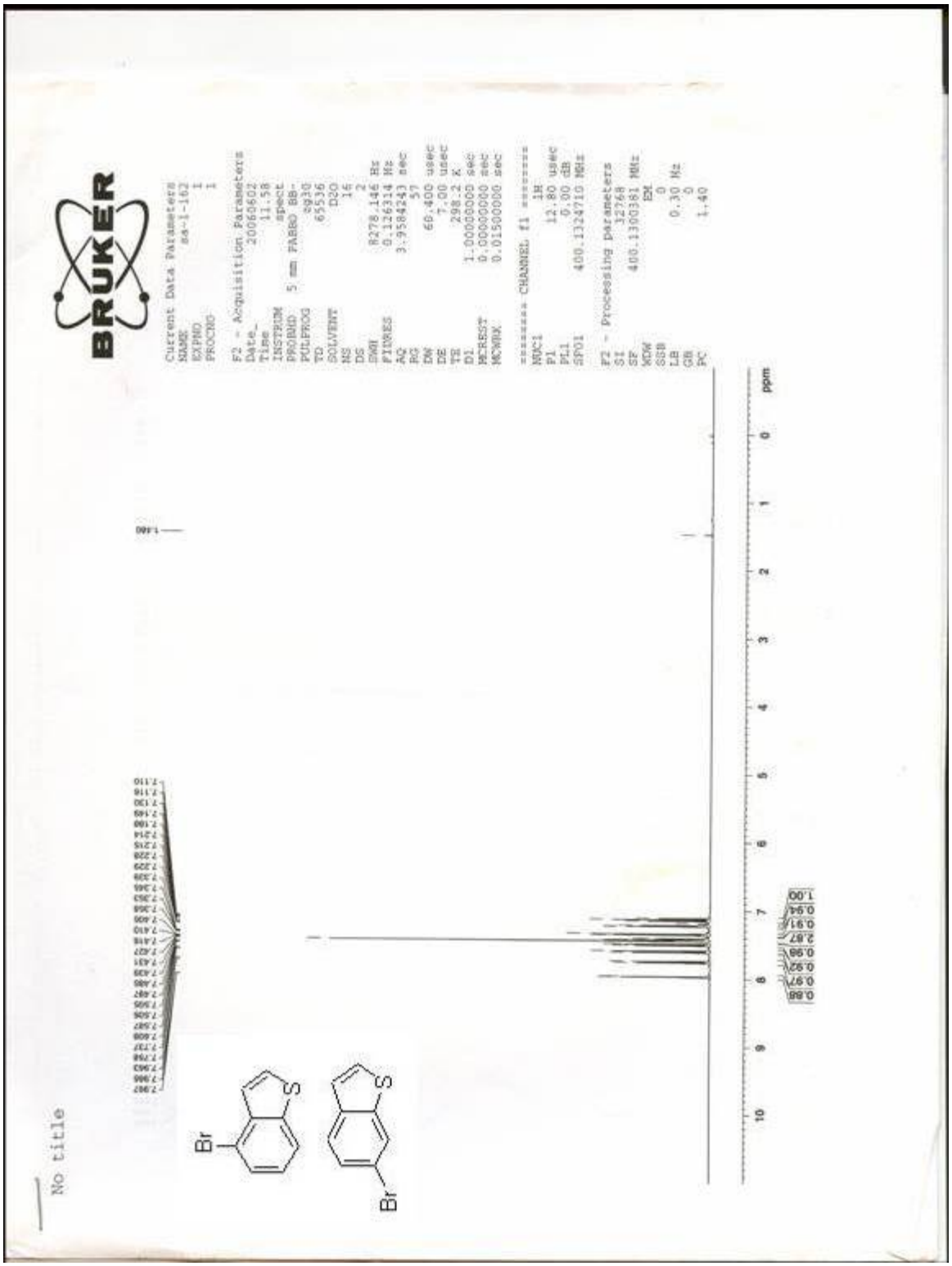
No title
BRUKER
Current Data Parameters
NAME sa-1-162
EXPNO 1
PROCNO 1
F2 - Acquisition Parameters
Date_ 20060602
Time 11.58
INSTRUM spect
PROBHD 5 mm PABBO BB-
PULPROG zg30
TD 65536
SOLVENT D2O
NS 16
DS 2
SWH 8278.146 Hz
FIDRES 0.126314 Hz
AQ 3.9584243 sec
RG 57
DW 60.400 usec
DE 7.00 usec
TE 298.2 K
D1 1.00000000 sec
MCREST 0.00000000 sec
MCWRK 0.01500000 sec
======= CHANNEL f1 ========
NUC1 1H
P1 12.80 usec
PL1 0.00 dB
SFO1 400.1324710 MHz
F2 - Processing parameters
SI 32768
SF 400.1300381 MHz
WDW EM
SSB 0
LB 0.30 Hz
GB 0
PC 1.40
Br
Br
ppm
0.88
0.97
0.92
0.98
2.87
0.91
0.94
1.00

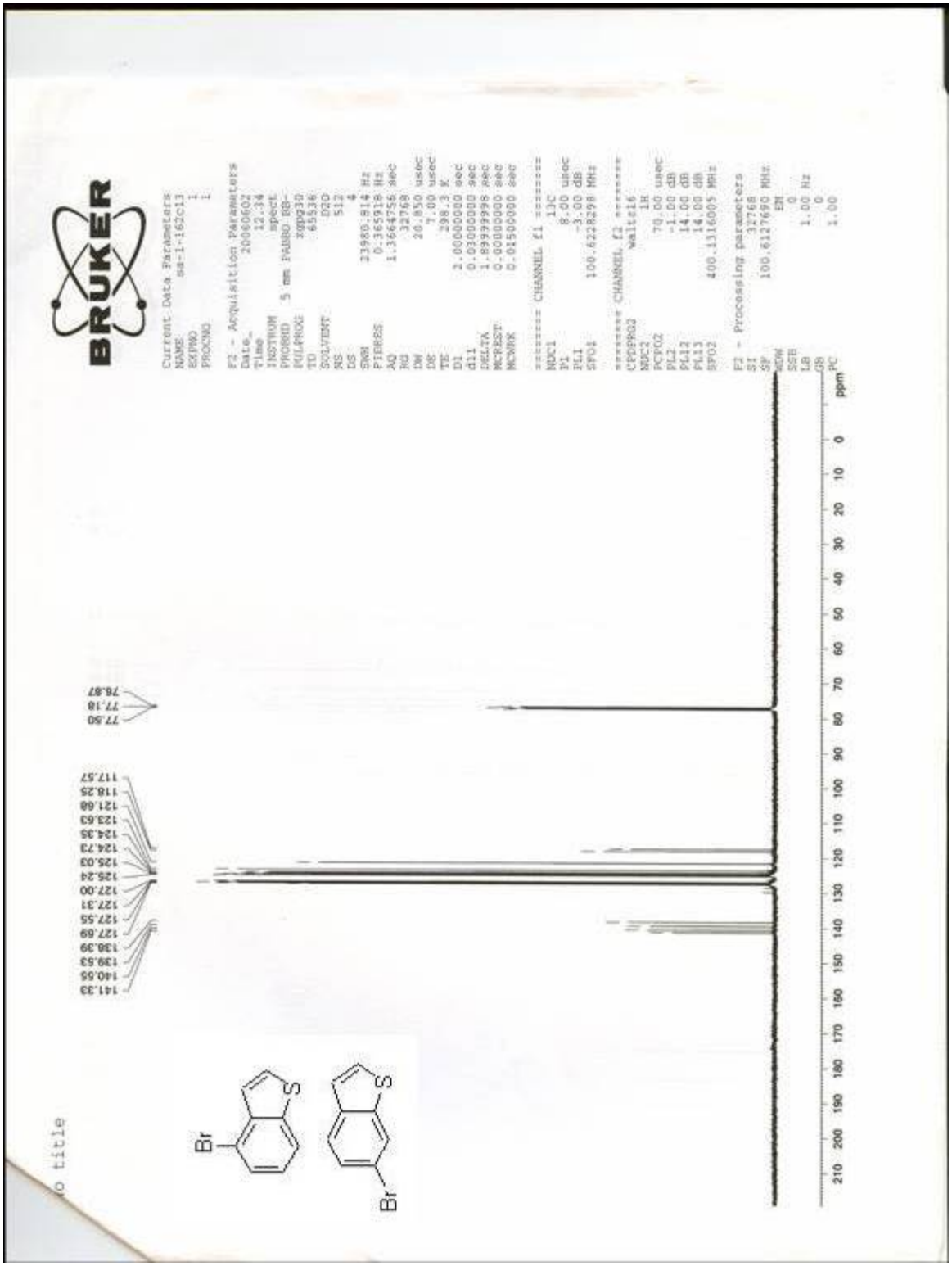
BRUKER
Current Data Parameters
NAME sa-1-162c13
EXPNO 1
PROCNO 1
F2 - Acquisition Parameters
Date_ 20060602
Time 12.34
INSTRUM spect
PROBHD 5 mm PABBO BB-
PULPROG zgpg30
TD 65536
SOLVENT D2O
NS 512
DS 4
SWH 23980.814 Hz
FIDRES 0.365918 Hz
AQ 1.3664756 sec
RG 32768
DW 20.850 usec
DE 7.00 usec
TE 298.3 K
D1 2.00000000 sec
d11 0.03000000 sec
DELTA 1.89999998 sec
MCREST 0.00000000 sec
MCWRK 0.01500000 sec
======== CHANNEL f1 ========
NUC1 13C
P1 8.00 usec
PL1 -3.00 dB
SFO1 100.6228298 MHz
======== CHANNEL f2 ========
CPDPRG2 waltz16
NUC2 1H
PCPD2 70.00 usec
PL2 -1.00 dB
PL12 14.00 dB
PL13 14.00 dB
SFO2 400.1316005 MHz
F2 - Processing parameters
SI 32768
SF 100.6127690 MHz
WDW EM
SSB 0
LB 1.00 Hz
GB 0
PC 1.00
141.33
140.55
139.53
138.39
127.69
127.55
127.31
127.00
125.24
125.03
124.73
124.35
123.63
121.68
118.25
117.57
77.50
77.18
76.87
Br
S
Br
S
ppm
o title

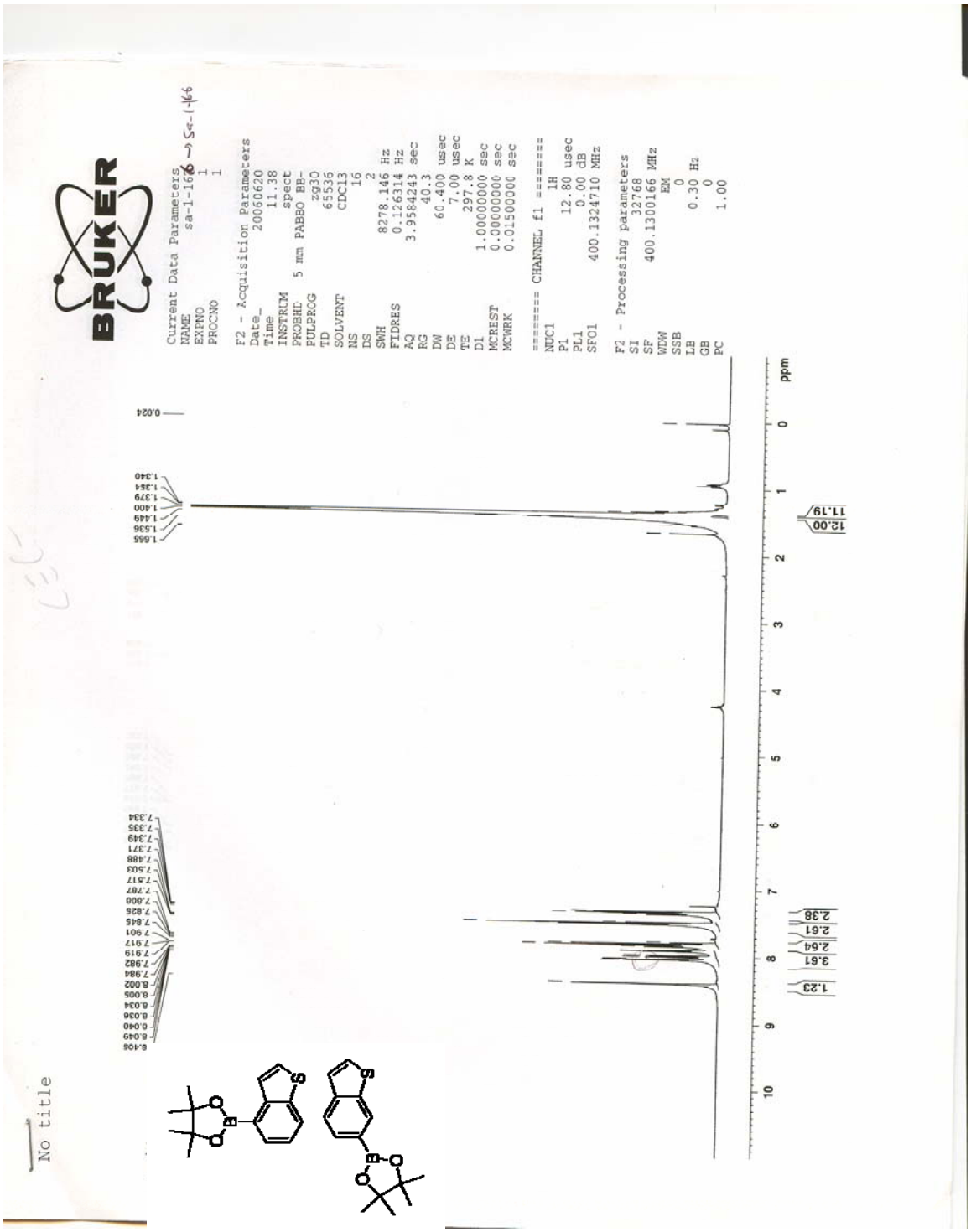
No title
BRUKER
Current Data Parameters
NAME sa-1-166 → Sa-I-166
EXPNO 1
PROCNO 1
F2 - Acquisition Parameters
Date_ 20060620
Time 11.38
INSTRUM spect
PROBHD 5 mm PABBO BB-
PULPROG zg30
TD 65536
SOLVENT CDCl3
NS 16
DS 2
SWH 8278.146 Hz
FIDRES 0.126314 Hz
AQ 3.9584243 sec
RG 40.3
DW 60.400 usec
DE 7.00 usec
TE 297.8 K
D1 1.00000000 sec
MCREST 0.00000000 sec
MCWRK 0.01500000 sec
======== CHANNEL f1 ========
NUC1 1H
P1 12.80 usec
PL1 0.00 dB
SFO1 400.1324710 MHz
F2 - Processing parameters
SI 32768
SF 400.1300166 MHz
WDW EM
SSB 0
LB 0.30 Hz
GB 0
PC 1.00
ppm
12.00
11.19
3.61
2.64
2.61
2.38
1.23

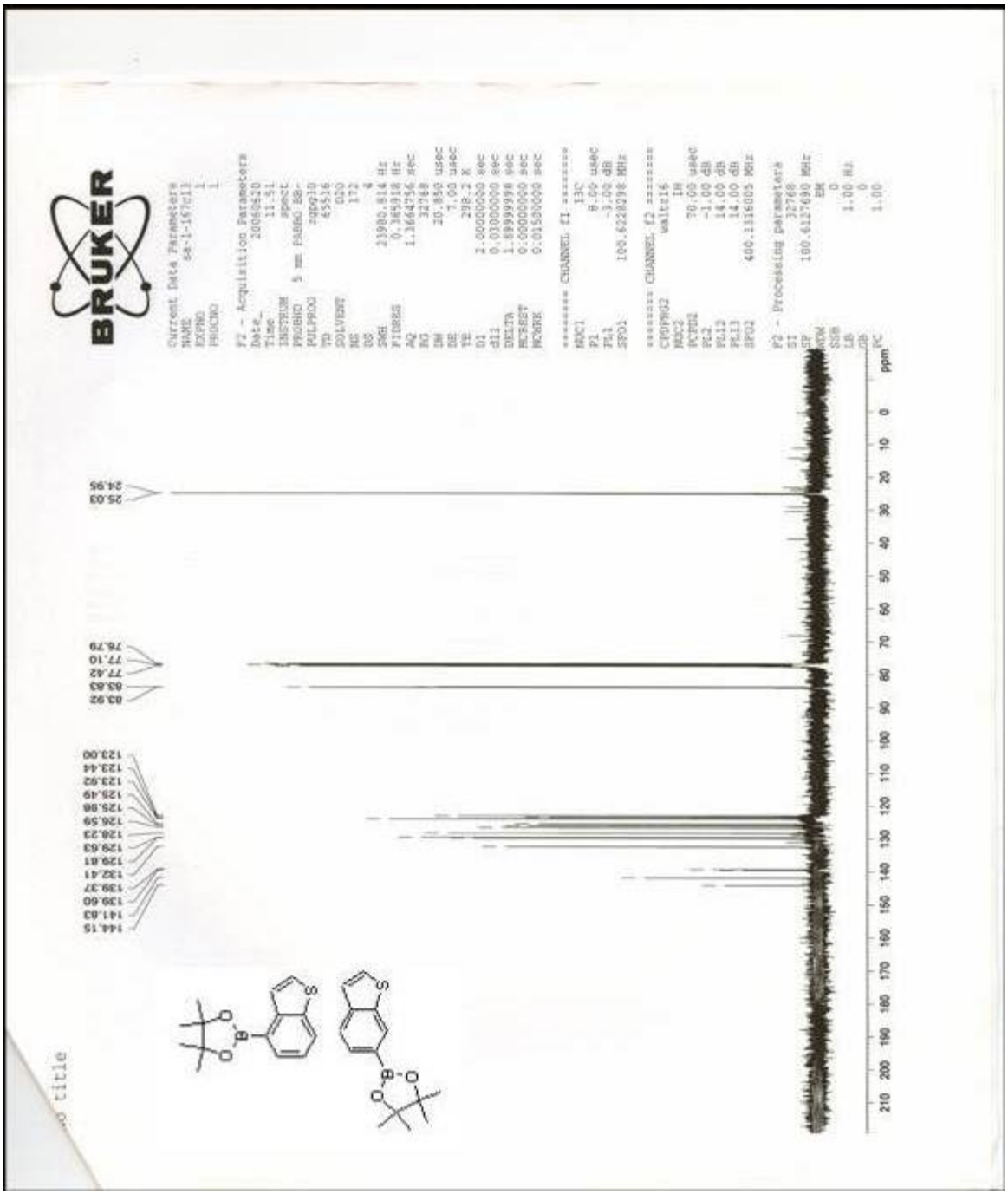
BRUKER
Current Data Parameters
NAME ea-1-167c13
EXPNO 1
PROCNO 1
F2 - Acquisition Parameters
Date_ 20060610
Time 11.51
INSTRUM spect
PROBHD 5 mm PABBO BB-
PULPROG zgpg30
TD 65536
SOLVENT CDCl3
NS 172
DS 4
SWH 21980.814 Hz
FIDRES 0.335318 Hz
AQ 1.3664736 sec
RG 32768
DW 20.850 usec
DE 7.00 usec
TE 298.2 K
D1 2.00000000 sec
d11 0.03000000 sec
DELTA 1.89999998 sec
MCREST 0.00000000 sec
MCWRK 0.01500000 sec
======== CHANNEL f1 ========
NUC1 13C
P1 8.00 usec
PL1 -3.00 dB
SFO1 100.6228298 MHz
======== CHANNEL f2 ========
CPDPRG2 waltz16
NUC2 1H
PCPD2 70.00 usec
PL2 -1.00 dB
PL12 14.00 dB
PL13 14.00 dB
SFO2 400.1316005 MHz
F2 - Processing parameters
SI 32768
SF 100.6127690 MHz
WDW EM
SSB 0
LB 1.00 Hz
GB 0
PC 1.00
ppm
144.15
141.63
139.60
139.37
132.41
129.81
129.63
128.23
126.59
125.86
125.49
123.92
123.44
123.00
83.92
83.83
77.42
77.10
76.79
25.03
24.95
S
O
O
B
S
O
O
B

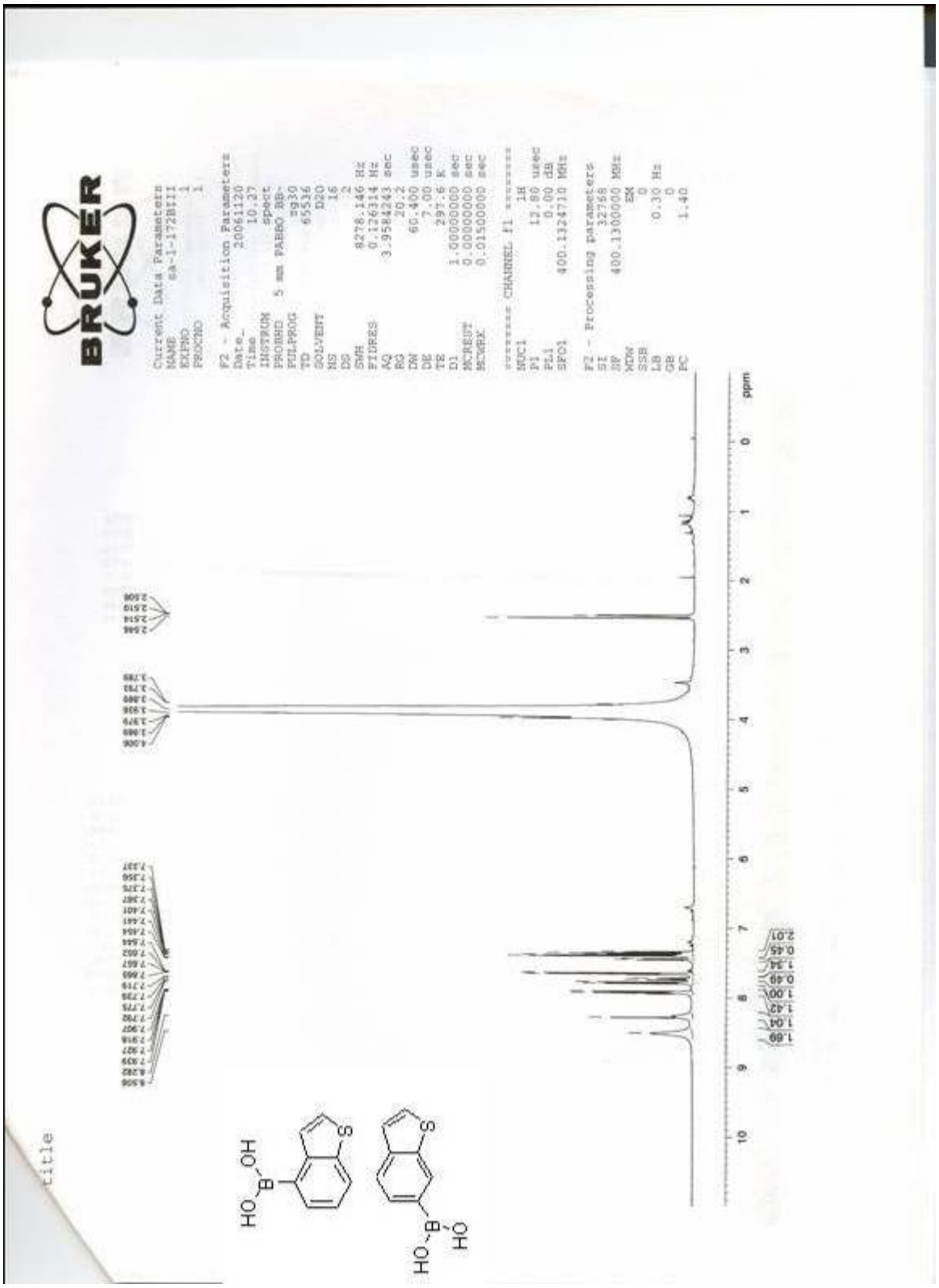
BRUKER
Current Data Parameters
NAME ea-1-172BIII
EXPNO 1
PROCNO 1
F2 - Acquisition Parameters
Date_ 20061120
Time 10.27
INSTRUM spect
PROBHD 5 mm PABBO BB-
PULPROG zg30
TD 65536
SOLVENT D2O
NS 16
DS 2
SWH 8278.146 Hz
FIDRES 0.126314 Hz
AQ 3.9584243 sec
RG 20.2
DW 60.400 usec
DE 7.00 usec
TE 297.6 K
D1 1.00000000 sec
MCREST 0.00000000 sec
MCWRK 0.01500000 sec
======== CHANNEL f1 ========
NUC1 1H
P1 12.80 usec
PL1 0.00 dB
SFO1 400.1324710 MHz
F2 - Processing parameters
SI 32768
SF 400.1300000 MHz
WDW EM
SSB 0
LB 0.30 Hz
GB 0
PC 1.40
ppm
HO
OH
B
S
HO
OH
B
S

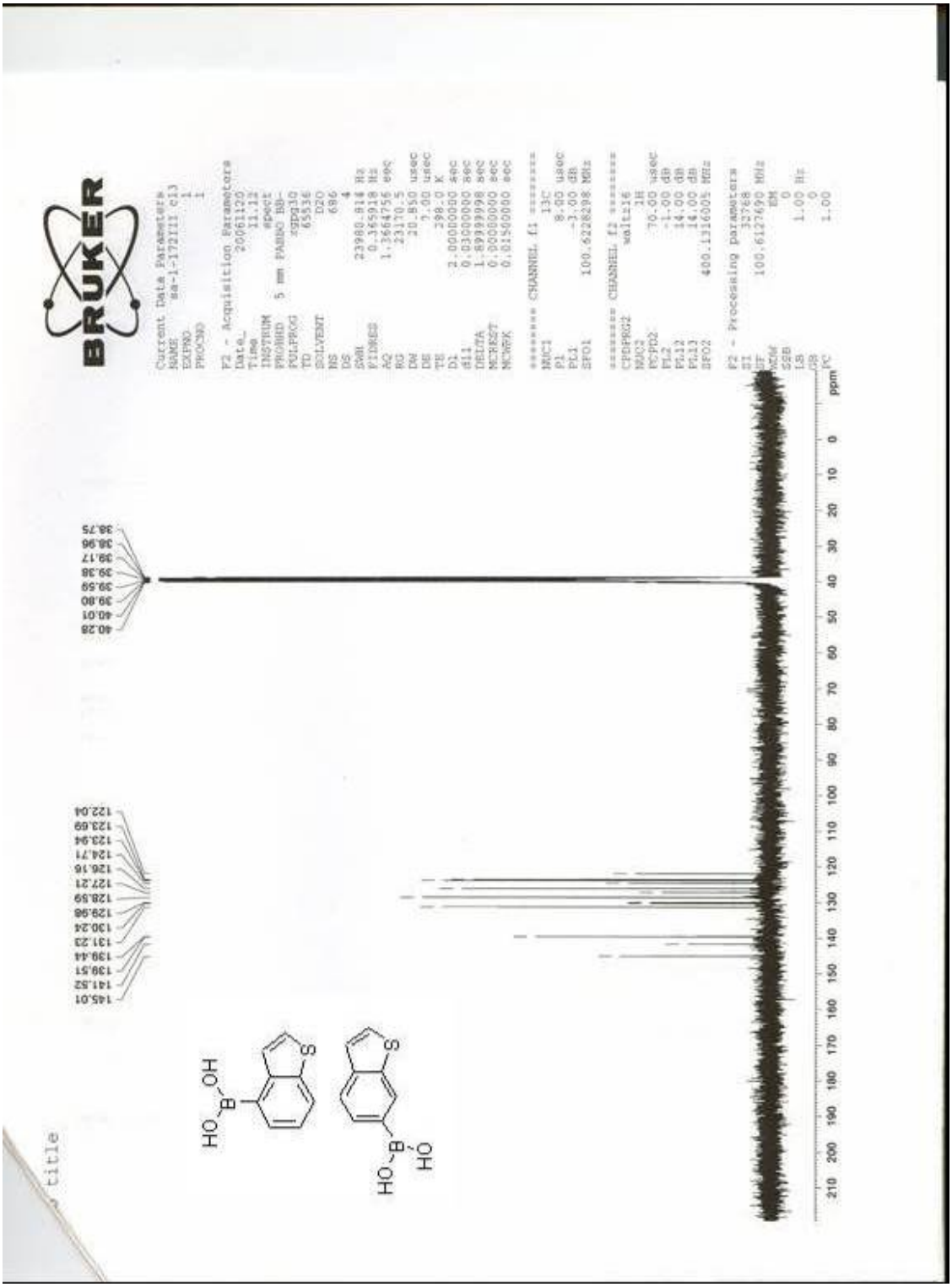
BRUKER
38.75
38.96
39.17
39.38
39.59
39.80
40.01
40.28
122.04
123.69
123.94
124.71
126.16
127.21
128.59
129.98
130.24
131.23
139.44
139.51
141.52
145.01
S
B
OH
HO
S
B
HO
OH
ppm

APPENDIX B

Supporting Information:

Design and Synthesis of Linear Diamidine Molecules as Antiparasitic Agents

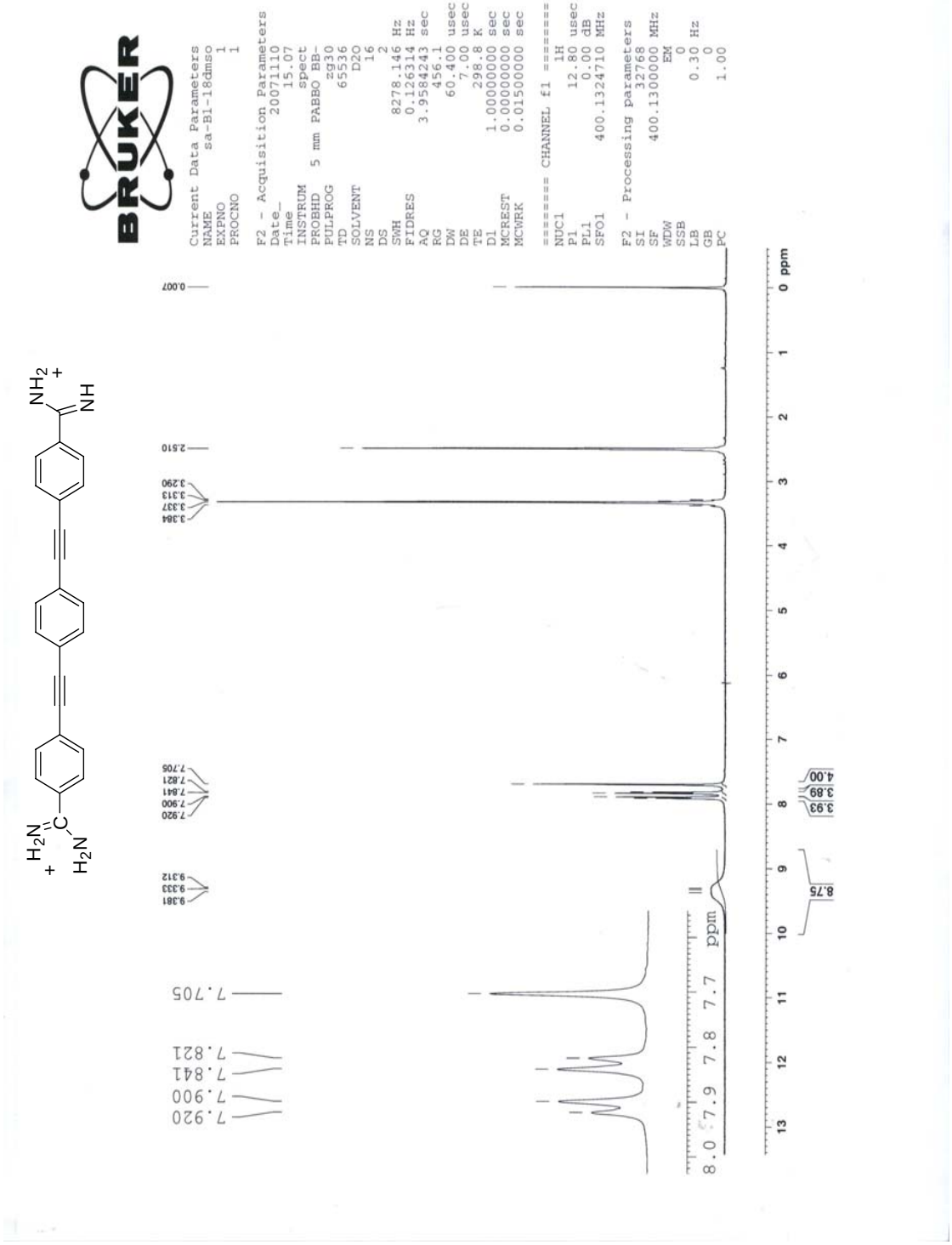
BRUKER
Current Data Parameters
NAME sa-B1-18dmso
EXPNO 1
PROCNO 1
F2 - Acquisition Parameters
Date_ 20071110
Time 15.07
INSTRUM spect
PROBHD 5 mm PABBO BB-
PULPROG zg30
TD 65536
SOLVENT D2O
NS 16
DS 2
SWH 8278.146 Hz
FIDRES 0.126314 Hz
AQ 3.9584243 sec
RG 456.1
DW 60.400 usec
DE 7.00 usec
TE 298.8 K
D1 1.00000000 sec
MCREST 0.00000000 sec
MCWRK 0.01500000 sec
======== CHANNEL f1 ========
NUC1 1H
P1 12.80 usec
PL1 0.00 dB
SFO1 400.1324710 MHz
F2 - Processing parameters
SI 32768
SF 400.1300000 MHz
WDW EM
SSB 0
LB 0.30 Hz
GB 0
PC 1.00
0.007
2.510
3.290
3.313
3.337
3.364
7.705
7.821
7.841
7.900
7.920
9.312
9.333
9.381
3.93
3.89
4.00
8.75
7.705
7.821
7.841
7.900
7.920
8.0 7.9 7.8 7.7 ppm
0 ppm
NH2+
NH
H2N
+
C
H2N

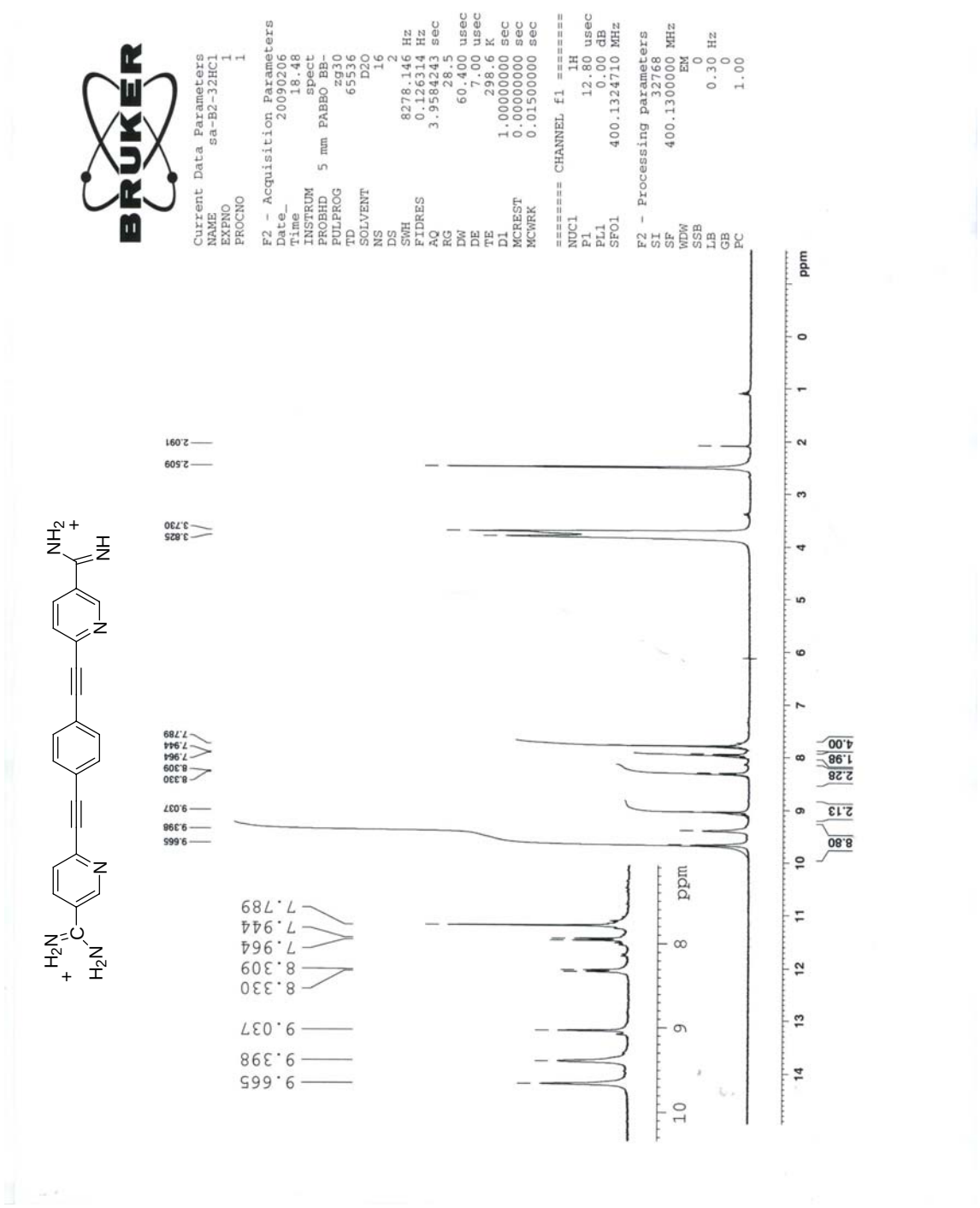
BRUKER
Current Data Parameters
NAME sa-B2-32HCl
EXPNO 1
PROCNO 1
F2 - Acquisition Parameters
Date_ 20090206
Time 18.48
INSTRUM spect
PROBHD 5 mm PABBO BB-
PULPROG zg30
TD 65536
SOLVENT D2O
NS 16
DS 2
SWH 8278.146 Hz
FIDRES 0.126314 Hz
AQ 3.9584243 sec
RG 28.5
DW 60.400 usec
DE 7.00 usec
TE 298.6 K
D1 1.00000000 sec
MCREST 0.00000000 sec
MCWRK 0.01500000 sec
======== CHANNEL f1 ========
NUC1 1H
P1 12.80 usec
PL1 0.00 dB
SFO1 400.1324710 MHz
F2 - Processing parameters
SI 32768
SF 400.1300000 MHz
WDW EM
SSB 0
LB 0.30 Hz
GB 0
PC 1.00
ppm
9.665
9.398
9.037
8.330
8.309
7.964
7.944
7.789
2.091
2.509
3.730
3.825
8.80
2.13
1.98
2.28
4.00
NH2+
NH
N
N
H2N+
C
NH2

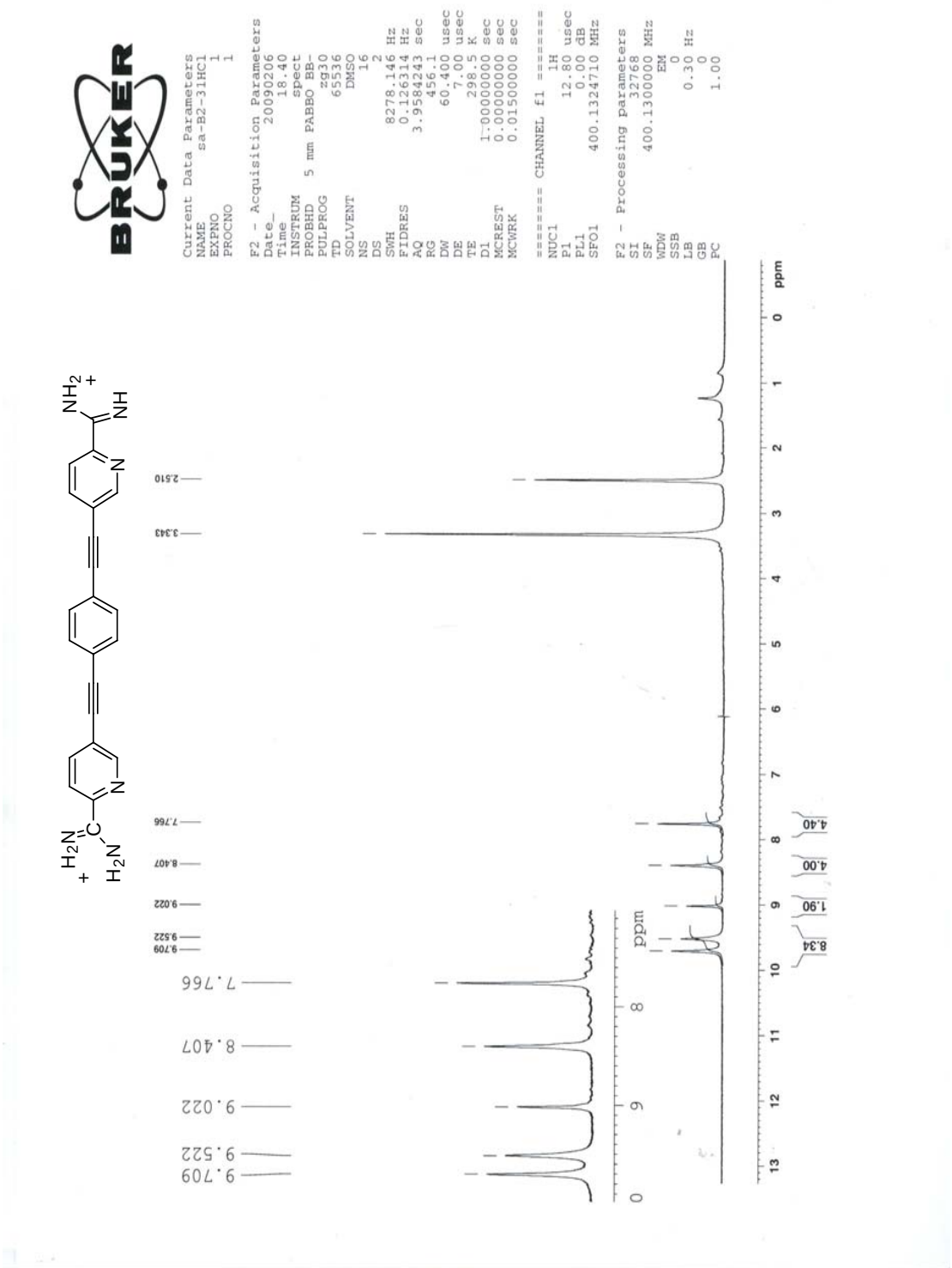
BRUKER
Current Data Parameters
NAME sa-B2-31HCl
EXPNO 1
PROCNO 1
F2 - Acquisition Parameters
Date_ 20090206
Time 18.40
INSTRUM spect
PROBHD 5 mm PABBO BB-
PULPROG zg30
TD 65536
SOLVENT DMSO
NS 16
DS 2
SWH 8278.146 Hz
FIDRES 0.126314 Hz
AQ 3.9584243 sec
RG 456.1
DW 60.400 usec
DE 7.00 usec
TE 298.5 K
D1 1.00000000 sec
MCREST 0.00000000 sec
MCWRK 0.01500000 sec
======== CHANNEL f1 ========
NUC1 1H
P1 12.80 usec
PL1 0.00 dB
SFO1 400.1324710 MHz
F2 - Processing parameters
SI 32768
SF 400.1300000 MHz
WDW EM
SSB 0
LB 0.30 Hz
GB 0
PC 1.00
2.510
3.343
7.766
8.407
9.022
9.522
9.709
4.40
4.00
1.90
8.34
ppm

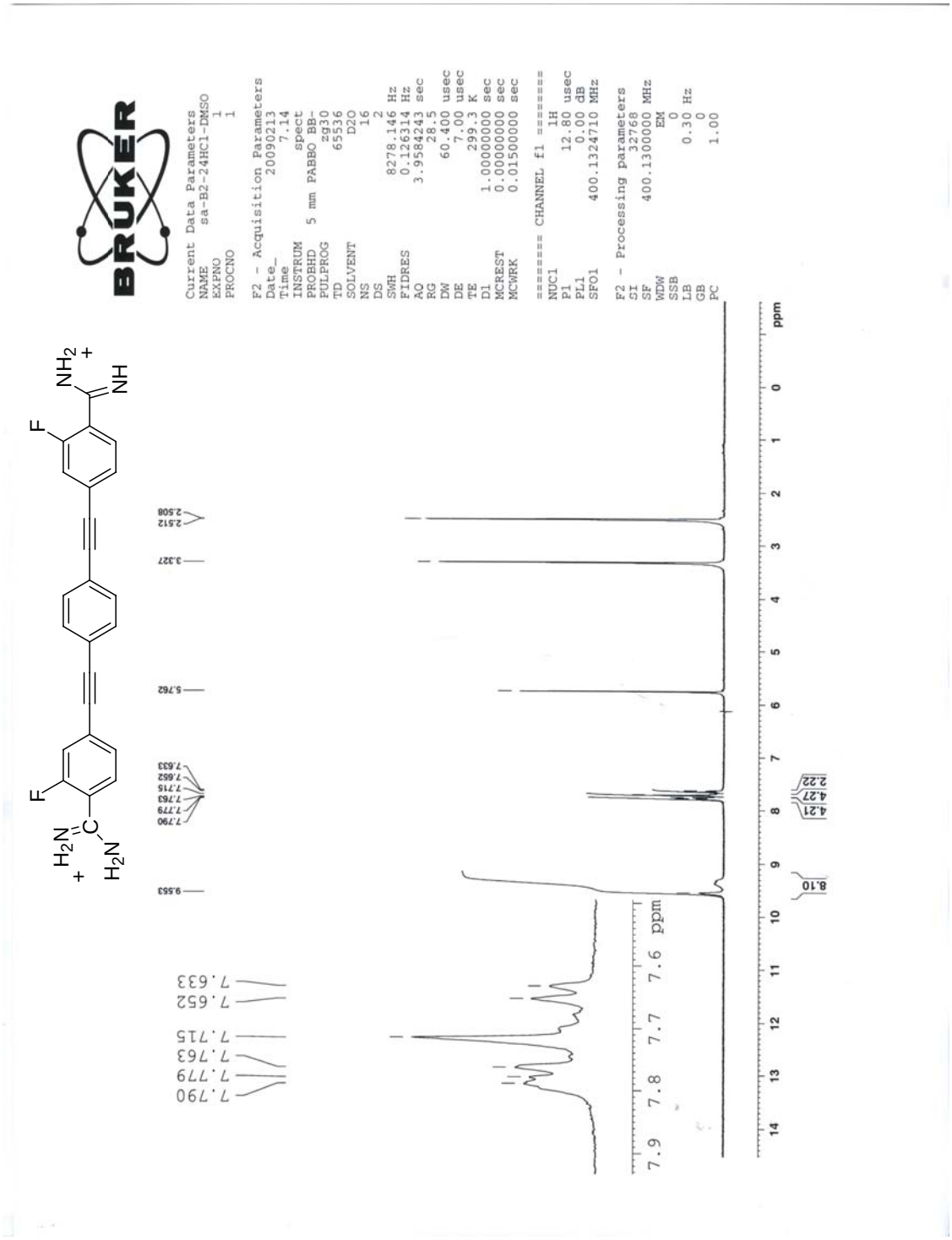
Current Data Parameters
NAME sa-B2-24HCl-DMSO
EXPNO 1
PROCNO 1
F2 - Acquisition Parameters
Date_ 20090213
Time 7.14
INSTRUM spect
PROBHD 5 mm PABBO BB-
PULPROG zg30
TD 65536
SOLVENT D2O
NS 16
DS 2
SWH 8278.146 Hz
FIDRES 0.126314 Hz
AQ 3.9584243 sec
RG 28.5
DW 60.400 usec
DE 7.00 usec
TE 299.3 K
D1 1.00000000 sec
MCREST 0.00000000 sec
MCWRK 0.01500000 sec
======== CHANNEL f1 ========
NUC1 1H
P1 12.80 usec
PL1 0.00 dB
SFO1 400.1324710 MHz
F2 - Processing parameters
SI 32768
SF 400.1300000 MHz
WDW EM
SSB 0
LB 0.30 Hz
GB 0
PC 1.00
9.553
7.790
7.779
7.763
7.715
7.652
7.633
5.762
3.327
2.512
2.508
8.10
4.21
4.27
2.22
ppm

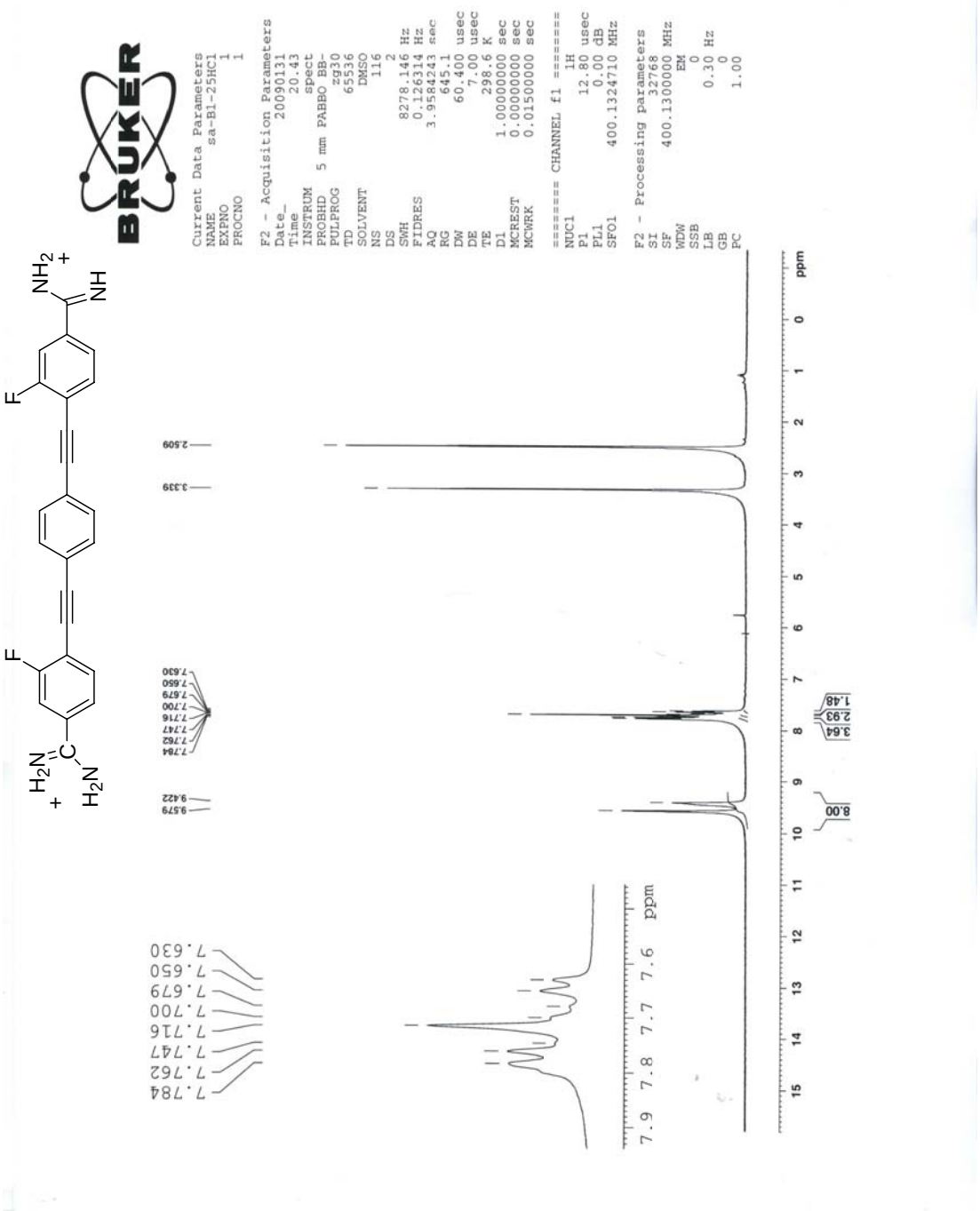
BRUKER
Current Data Parameters
NAME sa-B1-25HCl
EXPNO 1
PROCNO 1
F2 - Acquisition Parameters
Date_ 20090131
Time_ 20.43
INSTRUM spect
PROBHD 5 mm PABBO BB-
PULPROG zg30
TD 65536
SOLVENT DMSO
NS 116
DS 2
SWH 8278.146 Hz
FIDRES 0.126314 Hz
AQ 3.9584243 sec
RG 645.1
DW 60.400 usec
DE 7.00 usec
TE 298.6 K
D1 1.00000000 sec
MCREST 0.00000000 sec
MCWRK 0.01500000 sec
======== CHANNEL f1 ========
NUC1 1H
P1 12.80 usec
PL1 0.00 dB
SFO1 400.1324710 MHz
F2 - Processing parameters
SI 32768
SF 400.1300000 MHz
WDW EM
SSB 0
LB 0.30 Hz
GB 0
PC 1.00
2.509
3.339
7.630
7.650
7.679
7.700
7.716
7.747
7.762
7.784
9.422
9.579
8.00
3.64
2.93
1.48
ppm
F
NH2+
NH
H2N+
H2N

APPENDIX C

Supporting Information:

Synthesis of Arylimidamides as Potential Leishmanisis Treatment Agents

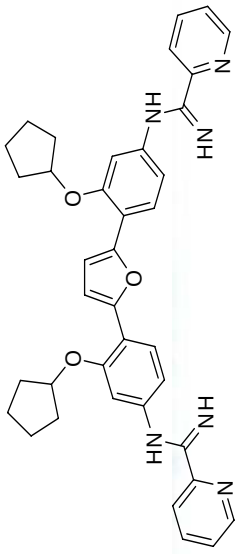

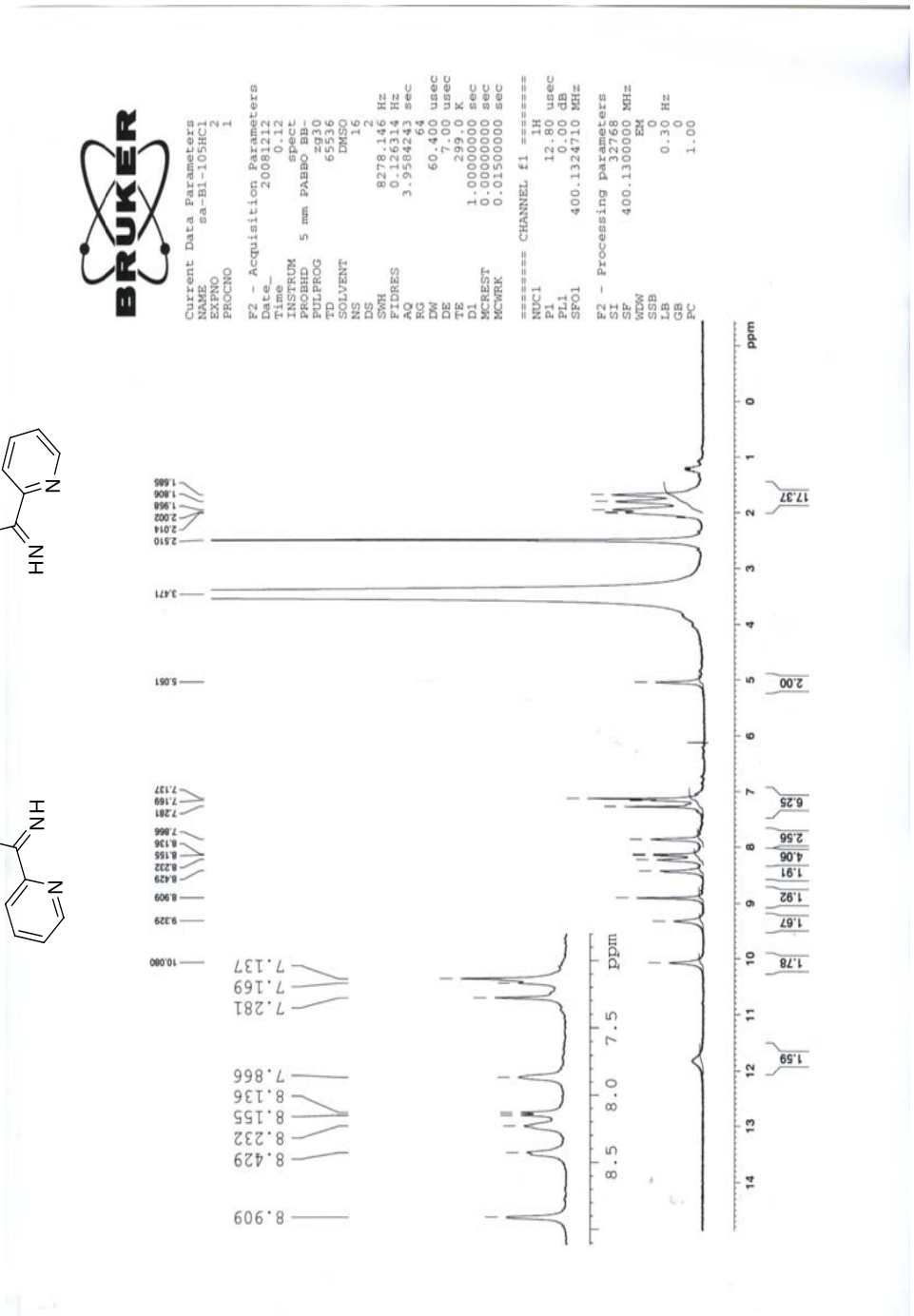
BRUKER
Current Data Parameters
NAME sa-B1-105HCl
EXPNO 2
PROCNO 1
F2 - Acquisition Parameters
Date_ 20081212
Time 0.12
INSTRUM spect
PROBHD 5 mm PABBO BB-
PULPROG zg30
TD 65536
SOLVENT DMSO
NS 16
DS 2
SWH 8278.146 Hz
FIDRES 0.126314 Hz
AQ 3.958424 sec
RG 64
DW 60.400 usec
DE 7.00 usec
TE 299.0 K
D1 1.00000000 sec
MCREST 0.00000000 sec
MCWRK 0.01500000 sec
======== CHANNEL f1 ========
NUC1 1H
P1 12.80 usec
PL1 0.00 dB
SFO1 400.1324710 MHz
F2 - Processing parameters
SI 32768
SF 400.1300000 MHz
WDW EM
SSB 0
LB 0.30 Hz
GB 0
PC 1.00
ppm
17.37
2.00
6.25
2.56
4.06
1.91
1.92
1.67
1.78
1.59
10.080
9.329
8.909
8.429
8.232
8.155
8.136
7.866
7.281
7.169
7.137
5.051
3.471
2.510
2.014
2.002
1.964
1.806
1.686

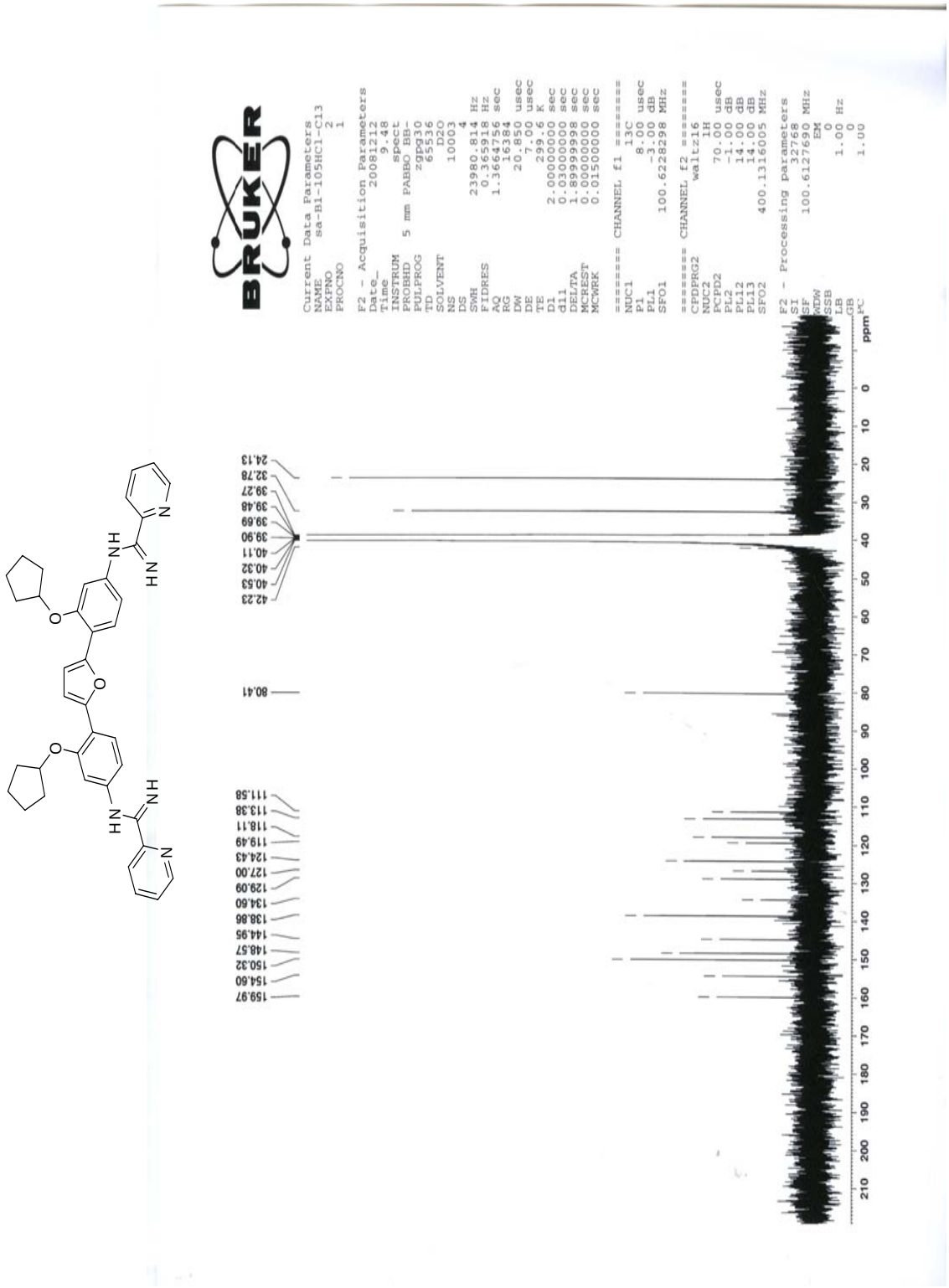
BRUKER
Current Data Parameters
NAME sa-B1-105HCl-C13
EXPNO 2
PROCNO 1
F2 - Acquisition Parameters
Date_ 20081212
Time 9.48
INSTRUM spect
PROBHD 5 mm PABBO BB-
PULPROG zgpg30
TD 65536
SOLVENT D2O
NS 10003
DS 4
SWH 23980.814 Hz
FIDRES 0.365918 Hz
AQ 1.3664756 sec
RG 16384
DW 20.850 usec
DE 7.00 usec
TE 299.6 K
D1 2.00000000 sec
d11 0.03000000 sec
DELTA 1.89999998 sec
MCREST 0.00000000 sec
MCWRK 0.01500000 sec
======== CHANNEL f1 ========
NUC1 13C
P1 8.00 usec
PL1 -3.00 dB
SFO1 100.6228298 MHz
======== CHANNEL f2 ========
CPDPRG2 waltz16
NUC2 1H
PCPD2 70.00 usec
PL2 -1.00 dB
PL12 14.00 dB
PL13 14.00 dB
SFO2 400.1316005 MHz
F2 - Processing parameters
SI 32768
SF 100.6127690 MHz
WDW EM
SSB 0
LB 1.00 Hz
GB 0
1.00
ppm
24.13
32.78
39.27
39.48
39.69
39.90
40.11
40.32
40.53
42.23
80.41
111.58
113.38
118.11
119.49
124.43
127.00
129.09
134.60
138.86
144.95
148.57
150.32
154.60
159.97

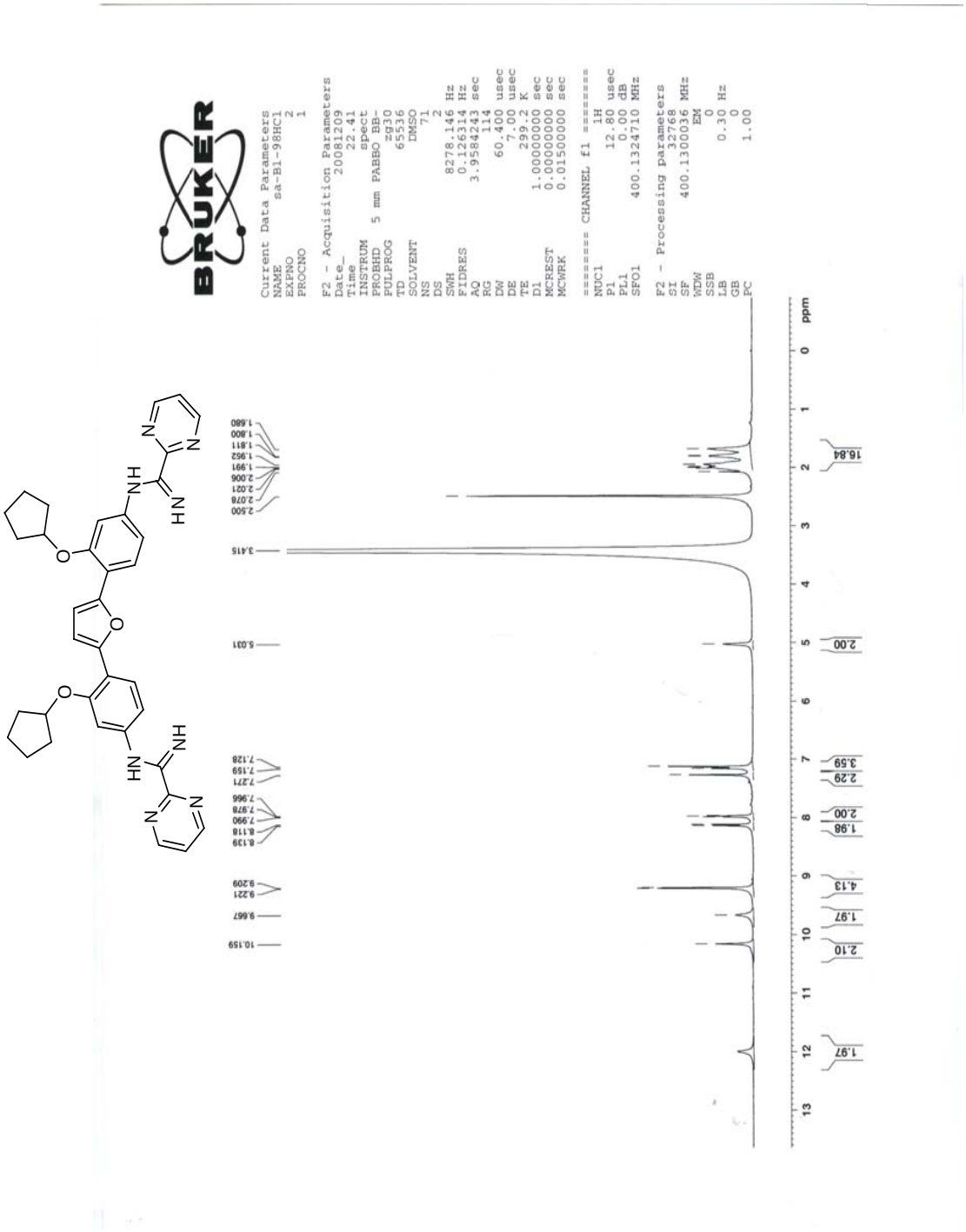
BRUKER
Current Data Parameters
NAME sa-B1-98HCl
EXPNO 2
PROCNO 1
F2 - Acquisition Parameters
Date_ 20081209
Time 22.41
INSTRUM spect
PROBHD 5 mm PABBO BB-
PULPROG zg30
TD 65536
SOLVENT DMSO
NS 71
DS 2
SWH 8278.146 Hz
FIDRES 0.126314 Hz
AQ 3.9584243 sec
RG 114
DW 60.400 usec
DE 7.00 usec
TE 299.2 K
D1 1.00000000 sec
MCREST 0.00000000 sec
MCWRK 0.01500000 sec
======== CHANNEL f1 ========
NUC1 1H
P1 12.80 usec
PL1 0.00 dB
SFO1 400.1324710 MHz
F2 - Processing parameters
SI 32768
SF 400.1300036 MHz
WDW EM
SSB 0
LB 0.30 Hz
GB 0
PC 1.00
ppm
16.84
2.00
3.59
2.29
1.98
2.00
4.13
1.97
2.10
1.97
1.680
1.800
1.811
1.952
1.991
2.006
2.021
2.078
2.500
3.415
5.031
7.128
7.159
7.271
7.966
7.978
7.990
8.118
8.139
9.209
9.221
9.667
10.159

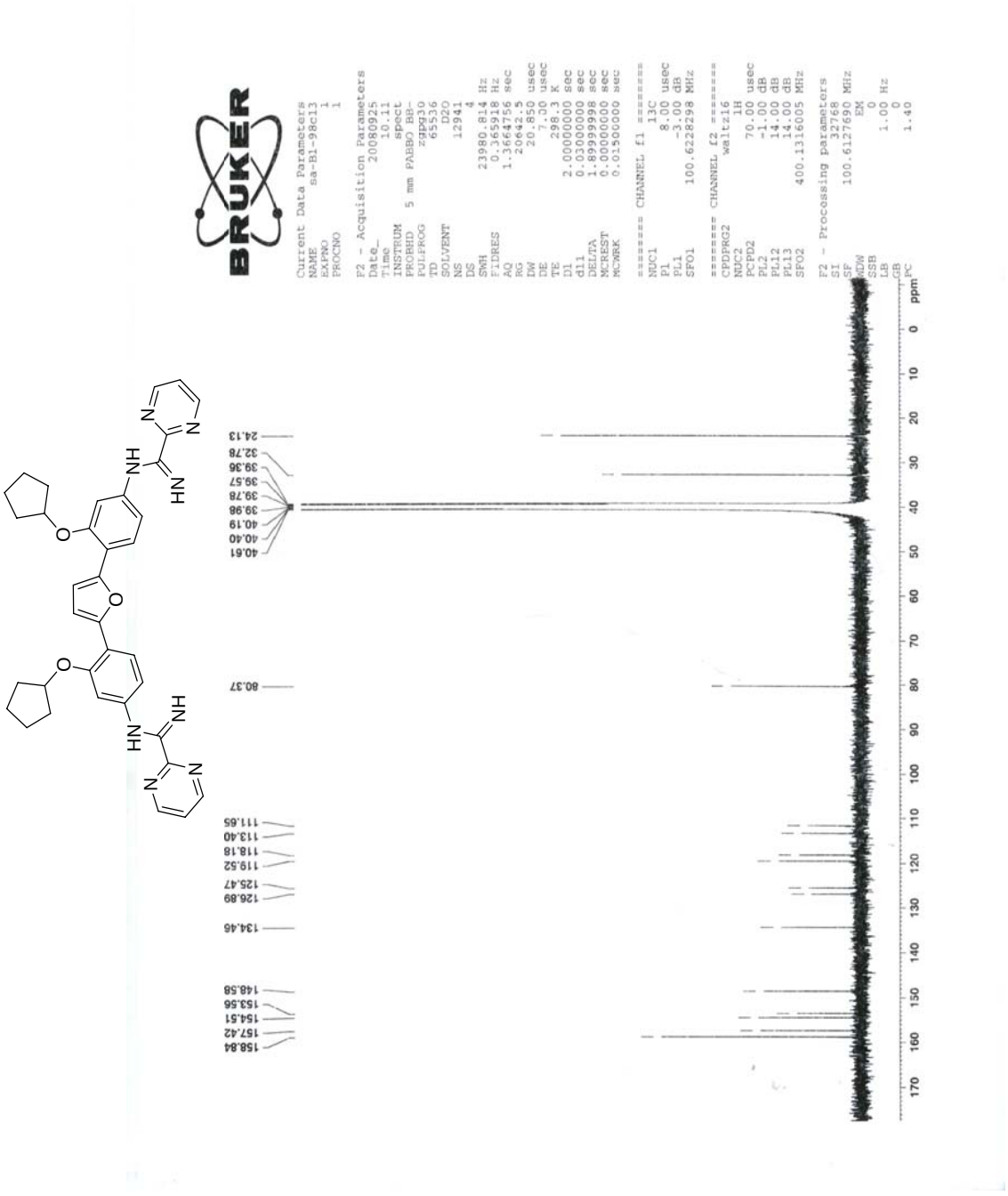
BRUKER
Current Data Parameters
NAME sa-B1-98c13
EXPNO 1
PROCNO 1
F2 - Acquisition Parameters
Date_ 20080925
Time 10.11
INSTRUM spect
PROBHD 5 mm PABBO BB-
PULPROG zgpg30
TD 65536
SOLVENT D2O
NS 12941
DS 4
SWH 23980.814 Hz
FIDRES 0.365918 Hz
AQ 1.3664756 sec
RG 20642.5
DW 20.850 usec
DE 6.00 usec
TE 298.1 K
D1 2.00000000 sec
d11 0.03000000 sec
DELTA 1.89999998 sec
MCREST 0.00000000 sec
MCWRK 0.01500000 sec
======== CHANNEL f1 ========
NUC1 13C
P1 8.00 usec
PL1 -3.00 dB
SFO1 100.6228298 MHz
======== CHANNEL f2 ========
CPDPRG2 waltz16
NUC2 1H
PCPD2 70.00 usec
PL2 -1.00 dB
PL12 14.00 dB
PL13 14.00 dB
SFO2 400.1316005 MHz
F2 - Processing parameters
SI 32768
SF 100.6127690 MHz
WDW EM
SSB 0
LB 1.00 Hz
GB 0
PC 1.40
24.13
32.78
39.36
39.57
39.78
39.98
40.19
40.40
40.61
80.37
111.65
113.40
118.18
119.52
125.47
126.89
134.46
148.58
153.56
154.51
157.42
158.84
ppm

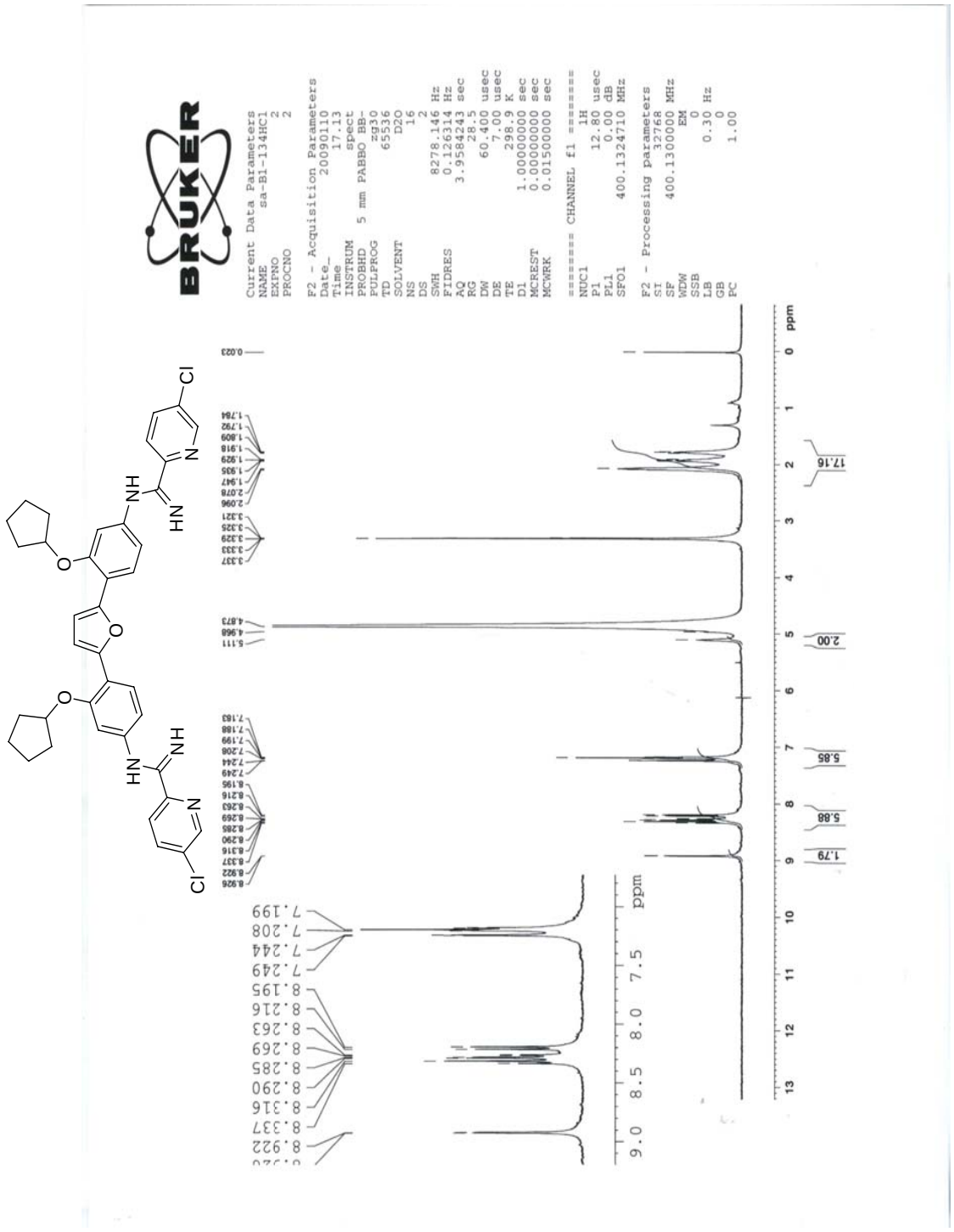
BRUKER
Current Data Parameters
NAME sa-B1-134HCl
EXPNO 2
PROCNO 2
F2 - Acquisition Parameters
Date_ 20090110
Time 17.13
INSTRUM spect
PROBHD 5 mm PABBO BB-
PULPROG zg30
TD 65536
SOLVENT D2O
NS 16
DS 2
SWH 8278.146 Hz
FIDRES 0.126314 Hz
AQ 3.9584243 sec
RG 28.5
DW 60.400 usec
DE 7.00 usec
TE 298.9 K
D1 1.00000000 sec
MCREST 0.00000000 sec
MCWRK 0.01500000 sec
======== CHANNEL f1 ========
NUC1 1H
P1 12.80 usec
PL1 0.00 dB
SFO1 400.1324710 MHz
F2 - Processing parameters
SI 32768
SF 400.1300000 MHz
WDW EM
SSB 0
LB 0.30 Hz
GB 0
PC 1.00
17.16
2.00
5.85
5.88
1.79
ppm


BRUKER
Current Data Parameters
NAME sa-B1-134c13
EXPNO 1
PROCNO 1
F2 - Acquisition Parameters
Date_ 20090106
Time 16.43
INSTRUM spect
PROBHD 5 mm PABBO BB-
PULPROG zgpg30
TD 65536
SOLVENT D2O
NS 512
DS 4
SWH 23980.814 Hz
FIDRES 0.365918 Hz
AQ 1.3664756 sec
RG 32768
DW 20.850 usec
DE 7.00 usec
TE 299.8 K
D1 2.00000000 sec
d11 0.03000000 sec
DELTA 1.89999998 sec
MCREST 0.00000000 sec
MCWRK 0.01500000 sec
======== CHANNEL f1 ========
NUC1 13C
P1 8.00 usec
PL1 -3.00 dB
SFO1 100.6228298 MHz
======== CHANNEL f2 ========
CPDPRG2 waltz16
NUC2 1H
PCPD2 70.00 usec
PL2 -1.00 dB
PL12 14.00 dB
PL13 14.00 dB
SFO2 400.1316005 MHz
F2 - Processing parameters
SI 32768
SF 100.6127690 MHz
WDW EM
SSB 0
LB 1.00 Hz
GB 0
PC 1.00
No title
ppm
-0.00
0.25
24.18
33.08
76.70
77.02
77.22
77.33
79.54
79.61
106.61
111.07
113.09
116.08
122.62
126.91
133.88
136.57
146.79
148.69
149.30
149.78
151.86
154.94
NH
HN
N
Cl
O

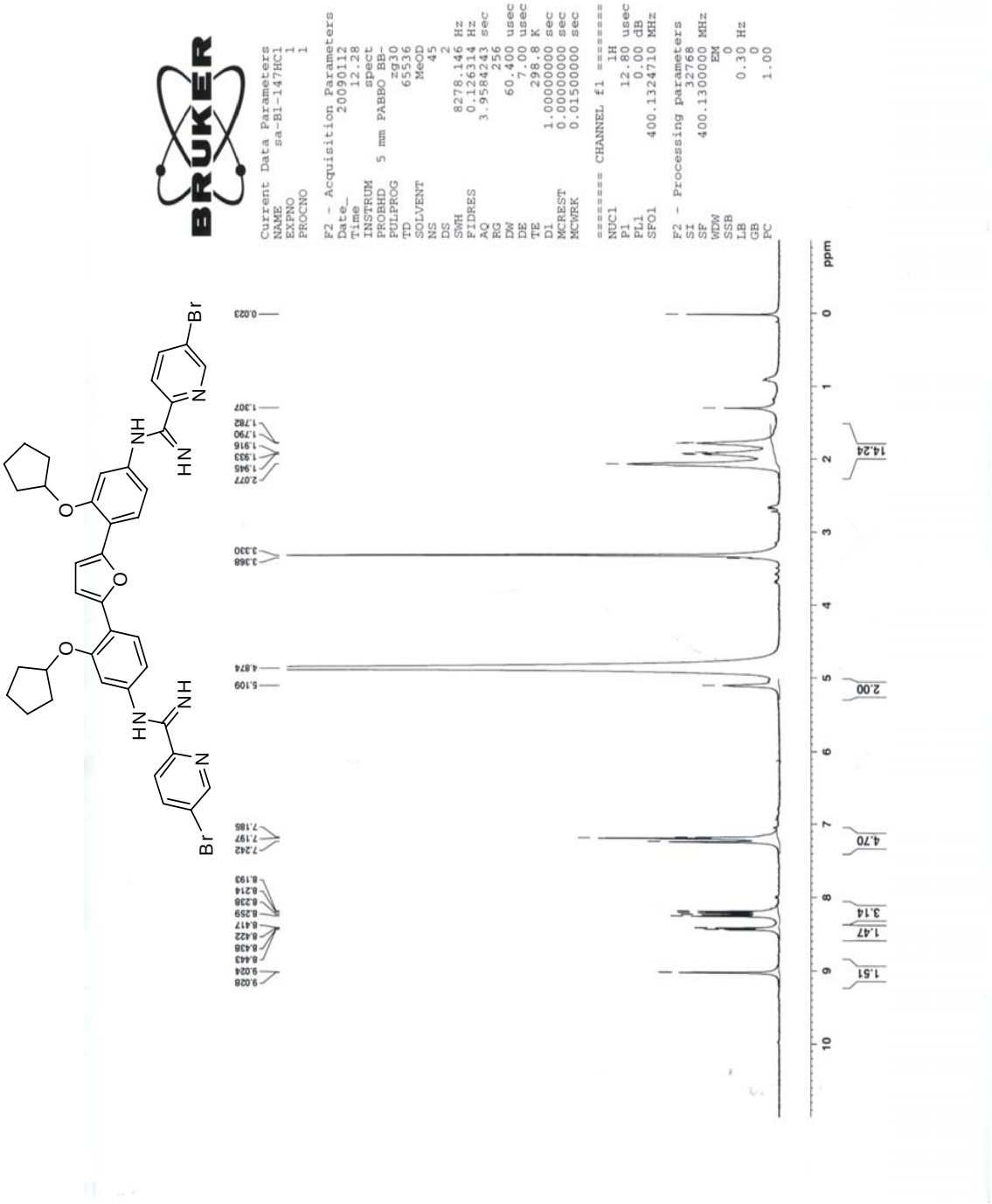
BRUKER
Current Data Parameters
NAME sa-B1-147HCl
EXPNO 1
PROCNO 1
F2 - Acquisition Parameters
Date_ 20090112
Time 12.28
INSTRUM spect
PROBHD 5 mm PABBO BB-
PULPROG zg30
TD 65536
SOLVENT MeOD
NS 45
DS 2
SWH 8278.146 Hz
FIDRES 0.126314 Hz
AQ 3.958243 sec
RG 256
DW 60.400 usec
DE 7.00 usec
TE 298.8 K
D1 1.00000000 sec
MCREST 0.00000000 sec
MCWRK 0.01500000 sec
======== CHANNEL f1 ========
NUC1 1H
P1 12.80 usec
PL1 0.00 dB
SFO1 400.1324710 MHz
F2 - Processing parameters
SI 32768
SF 400.1300000 MHz
WDW EM
SSB 0
LB 0.30 Hz
GB 0
PC 1.00
0.023
1.307
1.782
1.790
1.916
1.933
1.945
2.077
3.330
3.368
4.874
5.109
7.185
7.197
7.242
8.193
8.214
8.238
8.259
8.417
8.422
8.436
8.443
9.024
9.028
14.24
2.00
4.70
1.47
3.14
1.51
ppm

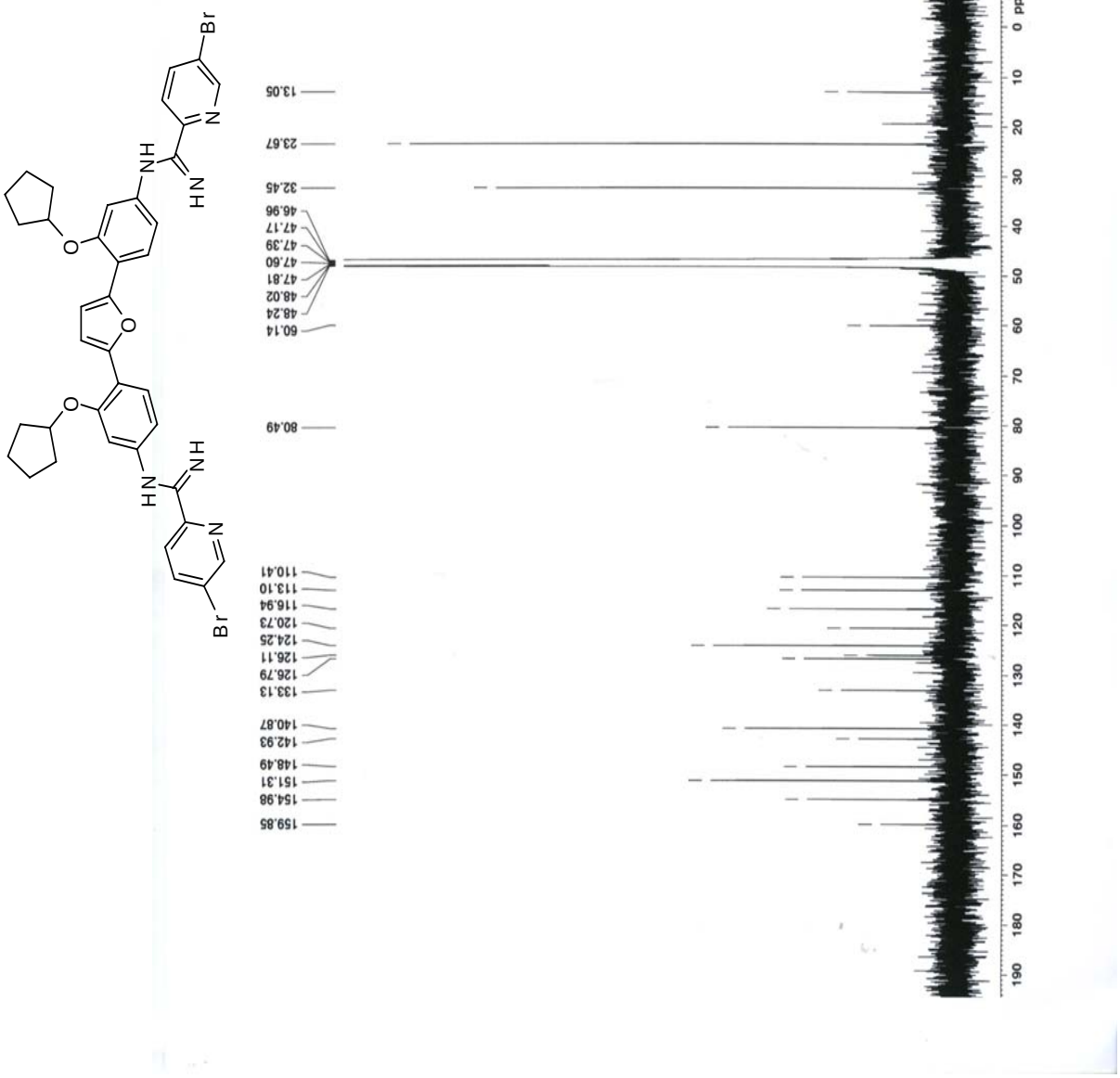
Br
NH
HN
O
O
O
HN
NH
N
Br
13.05
23.67
32.45
46.96
47.17
47.39
47.60
47.81
48.02
48.24
60.14
80.49
110.41
113.10
116.94
120.73
124.25
126.11
126.79
133.13
140.87
142.93
148.49
151.31
154.98
159.85
0 ppm

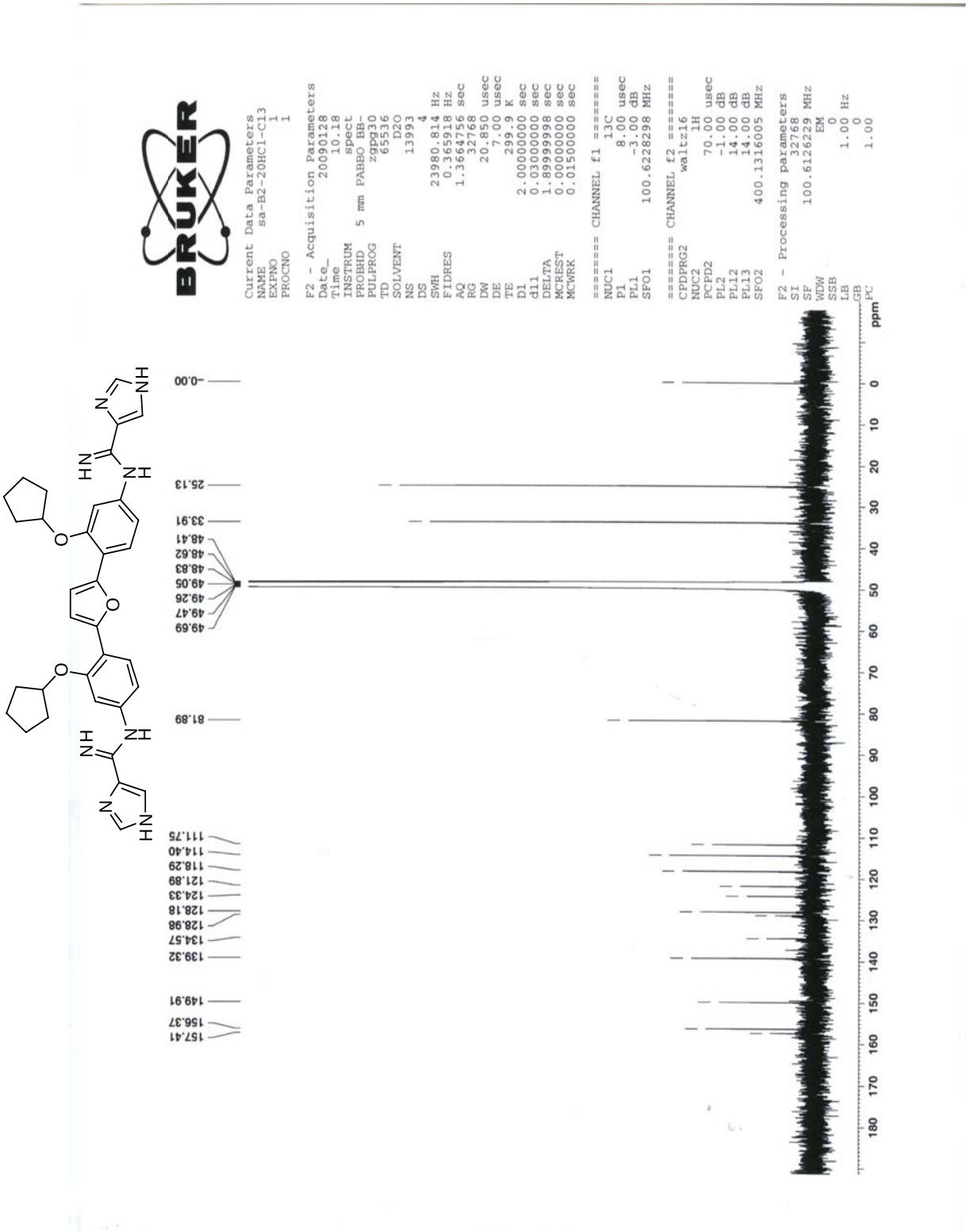
BRUKER
Current Data Parameters
NAME sa-B2-20HCl-C13
EXPNO 1
PROCNO 1
F2 - Acquisition Parameters
Date_ 20090128
Time_ 10.18
INSTRUM spect
PROBHD 5 mm PABBO BB-
PULPROG zgpg30
TD 65536
SOLVENT D2O
NS 13993
DS 4
SWH 23980.814 Hz
FIDRES 0.365918 Hz
AQ 1.3664756 sec
RG 32768
DW 20.850 usec
DE 7.00 usec
TE 299.9 K
D1 2.00000000 sec
d11 0.03000000 sec
DELTA 1.89999998 sec
MCREST 0.00000000 sec
MCWRK 0.01500000 sec
======== CHANNEL f1 ========
NUC1 13C
P1 8.00 usec
PL1 -3.00 dB
SFO1 100.6228298 MHz
======== CHANNEL f2 ========
CPDPRG2 waltz16
NUC2 1H
PCPD2 70.00 usec
PL2 -1.00 dB
PL12 14.00 dB
PL13 14.00 dB
SFO2 400.1316005 MHz
F2 - Processing parameters
SI 32768
SF 100.6126229 MHz
WDW EM
SSB 0
LB 1.00 Hz
GB 0
PC 1.00
ppm
0.00
25.13
33.91
48.41
48.62
48.83
49.05
49.26
49.47
49.69
81.89
111.75
114.40
118.29
121.89
124.33
128.18
128.98
134.57
139.32
149.91
156.37
157.41

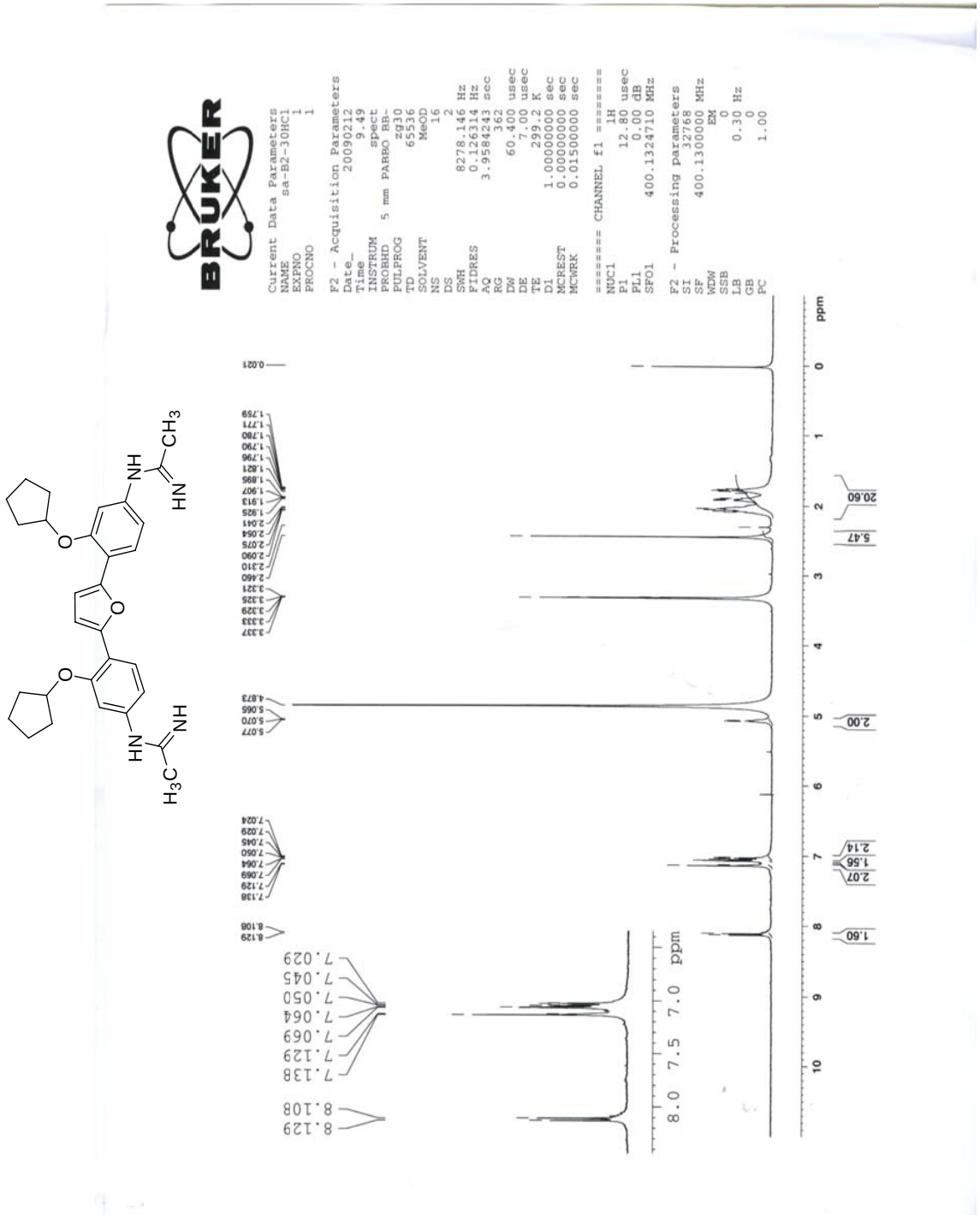
BRUKER
Current Data Parameters
NAME sa-B2-30HCl
EXPNO 1
PROCNO 1
F2 - Acquisition Parameters
Date_ 20090212
Time 9.49
INSTRUM spect
PROBHD 5 mm PABBO BB-
PULPROG zg30
TD 65536
SOLVENT MeOD
NS 16
DS 2
SWH 8278.146 Hz
FIDRES 0.126314 Hz
AQ 3.9584243 sec
RG 362
DW 60.400 usec
DE 7.00 usec
TE 299.2 K
D1 1.00000000 sec
MCREST 0.00000000 sec
MCWRK 0.01500000 sec
======== CHANNEL f1 ========
NUC1 1H
P1 12.80 usec
PL1 0.00 dB
SFO1 400.1324710 MHz
F2 - Processing parameters
SI 32768
SF 400.1300000 MHz
WDW EM
SSB 0
LB 0.30 Hz
GB 0
PC 1.00
NH
CH3
HN
O
O
O
NH
HN
H3C
ppm
20.60
5.47
2.00
2.14
1.56
2.07
1.60

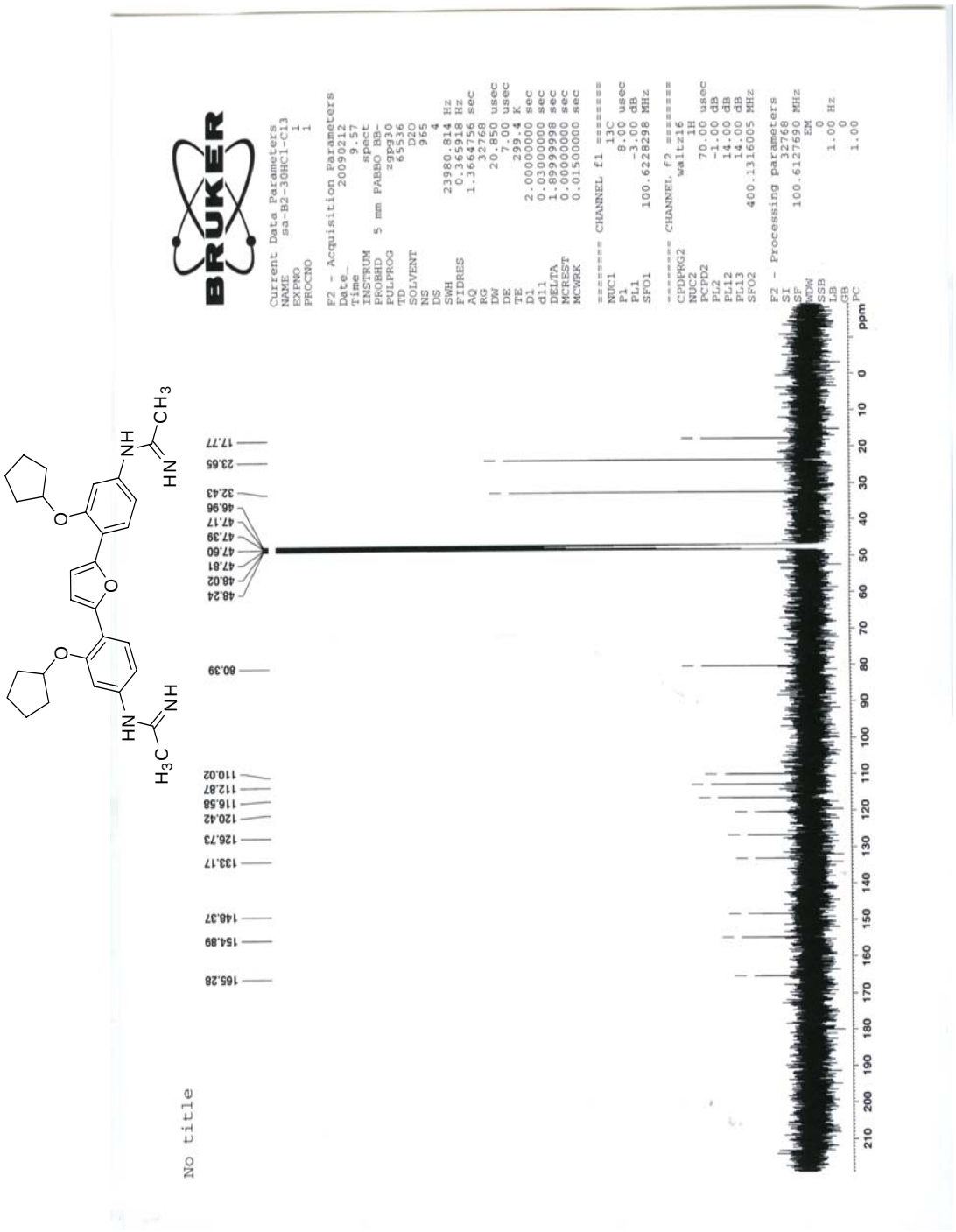
No title
BRUKER
Current Data Parameters
NAME sa-B2-30HCl-C13
EXPNO 1
PROCNO 1
F2 - Acquisition Parameters
Date_ 20090212
Time 9.57
INSTRUM spect
PROBHD 5 mm PABBO BB-
PULPROG zgpg30
TD 65536
SOLVENT D2O
NS 964
DS 4
SWH 23980.814 Hz
FIDRES 0.365918 Hz
AQ 1.3664756 sec
RG 32768
DW 20.850 usec
DE 7.00 usec
TE 299.4 K
D1 2.00000000 sec
d11 0.03000000 sec
DELTA 1.89999998 sec
MCREST 0.00000000 sec
MCWRK 0.01500000 sec
======== CHANNEL f1 ========
NUC1 13C
P1 8.00 usec
PL1 3.00 dB
SFO1 100.6228298 MHz
======== CHANNEL f2 ========
CPDPRG2 waltz16
NUC2 1H
PCPD2 70.00 usec
PL2 -1.00 dB
PL12 14.00 dB
PL13 14.00 dB
SFO2 400.1316005 MHz
F2 - Processing parameters
SI 32768
SF 100.6127690 MHz
WDW EM
SSB 0
LB 1.00 Hz
GB 0
PC 1.00
17.77
23.65
32.43
46.96
47.17
47.39
47.60
47.81
48.02
48.24
80.39
110.02
112.87
116.58
120.42
126.73
133.17
148.37
154.89
165.28
ppm
NH
CH3
HN
O
O
O
HN
NH
H3C

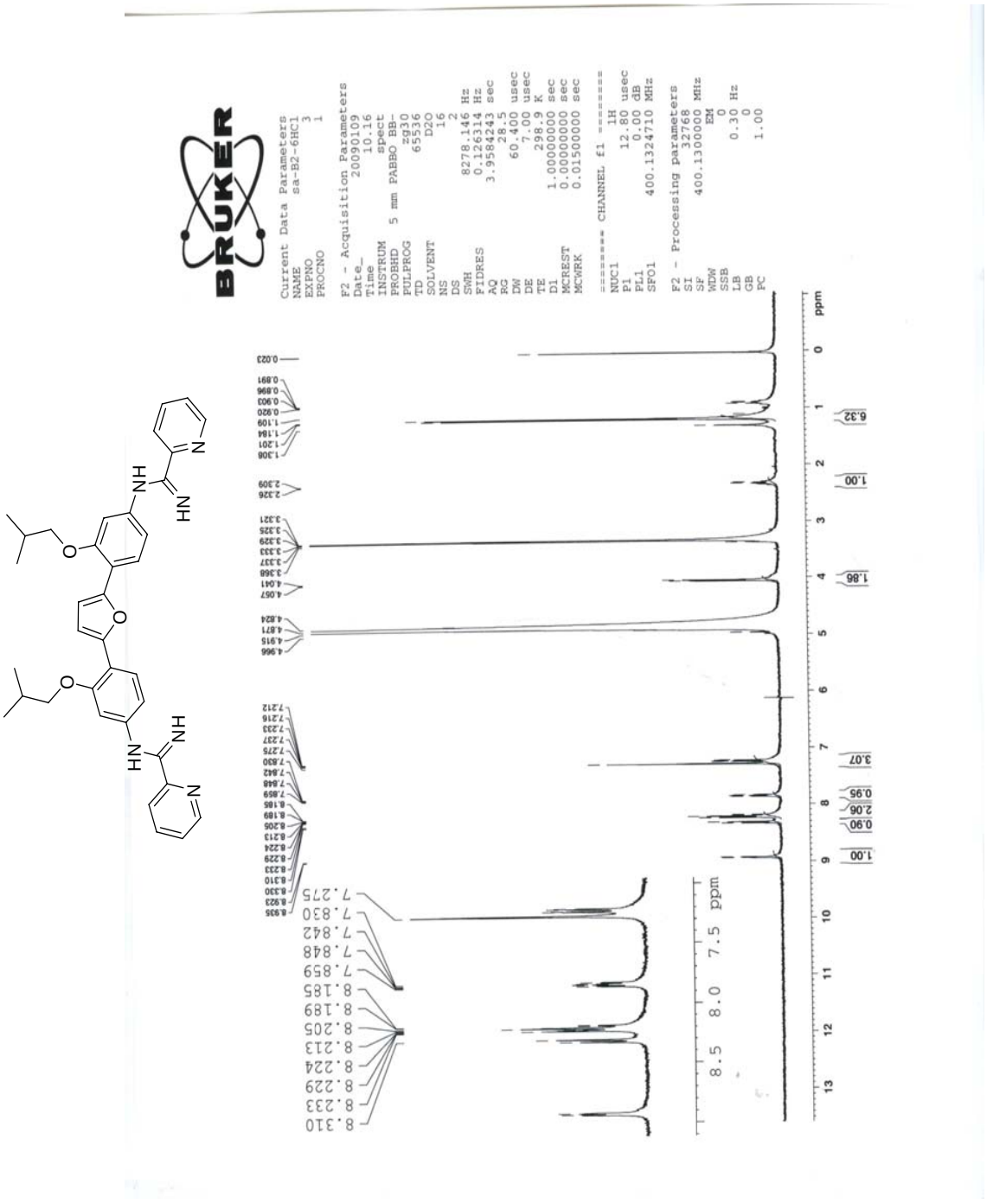
BRUKER
Current Data Parameters
NAME sa-B2-6HCl
EXPNO 3
PROCNO 1
F2 - Acquisition Parameters
Date_ 20090109
Time 10.16
INSTRUM spect
PROBHD 5 mm PABBO BB-
PULPROG zg30
TD 65536
SOLVENT D2O
NS 16
DS 2
SWH 8278.146 Hz
FIDRES 0.126314 Hz
AQ 3.9584243 sec
RG 28.5
DW 60.400 usec
DE 6.00 usec
TE 298.9 K
D1 1.00000000 sec
MCREST 0.00000000 sec
MCWRK 0.01500000 sec
======== CHANNEL f1 ========
NUC1 1H
P1 12.80 usec
PL1 0.00 dB
SFO1 400.1324710 MHz
F2 - Processing parameters
SI 32768
SF 400.1300000 MHz
WDW EM
SSB 0
LB 0.30 Hz
GB 0
PC 1.00
ppm
6.32
1.00
1.86
3.07
0.95
2.06
0.90
1.00
8.5 8.0 7.5 ppm

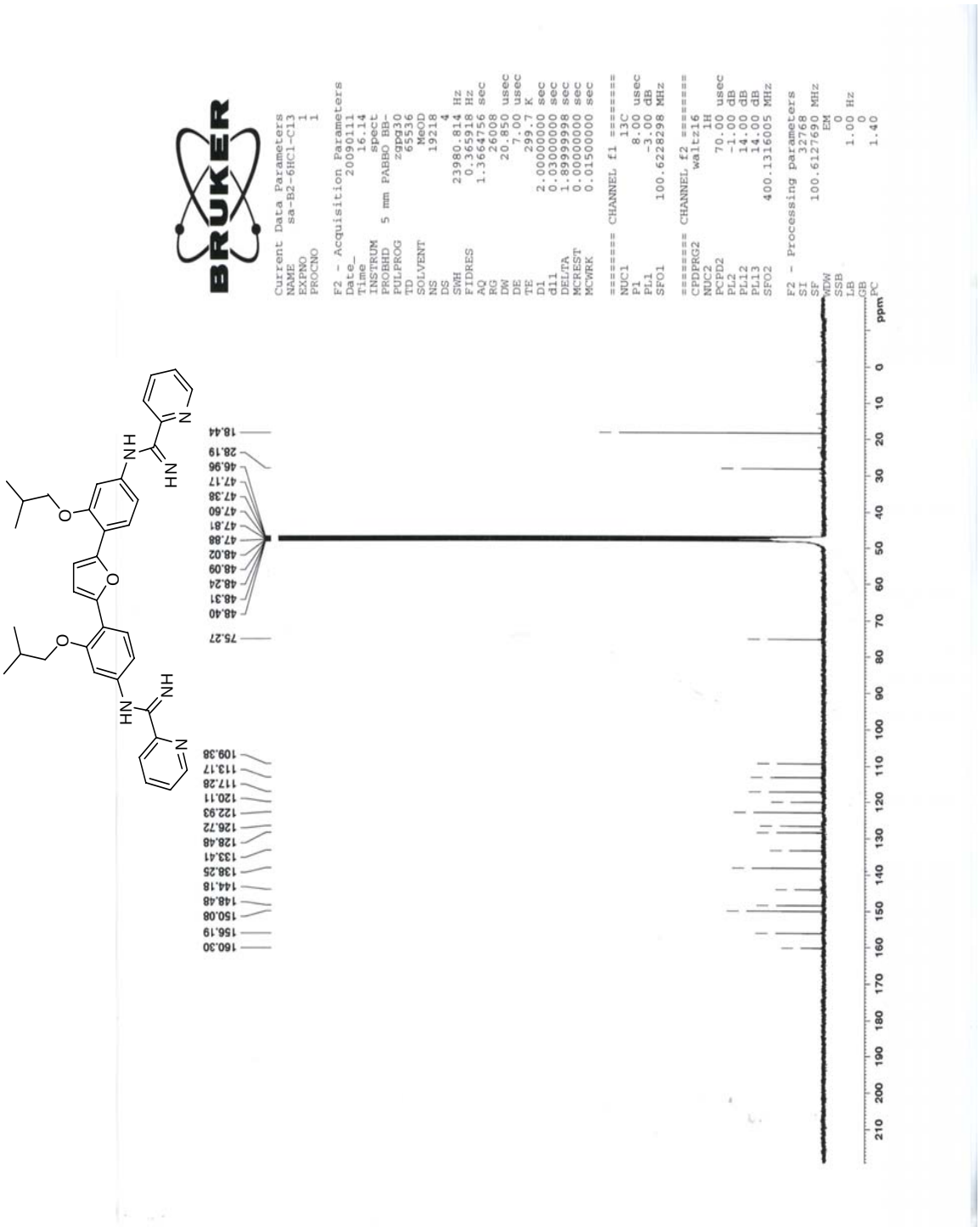
BRUKER
Current Data Parameters
NAME sa-82-6HCl-C13
EXPNO 1
PROCNO 1
F2 - Acquisition Parameters
Date_ 20090111
Time_ 16.14
INSTRUM spect
PROBHD 5 mm PABBO BB-
PULPROG zgpg30
TD 65536
SOLVENT MeOD
NS 19218
DS 4
SWH 23980.814 Hz
FIDRES 0.365918 Hz
AQ 1.3664756 sec
RG 26008
DW 20.850 usec
DE 7.00 usec
TE 299.7 K
D1 2.00000000 sec
d11 0.03000000 sec
DELTA 1.89999998 sec
MCREST 0.00000000 sec
MCWRK 0.01500000 sec
======== CHANNEL f1 ========
NUC1 13C
P1 8.00 usec
PL1 -3.00 dB
SFO1 100.6228298 MHz
======== CHANNEL f2 ========
CPDPRG2 waltz16
NUC2 1H
PCPD2 70.00 usec
PL2 1.00 dB
PL12 14.00 dB
PL13 14.00 dB
SFO2 400.1316005 MHz
F2 - Processing parameters
SI 32768
SF 100.6127690 MHz
WDW EM
SSB 0
LB 1.00 Hz
GB 0
PC 1.40
18.44
28.19
46.96
47.17
47.38
47.60
47.81
47.88
48.02
48.09
48.24
48.31
48.40
75.27
109.38
113.17
117.28
120.11
122.93
126.72
128.48
133.41
138.25
144.18
148.48
150.08
156.19
160.30
ppm

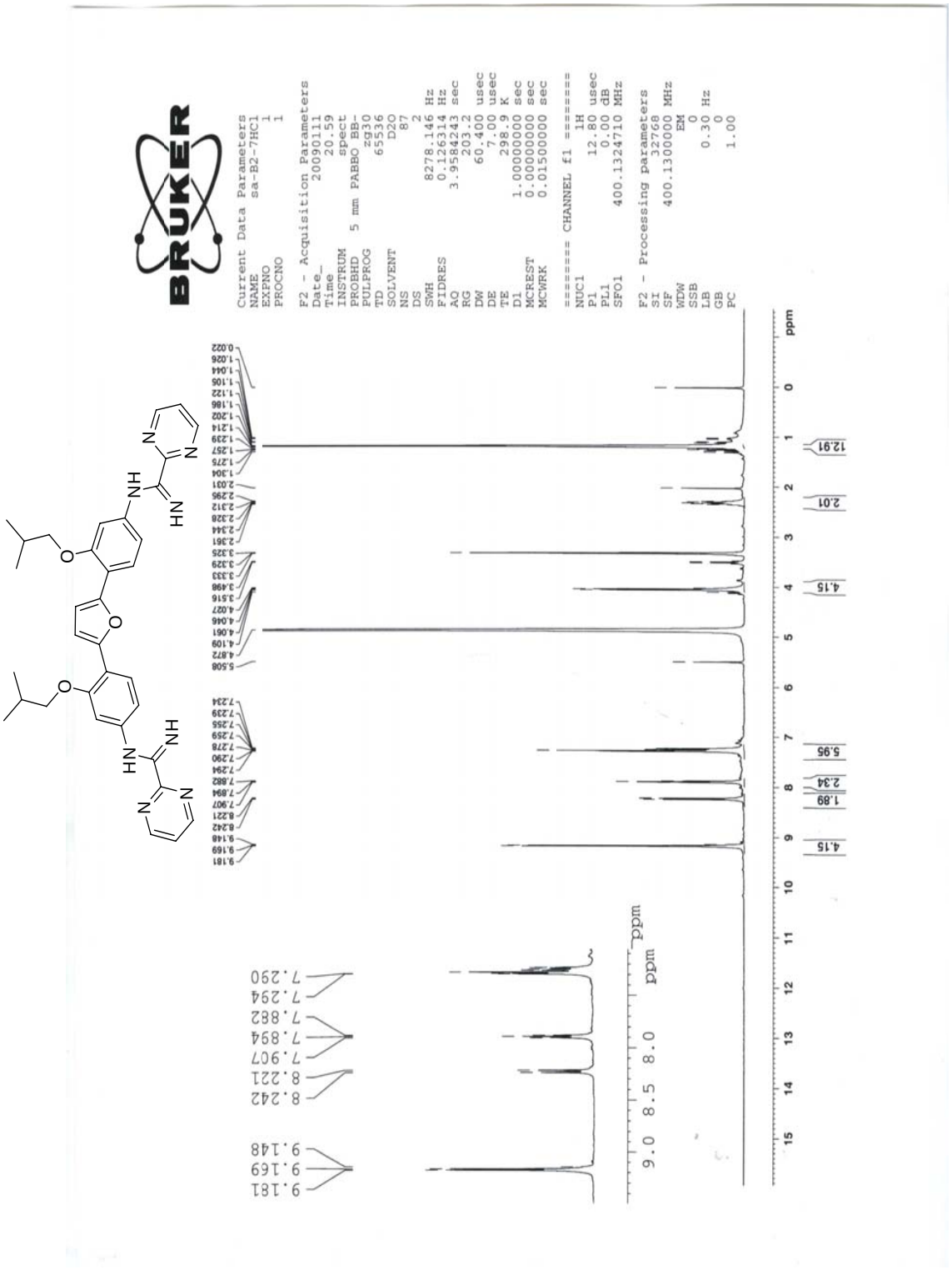
BRUKER
Current Data Parameters
NAME sa-B2-7HCl
EXPNO 1
PROCNO 1
F2 - Acquisition Parameters
Date_ 20090111
Time_ 20.59
INSTRUM spect
PROBHD 5 mm PABBO BB-
PULPROG zg30
TD 65536
SOLVENT D2O
NS 87
DS 2
SWH 8278.146 Hz
FIDRES 0.126314 Hz
AQ 3.9584243 sec
RG 203.2
DW 60.400 usec
DE 7.00 usec
TE 298.9 K
D1 1.00000000 sec
MCREST 0.00000000 sec
MCWRK 0.01500000 sec
======== CHANNEL f1 ========
NUC1 1H
P1 12.80 usec
PL1 0.00 dB
SFO1 400.1324710 MHz
F2 - Processing parameters
SI 32768
SF 400.1300000 MHz
WDW EM
SSB 0
LB 0.30 Hz
GB 0
PC 1.00
ppm
12.91
2.01
4.15
5.95
1.89
2.34
4.15
9.181
9.169
9.148
8.242
8.221
7.907
7.894
7.882
7.294
7.290
9.0 8.5 8.0 ppm

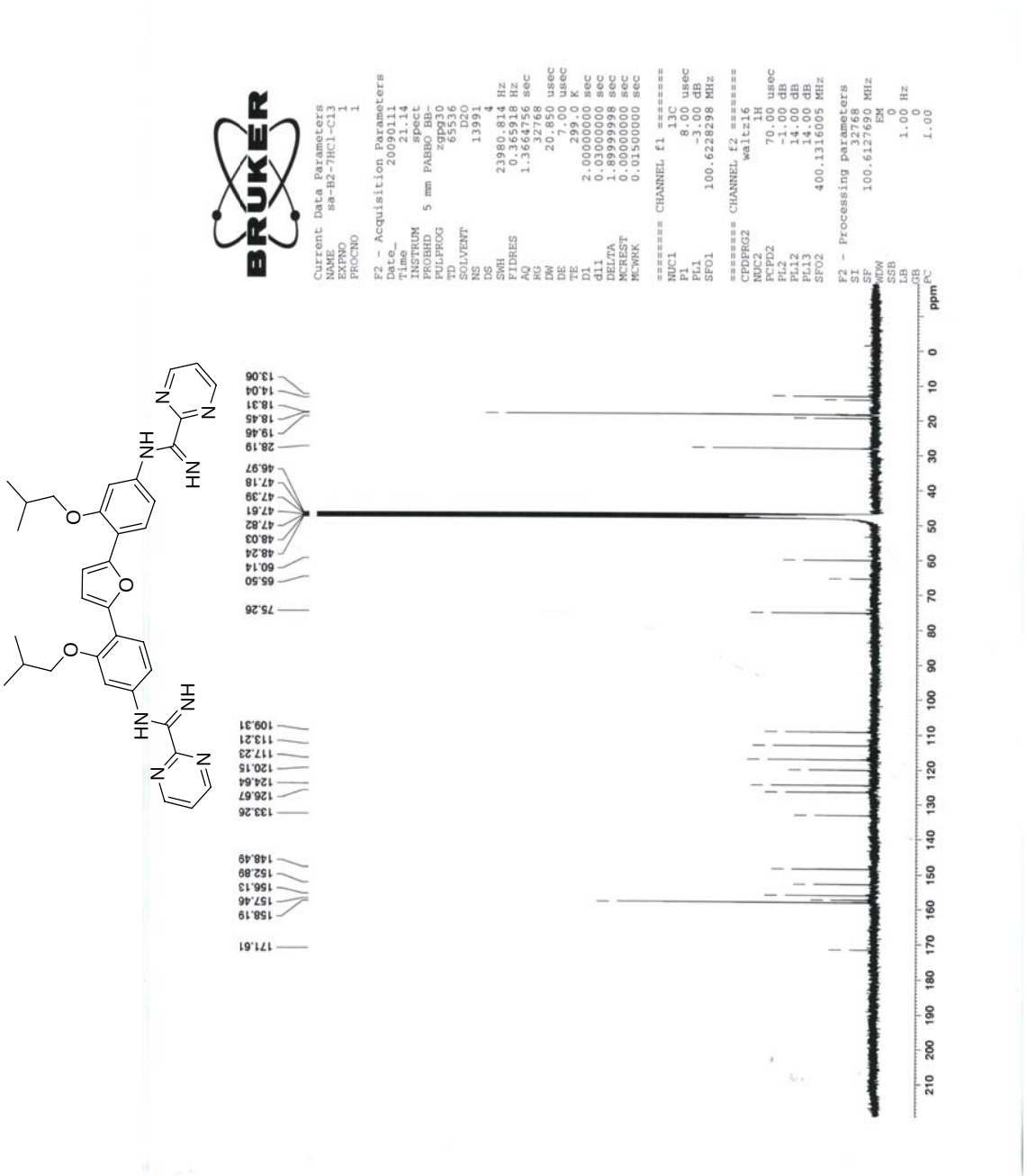
BRUKER
Current Data Parameters
NAME sa-B2-7HCl-C13
EXPNO 1
PROCNO 1
F2 - Acquisition Parameters
Date_ 20090111
Time 21.14
INSTRUM spect
PROBHD 5 mm PABBO BB-
PULPROG zgpg30
TD 65536
SOLVENT D2O
NS 13991
DS 4
SWH 23980.814 Hz
FIDRES 0.365918 Hz
AQ 1.3664756 sec
RG 32768
DW 20.850 usec
DE 7.00 usec
TE 299.0 K
D1 2.00000000 sec
D11 0.03000000 sec
DELTA 1.89999998 sec
MCREST 0.00000000 sec
MCWRK 0.01500000 sec
======== CHANNEL f1 ========
NUC1 13C
P1 8.00 usec
PL1 -3.00 dB
SFO1 100.6228298 MHz
======== CHANNEL f2 ========
CPDPRG2 waltz16
NUC2 1H
PCPD2 70.00 usec
PL2 -1.00 dB
PL12 14.00 dB
PL13 14.00 dB
SFO2 400.1316005 MHz
F2 - Processing parameters
SI 32768
SF 100.6127690 MHz
WDW EM
SSB 0
LB 1.00 Hz
GB 0
PC 1.00
13.06
14.04
18.31
18.45
18.46
28.19
46.97
47.18
47.39
47.61
47.82
48.03
48.24
60.14
65.50
75.26
109.31
113.21
117.23
120.15
124.64
126.67
133.26
148.49
152.89
156.13
157.46
158.19
171.61
ppm

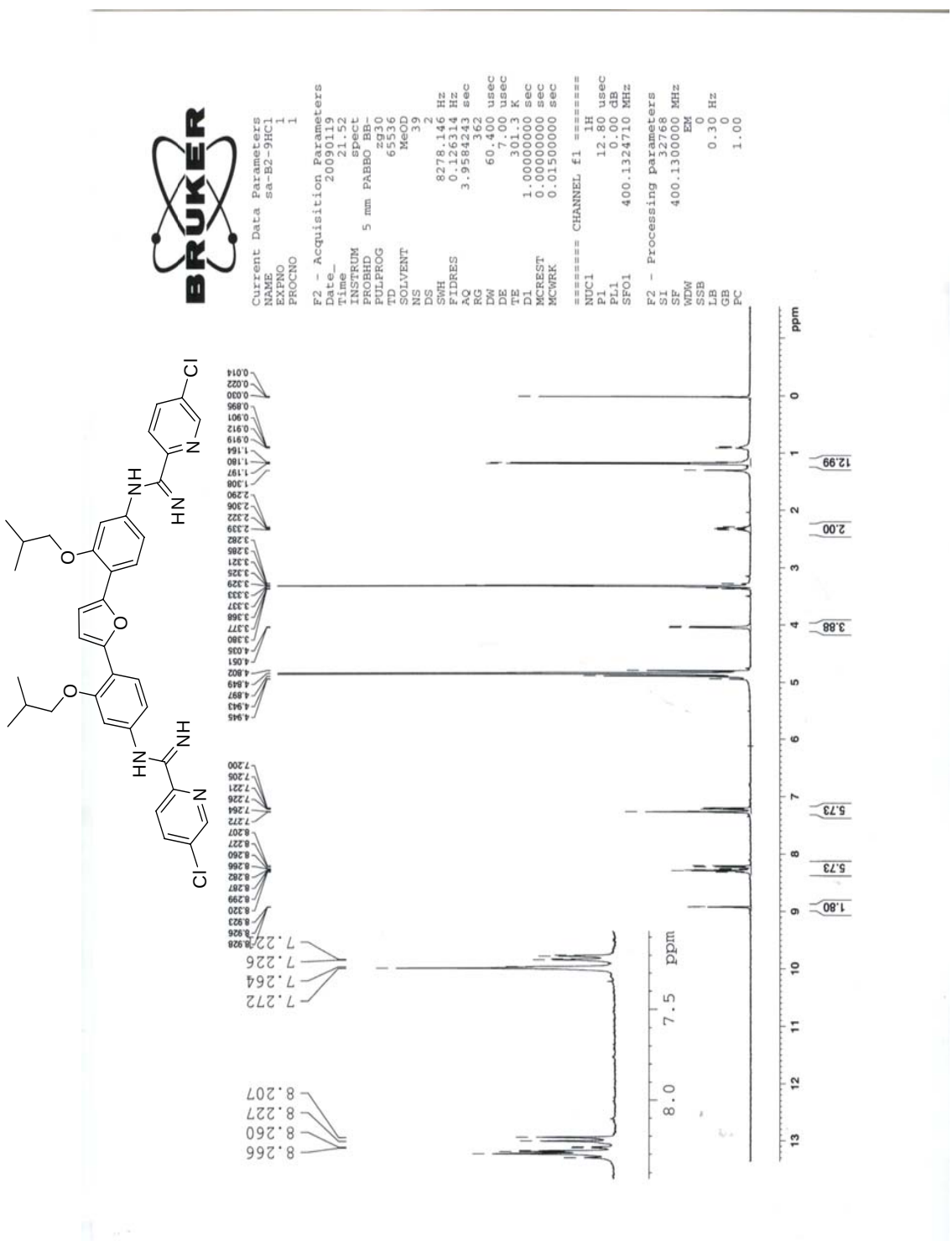
BRUKER
Current Data Parameters
NAME sa-B2-9HCl
EXPNO 1
PROCNO 1
F2 - Acquisition Parameters
Date_ 20090119
Time 21.52
INSTRUM spect
PROBHD 5 mm PABBO BB-
PULPROG zg30
TD 65536
SOLVENT MeOD
NS 39
DS 2
SWH 8278.146 Hz
FIDRES 0.126314 Hz
AQ 3.9584243 sec
RG 362
DW 60.400 usec
DE 7.00 usec
TE 301.3 K
D1 1.00000000 sec
MCREST 0.00000000 sec
MCWRK 0.01500000 sec
======== CHANNEL f1 ========
NUC1 1H
P1 12.80 usec
PL1 0.00 dB
SFO1 400.1324710 MHz
F2 - Processing parameters
SI 32768
SF 400.1300000 MHz
WDW EM
SSB 0
LB 0.30 Hz
GB 0
PC 1.00
ppm
12.99
2.00
3.88
5.73
5.73
1.80
8.266
8.260
8.227
8.207
7.272
7.264
7.226
7.221
8.0
7.5
ppm
HN
NH
NH
HN
N
N
O
O
O
Cl
Cl

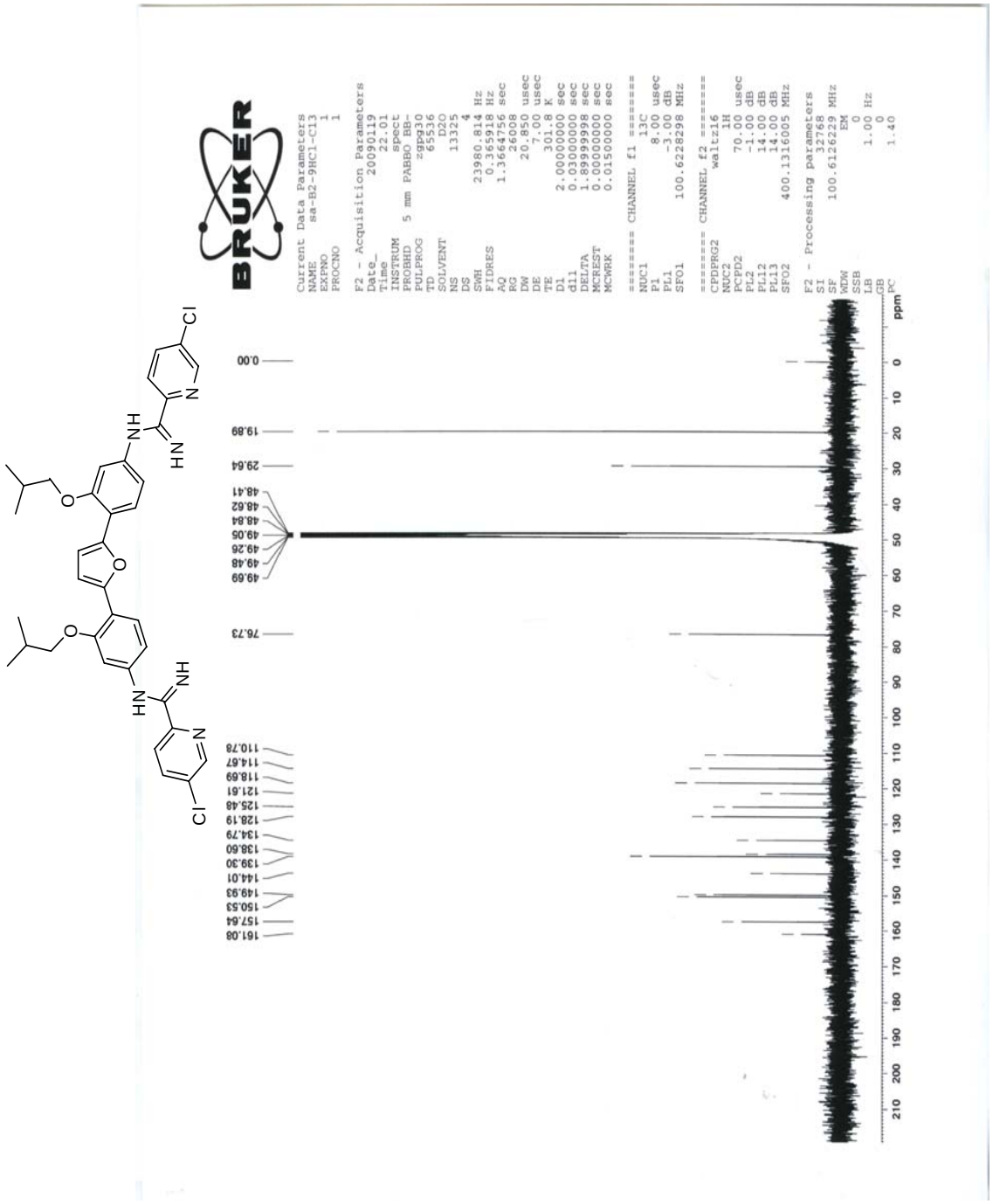
BRUKER
Current Data Parameters
NAME sa-B2-9HCl-C13
EXPNO 1
PROCNO 1
F2 - Acquisition Parameters
Date_ 20090119
Time_ 22.01
INSTRUM spect
PROBHD 5 mm PABBO BB-
PULPROG zgpg30
TD 65536
SOLVENT D2O
NS 13325
DS 4
SWH 23980.814 Hz
FIDRES 0.365918 Hz
AQ 1.3664756 sec
RG 26008
DW 20.850 usec
DE 7.00 usec
TE 301.8 K
D1 2.00000000 sec
d11 0.03000000 sec
DELTA 1.89999998 sec
MCREST 0.00000000 sec
MCWRK 0.01500000 sec
======== CHANNEL f1 ========
NUC1 13C
P1 8.00 usec
PL1 -3.00 dB
SFO1 100.6228298 MHz
======== CHANNEL f2 ========
CPDPRG2 waltz16
NUC2 1H
PCPD2 70.00 usec
PL2 -1.00 dB
PL12 14.00 dB
PL13 14.00 dB
SFO2 400.1316005 MHz
F2 - Processing parameters
SI 32768
SF 100.6126229 MHz
WDW EM
SSB 0
LB 1.00 Hz
GB 0
PC 1.40
ppm
0.00
19.89
29.64
48.41
48.62
48.84
49.05
49.26
49.48
49.69
76.73
110.78
114.67
118.69
121.61
125.48
128.19
134.79
138.60
139.30
144.01
149.93
150.53
157.64
161.08
NH
HN
O
N
Cl

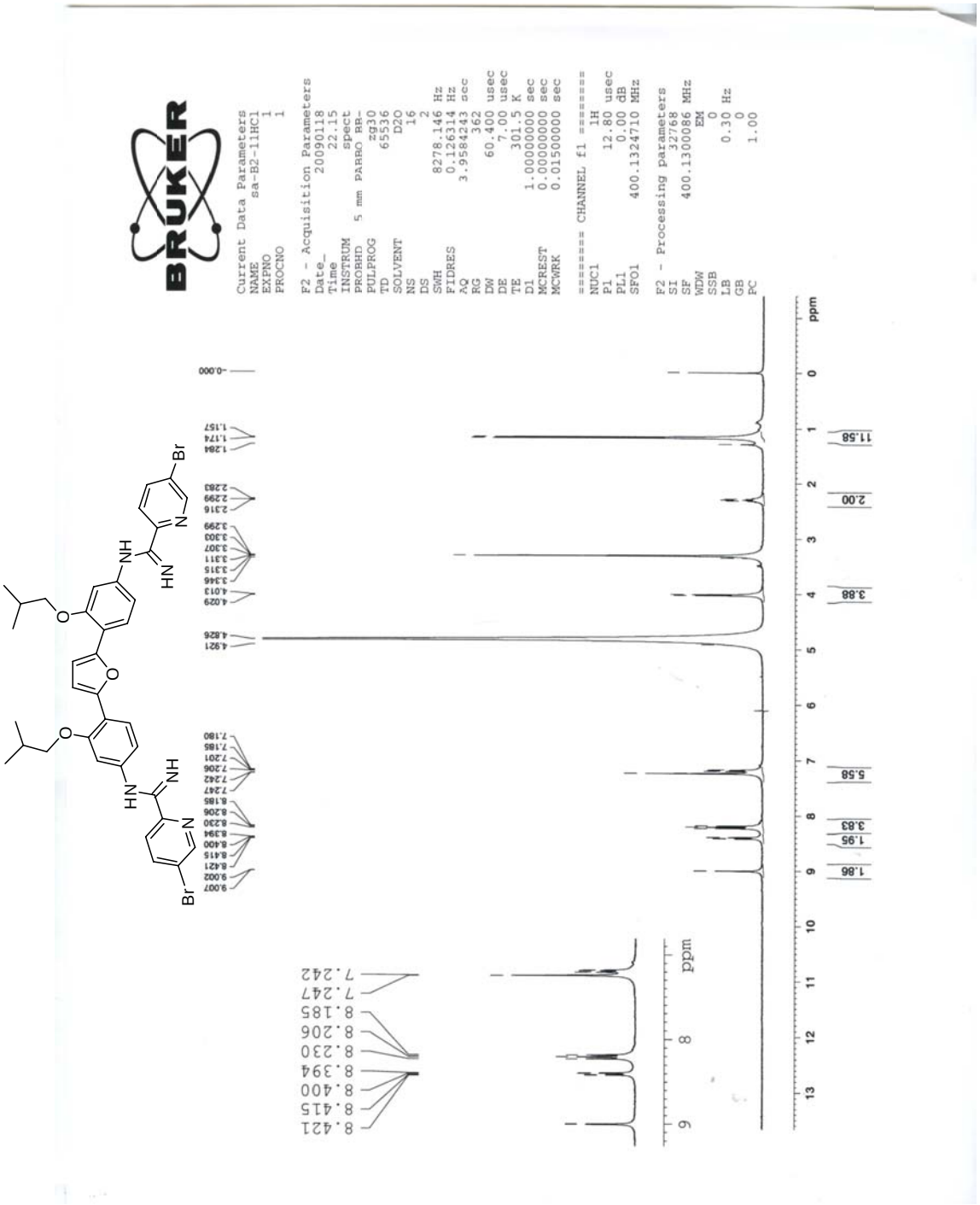
BRUKER
Current Data Parameters
NAME sa-B2-11HCl
EXPNO 1
PROCNO 1
F2 - Acquisition Parameters
Date_ 20090118
Time 22.15
INSTRUM spect
PROBHD 5 mm PABBO BB-
PULPROG zg30
TD 65536
SOLVENT D2O
NS 16
DS 2
SWH 8278.146 Hz
FIDRES 0.126314 Hz
AQ 3.95842432 sec
RG 362
DW 60.400 usec
DE 7.00 usec
TE 301.5 K
D1 1.00000000 sec
MCREST 0.00000000 sec
MCWRK 0.01500000 sec
======== CHANNEL f1 ========
NUC1 1H
P1 12.80 usec
PL1 0.00 dB
SFO1 400.1324710 MHz
F2 - Processing parameters
SI 32768
SF 400.1300086 MHz
WDW EM
SSB 0
LB 0.30 Hz
GB 0
PC 1.00
Br
NH
HN
N
O
ppm
11.58
2.00
3.88
5.58
3.83
1.95
1.86

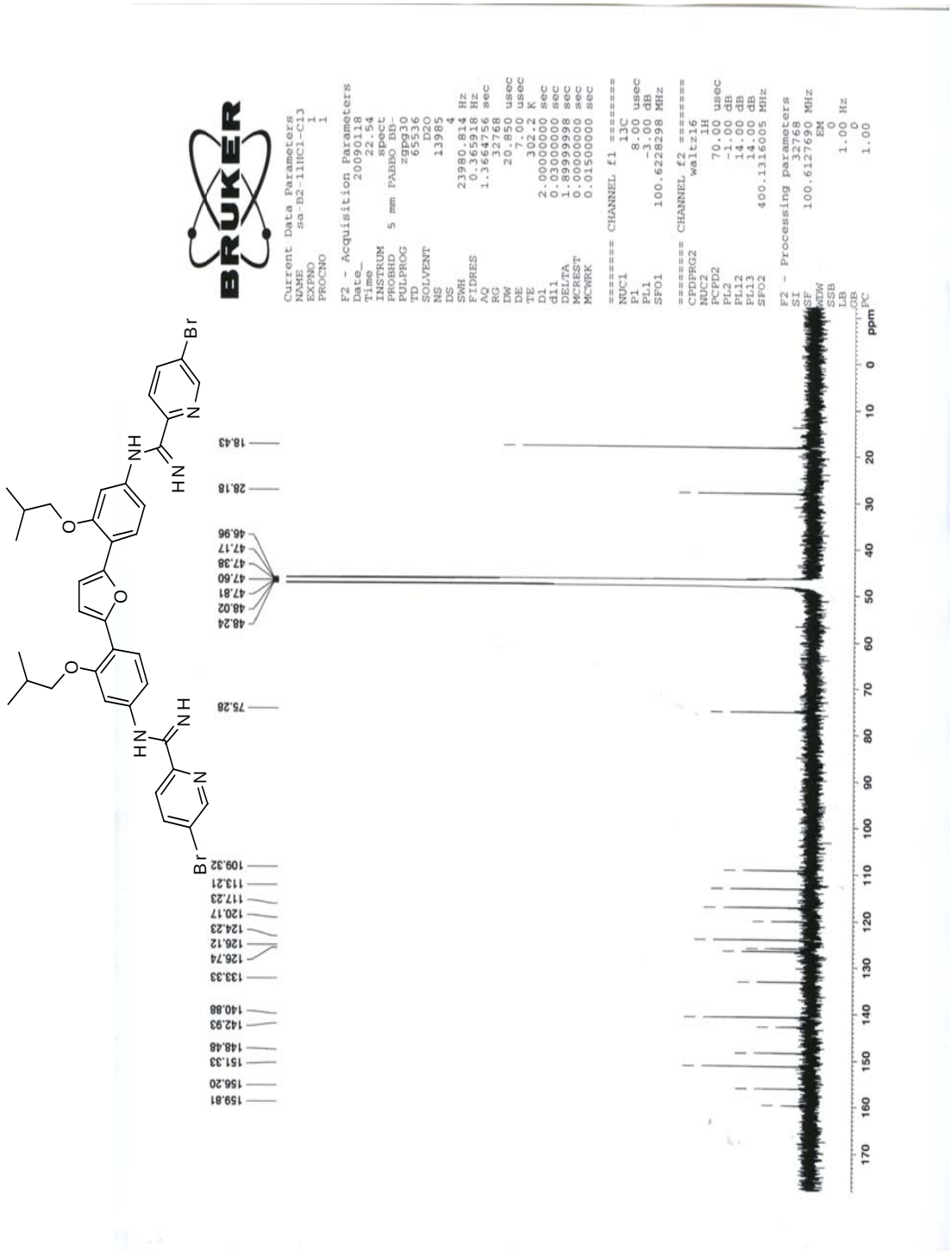
Br
NH
HN
N
O
O
NH
HN
N
Br
18.43
28.18
46.96
47.17
47.38
47.60
47.81
48.02
48.24
75.28
109.32
113.21
117.23
120.17
124.23
126.12
126.74
133.33
140.88
142.93
148.48
151.33
156.20
159.81
ppm

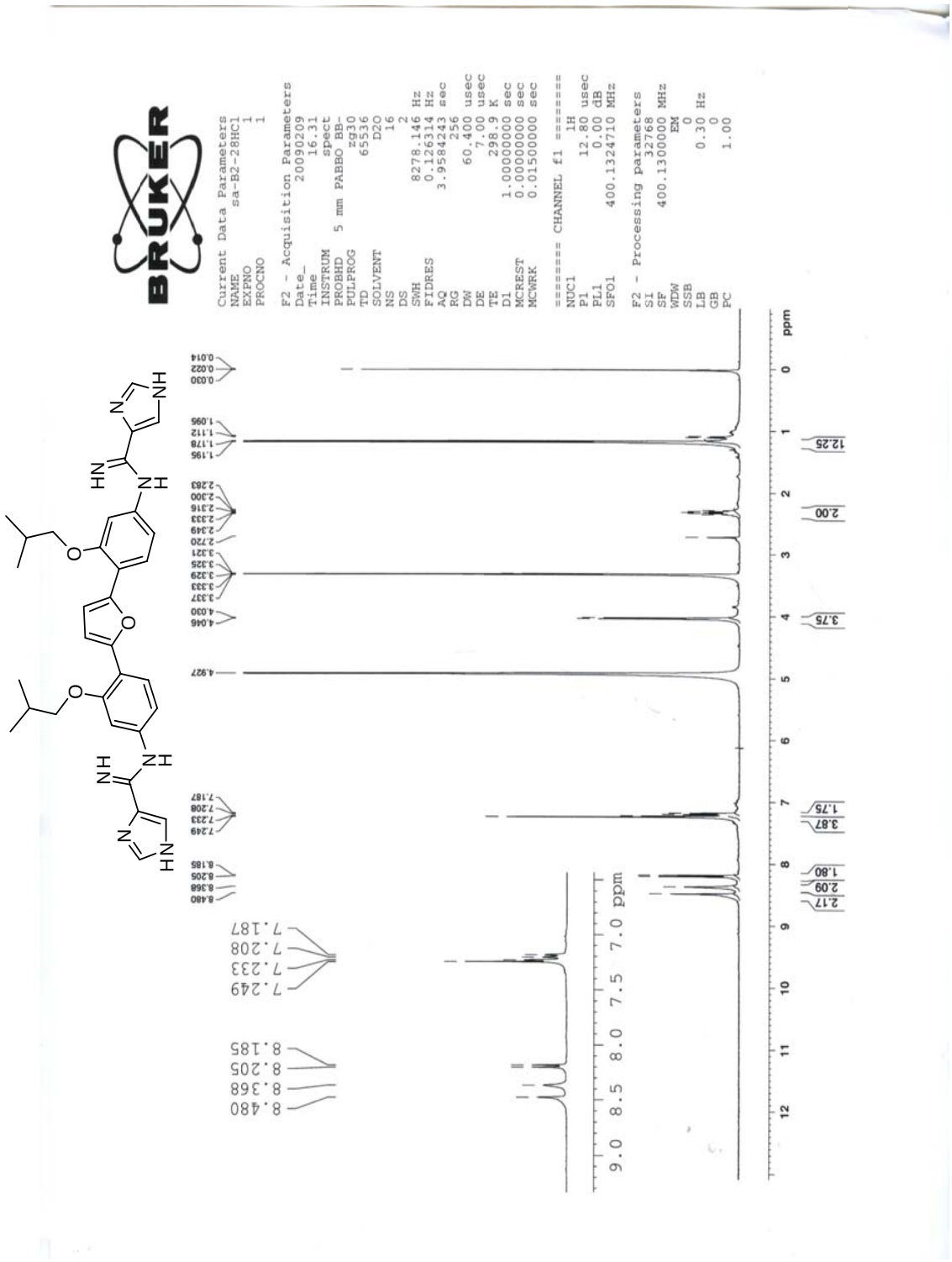
BRUKER
Current Data Parameters
NAME sa-B2-28HCl
EXPNO 1
PROCNO 1
F2 - Acquisition Parameters
Date_ 20090209
Time_ 16.31
INSTRUM spect
PROBHD 5 mm PABBO BB-
PULPROG zg30
TD 65536
SOLVENT D2O
NS 16
DS 2
SWH 8278.146 Hz
FIDRES 0.126314 Hz
AQ 3.9584243 sec
RG 256
DW 60.400 usec
DE 7.00 usec
TE 298.9 K
D1 1.00000000 sec
MCREST 0.00000000 sec
MCWRK 0.01500000 sec
======== CHANNEL f1 ========
NUC1 1H
P1 12.80 usec
PL1 0.00 dB
SFO1 400.1324710 MHz
F2 - Processing parameters
SI 32768
SF 400.1300000 MHz
WDW EM
SSB 0
LB 0.30 Hz
GB 0
PC 1.00
ppm
12.25
2.00
3.75
3.87
1.75
1.80
2.09
2.17
8.480
8.368
8.205
8.185
7.249
7.233
7.208
7.187

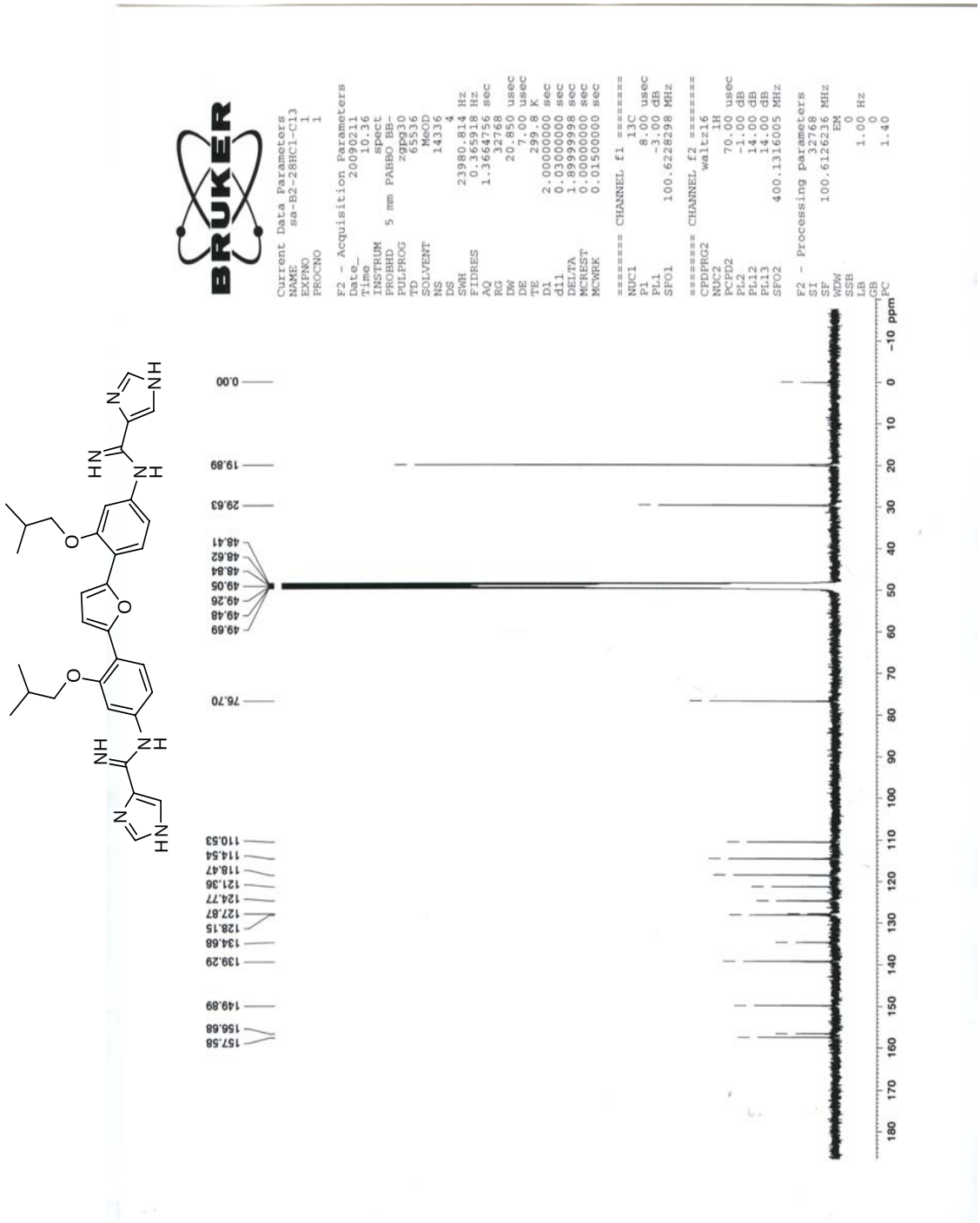
BRUKER
Current Data Parameters
NAME sa-B2-28HCl-C13
EXPNO 1
PROCNO 1
F2 - Acquisition Parameters
Date_ 20090211
Time 10.36
INSTRUM spect
PROBHD 5 mm PABBO BB-
PULPROG zgpg30
TD 65536
SOLVENT MeOD
NS 14336
DS 4
SWH 23980.814 Hz
FIDRES 0.365918 Hz
AQ 1.3664756 sec
RG 32768
DW 20.850 usec
DE 7.00 usec
TE 299.8 K
D1 2.00000000 sec
d11 0.03000000 sec
DELTA 1.89999998 sec
MCREST 0.00000000 sec
MCWRK 0.01500000 sec
======== CHANNEL f1 ========
NUC1 13C
P1 8.00 usec
PL1 -3.00 dB
SFO1 100.6228298 MHz
======== CHANNEL f2 ========
CPDPRG2 waltz16
NUC2 1H
PCPD2 70.00 usec
PL2 -1.00 dB
PL12 14.00 dB
PL13 14.00 dB
SFO2 400.1316005 MHz
F2 - Processing parameters
SI 32768
SF 100.6126236 MHz
WDW EM
SSB 0
LB 1.00 Hz
GB 0
PC 1.40
0.00
19.89
29.63
48.41
48.62
48.84
49.05
49.26
49.48
49.69
76.70
110.53
114.54
118.47
121.36
124.77
127.87
128.15
134.68
139.29
149.89
156.68
157.58
ppm